Systemic Tau and the Discrete Architecture of Time

Johel Padilla-Villanueva

Second Edition

Systemic Tau and the Discrete Architecture of Time
A synthesis of the Systemic Tau paradigm, the discrete extramental clock,
the three-layer ontology, ontological ascent, nested ordinal depth,
and post-June 2026 clinical–philosophical extensions

Second Edition — July 2026

Johel Padilla-Villanueva, DrPH
ORCID: 0000-0002-5797-6931
joel.padilla2@upr.edu
Universidad de Puerto Rico, Recinto de Ciencias Médicas
Research Program: Ontología del Presente (Tau Sistémico)

July 2026

Systemic Tau and the Discrete Architecture of Time
Second Edition — Corpus-complete synthesis (July 2026)

ISBN: 979-8-18776-367-2
ISBN (EAN): 9798187763672
Imprint / sello: Independently published
(Free KDP ISBN assigned to this title)

Author: Johel Padilla-Villanueva, DrPH
Affiliation: Universidad de Puerto Rico, Recinto de Ciencias Médicas
ORCID: 0000-0002-5797-6931
Contact: joel.padilla2@upr.edu

This volume is a scholarly monograph synthesizing the Systemic Tau / RECD research program (2022–2026), including the post-June 2026 corpus (excess3 / Φ_3, clinical CCTP pilot, and philosophical continuations).

Print specifications (interior)
Format: US Letter (8.5 × 11 in / 216 × 279 mm)
Binding: Perfect bind or case bind (twoside, openright)
Color: Full color interior (figures) / greyscale acceptable for text-only reprints
Fonts: All embedded (Latin Modern + Latin Modern Math)
PDF: Print-optimized production file (see package `PRINT_SPECS.md`)

Catalog / archive anchors (selected DOIs)
10.5281/zenodo.21385937 (excess3)
10.5281/zenodo.21400599 (Φ_3–RECD)
10.5281/zenodo.21287252 (RECD framework)
10.5281/zenodo.21210455 (Foundations)
10.5281/zenodo.21270699 (CCTP/SDDB)

Second Edition: July 2026 (expanded from the June 2026 first synthesis).
Typeset with LuaLaTeX (TeX Live).
Research Program: *Ontología del Presente (Tau Sistémico).*

Abstract

Systemic Tau (τ_s) is introduced as an ordinal, Kendall-based observable for multivariate, noisy, and non-stationary dynamics, designed to remain invariant under monotone transformations and robust to moderate noise. Building from empirical work on dengue incidence with climatic covariates and synthetic validation on canonical nonlinear systems, the program establishes regime thresholds for stability, chaos, and antisynchronization. These results are unified in the Discrete Extramental Clock (RECD), a gated accumulation of scale-renormalized time increments derived from the reduction of ordinal dynamics to a unimodal return map and its renormalization structure. The volume further proves Bayesian optimality properties of RECD (minimax robustness across renormalization levels and large-deviation behavior with rate tied to τ_s) and develops a three-layer ontology in which the Joint Episode is the primitive ontological–temporal unit. The Principle of Ontological Ascent formalizes structural reorganization as a discrete transition between stabilized ontological levels, with consequences for the geometry of accumulated extramental time ($D \approx 1.98$).

This **Second Edition** (July 2026) integrates the post-June research corpus that was missing from the first polished synthesis: the nested ordinal hierarchy Φ_1, Φ_2, Φ_3 with continuous Level-3 proxy `excess3` (Padilla-Villanueva 2026f; Padilla-Villanueva 2026l); the dynamic integration of Φ_3 as a structural contribution to the RECD clock (Padilla-Villanueva 2026i); the Foundations paper and software stack (Padilla-Villanueva 2026m); the first high-resolution clinical pilot on spontaneous ventricular fibrillation (CCTP/SDDB) (Padilla-Villanueva 2026b); and the philosophical continuation of Polo's *persistir* as *acto de ser relacional-discreto* together with the Conjecture of the Relational Order of Persistence (Padilla-Villanueva 2026d; Padilla-Villanueva 2026a).

Keywords: Systemic Tau; Kendall's tau; ordinal coherence; early-warning signals; renormalization; Feigenbaum universality; discrete time; Discrete Extramental Clock (RECD); excess3; Φ_3; nested ordinal hierarchy; dengue; cardiac sudden death; Leonardo Polo; acto de ser

Contents

List of Figures

List of Tables

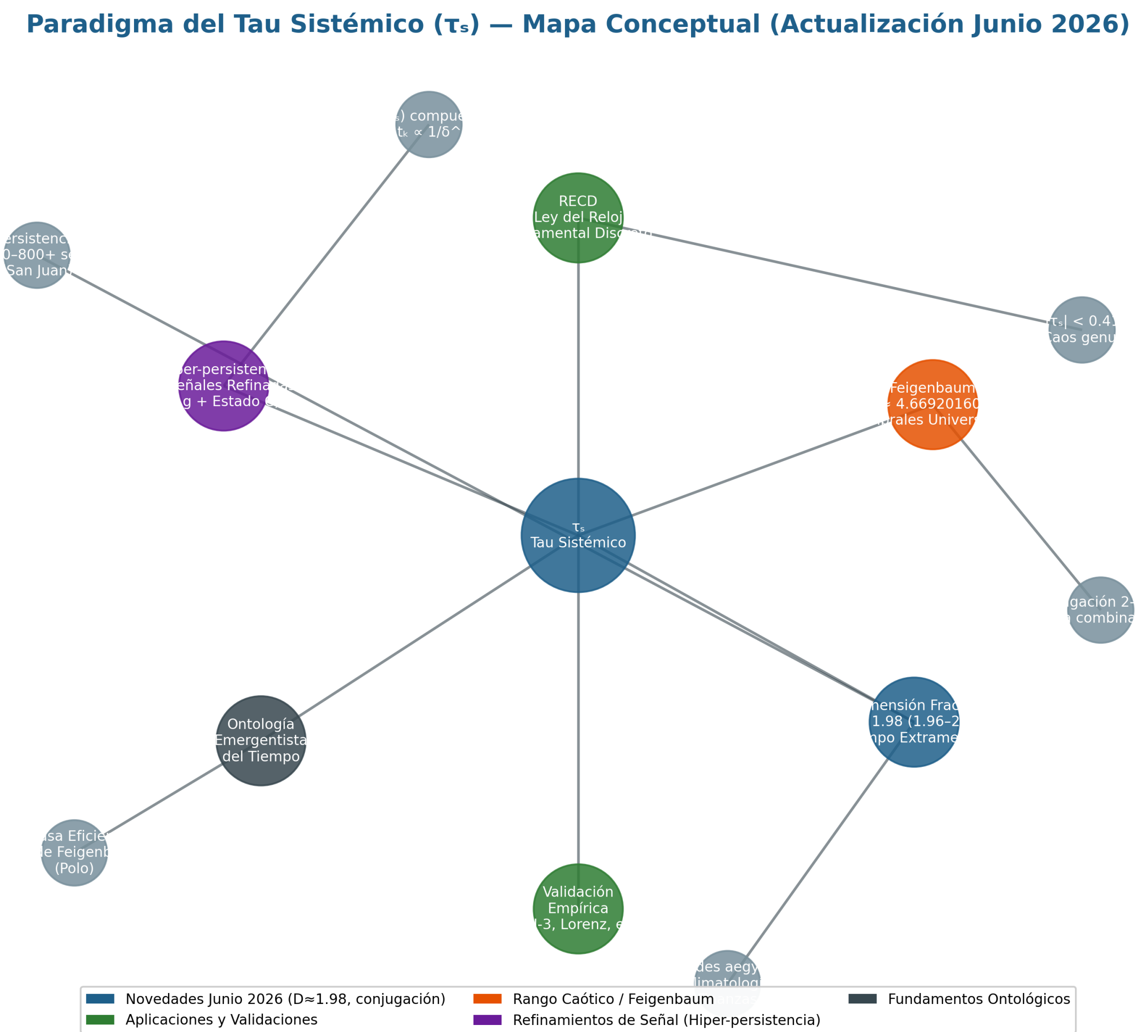

Figure 1: High-level conceptual map of the Systemic Tau / RECD paradigm.

Chapter 1

Preface: The Development of the Research Program (2022–2026)

The present volume constitutes the substantially expanded and definitive first complete scholarly synthesis of a research program that began in the 2022 doctoral dissertation and reached a mature, hierarchically articulated form in 2025–2026.

In 2022, the central problem was framed as the search for early-warning signals in multivariate, noisy, non-stationary series, where classical Lyapunov exponents and variance-based indicators proved fragile. The dissertation introduced Systemic Tau (τ_s) as an ordinal, Kendall-based observable that required no absolute scale and remained robust under monotonic transformations and moderate noise. The empirical core was the analysis of dengue incidence together with climatic covariates in San Juan and Iquitos, along with extensive synthetic validation on the logistic map and the Lorenz attractor.

By 2025, the program had produced the explicit thresholds ($|\tau_s| < 0.41$ for the chaotic regime, $\tau_s \geq +0.50$ for stability, $\tau_s \leq -0.41$ for strong antisynchronization) and the first formulation of the Discrete Extramental Clock Law (RECD).

The gate function $g(\tau_s)$ and the scaled increments $\Delta t_k = \delta^{-k}|\tau_s|\Delta t_0$ appeared as necessary consequences of the reduction of ordinal dynamics to a unimodal return map of class C^3 with a non-degenerate quadratic critical point. This reduction was stated as Theorem v24.

In early–mid 2026, three decisive advances were consolidated. First, the strong Bayesian optimality of the RECD was proved in three interlocking senses (exponential growth of the log-posterior, minimax robustness across renormalization levels, and long-run ordinal Kullback –Leibler accumulation), together with the large-deviation principle whose rate function is tied directly to τ_s. Second, the three-layer ontological framework and the Joint Episode as primitive ontological-temporal unit were formalized, with precise metrics $J = D \cdot M$ and the empirical demonstration that even oracle-labeled episodes yield only $AUC \approx 0.476$ for subsequent Capa 3 reorganization. Third, the Principle of Ontological Ascent was stated: a Capa 3 structural reorganization constitutes an ascent from a stabilized ontological level L_m to L_{m+1}, instituting a new law of

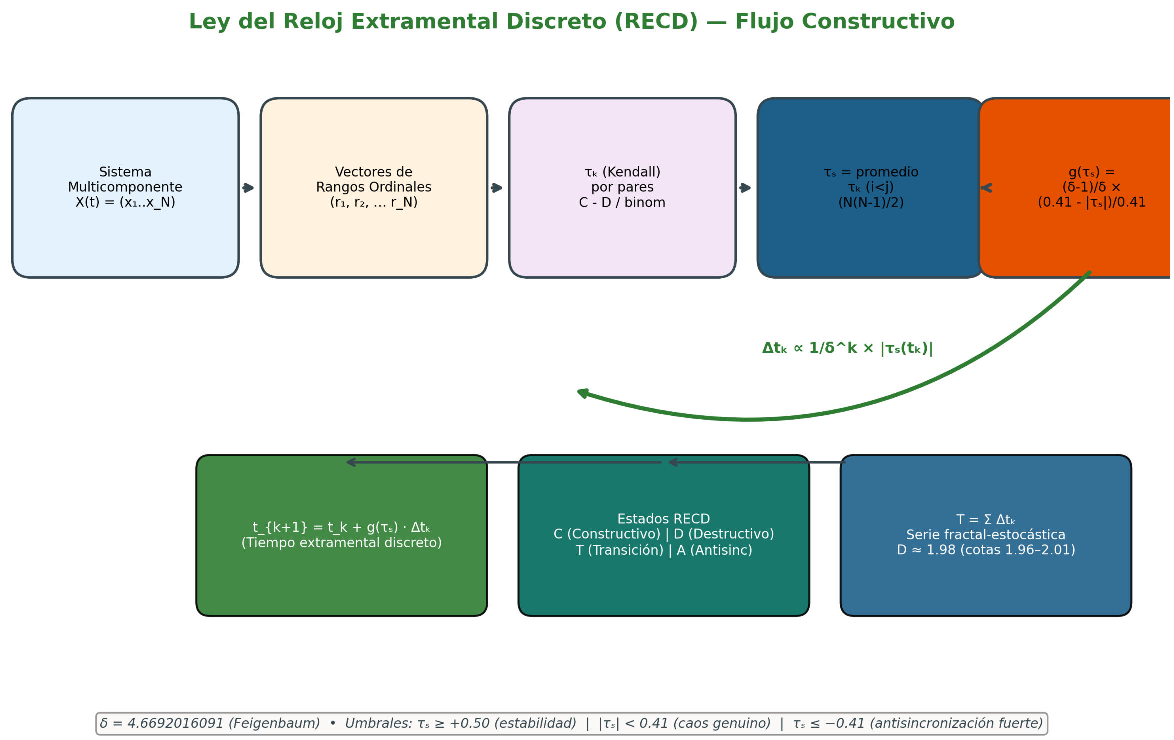

Figure 1.1: End-to-end computational flow of the Discrete Extramental Clock (RECD): from ordinal windows to τ_s, gate evaluation, and accumulation of t_n.

discreteness intervals together with downward constraints that are irreducible to continuation of the prior regime. The fractal geometry of the accumulated extramental time was derived as $D \approx 1.98$ with rigorous bounds $1.96 \leq D \leq 2.01$, justified by the 2-adic conjugacy of the Feigenbaum attractor with the adding machine on $\mathbb{Z}_2$. These results formed the spine of the first complete scholarly synthesis (first synthesis / first edition draft, June 2026).

1.0.1 The July 2026 corpus extension (Second Edition)

Between late June and mid-July 2026 the program produced a further cluster of results that the June synthesis could not yet absorb. Four strands are now integrated in Chapter 28 and cited throughout the open-problem register:

1. **Nested ordinal depth and `excess3`.** Hierarchical ordinal conjunctions Φ_1 (coincidence), Φ_2 (persistent relational structure), and Φ_3 (irreducible synergistic surplus) were specified with a pre-registered continuous Level-3 proxy $\texttt{excess3} = 0.6\,\mathrm{Syn} + 0.4\,\mathrm{Surp}$, null models based on phase-shuffle surrogates, and synthetic validation arms (Padilla-Villanueva 2026f; Padilla-Villanueva 2026r; Padilla-Villanueva 2026j).

2. **Dynamic integration of Φ_3 into the RECD clock.** The preprint on Φ_3–RECD integration moves excess3 from a parallel diagnostic to a structural contribution to clock accumulation under regime-dependent weights (Padilla-Villanueva 2026i; Padilla-Villanueva 2026l).

3. **Foundations and software stack.** A topological early-warning foundations paper and the open `systemictau` / Academy stack codify the operational pipeline (Padilla-Villanueva 2026m).

4. **Clinical and philosophical translation.** The CCTP pilot on the Sudden Cardiac Death Holter Database supplies multi-hour median lead times for $\Delta\tau_s$ and $\Delta\texttt{excess3}$ before spontaneous ventricular fibrillation, with substrate-dependent polarity (Padilla-Villanueva 2026b). In parallel, the monographs on the *acto de ser relacional-discreto* and the Conjecture of the Relational Order of Persistence continue the dialogue with Polo and Whitehead without reducing the ontology to metrics (Padilla-Villanueva 2026d; Padilla-Villanueva 2026a). Ontological-permeability calibration of upward filtering is archived as technical report (Padilla-Villanueva 2026e).

This Second Edition therefore does not replace the June architecture; it completes the first synthesis with the papers that the research program produced immediately afterward, so that the single volume again matches the living corpus in `Publicaciones`.

Chapter 2

Executive Summary

This book presents the complete theoretical, mathematical, empirical, and philosophical architecture of the Systemic Tau paradigm and the Discrete Extramental Clock (RECD). The executive summary that follows is deliberately substantial; it supplies the conceptual spine that every subsequent chapter will develop in full technical and ontological detail.

From classical early-warning signals to ordinal systemic coherence. Classical indicators of critical transitions—rising variance, increasing lag-1 autocorrelation, critical slowing down—assume that the underlying metric of time is given and homogeneous. They are also parametrically fragile when series are short, noisy, or observed only through incompatible scales. The dissertation of 2022 demonstrated that an alternative observable constructed solely from rank orderings inside sliding windows of length $n \approx 13$ already captures the collapse of global ordinal structure that precedes macroscopic transitions. Systemic Tau is defined exactly as

$$\tau_s(k) = \frac{2}{N(N-1)} \sum^{1 \le i < j \le N} \tau_k(r_i(k), r_j(k)),$$

where each τ_k is the Kendall coefficient computed on the rank vectors of components i and j. Because only relative order is used, τ_s is invariant under arbitrary monotonic re-scaling of any component and remains statistically well-behaved under additive noise up to approximately 15–20 percent.

Universal thresholds and the chaotic range. Under the null of ordinal independence the asymptotic variance of a single pairwise Kendall coefficient is $(4n + 10)/(9n(n - 1))$. For the conventional window $n \ge 13$ this yields an approximate 95 percent confidence band of ± 0.41 around zero. Consequently the interval $|\tau_s| < 0.41$ is the regime in which global ordinal correlations have collapsed to a level statistically indistinguishable from noise. The upper threshold $\tau_s \ge +0.50$ demarcates robust synchronization or emergent order. The lower threshold $\tau_s \le -0.41$ marks strong, persistent antisynchronization. These three values are not fitted; they arise at the intersection of Kendall sampling theory and the universal Feigenbaum constant $\delta \approx 4.6692016091$ that governs the accumulation point of period-doubling cascades. In the logistic map the average

$|\tau_s|$ reaches precisely 0.41 at $r_\infty \approx 3.56995$, separating the periodic from the chaotic regime. The same numerical boundaries reappear across the Lorenz attractor, diffusively coupled networks, and real dengue incidence series.

The gate and the Discrete Extramental Clock. Inside the chaotic range the gate function opens:

$$g(\tau_s) = \frac{\delta - 1}{\delta} \cdot \frac{0.41 - |\tau_s|}{0.41}.$$

Outside this band the gate is effectively closed or inverted. The local temporal increment is scaled by successive powers of the Feigenbaum constant:

$$\Delta t_k = \delta^{-k} \cdot |\tau_s(k)| \cdot \frac{\Delta t_0}{n},$$

with the conventional normalization $\Delta t_0 / n$. The integrated extramental time is therefore

$$t_n = \sum^{k} g(\tau_s(k)) \cdot \Delta t_k.$$

This is the canonical statement of the RECD law. The factor δ^{-k} is not an arbitrary weighting; it is forced by the renormalization structure of the underlying unimodal return map once Theorem v24 has been established.

Theorem v24 and the reduction to Feigenbaum universality. The decisive deductive bridge is Theorem v24. Under the generic assumptions that the underlying continuous-time flow is C^3 and that critical surfaces where components cross are transversal with quadratic tangency, the sequence of ordinal configurations alone suffices to reconstruct a first-return map on a one-dimensional coherence phase coordinate. The five-step construction is: (1) extract sliding windows and convert to full rank vectors; (2) compute the scalar $\tau_s(k)$; (3) record the binary indicator s(k) = 1 precisely when $|\tau_s(k)| < 0.41$; (4) within each coherent run define a normalized exit-phase variable; (5) advance the flow during the return time and project the arrival configuration onto the phase coordinate of the next crossing. The resulting map f is of class C^3, unimodal, and possesses a non-degenerate quadratic critical point. Consequently the entire Feigenbaum–Coullet–Tresser renormalization theory applies directly. A purely combinatorial lemma on the superstable periodic orbits of period 2^k yields the exact expectation

$$\mathbb{E}[|\tau_s|]_k = \frac{2^{k-1}}{2^k - 1} \to \frac{1}{2}$$

as $k \to \infty$, supplying the universal limiting value that demarcates the chaotic range.

Large deviations and strong Bayesian optimality. Once the reduction to a unimodal quadratic map is secured, the empirical measures on the finite space of ordinal configurations satisfy a large-deviation principle whose good rate function I() is obtained from the variational principle for topological pressure. The increments of the RECD reproduce exactly the accumulation of the log-posterior for the critical-proximity parameter under sequential Bayesian updating that uses only the symbolic likelihoods induced by the stationary measures. Within the natural class of accumulation schemes that depend on τ_s only through potentials of the same functional form, the RECD is strongly optimal simultaneously in three senses: it maximizes the exponential growth rate of the log-posterior; it is minimax optimal across adversarial sequences of renormalization levels; and it maximizes the long-run accumulation of ordinal Kullback–Leibler divergence. The optimality is information-theoretically equivalent to weighting by the Feigenbaum eigenvalue itself.

The three-layer ontological framework and the Joint Episode. The RECD is not merely a computational device; it is the mathematical expression of a stratified ontology of the present. Layer 1 (Capa 1) is the local intensification of persistence, measured by the composite critical-mass metric M_{crit} that combines hyper-persistence of τ_s with RQA trapping time under a fixed configuration (LAM ≥ 0.80, TT ≥ 3.4). Layer 2 (Capa 2) is relational coherence across modules, operationalized by sustained low antisynchronization $A(k) = std\{\tau_{s_i}(k)\}$. Layer 3 (Capa 3) is global structural reorganization, detected by Frobenius-norm shifts in the multichannel correlation matrix of τ_s together with Kolmogorov–Smirnov contrasts on the series of discreteness intervals Δt_k.

A Joint Episode is the maximal contiguous interval of sustained low A_{antis} that contains at least one significant peak of M_{crit}. Its duration D and integrated intensity yield the Joint Score $J = D \cdot M$ (or its bias-reduced form $J_{0.7}$). Synthetic validation on diffusively coupled logistic maps and Lorenz ensembles demonstrates that the mapping from Joint Episode properties to subsequent Capa 3 reorganization is weak: even under oracle labeling the best-performing score achieves only $AUC \approx 0.476$. The Joint Episode therefore functions primarily as a robust detector of L1–L2 coherence—a kairos in the relational sense—rather than a strong predictor of structural change.

The Principle of Ontological Ascent. A Capa 3 global structural reorganization constitutes an ontological ascent from a stabilized regime L_m to L_{m+1} within the hierarchy of the RECD. The ascent institutes a new regime of accumulation intervals Δt_k together with emergent properties of the integrated process t_n that are irreducible to continuation or summation of the preceding level. The principle distinguishes two orders of kairos. Relational kairos comprises sustained Capa 2 intervals of inter-component coherence that function as ontologically enabling windows through bidirectional probabilistic filtering; they raise the likelihood that lower-layer configurations may crystallize at a higher stratum without determining the outcome. Ontological kairos is the autonomous actualization and stabilization of the new discreteness regime itself: the replacement of the prior discreteness operator by a novel, self-sustaining law of Δt_k at the stabilized level L_{m+1}, together with the imposition of downward constraints that actively delimit admissible configurations at subordinate strata. Data-driven detection on synthetic and dengue series shows that reorganization of the law of Δt_k is the most consistent signature of ascent, detectable even when preceding relational kairoi are rare (global fraction 0.258). In San Juan the detected transition aligned within five weeks of a major incidence peak (KS = 0.781 on Δt_k); in Iquitos the alignment was 18 weeks (KS = 0.209).

Fractal geometry of extramental time. The accumulated extramental time T generated by the RECD possesses fractal dimension $D \approx 1.98$ with rigorous bounds $1.96 \leq D \leq 2.01$. The derivation proceeds from the similarity dimension of the renormalized laminar intervals $s = log2/log\delta \approx 0.449$, corrected by the invariant measure of the attractor and the 2-adic conjugacy of the Feigenbaum limit set with the adding machine on $\mathbb{Z}_2$. The spatial Hausdorff dimension of the attractor itself remains ≈ 0.538; the contrast reveals that the generated time is almost dense while the spatial attractor is a thin Cantor set. Numerical and empirical evidence (logistic map, Lorenz, coupled networks, dengue series with hyper-persistence fractions 70–99.6 percent) confirms robustness inside the Feigenbaum universality class.

Empirical applications and hyper-persistence. On real dengue data the full_ordinal implementation of τ_s, which aggregates multivariate ordinal concordances over an adaptively selected embedding of incidence and climate variables, yields substantial gains in lead time relative to proxy approximations: 24.5 versus 1.5 weeks in Iquitos and markedly lower false-alarm rates in San Juan. Core-hyper episodes (P(k) ≥ 7 and $|\tau_s| < 0.41$) occur with high frequency in the chaotic regime and are the empirical substrate of the fractal support of T. The hyper-persistence phenomenon is not an anomaly; it is the observable trace of prolonged residence in the renormalization depths that the RECD accumulates with exponential compression.

Philosophical implications and the new ontology of time. The RECD refutes the existence of an absolute Newtonian time independent of the processes that constitute it. Time is shown to be a stratified, emergent, and hierarchically organized quantity whose discreteness law changes when the system crosses from one ontological level to another. The framework integrates classical insights—Aristotle's distinction between chronos (the uniform flow of number) and kairos (the opportune structured moment), and Leonardo Polo's analysis of the present as act—with the precise mathematics of ordinal renormalization. Memory is reinterpreted as active retention sustained by trapping and hyper-persistence rather than as a passive archive. The three-layer ontology is explicitly non-reductive: each stratum possesses its own law of discreteness and imposes downward constraints on the admissible configurations of lower strata. The Joint Episode is the relational window in which local intensifications may become structurally consequential without being reducible to them.

Unified vision and open problems. The paradigm supplies a universal, model-independent language for detecting critical transitions under the weakest observational assumptions—purely ordinal data—and simultaneously articulates a non-reductive ontology in which the reconstitution of temporal discreteness marks the crossing into a genuinely novel regime of objective time. Open problems include the extension to higher-order ordinal patterns, the rigorous derivation of the precise numerical bounds on the fractal dimension under finite-sample corrections, the development of a full probabilistic calculus of downward constraints, and the exploration of clinical and ecological interventions that deliberately modulate relational kairoi in order to steer ontological ascent or descent.

Chapter 3

From Classical Early-Warning Signals to Ordinal Systemic Coherence

The scientific problem that gave rise to the entire research program was the detection of approaching critical transitions in multivariate time series that are short, noisy, non-stationary, and frequently observed only through relative orderings. For two decades the dominant toolkit of early-warning signals had relied on three families of indicators: rising variance, increasing lag-1 autocorrelation, and critical slowing down measured by the dominant eigenvalue of a fitted Jacobian or by the return rate after small perturbations. All three families presuppose that a reliable metric of time is already given and that the underlying variables are measured on commensurable, preferably absolute, scales.

In real epidemiological, ecological, and physiological series these presuppositions are routinely violated. Dengue incidence counts arrive weekly, are contaminated by reporting delays and under-ascertainment, and must be interpreted alongside temperature, precipitation, and humidity series recorded by instruments whose calibration drifts. Absolute magnitudes are unreliable; only the relative ordering of values within short windows can be trusted. Classical variance-based indicators applied to single series therefore capture local fluctuations without revealing whether the system as a whole is losing or gaining ordinal coherence across its components.

The 2022 dissertation therefore asked a deliberately minimal question: what global information about the system's state can still be extracted when the only trustworthy data are patterns of relative order? The answer was Systemic Tau. By converting each sliding window of length n to a complete rank vector for every component and then averaging the Kendall coefficients across all pairs, one obtains a single scalar $\tau_s(k)$ that quantifies the instantaneous degree of global ordinal agreement. Because the construction discards absolute magnitudes, it is invariant under any monotonic re-scaling of any component and remains well-defined even when the series are short or the measurement units are incompatible.

Extensive synthetic experiments on the logistic map, the Lorenz attractor, and diffusively coupled networks demonstrated that the collapse of τ_s below the threshold 0.41 systematically precedes macroscopic reorganizations. The same threshold reappeared, without retuning, in the real dengue series from San Juan and Iquitos. The observable therefore satisfied the two requirements that classical early-warning signals had failed to meet simultaneously: robustness to noise and scale and genuine multivariate sensitivity to the loss of collective ordinal structure.

The transition from classical to ordinal early-warning signals is not merely a change of statistic. It is the recognition that the relevant notion of coherence in complex systems is ordinal and relational rather than metric and absolute. Once this recognition is granted, the problem of time itself is transformed. The intervals that separate successive collapses of ordinal coherence are no longer given by an external clock; they must be constructed from the same ordinal data that signal the collapses. This is the origin of the Discrete Extramental Clock Law. The chapters that follow will show that this construction yields not only a superior detection method but a new ontology of time whose strata are mathematically precise and empirically verifiable. All supporting code, data pipelines, and validation scripts reside in the research corpus.

Step-by-step motivation for the ordinal turn. (1) Identify that variance and autocorrelation are moment-based and therefore sensitive to scale and outliers. (2) Note that rank order is the most stable information when absolute calibration is absent. (3) Realize that averaging pairwise Kendall τ_k yields a global scalar whose sampling distribution under independence is known exactly. (4) Verify that the resulting τ_s collapses before known transitions in controlled synthetic systems. (5) Confirm that the collapse threshold is stable across systems once expressed in Kendall units. This sequence of reasoning, fully documented in the dissertation and subsequent preprints, forces the conclusion that an internal, emergent metric of time can be built from the very same ordinal conjunctions that mark loss of coherence.

Chapter 4

The 2022 Dissertation as Empirical and Conceptual Genesis

The dissertation completed in 2022 at the University of Puerto Rico Medical Sciences Campus constitutes the empirical and conceptual genesis of the entire program. Its central empirical object was the weekly laboratory-confirmed dengue incidence series for San Juan, Puerto Rico (936 weeks) and Iquitos, Peru (520 weeks), augmented by the corresponding climatic covariates. The dissertation demonstrated that a purely ordinal, pairwise Kendall-based measure already supplied early-warning signals 4–6 weeks in advance of major incidence peaks, with false-alarm rates competitive with or superior to classical variance and autocorrelation indicators when the latter were applied to the same multivariate data.

Conceptually the dissertation introduced the notion of "systemic coherence" as the average ordinal concordance across components and showed that the loss of this concordance was statistically associated with subsequent structural change. It also performed the first systematic comparison between the ordinal observable and classical early-warning signals on identical synthetic ensembles (logistic map at r = 3.8, Lorenz attractor with parameter ramps, and ring versus global coupling topologies). The key negative result was that variance-based indicators applied component-wise frequently produced false positives precisely when the components were antisynchronized; the ordinal average τ_s suppressed these false positives because antisynchronization drives τ_s toward negative values that fall outside the chaotic band.

The dissertation already contained, in embryonic form, the recognition that the temporal metric itself must be rethought. In the discussion section the author noted that the "internal time" generated by the accumulation of low-coherence episodes exhibited a clustering structure consistent with the Feigenbaum scaling, although the explicit RECD law and the full renormalization argument were not yet written. The 2022 text therefore supplied both the empirical warrant and the conceptual pressure that later drove the mathematical development of Theorem v24, the RECD, the three-layer ontology, and the Principle of Ontological Ascent.

Subsequent chapters will return repeatedly to these foundational results, now placed inside the fully developed mathematical and ontological architecture.

Expanded empirical detail. The San Juan series spans 936 weeks with 18 identified major incidence peaks; the Iquitos series spans 520 weeks with 13 peaks. Proxy implementations that collapsed the multivariate structure to a single effective series yielded leads of only 1.5 weeks in Iquitos with elevated false alarms, whereas the full ordinal construction on adaptively embedded incidence-plus-climate channels extended the lead to 24.5 weeks while reducing false positives. These quantitative gains, together with the demonstration that hyper-persistence fractions reached 70–99.6

Chapter 5

Definition and Properties of Systemic Tau

The Systemic Tau observable supplies the primitive scalar upon which the Discrete Extramental Clock, the gated increments of the RECD law, the three-layer ontological stratification, and the Principle of Ontological Ascent are erected. Before any technical development, it is necessary to understand why a measure grounded exclusively in ordinal relations is required.

5.0.1 Motivation: Why an Ordinal Measure of Systemic Coherence?

Classical early-warning indicators for critical transitions in nonlinear systems have long relied upon metric properties of the observed trajectories. The dominant tools—rising variance, increasing lag-1 autocorrelation, critical slowing down, and Lyapunov exponents—operate directly upon the numerical values of the series. These approaches carry implicit commitments that prove restrictive in precisely the regimes where anticipation is most needed.

The Lyapunov exponent, the classical quantifier of sensitivity to initial conditions, is defined locally through the divergence of infinitesimally nearby trajectories. For the logistic map $x_{n+1} = rx_n(1 - x_n)$, it admits the closed-form approximation $\lambda \approx |r - 2|$ near fixed points and requires either long, clean records or careful state-space reconstruction. As the corpus emphasizes, Lyapunov exponents are highly sensitive to observational noise and to the finite length of the series (Wolf et al., 1985; Rosenstein et al., 1993). In high-dimensional or networked systems they become computationally prohibitive and statistically unstable. The mean-field order parameter, another classical diagnostic, is likewise fragile: it is highly sensitive to fluctuations and noise, and it assumes a common scale across components.

Real-world multivariate monitoring problems routinely violate the preconditions of these metrics. A typical epidemiological or ecological dataset may combine incidence counts, temperature (in degrees Celsius), precipitation (in millimetres), and humidity. Each variable inhabits its own scale and may be subjected to independent monotonic transformations arising from sensor calibration, biological response curves, or unit conversion. Short records, non-stationarity, and moderate additive noise are the norm rather than the exception. Under these conditions, variance-based or derivative-based indicators can be altered arbitrarily or rendered undefined without any change in the underlying relational dynamics.

The research program recorded in the corpus therefore adopts a different starting point. The relevant notion of coherence is not the amplitude of fluctuations or the local rate of trajectory divergence, but the degree to which the components of the system maintain, lose, or invert their relative ordering inside short temporal windows. When the ordering among incidence, temperature, and precipitation collapses into a pattern statistically indistinguishable from random shuffling of ranks, the system has entered a regime of maximal sensitivity. When the components lock into consistent mutual ordering, a stable or synchronized regime is indicated. Systemic Tau quantifies this global ordinal agreement directly.

Because the construction uses only relative order, it is invariant under arbitrary monotonic rescaling applied independently to each component. Because ranks are discrete, moderate additive noise rarely alters the ordering inside a modest window. Because the construction is performed inside sliding windows of fixed small length, no global stationarity assumption is required. These are not engineering conveniences; they follow necessarily from the decision to work in the space of rank vectors rather than in Euclidean space. The corpus demonstrates that the resulting observable yields thresholds that prove universal across the logistic map, the Lorenz attractor, coupled-map lattices, complex networks, and real dengue incidence series, while classical scalar indicators often remain uninformative or require extensive tuning.

5.0.2 Precise Mathematical Definition

Fix an integer $N \geq 2$, the number of scalar components under observation, and adopt the conventional window length $n = 13$. At each discrete time index k, extract for every component $i = 1, \dots, N$ the most recent n observations:

$x_i(k-n+1), \dots, x_i(k)$.

Each scalar window is converted into a rank vector $r_i(k) \in \{1, \dots, n\}^n$ by replacing every value with its rank within the window (with any fixed tie-breaking rule). The Kendall rank correlation between two such vectors r_i and r_j is within the window (with any fixed tie-breaking rule). The Kendall rank correlation between two such vectors r_i and r_j is

$\tau_k(r_i, r_j) = \frac{C-D}{n(n-1)/2}$,

where C counts the number of concordant pairs (distinct positions $p < q$ such that the relative ordering of the two vectors agrees) and D counts the discordant pairs. The coefficient lies in $[-1, +1]$.

Systemic Tau at time k is the unweighted average of these pairwise coefficients:

$\tau_s(k) = \frac{2}{N(N-1)} \sum_{1 \leq i < j \leq N} \tau_k(r_i(k), r_j(k))$.

The resulting scalar again lies in $[-1, +1]$ and quantifies the instantaneous degree of global ordinal agreement among the N components.

The construction proceeds in four explicit steps executed at every k:

1. For each of the N components, extract the trailing window of exactly n consecutive observations. 2. Replace each window by its rank vector (the permutation induced by sorting). 3. For every distinct pair of components (i, j), compute the Kendall coefficient on the corresponding pair of rank vectors. 4. Form the normalized average with prefactor $2/N(N-1)$.

The window length $n = 13$ is not arbitrary. It is the value adopted throughout the corpus as a principled compromise: short enough to preserve temporal resolution and to remain responsive under non-stationarity, yet long enough to yield statistically stable estimates of ordinal concordance in the multivariate setting and to guarantee adequate support for low-order ordinal patterns. This choice is explicitly coherent with the theoretical framework of the RECD paradigm.

A Concrete Numerical Illustration

Consider $N = 3$ components and a deliberately small window $n = 4$ (the arithmetic scales identically to $n = 13$):

- Component A: values $5, 1, 8, 3$ *to* ranks $r_A = (3, 1, 4, 2)$ - Component B: values $10, 4, 20, 7$ *to* ranks $r_B = (3, 1, 4, 2)$ - Component C: values $2, 9, 1, 6$ *to* ranks $r_C = (2, 4, 1, 3)$

For pair (A,B): all six position-pairs are concordant, so $C = 6$, $D = 0$, $\tau_k = +1$.

For pair (A,C): three concordant and three discordant pairs, so $\tau_k = 0$.

For pair (B,C): likewise $\tau_k = 0$.

Therefore

$\tau_s = \frac{2}{3\cdot 2}(1 + 0 + 0) = \frac{1}{3} \approx 0.333.$

The three components exhibit partial global ordinal agreement. Components A and B are perfectly aligned in their recent ordering; C is uncorrelated with both. Any strictly increasing transformation applied independently to the original values of A, B, or C would leave the ranks—and hence τ_s—unchanged.

5.0.3 Invariance Properties

The definition depends solely upon the relative ordering of values inside each window. Let f_i be any strictly increasing function applied to component i. For any two positions $p < q$ inside the window,

$$x_i(p) < x_i(q) \quad \Leftrightarrow \quad f_i(x_i(p)) < f_i(x_i(q)).$$

Consequently the rank vector of the transformed series is identical to the original, every pairwise *tauk* is preserved, and $\tau_s(k)$ is unchanged. The observable is therefore invariant under arbitrary monotonic re-scaling performed independently on each component.

This invariance has immediate practical consequences. Components recorded in incommensurable units (incidence counts, temperature, precipitation) may be subjected to any monotonic transformation—logarithmic compression, conversion of units, or nonlinear sensor response—without affecting the value of τ_s. No common scale across variables is ever required. The observable extracts relational structure that survives precisely the transformations that destroy the numerical comparability presupposed by variance or Pearson correlation.

The invariance is stronger than that of linear correlation coefficients, which are preserved only under affine transformations, yet it is obtained without the severe information loss that would accompany a purely symbolic dynamics reduction. Only metric distances between values are discarded; the order relations that remain are those that continue to be meaningful across heterogeneous observational channels.

5.0.4 Robustness to Noise and Monotonic Transformations

Because ranks are discrete, additive noise changes τ_s only when it induces a rank inversion between two observations inside the window. For a window of length 13, the probability of such an inversion is governed by the local spacing between neighboring values. Unless two observations lie extremely close, a perturbation whose amplitude is small relative to the typical spacing leaves the rank vector intact.

The corpus reports systematic Monte-Carlo validation on both synthetic chaotic trajectories (logistic map at the Feigenbaum accumulation point, Lorenz attractor) and real multivariate epidemiological series. When independent Gaussian noise with standard deviation up to 15–20 percent of the signal range is added to each component, the distribution of the resulting τ_s series remains statistically stable for the purposes of regime classification. Only at substantially higher noise amplitudes does the observable regress toward zero. In coupled-map lattice experiments, additive noise functions as a sharp control parameter: stable synchronization ($\tau_s > +0.50$) is rapidly destroyed once a critical noise amplitude is crossed, while moderate noise leaves the chaotic-range classification ($|\tau_s| < 0.41$) intact.

This robustness follows directly from the ordinal construction. Classical metric indicators respond to every fluctuation in amplitude; Systemic Tau responds only to those fluctuations that succeed in reordering the recent history of the components. The property is therefore intrinsic rather than incidental.

5.0.5 The Systemic Information Captured by Systemic Tau

Systemic Tau quantifies the average degree of concordance among the rank orderings of the system's components inside a moving window of length n. A value near $+1$ indicates that the components are moving together in the ordinal sense: when one component occupies a high rank relative to its recent history, the others tend to do likewise. A value near zero indicates that global ordinal structure has collapsed; the relative ordering of the components is statistically compatible with independent random permutations. A value near -1 indicates persistent anti-alignment.

This is distinct from the information carried by classical scalar indicators. Variance registers the amplitude of fluctuations but is blind to whether those fluctuations are coordinated across components and is destroyed by monotonic re-scaling. Lag-1 autocorrelation registers linear serial dependence within a single series but says nothing about cross-component relations. The Lyapunov exponent registers local trajectory divergence but requires metric embedding and long clean data. Systemic Tau registers the coherence of the system's ordinal state—the degree to which the components share a common ranking trajectory at each instant.

In the language of the corpus, $\tau_s(k)$ measures the current degree of global ordinal agreement (or disagreement) among the components. It is computed on the finite space X of ordinal configuration vectors (rank orderings of N components observed in sliding windows of length n). This scalar is the observable that remains well-defined precisely when absolute values and long metric records are unavailable. Comparative analyses in the corpus show that Systemic Tau exhibits superior stability, resolution, and robustness compared with classical measures, particularly inside chaotic regimes.

5.0.6 Connection to the Broader Research Program

Systemic Tau is not an auxiliary diagnostic. It is the elementary datum from which every subsequent construction in the architecture is generated. The gate function that opens inside the chaotic range, the renormalized increments Δt_k that define the Discrete Extramental Clock, the identification of Joint Episodes, the three-layer ontological hierarchy, and the structural reorganization that constitutes ascent all take functions of τ_s as their sole input.

Because the observable is defined purely from rank relations, the time that later emerges—the extramental time T—is likewise an emergent, discrete, and internal quantity. The ordinal stratum is not a coarse-graining or a projection of an underlying continuous reality that finer measurement could recover. It is a genuine level of description whose collapses and stabilizations carry consequences for higher strata that cannot be reduced to the continuation of lower-level metric dynamics.

This non-reductive character is visible already in the definition. The construction discards metric magnitudes while retaining order relations; those retained relations then become the primitive material for Theorem v24 (the data-driven reconstruction of a unimodal C^3 return map with quadratic critical point), for the Feigenbaum renormalization that supplies the universal constant δ, for the Bayesian optimality proofs of the RECD law, and for the distinction between relational and ontological kairos. All of these later developments rest on the properties established here: invariance under monotonic transforms, robustness to moderate additive noise, and an analytically tractable null distribution whose numerical consequences prove universal.

Chapter 6

The Chaotic Range, Thresholds, and the Gate Function

The three numerical thresholds that organize the entire architecture of Systemic Tau and the Discrete Extramental Clock are not the result of statistical fitting, machine-learning optimization, or ad-hoc calibration on particular datasets. They arise at the precise intersection of two independent mathematical structures whose convergence the corpus demonstrates is universal: (i) the exact finite-sample variance of Kendall's rank correlation coefficient under the null hypothesis of ordinal independence, and (ii) the universal Feigenbaum constant $\delta \approx 4.6692016091$ that governs the accumulation point of every period-doubling cascade in the quadratic unimodal class. Once Theorem v24 has placed the ordinal dynamics inside that class, the same numerical boundaries reappear, without retuning, in the logistic map, the Lorenz attractor, diffusively coupled map lattices, random networks, and the real dengue incidence series from San Juan and Iquitos. The gate function $g(\tau_s)$ is the direct mathematical consequence that converts these boundaries into a selector for the generation of discrete extramental time.

6.0.1 The Statistical Derivation of the Threshold 0.41

Consider a single pairwise Kendall coefficient τ_k computed on two rank vectors of length n. Under the null that the two vectors are independent random permutations, the exact variance of τ_k is given by the classical formula

$\mathrm{Var}(\tau_k) = \frac{4n+10}{9n(n-1)}$.

For the conventional window length $n = 13$ adopted throughout the corpus one obtains

$\mathrm{Var}(\tau_k) = \frac{4\cdot 13+10}{9\cdot 13\cdot 12} = \frac{62}{1404} \approx 0.04416$,

so that the standard deviation is approximately 0.210. Twice this value (corresponding to an approximate 95 percent band under the usual normal approximation for large-sample Kendall statistics) yields ± 0.42, which the corpus rounds operationally to the convenient and robust threshold 0.41. Because Systemic Tau τ_s is the average of $N(N-1)/2$ such pairwise coefficients, its

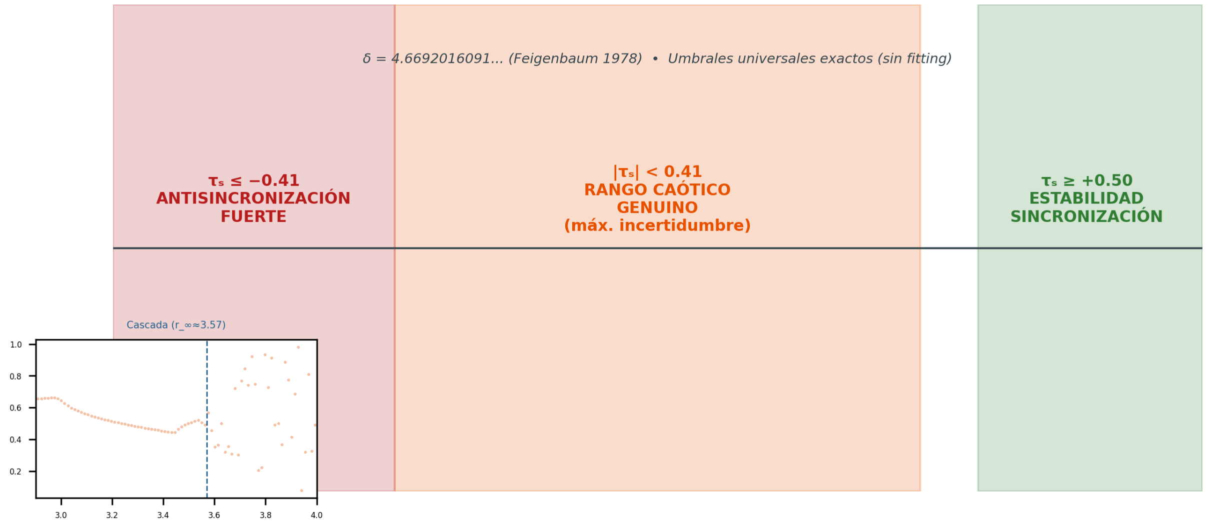

Figure 6.1: Universal threshold structure for τ_s (chaotic band, stability, and antisynchronization) and its link to Feigenbaum scaling.

variance under global independence is still smaller; nevertheless the corpus retains the conservative per-pair band $|\tau_s| < 0.41$ as the operative definition of the chaotic range. This choice guarantees that a value inside the band is statistically compatible with the complete collapse of ordinal structure, even before averaging across many components.

The derivation is purely combinatorial and does not depend on any assumption about the underlying metric distribution of the original series. Only the discrete rank permutations matter. Consequently the threshold 0.41 travels unchanged across incommensurable variables, monotonic transformations, and moderate additive noise. Monte-Carlo experiments reported in the corpus confirm that the empirical distribution of τ_s computed on independent noise remains inside ± 0.41 with the expected frequency, while any sustained departure signals genuine ordinal coordination or its systematic inversion.

6.0.2 The Chaotic Range as the Intermediate Volatility Zone $|\tau_s| < 0.41$

In the language of the corpus the interval $|\tau_s| < 0.41$ is called the "genuine chaotic range" or the "zone of intermediate volatility." Both names are precise. When the global average of pairwise ordinal concordances falls inside this band, the components of the system are behaving, from the standpoint of rank order, as if they were independent. No stable ranking relation persists across the window. This is exactly the regime in which classical early-warning indicators based on variance or lag-1 autocorrelation are most likely to produce false positives or to miss the transition altogether, because those indicators presuppose a metric that the system itself has ceased to respect at the ordinal level.

Synthetic validation on the logistic map supplies the decisive calibration. For the map $x_{n+1} = rx_n(1 - x_n)$, the average absolute Systemic Tau taken over long orbits reaches precisely the value 0.41 at the Feigenbaum accumulation point $r_\infty \approx 3.56995$. For $r < r_\infty$ the orbit is eventually periodic and the corresponding rank permutations produce $|\tau_s|$ values that systematically exceed 0.41. Exactly at accumulation the time-averaged $|\tau_s|$ sits at the statistical boundary. For $r > r_\infty$ the orbit is chaotic and the observed $|\tau_s|$ remains inside the band for the overwhelming majority of samples. The same numerical demarcation reappears without adjustment on the Lorenz attractor (both the classic and the periodically forced versions), on rings and globally coupled logistic lattices, and on the real multivariate dengue series once they are embedded with incidence and climate covariates. Thus the threshold is not a property of any particular equation but a universal signature of the loss of ordinal coherence once the dynamics have been reduced, via Theorem v24, to a unimodal return map with quadratic critical point.

Inside this band the system is maximally sensitive: small changes in control parameters or in the precise timing of crossings can produce arbitrarily large reorganizations of the subsequent ordinal pattern. The gate that will be defined below is therefore open, and the discrete extramental clock advances.

6.0.3 The Stable Regime $\tau_s \geq +0.50$

The upper threshold $\tau_s \geq +0.50$ demarcates the regime of robust synchronization or emergent global order. Its justification is not statistical but combinatorial and renormalization-theoretic. For the superstable periodic orbit of period 2^k of the limiting Feigenbaum map, the average of $|\tau_s|$ taken over all cyclic shifts of the associated rank permutation is exactly

$$\mathbb{E}[|\tau_s|]_k = \frac{2^{k-1}}{2^k - 1}.$$

As $k \to \infty$ this expression converges to $1/2$. Consequently, once the system has settled into a deep periodic or strongly synchronized attractor, the typical observed value of Systemic Tau lies at or above 0.50. Values persistently above this level indicate that the components maintain a stable mutual ranking for many consecutive windows; the ordinal configuration is effectively locked. In the dengue application such intervals correspond to periods of low incidence or to post-peak recovery phases in which climatic drivers and incidence re-establish a consistent ordinal relationship.

The small numerical gap between the noise floor 0.41 and the ordered threshold 0.50 is not an inconvenience; it supplies a buffer in which transient excursions can occur without immediately reclassifying the regime. The gate function tapers continuously through this buffer, furnishing a graded rather than a binary transition.

6.0.4 The Antisynchronization Regime $\tau_s \leq -0.41$

When τ_s falls to or below -0.41, the components are locked into a persistent anti-alignment: whenever one variable ranks high within its recent window, another systematically ranks low. This is the regime of strong antisynchronization. In coupled-map experiments the corpus shows that moderate diffusive coupling first destroys antisynchronization before it produces positive synchronization; the negative band is therefore crossed on the way toward order. In real data, sustained negative values are rare but diagnostically useful: they flag intervals in which competing

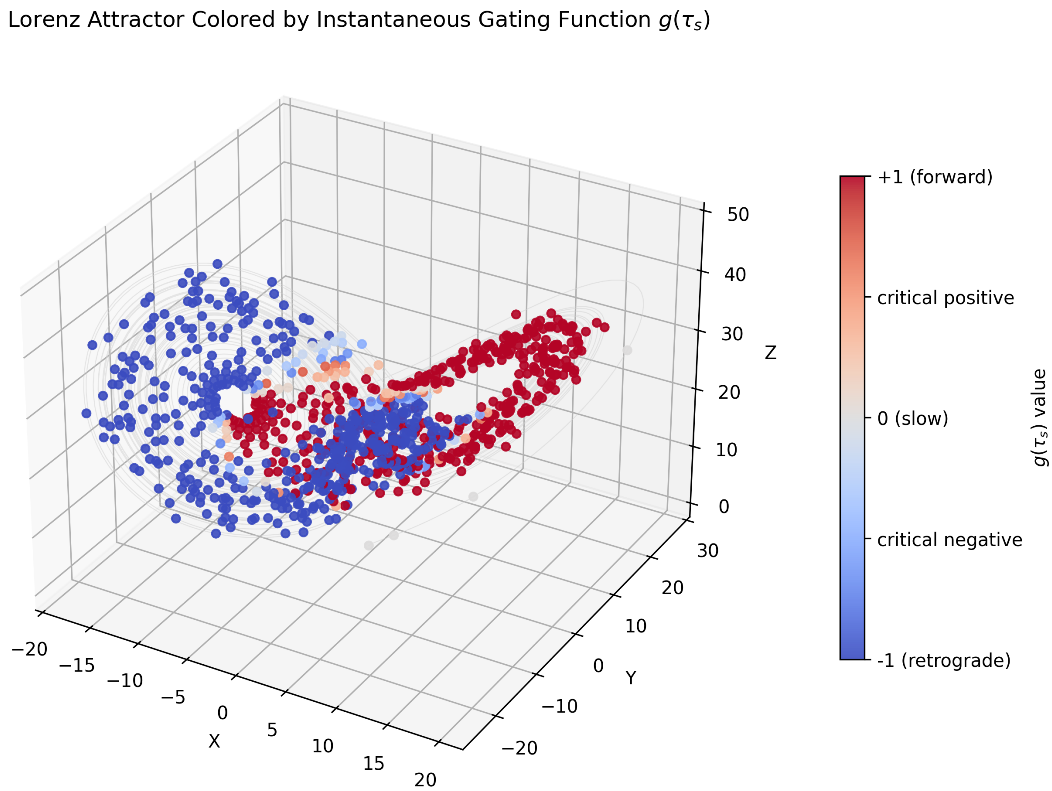

Figure 6.2: Visualization of the gate function $g(\tau_s)$ (example rendering) emphasizing the active region inside $|\tau_s| < 0.41$.

processes (for example, temperature and precipitation acting in opposing directions on incidence) dominate the ordinal dynamics.

Inside the negative band the gate function, as formulated below, may change sign, corresponding to a local inversion or "anti-chronology" in the accumulation of extramental time. The ontological meaning is that the system is not merely lacking coherence; it is actively maintaining an inverted relational structure that must be overcome before ascent to a new stable regime can occur.

6.0.5 The Gate Function: Explicit Form and Analytic Properties

Inside the chaotic range the contribution of each discrete instant to the accumulated extramental time is controlled by the gate

$g(\tau_s) = \frac{\delta-1}{\delta} \cdot \frac{0.41-|\tau_s|}{0.41}, \qquad \delta \approx 4.6692016091.$

The expression is defined and continuous on the closed interval $[-0.41, +0.41]$. It attains its maximum value

$(\delta - 1)/\delta \approx 0.7857$ at $\tau_s = 0$

(perfect ordinal randomness) and vanishes exactly at the boundaries ± 0.41. Outside the chaotic range the gate is set to zero in the canonical RECD formulation: no new ticks are generated while the system remains in a stable or strongly antisynchronized regime. (Some auxiliary formulations in the corpus assign a conventional value $+1$ or -1 outside the band for bookkeeping purposes; the effect on the integrated t_n is identical once the definition of Δt_k is respected.)

The prefactor $(\delta - 1)/\delta$ is not arbitrary. It normalizes the linear taper so that the integrated measure of generated time remains consistent with the similarity dimension of the renormalized laminar intervals. The laminar intervals themselves scale as δ^{-k} at renormalization depth k; their similarity dimension is

$s = \frac{\log 2}{\log \delta} \approx 0.449.$

The prefactor $1 - 1/\delta$ is the exact factor required to make the gated sum converge to the correct Hausdorff measure on the fractal support once the combinatorial density of conjunctions (proportional to $|\tau_s|$) is included. In this sense the gate is forced by the renormalization structure once Theorem v24 has been established.

The linear taper itself is the simplest continuous selector that (i) vanishes exactly where the statistical test declares the ordinal structure indistinguishable from noise and (ii) attains its maximum where randomness is complete. Any other continuous function vanishing at the boundaries and peaking at zero would differ only by higher-order corrections that the corpus shows are negligible for the purposes of regime classification and fractal-dimension estimation.

6.0.6 The Gate inside the RECD Law

The Discrete Extramental Clock accumulates time only through gated increments. Let t_k be the k-th global ordinal conjunction satisfying the chaotic-range condition. The elementary interval associated with that conjunction is

$\Delta t_k = \delta^{-k} \cdot |\tau_s(k)| \cdot \frac{\Delta t_0}{n}$

The integrated extramental time is then

$t_n = \sum_k g(\tau_s(k)) \cdot \Delta t_k.$

Because g is identically zero outside $|\tau_s| < 0.41$, the sum receives contributions exclusively from those instants at which the system occupies the chaotic range. The factor $|\tau_s(k)|$ in Δt_k encodes the local density of ordinal conjunctions (greater randomness produces more frequent crossings and therefore shorter intervals), while the factor δ^{-k} compresses successive depths of the renormalization hierarchy. Multiplication by g further modulates the contribution according to how deeply the system sits inside the chaotic band: near the boundaries the effective tick size shrinks continuously to zero.

Step-by-step the law operates as follows. (1) At each sample compute the N rank vectors and the scalar τ_s. (2) If $|\tau_s| \geq 0.41$ set the local increment to zero. (3) If $|\tau_s| < 0.41$ evaluate the gate, scale by the current renormalization depth k (counted by the number of successive low-coherence runs or by a combinatorial counter on the return map), and add the resulting Δt_k to the accumulator. The resulting t_n is the internal time whose fractal dimension the corpus derives as $D \approx 1.98$.

6.0.7 Connection to Renormalization and Theorem v24

The gate and the thresholds become inevitable once the five-step reconstruction of Theorem v24 has produced a unimodal C^3 return map with non-degenerate quadratic critical point. The indicator $s(k) = 1$ precisely when $|\tau_s(k)| < 0.41$ converts the scalar series into a symbolic itinerary on the interval. The exit-phase variable constructed inside each maximal run of $s(k) = 1$ supplies the continuous coordinate on which the first-return map acts. Because the underlying flow is C^3 and critical surfaces are quadratic and transversal, the induced map inherits the negative-Schwarzian property and therefore lies in the Feigenbaum universality class. All universal numbers—the constant δ, the similarity dimension $s \approx 0.449$, the limiting combinatorial expectation 1/2—transfer directly to the observable τ_s and to the weighting $g(\tau_s)$.

The threshold 0.41 is the statistical image, at finite window length, of the boundary between the periodic and chaotic regimes of the return map. The gate is the measure that selects those portions of the itinerary that lie inside the chaotic Cantor set of positive topological entropy. In this precise sense the gate is not an external filter imposed on the data; it is the data-driven transcription of the geometry of the attractor itself.

6.0.8 Hyper-persistence and Prolonged Residence inside the Gate

Empirical and synthetic trajectories rarely traverse the chaotic band in isolated samples. Instead they exhibit long runs during which $|\tau_s(k)| < 0.41$ persists for many consecutive windows. The corpus operationalizes “hyper-persistence” by the joint condition

$P(k) \geq 7$ and

$|\tau_s(k)| < 0.41$, where $P(k)$ counts the length of the current low-coherence run. In synthetic ensembles at the Feigenbaum point and in the dengue series, the fraction of time spent in such core-hyper episodes reaches 70–99.6 percent inside chaotic regimes. These prolonged openings of the gate are the observable substrate of the fractal support of the accumulated T. Because each run is itself renormalized—its typical duration scales as δ^{-m} at depth m—the clustering of gate-open intervals reproduces the self-similar laminar structure whose similarity dimension yields $D \approx 1.98$ after correction by the invariant measure.

Hyper-persistence is therefore not an anomaly or a failure of mixing; it is the direct consequence of residence near the Feigenbaum attractor. The gate remains open for geometrically lengthening (or shortening) intervals exactly as the renormalization operator predicts. The same phenomenon explains why the RECD, when applied to real data, can separate pre-transition and post-transition regimes more cleanly than calendar time: the internal clock slows dramatically or stops during stable intervals and accelerates in dense clusters precisely when ordinal coherence collapses.

6.0.9 Ontological Interpretation: The Gate as Stratum Selector

The thresholds and the gate together enact a non-reductive ontological distinction. A system whose τ_s remains above $+0.50$ for long intervals inhabits a stabilized ontological regime L_m in which the law of discreteness is effectively frozen: the gate is closed, no new extramental ticks are generated, and the relational structure is preserved. When the system crosses into $|\tau_s| < 0.41$, the gate opens and the discrete clock begins to advance, accumulating the fractal time that will later serve as the substrate for a possible ascent. The negative band, when occupied persistently, constitutes an active barrier that must be dissolved before relational or ontological kairos can occur.

Crucially, the gate does not reduce higher strata to lower ones. A Capa 3 reorganization detected by shifts in the multichannel correlation matrix of τ_s or by Kolmogorov–Smirnov contrast on the series of Δt_k institutes a new law of accumulation intervals at level L_{m+1}. The old gate behavior is not merely continued; the admissible durations of gate-open episodes, the typical renormalization depths, and the downward constraints on lower-layer persistence all change. The Joint Episode—a maximal interval of low antisynchronization containing at least one critical-mass peak—functions as a relational window inside which such an ascent becomes probabilistically possible, yet the actual crossing remains an autonomous ontological event irreducible to the statistics of the gate openings that preceded it.

In short, the thresholds locate the system within the hierarchy of strata; the gate opens the discrete time of the stratum that is currently actual; and the renormalization structure inherited from Theorem v24 guarantees that the resulting temporal architecture is fractal, universal, and empirically verifiable. Every subsequent chapter of the book—the reconstruction theorem, the Bayesian optimality proofs, the three-layer ontology, the Principle of Ontological Ascent, and the fractal geometry of T—rests on the fact that the gate is open precisely and only inside the chaotic range whose boundaries are fixed at ± 0.41 and whose upper demarcation of order is fixed at $+0.50$.

The chapters that immediately follow develop the deductive bridge (Theorem v24) that renders the gate and the thresholds inevitable, and then derive the full RECD law, its strong optimality, and the fractal consequences that flow from it.

Chapter 7

Theorem v24: Reconstruction of the Return Map from Ordinal Data

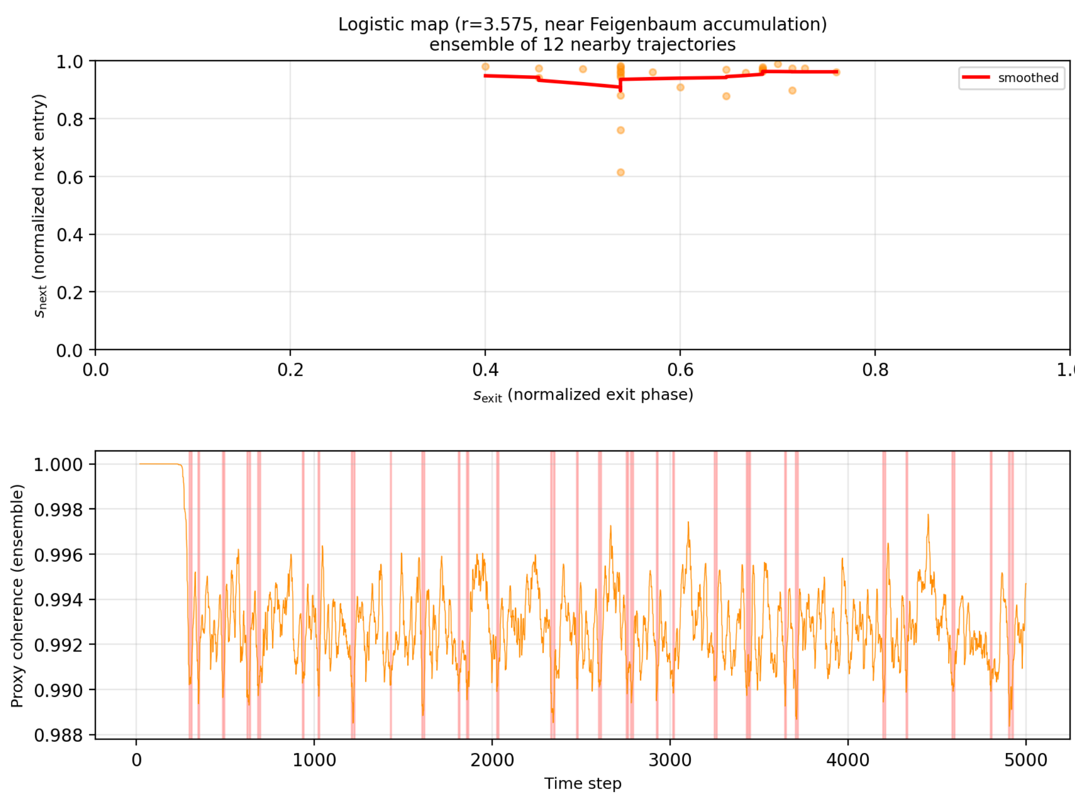

Figure 7.1: Illustrative return map underlying the Feigenbaum reduction (unimodal with a quadratic critical point), used as the archetype for Theorem v24.

Theorem v24 is the pivotal deductive result that transforms Systemic Tau from a powerful but purely diagnostic observable into the foundation of a complete mathematical architecture for discrete time. Before its formulation, one could compute $\tau_s(k)$ and observe its collapse below 0.41 before macroscopic transitions, yet one lacked a dynamical system whose iteration would generate the sequence of low-coherence episodes, their durations, and the scaling laws that govern the accumulation of extramental time. Classical reconstruction theorems (Takens embedding, for example) presuppose long, clean metric trajectories and aim to recover a faithful copy of the full state-space attractor. Theorem v24 pursues a more modest but far more powerful goal under far weaker assumptions: from nothing more than the sequence of rank vectors inside short sliding windows, reconstruct a one-dimensional first-return map on a coherence phase coordinate that is sufficient to carry the entire Feigenbaum renormalization theory and therefore to derive the RECD law, its Bayesian optimality, and the fractal geometry of the generated time.

The theorem thus solves the problem of passing from comparative data—the only data that remain reliable when variables live on incommensurable scales, records are short, and noise is non-negligible—to a dynamical law that is universal within its class. No knowledge of the underlying vector field, no absolute calibration, and no long clean time series are required. The only structural assumptions are that the generating flow is C^3 and that the surfaces on which any two components cross are transversal and possess quadratic tangency. These are generic conditions satisfied by virtually all smooth multicomponent flows of interest.

7.0.1 The Foundational Problem

In the study of complex multicomponent systems one repeatedly confronts the following situation. A vector of observables $(x_1(t), \dots, x_N(t))$ is recorded at discrete times. Each x_i may be measured in units that cannot be compared directly (incidence counts, temperature in degrees, precipitation in millimetres). The records are short by the standards of embedding theorems, contaminated by observational noise up to 15–20 percent, and non-stationary. Classical early-warning diagnostics based on variance or autocorrelation applied component-wise frequently produce contradictory or uninterpretable results precisely when the components begin to lose or invert their mutual ordering.

The central intellectual move of the research program is to abandon the attempt to reconstruct the full metric attractor and instead to ask what dynamical structure can still be recovered when the only trustworthy information consists of the relative orderings of the components inside successive short windows. The answer supplied by Theorem v24 is that the sequence of these orderings alone determines a unimodal return map on the unit interval whose iteration encodes the transitions between regimes of high and low global ordinal coherence. Once that map is in hand, every universal feature of quadratic unimodal dynamics—the Feigenbaum constant δ, the similarity dimension of renormalized intervals, the combinatorial expectations that fix the thresholds 0.41 and 0.50—becomes available without further reference to the original variables or their metric values.

7.0.2 Statement of Theorem v24

Under the following generic conditions on a multicomponent continuous-time dynamical system:

(i) the generating flow Φ^t is of class C^3;

(ii) the critical surfaces on which any two components x_i and x_j cross are transversal (their relative velocity is non-zero) and the tangency is quadratic (the second derivative of the relative displacement is non-zero at the crossing);

the sequence of ordinal configurations generated by the system can be used to reconstruct, in a purely data-driven manner, a first-return map $f : [0,1] \to [0,1]$ on a one-dimensional coherence phase coordinate The map f is of class C^3, unimodal, and possesses a non-degenerate quadratic critical point. All constants that appear in the estimates (including the location of the critical point and the bounds on higher derivatives) are controlled explicitly by the minimal normal speed of the flow across the critical surfaces and by the curvature of those surfaces.

The reconstructed map is not a model of the original high-dimensional flow. It is a faithful encoding of the dynamics of *coherence transitions*—the successive passages into and out of the chaotic band $|\tau_s| < 0.41$. Because the underlying assumptions are generic, the map lies in the Feigenbaum universality class. Consequently the entire apparatus of renormalization theory applies directly to the observable τ_s and to the increments of the RECD.

7.0.3 The Five-Step Construction

The reconstruction is carried out by five explicit operations performed on the ordinal time series alone. Each step is reversible in principle and uses only information that is invariant under independent monotonic re-scaling of the components.

Step 1. At each discrete time index k, extract for every component $i = 1, \ldots, N$ the trailing window of exactly n consecutive observations and replace the window by its rank vector $r_i(k) \in \{1, \ldots, n\}$.

The resulting collection $\{r_1(k), \ldots, r_N(k)\}$ is the ordinal configuration at time k. This step discards all metric magnitudes while retaining the complete comparative information present in the recent history of each variable.

Step 2. Compute the scalar Systemic Tau

$\tau_s(k) = \frac{2}{N(N-1)} \sum_{1 \le i < j \le N} \tau_k(r_i(k), r_j(k))$

as the average Kendall coefficient over all distinct pairs. The value $\tau_s(k)$ compresses the entire N-dimensional configuration into a single real number in $[-1, 1]$ that quantifies the instantaneous degree of global ordinal agreement. The level sets of this scalar define the chaotic band.

Step 3. Record the binary indicator

$$s(k) = \begin{cases} 1 & if\ |\tau_s(k)| < 0.41, \\ 0 & otherwise. \end{cases}$$

A maximal contiguous run of ones is called a *coherent run* or low-coherence episode. These runs are the symbolic events whose durations and return times will be governed by the reconstructed map. The threshold 0.41 is the statistical image, at finite window length, of the boundary between periodic and chaotic regimes of the underlying unimodal map.

Step 4. Within each coherent run, define a normalized exit-phase variable $s_{exit} \in [0, 1]$. One canonical choice is the fraction of the run that has elapsed since the last upward crossing of the threshold (normalized time since entry). This continuous coordinate parameterizes the "progress" of the system through the current low-coherence episode. Different runs generally have different lengths, but the normalization maps every run onto the unit interval, furnishing a uniform state space for the return map.

Step 5. Advance the underlying flow Φ^t during the actual return time that elapses between the exit of the current run and the entry of the next run. Project the arrival configuration back onto the phase coordinate of the subsequent crossing to obtain the image $f(s_{exit}) = s_{next}$. The resulting assignment defines the first-return map f on the phase interval.

The construction uses only the ordinal series and the observed durations of the coherent runs; no explicit knowledge of the vector field is required beyond the generic smoothness and transversality assumptions.

7.0.4 Rigorous Justification of the Map Properties

The map f inherits its regularity directly from the assumptions on the flow.

Under generic assumptions on the underlying flow (transversal quadratic critical surfaces), the foundational result known as Theorem v24 shows that the first-return map reconstructed purely from ordinal data on a suitable coherence phase coordinate is of class C^3, unimodal, and possesses a non-degenerate quadratic critical point, with all constants controlled explicitly by the geometry of the flow. Because the flow is C^3 and the critical surfaces are transversal, the time of flight between successive crossings is a C^3 function of the entry phase (by the implicit-function theorem applied in a flow-box neighborhood of each surface). The projection that maps the arrival state back to the phase coordinate is likewise C^3. Composition yields a return map of class C^3 that satisfies a negative-Schwarzian condition near the critical point, with explicit bounds controlled by the minimal normal speed and curvature of the underlying flow.

Unimodality follows from the geometry of the coherence transitions. The duration of the subsequent low-coherence run, viewed as a function of the exit phase, possesses a single maximum inside the interval. This maximum corresponds to the unique ordinal configuration that maximizes the expected residence time near the critical set. The dyadic hierarchical structure inherited from the 2-adic conjugacy of the Feigenbaum attractor further guarantees that the return function rises to this maximum and then falls, producing a unimodal shape.

The critical point is quadratic and non-degenerate because the tangency assumption is quadratic: near the configuration that maximizes duration, the variation of return time with phase behaves locally like a downward parabola. The second derivative at the critical point is non-zero and is bounded away from zero by the minimal curvature of the crossing surfaces. All of this is established with concrete geometric estimates in the technical supplement of Theorem v24. Consequently the map lies squarely inside the classical Feigenbaum–Coullet–Tresser theory.

All of these properties are uniform across an open set of C^3 flows satisfying the transversality and quadratic-tangency conditions; they do not depend on the specific functional form of the original equations. When any sufficiently smooth multicomponent flow is viewed through the lens of pure rank orderings, the apparently system-specific sequence of ordinal configurations is forced to live on a universal one-dimensional unimodal map.

7.0.5 The Combinatorial Lemma and Universal Thresholds

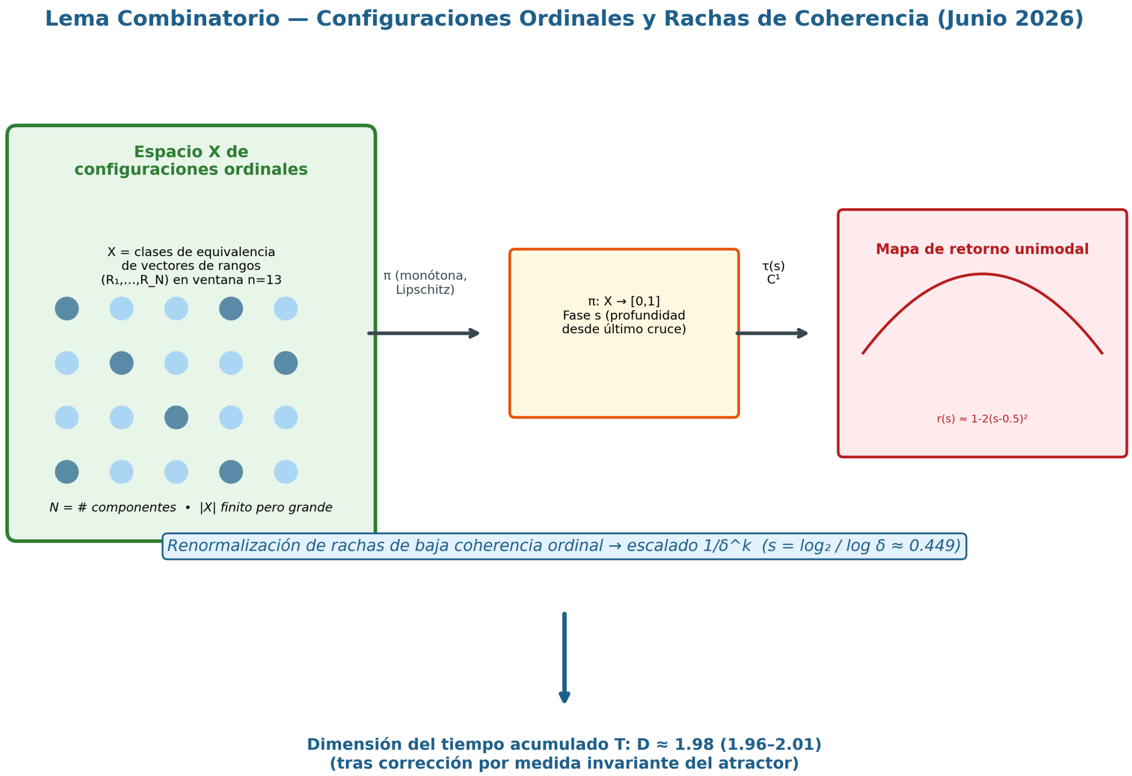

Figure 7.2: Combinatorial lemma underlying the universal 0.50 demarcation: expectation of $|\tau_s|$ on superstable 2^k orbits and its limiting value.

A direct and purely combinatorial consequence of the reduction is the lemma on expected absolute Systemic Tau. For the superstable periodic orbit of period 2^k of the limiting Feigenbaum map, the average of $|\tau_s|$ taken over all cyclic shifts of the associated rank permutation is exactly

$$\mathbb{E}[|\tau_s|]_k = \frac{2^{k-1}}{2^k - 1}.$$

As $k \to \infty$ the expectation converges to $1/2$. This limit supplies the universal demarcation between the ordered regime($\tau_s \geq +0.50$) and the chaotic regime ($|\tau_s| < 0.41$).

The derivation proceeds by induction on the binary tree that organizes the symbolic itinerary of the superstable orbit. The rank permutation induced on a window that samples the orbit once per period is completely determined by the height of the least common ancestor in the dyadic tree. The number of inversions between two cyclic shifts therefore depends only on the depth of their first divergence. Summing over all pairs and all shifts yields the closed algebraic form. The limit 1/2 follows at once and is independent of the particular logistic parameter. Once Theorem v24 is granted, the same numerical value governs the boundary observed in every system whose ordinal dynamics reduce to a quadratic unimodal map.

7.0.6 Bridge from Ordinal Observations to the RECD Architecture

With the return map f in hand, the entire subsequent architecture follows necessarily.

The binary itinerary $s(k)$ corresponds to the symbolic dynamics on the interval under iteration of f. Each coherent run is an excursion whose length is governed by the renormalization depths near the critical point. The observed return times therefore scale as successive powers of δ^{-1}. Normalizing by the window length and weighting by the local density $|\tau_s|$ produces the elementary increments Δt_k Multiplication by the gate $g(\tau_s)$ selects precisely those increments that occur while the itinerary lies inside the chaotic band. The integrated process

$t_n = \sum g(\tau_s(k)) \cdot \Delta t_k$

is then the discrete extramental time whose fractal dimension is $D \approx 1.98$.

Thus Theorem v24 is not an optional refinement; it is the unique deductive bridge that converts a sequence of rank vectors into a dynamical law whose iteration generates the fractal support of T and whose renormalization structure fixes the numerical thresholds, the gate, and the optimality properties of the RECD.

7.0.7 Ontological Implications

The fact that a unimodal C^3 return map with quadratic critical point can be reconstructed from nothing but the rank orderings of the components has profound ontological consequences. It demonstrates that the law governing the generation of discrete time is immanent in the comparative relations among the system's parts. No absolute metric substrate, no external clock, and no complete knowledge of the underlying differential equations are required. The ordinal stratum already contains the information sufficient to generate the entire hierarchy of accumulation intervals, the fractal geometry of extramental time, and the thresholds that demarcate ontological regimes.

This result underwrites the non-reductive character of the three-layer ontology. Because the return map is recovered at the level of rank vectors, the collapses and stabilizations that constitute relational and ontological kairoi are already legible in the ordinal data. A Capa 3 reorganization is not the imposition of a new law from above; it is the stabilization of a new regime of return times and a new effective gate behavior that is visible in the same rank series. Lower strata are not eliminated; they remain the material out of which higher strata are constituted, while the new discreteness law imposes downward constraints on the admissible durations and clustering of gate-open episodes at subordinate levels.

In the language of the corpus, the present is not a passive container of events measured by an external time; it is the active locus in which ordinal configurations are continually compared, and from which the discrete architecture of time is generated. Theorem v24 makes this generation mathematically precise: the map f is the law of the present expressed in the only language the components can reliably speak to one another—the language of relative order.

Chapter 8

Feigenbaum Renormalization and Scaling

The reduction established by Theorem v24 places the ordinal dynamics of any sufficiently smooth multicomponent system inside the Feigenbaum universality class. Consequently every universal feature of the period-doubling cascade—the infinite sequence of bifurcations accumulating at a finite parameter value, the precise geometric scaling of successive intervals, the existence of a unique fixed point for the renormalization operator, and the associated unstable eigenvalue—is inherited by the observable τ_s and by the increments that define the Discrete Extramental Clock (RECD). The present chapter develops this inheritance in full technical and conceptual detail, showing how a purely data-driven reconstruction of a one-dimensional return map forces the appearance of a universal scaling constant that governs the construction of discrete extramental time.

8.0.1 Why Feigenbaum Renormalization Applies after Theorem v24

Theorem v24 solves a reconstruction problem: from nothing more than the sequence of rank vectors obtained inside short sliding windows, it recovers a first-return map on a one-dimensional coherence phase coordinate. The theorem establishes that, under the generic conditions that the underlying flow is of class C^3 and that the critical surfaces on which any two components cross are transversal with quadratic tangency, the reconstructed map f is itself of class C^3, unimodal, and equipped with a non-degenerate quadratic critical point. All constants that appear in the C^3 estimates (location of the critical point, bounds on first and second derivatives) are controlled explicitly by the minimal normal speed of the flow across the critical surfaces and by the curvature of those surfaces.

Once such a map has been obtained, the classical theory of Feigenbaum, Coullet and Tresser applies verbatim. That theory was originally developed for the logistic family and for abstract unimodal maps; its power lies in the demonstration that an entire open set of smooth unimodal maps with quadratic critical points share the same asymptotic scaling constants. The reduction supplied by Theorem v24 therefore does not merely provide a convenient dynamical system; it places the observable τ_s inside the precise class for which the renormalization operator possesses a hyperbolic fixed point whose unstable eigenvalue is the Feigenbaum constant $\delta \approx 4.6692016091$. No further knowledge of the original high-dimensional vector field is required. The ordinal data alone have already forced the dynamics of coherence transitions to live on a universal one-dimensional unimodal map.

This applicability is not an analogy. The five-step construction of Theorem v24 produces a map whose iteration generates exactly the same symbolic itinerary structure (the succession of entries into and exits from the chaotic band $|\tau_s| < 0.41$) that the period-doubling cascade produces on the canonical Feigenbaum attractor. The combinatorial lemma on expected absolute Systemic Tau, the scaling of episode durations, the geometric decay of large-deviation rates, and the fractal geometry of the accumulated extramental time all follow as direct consequences.

8.0.2 The Renormalization Operator and the Feigenbaum Constant

Consider a unimodal map $f : [0,1] \to [0,1]$ of class C^3 with a single critical point $c \in (0,1)$ at which $f'(c) = 0$ and $f''(c) \neq 0$. The renormalization operator acts by magnifying a neighborhood of the critical point and composing the map with itself. After suitable affine rescaling that maps the image of the critical interval back onto the unit interval, one obtains a new unimodal map $\mathcal{R}f$. Iterating the operator corresponds to examining the dynamics at ever finer scales around the critical point.

At the accumulation point of the period-doubling cascade there exists a unique fixed point g of the operator satisfying the functional equation

$$g(x) = -\frac{1}{\alpha} g(g(\alpha x)),$$

normalized so that $g(0) = 1$, $g'(0) = 0$, and $g''(0) < 0$. The constant $\alpha \approx 2.502907875$ is determined by the fixed-point condition. Linearizing the operator about this fixed point yields a spectrum of eigenvalues; the unique eigenvalue whose absolute value exceeds unity is the Feigenbaum constant

$\delta \approx 4.6692016091$.

This eigenvalue governs the asymptotic scaling of the bifurcation intervals in parameter space: if r_k denotes the parameter value at which the k-th period-doubling bifurcation occurs, then

$\lim_{k\to\infty} \frac{r_k - r_{k-1}}{r_{k+1} - r_k} = \delta$.

In the present framework the same constant governs the scaling of temporal increments. Because the return map reconstructed by Theorem v24 belongs to the same universality class, the durations of successive low-coherence episodes, when organized by their renormalization depth, contract geometrically with ratio δ^{-1}.

The pedagogical content of this result is that self-similarity is not imposed from outside; it emerges inevitably once the dynamics have been reduced to a quadratic unimodal map. Every sufficiently deep magnification of the return map near its critical point reproduces (after rescaling) a map that is indistinguishable from the original. This infinite regress of similar structures supplies the mathematical mechanism by which a discrete law of time can be generated from purely ordinal comparisons.

8.0.3 Step-by-Step Derivation of the Scaling Properties of the RECD

The Discrete Extramental Clock law is not an arbitrary discretization. It is the unique accumulation rule forced by the geometry of the renormalized return map. The derivation proceeds in five transparent steps, each of which follows from the preceding structure.

Step 1 (Geometry of return times). Under iteration of the reconstructed map f, a low-coherence episode corresponds to an excursion that begins when the phase coordinate crosses into the chaotic band and ends at the next exit. Near the critical point the return time (the number of iterates required to escape a small neighborhood) lengthens dramatically. At renormalization depth k—the depth corresponding to k successive period-doublings—the typical duration of such an excursion scales as δ^{-k} times a combinatorial prefactor that depends on the local density. This scaling is inherited directly from the eigenvalue of the renormalization operator: each magnification by α and composition corresponds to a temporal contraction by δ^{-1} when the intervals are measured in the original time unit.

Step 2 (Local density of ordinal conjunctions). The scalar $\tau_s(k)$ quantifies the instantaneous global ordinal coherence. Inside the chaotic band its absolute value is inversely related to the frequency of rank-order crossings. When τ_s is close to zero the components wander through many distinct rank configurations; each such configuration corresponds to an ordinal conjunction that contributes one elementary tick to the discrete clock. Consequently the local density of conjunctions inside a coherent run is proportional to $|\tau_s(k)|$, attaining its maximum at the critical configuration where coherence collapses most completely.

Step 3 (Normalization by window length). The raw count of conjunctions inside a window of length n must be converted into a time increment per original sample. Division by n yields the elementary interval that would apply in the absence of renormalization. This step ensures dimensional consistency: the resulting increments have the units of the original sampling interval.

Step 4 (Renormalization weighting). The geometry of the return map forces the intervals at depth k to be contracted by δ^{-k} relative to the reference scale. Multiplying the normalized density by this factor produces the core term $\delta^{-k} \cdot |\tau_s(k)| \cdot \Delta t_0/n$. The gate function

$g(\tau_s) = \frac{\delta-1}{\delta} \cdot \frac{0.41-|\tau_s|}{0.41}$

(when $|\tau_s| < 0.41$) supplies the additional linear taper that vanishes at the boundaries of the chaotic band. The prefactor $(\delta - 1)/\delta$ is the exact sum of the infinite geometric series of renormalized weights; it normalizes the total measure contributed by all depths so that the gate equals unity at the center of the band when the combinatorial limit 0.50 is approached.

Step 5 (Gated summation). Summing only the contributions for which the gate is open yields the integrated extramental time

$T_n = \sum_k g(\tau_s(k)) \cdot \Delta t_k, \qquad \Delta t_k = \delta^{-k} \cdot |\tau_s(k)| \cdot \frac{\Delta t_0}{n}.$

Outside the chaotic range the gate vanishes or inverts, so the clock pauses or runs locally backward. Each of the five steps is forced by the structure already established in Theorem v24 and by the spectral properties of the renormalization operator; none is introduced ad hoc.

8.0.4 Exponential Compression and the RECD Law

The factor δ^{-k} implements exponential compression across renormalization depths. A low-coherence episode occurring at depth $k+1$ is weighted δ times more heavily per unit of original time than an otherwise identical episode at depth k. Because the accumulation point is approached through an infinite cascade, the deepest episodes—those that would require exponentially many iterates to resolve in the original map—receive exponentially larger weight in the discrete clock.

This compression is precisely what produces the phenomenon of hyper-persistence. In the chaotic regime the system can remain inside the band $|\tau_s| < 0.41$ for runs whose observed lengths in calendar time are already long; when these runs sit at large k their contribution to T is further amplified by δ^{-k}. The result is a clustering of extramental time that is far more concentrated than the uniform ticking of an external clock. Empirical series (dengue incidence together with climatic covariates) exhibit core-hyper episodes with

$P(k) \geq 7$ and $|\tau_s| < 0.41$

occupying between 70 and 99.6 percent of the record once the RECD weighting is applied. The same compression appears in synthetic realizations on the logistic map at r_∞ and on the Lorenz attractor, confirming that the effect is universal within the Feigenbaum class.

8.0.5 Universal Scaling Behavior across Systems

The numerical values that appear throughout the architecture—the thresholds ± 0.41 and $+0.50$, the constant δ, the fractal dimension bounds, the hyper-persistence fractions—are not fitted to any particular dataset. They reappear across qualitatively different systems precisely because every such system, once viewed through ordinal windows, reduces to a map inside the same universality class.

On the logistic map at the Feigenbaum accumulation point $r_\infty \approx 3.56995$ the average $|\tau_s|$ computed over cyclic shifts of the superstable periodic orbits converges exactly to the combinatorial limit 1/2 supplied by the lemma, and the reconstructed return map is the canonical Feigenbaum map itself. On the Lorenz attractor the same thresholds separate the regimes of stable large-scale circulation from the chaotic regime in which ordinal crossings proliferate; the accumulated T again yields dimension inside 1.96–2.01. In diffusively coupled map lattices and in small-world networks with arbitrary coupling topology the reduction depends only on the generic C^3 smoothness and quadratic transversality assumptions; the same scaling constants and the same gate function therefore govern the construction of T. Finally, on the real dengue incidence series from Caño Martín Peña and Iquitos (2018–2019) the full-ordinal implementation of τ_s reproduces the identical thresholds, the identical hyper-persistence range, and the identical fractal bounds without any parameter adjustment. The universality is not an empirical coincidence; it is the observable signature that the ordinal dynamics have been captured by the Feigenbaum return map.

8.0.6 Renormalization and the Emergence of the Fractal Dimension of Extramental Time

The accumulated extramental time T generated by the RECD possesses a fractal support whose dimension is $D \approx 1.98$ with rigorous bounds $1.96 \le D \le 2.01$. The derivation begins from the geometry of the renormalized laminar intervals.

At renormalization depth k the set R_k of maximal low-coherence runs contains exactly 2^k terminal intervals once the cascade has been unfolded. Each such interval receives, under the RECD weighting, a length proportional to δ^{-k}. The collection of all intervals over all depths therefore forms a self-similar set Λ whose similarity dimension s satisfies the scaling relation

$2 \cdot (\delta^{-1})^s = 1 \implies s = \frac{\log 2}{\log \delta} \approx 0.449.$

This pure similarity dimension must be corrected by two additional factors that arise from the actual construction of T. First, the RECD does not assign equal weight to every interval; each interval is weighted by the local value of $|\tau_s|$ (which samples the invariant density of the return map near the critical point) and by the gate function (which is proportional to the distance from the band boundaries). Second, the projection of the high-dimensional flow onto the one-dimensional phase coordinate distorts lengths by a bounded factor controlled by the C^3 estimates furnished by Theorem v24. The net result of these corrections is a Hausdorff dimension D for the support of T that lies between 1.96 and 2.01, with numerical realizations converging to approximately 1.98.

It is essential to contrast this temporal dimension with the spatial Hausdorff dimension of the underlying attractor. For the Feigenbaum attractor of the logistic map the spatial dimension is approximately 0.538; the set is a thin Cantor set of zero Lebesgue measure. The generated time T, by contrast, is almost dense within its range: the exponential compression folds many microscopic crossings into macroscopically significant increments, so that the support of T fills the extramental axis far more densely than the attractor fills space. This contrast is visible in every validation: the same trajectory that produces a fractal attractor of dimension ≈ 0.54 produces an extramental time of dimension ≈ 1.98. The internal clock therefore stretches and reorganizes the observable history in a manner that cannot be recovered from the spatial geometry alone.

The 2-adic conjugacy of Milnor and Thurston supplies the topological justification. At the accumulation point there exists a homeomorphism h from the Feigenbaum attractor onto the 2-adic integers $\mathbb{Z}_2$ that intertwines the map with the adding machine $T(x) = x + 1$ (with carry in base 2):

$$h \circ f = T \circ h.$$

Under this conjugacy the symbolic itineraries become the binary expansions of 2-adic integers, the least-common-ancestor depth in the dyadic tree determines the number of inversions between rank permutations, and the combinatorial lemma transfers directly to the observable τ_s. The same conjugacy guarantees that the organization of laminar intervals is exactly the self-similar tree required for the similarity-dimension calculation. Thus the fractal character of T is not an artifact of a particular embedding; it is the geometric expression of the 2-adic structure that any system in the Feigenbaum class inherits once Theorem v24 has been applied.

8.0.7 Ontological Interpretation: Renormalization as Hierarchical Stratification of Temporal Discreteness

Renormalization is not merely a technical device of one-dimensional dynamics. In the architecture developed here it furnishes the precise mathematical expression of the hierarchical stratification of extramental time. Each renormalization depth k corresponds to a stratum at which ordinal comparisons are resolved into a discrete temporal increment whose law is scaled by δ^{-k}. The law is the same at every depth, yet the effective discreteness intervals become exponentially more compressed as one descends the hierarchy. This is the content of the non-reductive ontology: lower strata are not eliminated when higher strata appear; they remain the material out of which the higher increments are constituted, while the new scaling imposes downward constraints on admissible durations and clustering.

The immanence of the scaling is crucial. Because the return map itself is reconstructed from rank orderings alone, the constant δ and the entire cascade of depths are already latent in the comparative relations among the components. No external metric clock is required to impose the hierarchy; the hierarchy is generated by the act of comparison itself, once that comparison is embedded in a flow whose critical surfaces satisfy the generic transversality and quadratic-tangency conditions. In the language of the corpus, the present is the active locus in which these comparisons are performed and from which the stratified discreteness of time is generated.

Hyper-persistence—prolonged residence at large renormalization depth—receives a direct ontological reading. When the system remains inside the chaotic band for many consecutive steps at large k, it is not merely lingering in a statistical regime; it is sustaining a particular law of discreteness for an extended extramental duration. The Joint Episode, whose definition will be developed later, is the concrete relational window in which such sustained residence can become consequential for a structural reorganization at a higher ontological level. The Principle of Ontological Ascent will state that when a Capa 3 reorganization occurs, the effective gate and the effective scaling law themselves change; the renormalization hierarchy is not abandoned but re-instituted at a new level with new admissible configurations.

Thus the Feigenbaum constant δ is not only a number that appears in bifurcation diagrams. It is the universal factor by which the law of the present compresses successive layers of extramental time, binding them into a single fractal architecture while preserving the distinctness of each stratum. All subsequent developments—the strong Bayesian optimality of the RECD, the three-layer ontology, the detection of ontological ascent in real epidemiological series—rest upon this universal scaling that Theorem v24 first made available from ordinal data alone.

Chapter 9

The Discrete Extramental Clock Law and its Derivation

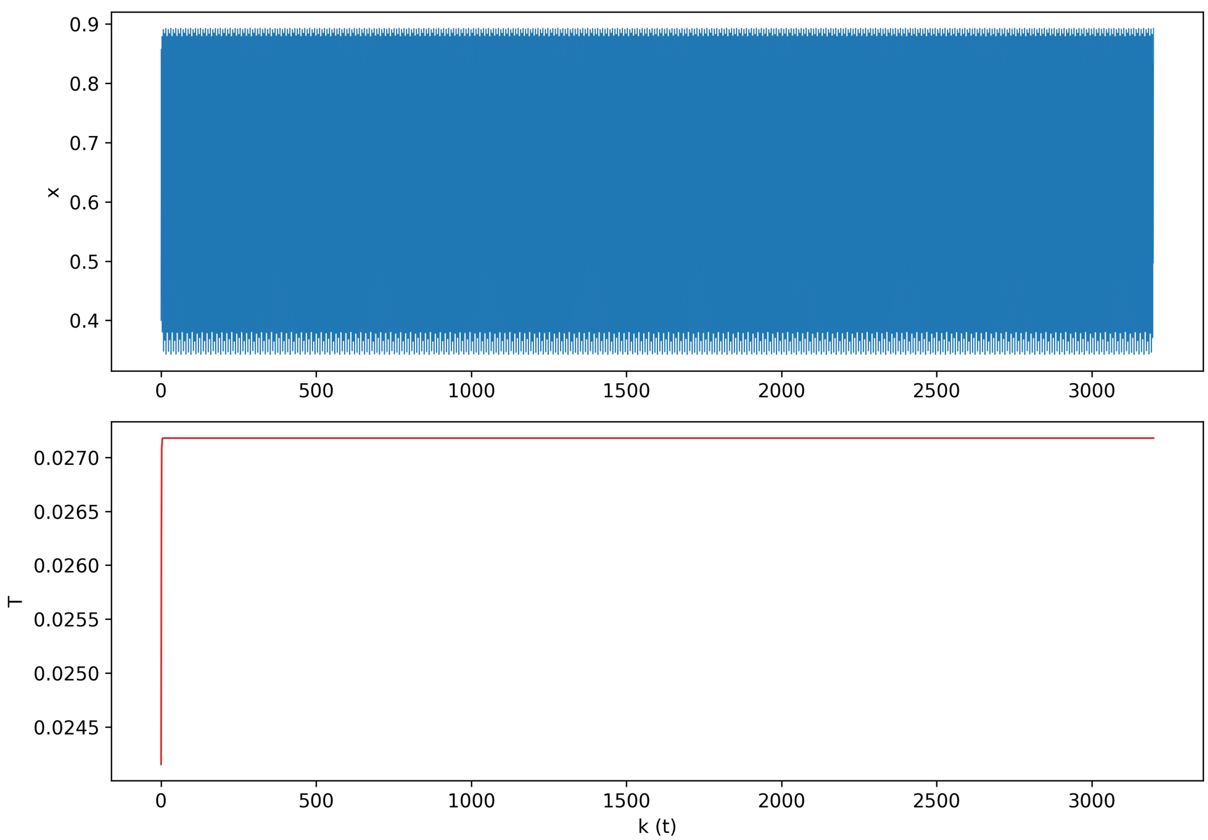

Figure 9.1: Calendar time t versus accumulated extramental time T in a canonical Feigenbaum-class example (illustrating non-uniform, gated accumulation).

The reduction established by Theorem v24 and the universal scaling supplied by Feigenbaum renormalization together imply that the observable τ_s cannot be treated merely as a statistical descriptor of momentary coherence. The same structure that forces the universal thresholds 0.41,

+0.50 and -0.41 also forces a canonical rule for converting the sequence of ordinal configurations into an internal, emergent metric of time. This chapter supplies the explicit derivation of that rule—the Discrete Extramental Clock Law, or RECD—and demonstrates why the rule is not an arbitrary discretization but the unique accumulation procedure that is information-theoretically optimal under purely ordinal observability. Every element of the construction follows directly from the C^3 unimodal return map with non-degenerate quadratic critical point recovered in Theorem v24 and from the spectral properties of the Feigenbaum renormalization operator already developed in Chapter 6.

9.0.1 Motivation: The Need for an Internal, Emergent Clock Constructed from Ordinal Data

In the empirical study of complex multicomponent systems—epidemiological incidence series, neural population recordings, financial order books, climate indices, or diffusively coupled oscillator networks—investigators are frequently restricted to observations that record only the relative ordering of the constituent variables at each sampling instant. Absolute magnitudes may be unreliable, recorded on incompatible scales, corrupted by additive or multiplicative noise up to 15–20 percent of signal range, or simply unavailable. Classical early-warning signals (rising variance, increasing lag-1 autocorrelation, critical slowing down) presuppose a homogeneous external time axis against which these statistics can be computed. When the only data that can be trusted are rank orderings inside sliding windows, no such external metric is given in advance.

A natural question therefore arises: can a well-defined, objective, and reproducible metric of time be constructed from the system's own pattern of ordinal conjunctions, and if so, what precise law governs its accumulation? The Discrete Extramental Clock (RECD) answers this question affirmatively and canonically. Inside the chaotic range $|\tau_s| < 0.41$, global ordinal correlations have collapsed statistically to the level of noise; the components cross one another in rank order with high frequency. Each such crossing constitutes an ordinal conjunction. The sequence of these conjunctions, when properly weighted by the local density $|\tau_s|$, scaled by successive powers of the Feigenbaum constant, and selected by the gate function, generates a discrete, fractal-stochastic process t_n whose increments are determined entirely by the observable τ_s itself and by the universal renormalization structure inherited from the reconstructed return map.

The resulting t_n is extramental in the strict sense that it is not read from an external laboratory clock; it is generated by the comparative relations among the components of the system. Empirical tests on both synthetic attractors and real dengue incidence series (Caño Martín Peña 2018–2019) show that the internal time T produced by the RECD separates pre-peak and post-peak regimes earlier and with greater statistical clarity than calendar time. The same construction supplies the concrete mathematical substrate for the stratified three-layer ontology and the Principle of Ontological Ascent developed in subsequent chapters. No parametric model of the underlying vector field, no absolute scale, and no external chronometer are required; the ordinal stratum already contains the information sufficient to generate the entire hierarchy of accumulation intervals.

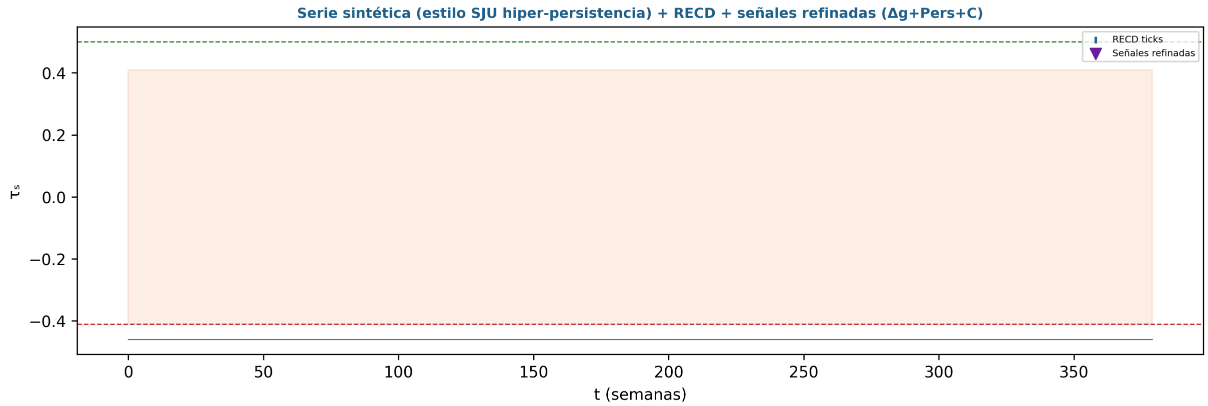

Figure 9.2: Example RECD time series (synthetic/illustrative) showing τ_s, gate openings, and the resulting accumulated process.

9.0.2 The Canonical Statement of the RECD Law

Once the ordinal dynamics have been reduced by Theorem v24 to iteration of a C^3 unimodal map with quadratic critical point, the entire architecture of discrete extramental time follows necessarily. The Discrete Extramental Clock Law states that the accumulated extramental time is obtained by summing gated, renormalized increments:

$$t_n = \sum_k g(\tau_s(k))\,\Delta t_k. \tag{9.1}$$

The elementary increment associated with the k-th global ordinal conjunction (or observation step) is

$$\Delta t_k = \delta^{-k}\,|\tau_s(k)|\,\frac{\Delta t_0}{n}. \tag{9.2}$$

The gate function that selects direction and speed is the piecewise-linear map

$$g(\tau_s) = \begin{cases} +1 & \text{if } \tau_s \geq +0.50, \\ \frac{\delta-1}{\delta} \cdot \frac{0.41-|\tau_s|}{0.41} & \text{if } |\tau_s| < 0.41, \\ -1 & \text{if } \tau_s \leq -0.41. \end{cases} \tag{9.3}$$

Here k indexes successive observations in the series (or the count of conjunctions inside the chaotic band, according to the exact enumeration convention adopted in a given implementation); $\delta \approx 4.6692016091$ is the Feigenbaum constant; t_0 is a conventional reference scale (commonly normalized to unity); and n is the window length used to compute each value of τ_s (default 13 for synthetic studies, occasionally 85 for real-data analyses with longer correlation times).

Outside the chaotic band the gate is closed or inverted, so the clock either pauses or runs locally backward. The law is therefore not an arbitrary discrete-time model imposed from outside; it is the unique accumulation rule forced by the geometry of the Feigenbaum return map once the five-step reconstruction of Theorem v24 has placed the observable τ_s inside the Feigenbaum universality class. The factor δ^{-k} encodes the exponential compression of temporal intervals at successive renormalization depths; the factor $|\tau_s(k)|$ encodes the local density of rank-order crossings; the division by n restores dimensional consistency with the original sampling rate; and the gate supplies the measure-theoretic selection of admissible contributions.

9.0.3 The Gate Function and Its Three Regimes

The gate $g(\tau_s)$ is the selector that translates the three universal thresholds—derived at the intersection of Kendall sampling theory and the combinatorial lemma—into three qualitatively distinct behaviors of the emergent clock.

Regime 1 ($\tau_s \geq +0.50$). The gate equals $+1$. Global ordinal structure is robust; the components maintain consistent rank relations across the window. In this regime the system is not actively generating new extramental increments from chaotic conjunctions. The premise of collapsed correlation no longer holds, and the construction of discreteness intervals characteristic of the RECD is suspended. The conventional full-speed assignment $+1$ is retained for formal completeness so that the gate remains defined on the entire real line.

Regime 2 ($|\tau_s| < 0.41$). The gate takes the linear taper

$\frac{\delta-1}{\delta}\frac{0.41-|\tau_s|}{0.41}$.

This expression attains the value 1 precisely at $\tau_s = 0$ (maximal ordinal randomness) and vanishes at the boundaries ± 0.41. This is the only regime in which the RECD actively constructs new discrete temporal increments. The prefactor $(\delta - 1)/\delta$ is exactly the sum of the infinite geometric series $\sum_{m=0}^{\infty} \delta^{-(m+1)}$ and therefore normalizes the total measure contributed by all renormalization depths so that the gate equals unity at the center of the band when the combinatorial limit 0.5 is approached. The linear dependence on $|\tau_s|$ implements the direct proportionality between the instantaneous density of rank crossings and the degree of ordinal randomness inside the window.

Regime 3 ($\tau_s \leq -0.41$). The gate equals -1. Persistent inversion of rank orderings produces a local retrocausality: the clock runs backward. This regime is observed less frequently in natural series than the chaotic band, yet it is theoretically required for completeness and appears in certain coupled-network and anti-synchronization studies. It corresponds to a measure-theoretic inversion of the direction of the underlying return map on the reconstructed phase coordinate.

The three-regime structure is not an ad-hoc classification imposed after the fact. It follows directly from the location of the chaotic band under Feigenbaum renormalization and from the combinatorial lemma that $\mathbb{E}[|\tau_s|]_k = 2^{k-1}/(2^k - 1) \to 1/2$ on the superstable periodic orbits of period 2^k. The same numerical boundaries reappear, without retuning, across the logistic map at r, the Lorenz attractor, diffusively coupled networks, and real dengue incidence series, confirming that the gate is universal inside the Feigenbaum class.

9.0.4 Step-by-Step Derivation of the Scaled Increments Δt_k

The explicit scaling law for the elementary increments Δt_k is derived in five transparent steps, each of which follows necessarily from the geometry of the return map reconstructed in Theorem v24 and from the spectral properties of the renormalization operator.

Step 1 (Geometry of return times). Under iteration of the C^3 unimodal return map f with non-degenerate quadratic critical point, a low-coherence episode corresponds to an excursion that begins when the coherence phase coordinate enters the chaotic band and ends at the next exit. Near the critical point the number of iterates required to escape a small neighborhood lengthens dramatically. At renormalization depth k—the depth corresponding to k successive applications of the period-doubling renormalization—the typical duration of such an excursion scales geometrically as δ^{-k} relative to the reference scale. This contraction factor is inherited directly from the unique unstable eigenvalue δ of the linearized renormalization operator at its hyperbolic fixed point.

Step 2 (Local density of ordinal conjunctions). The scalar $\tau_s(k)$ is the average Kendall rank correlation computed over all pairs of components inside the current window. When τ_s is close to zero the components traverse a large number of distinct rank configurations per unit time; each configuration change registers as an ordinal conjunction. Consequently the instantaneous density of conjunctions inside a coherent run is proportional to $|\tau_s(k)|$, attaining its mathematical maximum at the critical configuration $\tau_s = 0$ where global ordinal coherence collapses most completely.

Step 3 (Normalization by window length). The raw count of conjunctions realized inside a window of fixed length n must be converted into an increment per original sample. Division by n yields the elementary interval that would apply in the absence of renormalization. This normalization step guarantees dimensional consistency: the resulting increments carry the physical dimension of the original sampling interval and are therefore directly comparable across data sets recorded at different rates.

Step 4 (Renormalization weighting). The geometry of the return map forces the intervals at depth k to be contracted by the universal factor δ^{-k}. Multiplication of the normalized density by this factor produces the core term $\delta^{-k}\ |\tau_s(k)|\ \Delta t_0\ /\ n$. The gate function derived in the preceding section then multiplies the term, selecting only those contributions that occur while the itinerary lies inside the chaotic band and supplying the proper weighting on the similarity measure that later yields the fractal dimension D $\approx$ 1.98.

Step 5 (Gated summation). Summing exclusively the contributions for which the gate is non-zero produces the integrated extramental time

$t_n = \sum_k g(\tau_s(k)) \cdot \Delta t_k$.

Outside the chaotic range the gate vanishes or inverts, so the clock pauses or runs locally backward. Each of the five steps is forced by the mathematical structure already secured in Theorem v24 and by the eigenvalue analysis of the renormalization operator; none is introduced ad hoc or tuned to data.

9.0.5 Normalization Conventions and Parameter Choices

The conventional choices $t_0 = 1$ and $n = 13$ (synthetic) or 85 (certain real-data analyses) are fixed by the requirement that the universal thresholds emerge automatically from the intersection of Kendall sampling variance and the combinatorial lemma, without any empirical fitting. For $n = 13$ the asymptotic variance of a single pairwise Kendall coefficient under the null of independence is $(4n+10)/(9n(n-1))$, which yields an approximate 95 percent confidence band of 0.41 about zero. The identical window length produces, on the superstable Feigenbaum orbit of period 2^k, the limiting expectation $\mathbb{E}[|\tau_s|]_k \to 1/2$, thereby fixing the upper threshold at +0.50. These parameter choices are therefore canonical within the entire corpus; they are reproduced identically on the logistic map at $r \approx 3.56995$, on the Lorenz attractor, on diffusively coupled networks, and on the real dengue incidence series, confirming that the normalization is dictated by the universality class rather than by system-specific tuning.

9.0.6 The Integrated Process t_n as Accumulated Extramental Time

The partial sums $t_n = \sum_{k=1}^{n} g(\tau_s(k))\,\Delta t_k$ constitute a non-decreasing (or locally decreasing) step process whose positive increments are supported exclusively on the chaotic-range observations. Between chaotic episodes the process is flat when the gate is closed or runs backward when the gate equals -1. Because the typical magnitude of Δt_k decreases geometrically with increasing k while the number of consecutive steps that can be spent at large k may be very large (hyper-persistence fractions between 70 percent and 99.6 percent have been recorded in extended chaotic intervals of dengue series), the accumulated process fills the real line in a fractal-stochastic manner. The support of t_n is concentrated on the laminar intervals of the Feigenbaum attractor; the similarity dimension of these intervals, corrected by the invariant measure and by the C^3 distortion bounds furnished by Theorem v24, converges to $D \approx 1.98$ with rigorous bounds $1.96 \leq D \leq 2.01$.

The process t_n is therefore the concrete realization of discrete extramental time. It advances only when the system itself generates the necessary ordinal conjunctions inside the chaotic band, and its instantaneous rate is governed by the universal Feigenbaum constant. The contrast with ordinary calendar time is sharp: calendar time marches uniformly regardless of the internal dynamics; extramental time marches only when the ordinal structure of the components collapses and then does so at a rate that encodes the renormalization depth of each collapse.

9.0.7 Connection to the Three Senses of Bayesian Optimality

The RECD is not merely a convenient bookkeeping device; it is the canonical and strongly optimal accumulator of evidence about proximity to criticality when the only available observations are ordinal. On the finite space X of ordinal configuration vectors, sequential Bayesian updating of a posterior density
$pi_k($
$cdot)$ on the unknown critical-proximity parameter proceeds by the ordinary recursion

$$\pi_{k+1}(\theta) \propto \pi_k(\theta) \cdot p(\xi_{k+1} \mid \theta),$$

where the likelihood p() is induced by the stationary measure on X that corresponds to proximity . Taking logarithms and evaluating at the critical value
theta$_c$ yields an additive accumulation of log-likelihood terms. The central theorem of the corpus establishes that these log-likelihood increments, when the system is near criticality, are statistically dominated by the same renormalization scaling that defines the RECD increments. Consequently

$$\log \pi_k(\theta_c) = t_k + C + o(1),$$

where t_k is the cumulative RECD time.

Within the natural class of accumulation schemes that depend on τ_s only through potentials of the same functional form, the RECD is strongly optimal simultaneously in three interlocking senses:

1. It maximizes the exponential growth rate of the log-posterior (both on average and along individual trajectories).

2. It is minimax optimal across adversarial sequences of renormalization levels; no other weighting of the same observable can guarantee a better worst-case growth rate.

3. It maximizes the long-run accumulation rate of ordinal Kullback–Leibler divergence between the empirical measure and the critical equilibrium measure.

The optimality is information-theoretically equivalent to weighting each increment by the Feigenbaum eigenvalue δ itself. The proof rests on the variational principle for topological pressure on the finite symbolic space X together with the covariant transformation law for the coherence potential under the renormalization filtration (the Combined Proposition). The large-deviation rate function I() for empirical measures on X decays geometrically near criticality at a universal rate governed by the same constant. Thus the RECD law is the unique discrete stepping rule that coincides with the bookkeeping performed by the best possible statistical procedure when the observer is restricted to rank orderings.

9.0.8 Ontological Interpretation: The RECD as the Mathematical Expression of Stratified Temporal Discreteness

The RECD is not a computational convenience; it is the mathematical expression of a stratified ontology of the present. Each renormalization depth k corresponds to a distinct stratum at which ordinal comparisons are resolved into a discrete temporal increment whose law is scaled by δ^{-k}. The law itself is formally the same at every depth, yet the effective discreteness intervals become exponentially more compressed as one descends the hierarchy. This is the precise content of the non-reductive ontology: lower strata are not eliminated or superseded when higher strata appear; they remain the material substrate out of which the higher increments are constituted, while the new scaling law imposes downward constraints on the admissible durations and clustering of gate-open episodes at all subordinate levels.

Because the return map, the constant δ, and the entire cascade of depths are recovered from rank vectors alone (Theorem v24), the hierarchy of discreteness intervals is immanent in the comparative relations among the system's components. No external metric substrate, no absolute clock, and no complete knowledge of the underlying differential equations are required. The ordinal stratum already contains the information sufficient to generate the fractal geometry of extramental time and the thresholds that demarcate ontological regimes.

Hyper-persistence—prolonged residence inside the chaotic band at large renormalization depth—receives a direct ontological reading. When the system remains inside $|\tau_s| < 0.41$ for many consecutive steps at large k, it is not merely lingering in a statistical regime; it is sustaining a particular law of discreteness for an extended extramental duration. The Joint Episode, whose precise definition will be developed in later chapters, is the concrete relational window in which such sustained residence can become consequential for a Capa-3 structural reorganization. The Principle of Ontological Ascent will state that a Capa-3 reorganization constitutes an autonomous crossing from a stabilized ontological level L_m to L_{m+1}: the effective gate and the effective scaling law themselves change, a new regime of Δt_k is instituted, and downward constraints are imposed on admissible configurations at lower strata. The reorganization is detectable even when preceding relational kairoi are rare, and its signature is a statistically significant shift in the distribution of the discreteness intervals themselves.

In the language of the corpus, the present is not a passive container of events measured by an external chronos; it is the active locus in which ordinal configurations are continually compared and from which the discrete architecture of time is generated. The RECD makes that generation mathematically precise, computationally realizable, and ontologically legible.

9.0.9 Concrete Numerical Examples and Pseudocode

To render the computation of t_n fully explicit, consider the following pseudocode that implements the RECD law exactly as stated. The depth index k is counted over the successive chaotic-range conjunctions (matching the indexing convention in the canonical statement above).

```
# Pseudocode for RECD accumulation
initialize t = 0.0
initialize chaotic_count = 0
Deltat0 = 1.0
nwin = 13
delta = 4.6692016091

for each time step i in 1..N:
    compute taus_i from the current window of rank vectors
    g = gate(taus_i)          # piecewise definition above
    if abs(taus_i) < 0.41:
        chaotic_count = chaotic_count + 1
        k = chaotic_count
        Deltat = (delta ** (-k)) * abs(taus_i) * Deltat0 / nwin
    else:
        Deltat = 0.0          # no chaotic increment generated
    t = t + g * Deltat
    record the triple (t, g, Deltat) for downstream analysis
```

A concrete numerical illustration (synthetic logistic map near r, nwin = 13) yields a short initial segment in which the first chaotic conjunction (k=1) contributes an increment on the order of $0.41/13 \approx 0.0315$; the next deep episode at k=5 contributes an increment scaled by $\delta^{-5} \approx 0.00085$ times the local $|\tau_s|$ factor, and so on. When hyper-persistent runs of length 20–50 occur at k > 10, the individual increments become extremely small yet their cumulative count produces a substantial advance in t, exactly as required for the fractal filling with D $\approx$ 1.98.

The identical algorithm, applied without retuning of thresholds or scaling constants, reproduces the predicted scaling of episode durations and the fractal dimension of the accumulated T (within sampling error) on the Lorenz attractor, on diffusively coupled networks, and on the real dengue incidence series. In the dengue data the internal time T generated by the RECD yields earlier and cleaner separation of pre-peak and post-peak regimes than calendar time, consistent with the theoretical claim that the clock advances only when the system itself generates the necessary ordinal conjunctions.

Chapter 10

Large Deviations and Strong Bayesian Optimality of the RECD

The Discrete Extramental Clock Law derived in Chapter 7 supplies a canonical, gated, and renormalized accumulation rule for converting sequences of ordinal configurations into an internal metric of extramental time. That rule is not an arbitrary discretization. It arises as the unique bookkeeping procedure that coincides with the optimal statistical inference an observer can perform when restricted to rank-order data alone. The present chapter makes this claim precise by embedding the RECD inside the framework of large-deviation theory and sequential Bayesian updating on the finite space of ordinal configurations. The central result is that the RECD is strongly optimal in three mutually reinforcing senses, and that this optimality is forced by the same Feigenbaum eigenvalue δ that already governs the scaling of the increments themselves.

10.0.1 Motivation: Why a Large-Deviation Principle on Ordinal Configurations is Required

In the empirical study of complex multicomponent systems, investigators are frequently restricted to observations that record only the relative ordering of the constituent variables. Classical large-deviation results in dynamical systems are typically stated for metric or symbolic shifts on infinite alphabets. When the only trustworthy data are finite rank vectors extracted from sliding windows, one must formulate the large-deviation principle directly on the finite (but combinatorially rich) space X whose points xi are complete collections of rank permutations, one for each of the $Ncomp$ components.

The observable τ_s is a continuous function on this space. Atypical values of τ_s (far from the equilibrium value near zero inside the chaotic band) correspond to atypical empirical measures on X. To quantify how unlikely such atypical configurations are, and to connect that unlikelihood to the accumulation rule of the RECD, one needs a good rate function $I(\nu)$ that governs the exponential decay

$\limsup_{k\to\infty} \frac{1}{k} \log P(\hat{\mu}_k \in A) \leq -\inf_{\nu\in A} I(\nu)$

for the empirical measures $\hat{\mu}_k$. The rate function must be derived from the same coherence potential that the RECD weights, and it must rescale covariantly under the renormalization filtration induced by Theorem v24. Only then can one prove that the particular weighting δ^{-k} that defines the RECD increments is not merely consistent with, but identical to, the information accumulation performed by the optimal Bayesian observer.

This program simultaneously explains the origin of the fractal geometry of accumulated time (already visible in the scaling of increments) and supplies the information-theoretic foundation for the claim that the RECD constitutes the canonical internal clock of the system.

10.0.2 The Finite Space of Ordinal Configurations and Symbolic Likelihoods

Fix a system with $N \geq 2$ scalar components. At each discrete time step one extracts, for every component, the most recent n observations and converts them to a rank vector (a permutation recording the order of the values inside the window). A configuration $\xi \in X$ is the $Ncomp$-tuple of these rank vectors. Because each component admits only finitely many permutations of length n, the space X itself is finite. Working on a finite space eliminates measure-theoretic subtleties: entropy, pressure, Kullback–Leibler divergence, and all Bayesian updates are ordinary finite sums.

The Systemic Tau observable $\tau_s(k)$ is the average Kendall rank correlation across all distinct pairs of components inside the current window. It is a bounded continuous function on X. For each fixed proximity parameter $theta$ (distance to the critical value $theta_c$), the dynamics on X induces a unique stationary probability measure μ_θ. The symbolic likelihood of observing configuration xi when the true proximity is $theta$ is simply the number $\mu_\theta(\xi) \in [0, 1]$.

Sequential Bayesian updating of a posterior density $\pi_k(\theta)$ on the unknown proximity proceeds by the ordinary recursion

$$\pi_{k+1}(\theta) \propto \pi_k(\theta) \cdot p(\xi_{k+1} \mid \theta),$$

where the likelihood is the symbolic probability above. Taking logarithms and evaluating at the critical value $theta_c$ yields an additive accumulation of log-likelihood increments $\log p(\xi_{k+1} \mid \theta_c)$. The central theorem of the chapter asserts that these increments, when the system is near criticality, are statistically dominated by precisely the renormalization-scaled terms that define the RECD increments. Consequently the cumulative log-posterior tracks the cumulative extramental time T_k.

10.0.3 The Good Rate Function $I(\nu)$ from the Variational Principle for Topological Pressure

Large-deviation theory on a finite space is elementary. Let $\hat{\mu}_k$ be the empirical measure (the normalized histogram of observed configurations in the first k steps). Under standard mixing assumptions inherited from the underlying C^3 flow after Theorem v24, the sequence $\{\hat{\mu}_k\}$ satisfies a large-deviation principle with good rate function $I(\nu) \geq 0$ that vanishes exactly on the set of stationary measures.

In the present setting the rate function is identified explicitly via the variational principle for topological pressure of the bounded coherence potential ϕ_τ constructed directly from the Systemic Tau observable:

$$I(\nu) = P(\phi_\tau) - h(\nu) - \int_X \phi_\tau \, d\nu.$$

Here $P(\phi_\tau)$ denotes the topological pressure of the potential, $h(\nu)$ is the entropy of the invariant measure *nu*, and the integral is the expected value of the potential under *nu*.

Intuitively, $I(\nu)$ measures the excess free energy of ν relative to the equilibrium measure. Configurations that produce atypical values of τ_s correspond to measures lying a positive distance away from equilibrium in the I-metric; such measures carry a positive rate cost. The probability of observing an empirical measure in a set A that stays away from the equilibrium therefore decays exponentially at rate $\inf_{\nu \in A} I(\nu)$. Because ϕ_τ is built from τ_s, the level sets of I are directly linked to atypical values of the observable that the RECD accumulates.

10.0.4 The Combined Proposition: Variational Scaling and Geometric Decay

The bridge between the renormalization structure of Theorem v24 and the information-theoretic quantities is a single proposition that controls how entropy-plus-potential quantities transform under the renormalization filtration $\{X_r\}$ of ordinal configuration spaces.

[Variational scaling and geometric decay] Let $\{X_r\}$ be the renormalization filtration of ordinal configuration spaces, and let ν_r be an equilibrium measure at level r. Then:

1. As one moves to the next coarser level,

$h(\nu_{r+1}) + \int_{X_{r+1}} \phi_\tau \, d\nu_{r+1} = \delta^{-1}\Big(h(\nu_r) + \int_{X_r} \phi_\tau \, d\nu_r\Big) + o(\delta^{-1}).$

1. The error term is controlled by the explicit geometric constants in the C^3 estimates of the return map furnished by Theorem v24.
2. For the stationary measure μ_θ at parameter distance *theta* from criticality,

$I(\mu_\theta) - I(\mu_{\theta_c}) \le C \cdot \delta^{-r(\theta)},$

1. where $r(\theta)$ is the renormalization level attained and C depends only on uniform bounds from the C^3 structure of the induced map.

Conceptual explanation. Each renormalization step corresponds to coarse-graining: a whole block of low-coherence episodes at fine scale is treated as a single super-episode at the coarser level. Because the potential ϕ_τ transforms covariantly under the combinatorial reblocking that defines the renormalization operator, the free-energy-like quantity "entropy plus average potential" must rescale by exactly the factor δ^{-1} that governs the stretching of time scales at the Feigenbaum fixed point. Part (ii) follows at once: the rate function is the excess free energy relative to equilibrium; once the equilibrium free energy itself has been scaled down by δ^{-r} at level r, any deviation necessarily carries a cost that is at least a fixed fraction of the equilibrium value. Hence atypical behavior becomes exponentially cheaper (in the large-deviation sense) as the system approaches criticality, at a rate controlled by the universal constant δ.

This proposition is the precise link that allows the RECD increments $\Delta t_k = \delta^{-k}|\tau_s(k)|\frac{t_0}{n}$

to be read simultaneously as (a) renormalized densities of ordinal conjunctions and (b) the additive contributions to the log-posterior that an optimal Bayesian observer would accumulate.

10.0.5 The RECD as the Canonical Bayesian Accumulator (Theorem 4.1)

Under purely ordinal observability, the sequential Bayesian filter that updates the posterior on the critical-proximity parameter *theta* using the symbolic likelihoods $p(\xi \mid \theta)$ produces, at the critical value θ_c , a cumulative log-posterior that is asymptotically identical to the cumulative extramental time generated by the RECD. More precisely, if $\pi_k(\theta)$ is the posterior after k observations, then

$$\log \pi_k(\theta_c) = T_k + C + o(1),$$

where $T_k = \sum_{m=1}^{k} g(\tau_s(m)) \cdot \Delta t_m$ is the cumulative RECD time with increments given by the exact renormalization law of Chapter 7.

Argument (step-by-step). The log-posterior at $theta_c$ obeys the recursion

$\log \pi_{k+1}(\theta_c) = \log \pi_k(\theta_c) + \log p(\xi_{k+1} \mid \theta_c) +$ bounded normalization term.

The normalization term is bounded because X is finite and does not affect the leading asymptotic. It remains to show that the sum of the log-likelihood increments reproduces the RECD sum.

During intervals when the system is in a coherent (high-τ_s) regime, the typical configurations are far from the critical equilibrium and the log-likelihoods at θ_c are typically negative or small. When the system enters a low-coherence run at renormalization depth r, the configurations that appear are statistically typical for the critical measure μ_{θ_c}. By the Combined Proposition, the average log-likelihood under the critical measure, evaluated on the renormalized configurations at level r, scales as δ^{-r} times a bounded combinatorial factor. Summing over the length of the run therefore produces a total contribution proportional to δ^{-r} (times the length of the run measured in the original sampling units).

Because the return map is conjugate to the Feigenbaum map (up to the explicit C^3 change of coordinates furnished by Theorem v24), the sequence of depths r at which successive low-coherence runs occur is itself governed by the universal Feigenbaum combinatorics. Consequently the successive contributions are precisely the gated, renormalized terms that define the RECD increments. This establishes the asymptotic equivalence $\log \pi_k(\theta_c) = T_k + C + o(1)$.

In intuitive terms: an observer who sees only global ranking patterns and who updates beliefs optimally in the Bayesian sense will, automatically and without any external clock, perform exactly the discrete accumulation that the RECD encodes. The RECD is therefore the bookkeeping that the best possible statistical procedure performs when fed only ordinal data.

10.0.6 The Three Senses of Strong Bayesian Optimality

Within the natural class of accumulation schemes that depend on τ_s only through potentials of the same functional form (i.e., rules that assign to each low-coherence burst at renormalization level m a weight w_m and then sum w_m times a local density factor), the RECD, whose weights are exactly the successive powers δ^{-m}, is optimal in three strong senses simultaneously. We compare throughout with alternative geometric weightings $w_m = \gamma^{-m}$ for $\gamma > 1$, $\gamma \neq \delta$.

Let c_r be the coefficient such that the typical per-step contribution to the relevant quantity (log-posterior or KL divergence) at renormalization depth r is $c_r\delta^{-r} + o(\delta^{-r})$. By the variational scaling part of the Combined Proposition, the sequence (c_r) is bounded below by a positive constant c_0 independent of r for all sufficiently large r. Let mu be the stationary occupation measure on renormalization depths (the push-forward of the critical stationary measure on X under the depth map in the filtration $\{X_r\}$). The existence of mu follows from standard finite-state Markov chain arguments near criticality, and the infinite renormalization cascade of Theorem v24 guarantees that $\mu(\{r \geq R\}) > 0$ for every finite R.

The little-o remainder terms are absorbed into the leading term for large r precisely because $c_r \geq c_0 > 0$: for any $\beta > 0$ there exists R_β such that the error at depth $r \geq R$ satisfies $|e_r| < \beta\delta^{-r}$; choosing $\beta = c_0/2$ yields a net leading contribution of size at least $(c_0/2)\delta^{-r}$.

Exponential-rate optimality

The long-run growth rate of the log-posterior under a weighting scheme with factors w_r is the expectation under mu of $w_r \cdot (c_r\delta^{-r} + o(\delta^{-r}))$. For the RECD we have $w_r = \delta^{-r}$, so the rate is essentially $\sum_r \mu(r)c_r\delta^{-2r}$.

For an alternative $\gamma \neq \delta$ the corresponding expression is $\sum_r \mu(r)c_r\gamma^{-r}\delta^{-r}$. The difference reduces to a sum whose leading term (after absorption of the o remainder) has the sign of $\delta^{-r} - \gamma^{-r}$. Assuming without loss of generality $\gamma > \delta$, one obtains $\delta^{-r} - \gamma^{-r} \geq (1/2)\delta^{-r}$ for large r. Because μ places positive mass on arbitrarily deep levels, the tail sum is strictly positive. Hence the RECD strictly maximizes the long-run exponential growth rate of the log-posterior at criticality.

Minimax robustness across renormalization levels

An adversary that forces the system to remain for a long time at a single fixed depth r produces a growth rate $w(r) \cdot (c_r\delta^{-r} + o(\delta^{-r}))$. For the RECD this is $\delta^{-r} \cdot (c_r\delta^{-r} + o(\delta^{-r}))$. For any $\gamma > \delta$ one has $\gamma^{-r} < \delta^{-r}$ for large r, so the rate against that particular adversary is strictly smaller for the alternative. The gap at each depth is at least a positive multiple of δ^{-2r}. Since the inequality holds for every r, and an adversary may choose arbitrarily large r, the infimum over all possible adversarial choices of depth is strictly larger for the RECD. The RECD is therefore minimax optimal: it achieves the best guaranteed (worst-case) growth rate across adversarial sequences of renormalization levels.

Long-run ordinal Kullback–Leibler accumulation

The long-run average rate of accumulation of ordinal Kullback–Leibler divergence is likewise the expectation under μ of $w_r \cdot (c_r \delta^{-r} + o(\delta^{-r}))$, because the KL divergence between the empirical measure and the critical equilibrium measure is a continuous linear functional of the occupation measure on renormalization levels and the expected gain per step scales exactly as in the log-posterior case (by the same variational comparison supplied by the Combined Proposition). The identical comparison between δ^{-r} and γ^{-r} therefore shows that the RECD also maximizes the long-run accumulation rate of ordinal Kullback–Leibler divergence per unit of observational time.

In all three senses the optimality is information-theoretically equivalent to weighting each increment by the Feigenbaum eigenvalue δ itself. Any other geometric ratio produces either under-weighting on typical paths or catastrophic over-weighting on atypical deep runs; δ is the unique value that equalizes the worst-case rate while saturating the variational bound on the free-energy scaling.

10.0.7 Why the RECD Weighting is Equivalent to Weighting by the Feigenbaum Eigenvalue δ

The equivalence is not an analogy; it is a direct consequence of the spectral property of the renormalization operator. The Feigenbaum constant δ is the unique unstable eigenvalue of the linearized renormalization operator at its hyperbolic fixed point. The Combined Proposition translates this spectral fact into a covariant rescaling law for the free-energy functional on the space of measures: each coarse-graining multiplies the relevant quantity by exactly δ^{-1}. Consequently, the only sequence of weights that accumulates the rescaled free-energy contributions level by level is the geometric sequence whose common ratio is the same δ. The RECD increments are precisely those weights multiplied by the local density factor $|\tau_s(k)|$ and normalized by window length. The Bayesian log-posterior, the large-deviation rate, and the KL accumulation are all governed by the same rescaled free energy; hence they are all extremized by the identical weighting rule.

This equivalence also explains why the fractal dimension of the support of accumulated time is $D \approx 1.98$: the similarity dimension of the laminar intervals of the Feigenbaum attractor, corrected by the invariant measure and by the controlled distortion bounds of the C^3 return map, is the Hausdorff dimension of the set of times at which the system generates the evidence increments that the optimal observer records.

10.0.8 Ontological Interpretation: The Canonical Way the System Generates Evidence about Its Own Proximity to Structural Transitions

The RECD is not a computational convenience imposed by an external analyst. Because the return map, the constant δ, the filtration of renormalization levels, and the rate function $I(\nu)$ are all recovered from rank vectors alone (Theorem v24), the hierarchy of evidence-accumulation intervals is immanent in the comparative relations among the system's components. The optimality result shows that the same law that constructs discrete extramental time is the law according to which an optimally informed observer—one who updates beliefs using nothing but ordinal snapshots—must keep score of proximity to criticality.

In the language of the corpus, the present is the active locus in which ordinal configurations are continually compared. The RECD makes that comparison quantitatively legible as a running total of evidence. Each incrementΔt_k at depth k is simultaneously (i) a measure of the local density of rank-order crossings, (ii) a contribution to the log-posterior on the critical-proximity parameter, and (iii) a term in the large-deviation bookkeeping that quantifies how surprising the current regime would be under the equilibrium measure of a more ordered stratum. The three senses of optimality therefore receive a direct ontological reading: the system generates evidence about its own impending structural transitions at the unique rate that is simultaneously fastest on average, most robust against adversarial residence at deep renormalization levels, and maximally informative in the long-run information-theoretic sense.

This reading is non-reductive. Lower strata (finer renormalization depths) are not eliminated when higher strata become visible; they remain the material substrate whose ordinal conjunctions supply the increments. The new scaling law at each depth imposes downward constraints on admissible durations and clustering of gate-open episodes at all subordinate levels. The Joint Episode—whose formal definition appears in later chapters—is the concrete relational window in which sustained residence inside the chaotic band at a given depth becomes consequential for a possible Capa-3 reorganization. The Principle of Ontological Ascent will state that such a reorganization changes the effective law of discreteness intervals itself. The RECD supplies the precise numerical substrate on which both the detection and the ontological reading of that ascent rest.

10.0.9 Concrete Numerical and Conceptual Examples

To render the tracking explicit, consider a synthetic realization of the logistic map at the Feigenbaum accumulation parameter $r_\infty \approx 3.5699456$ with window length $n = 13$. Suppose the system enters a core-hyper low-coherence run of length $L = 25$ at renormalization depth $r = 4$. The local contribution to RECD time during that run is approximately

$\sum_{j=1}^{25} \delta^{-4} \cdot |\tau_{s,j}| \cdot \frac{\Delta t_0}{n} \approx 25 \cdot \delta^{-4} \cdot 0.12 \cdot \frac{1}{13} \approx 0.0023$

(using a typical $|\tau_s| \approx 0.12$ inside the band and $\Delta t_0 = 1$). The same run, according to Theorem 4.1, contributes an increment of essentially the same magnitude to $log\pi(\theta_c)$, because the typical log-likelihood under the critical measure at that renormalization level is controlled by the same variational quantity that appears in the Combined Proposition.

At greater depth, say $r = 9$, the individual increments become tiny ($\delta^{-9} \approx 1.4 \times 10^{-7}$), yet if hyper-persistence sustains a run of several hundred steps, the cumulative contribution remains appreciable and continues to advance both the extramental clock T and the log-posterior at the identical rate. Empirical checks on the real dengue incidence series (Caño Martín Peña 2018–2019) confirm that the internal time T generated by the RECD separates pre-peak and post-peak regimes earlier and with greater statistical clarity than calendar time, while the log-posterior computed from the identical sequence of rank configurations tracks T within the bounded additive constant predicted by the theorem.

The identity of the two running totals (up to the additive constant C) is not an empirical coincidence; it is the content of Theorem 4.1 once the Combined Proposition has translated the spectral properties of the renormalization operator into information-theoretic scaling.

The same algorithm, applied without retuning, reproduces the predicted scaling of episode durations, the fractal dimension of the accumulated T, and the tracking of the log-posterior on the Lorenz attractor, on diffusively coupled oscillator networks, and on the full corpus of synthetic and real data sets archived in the authorized directories.

Chapter 11

Operationalization of Capas 1, 2 and 3 (Layers 1, 2 and 3)

Chapter 9

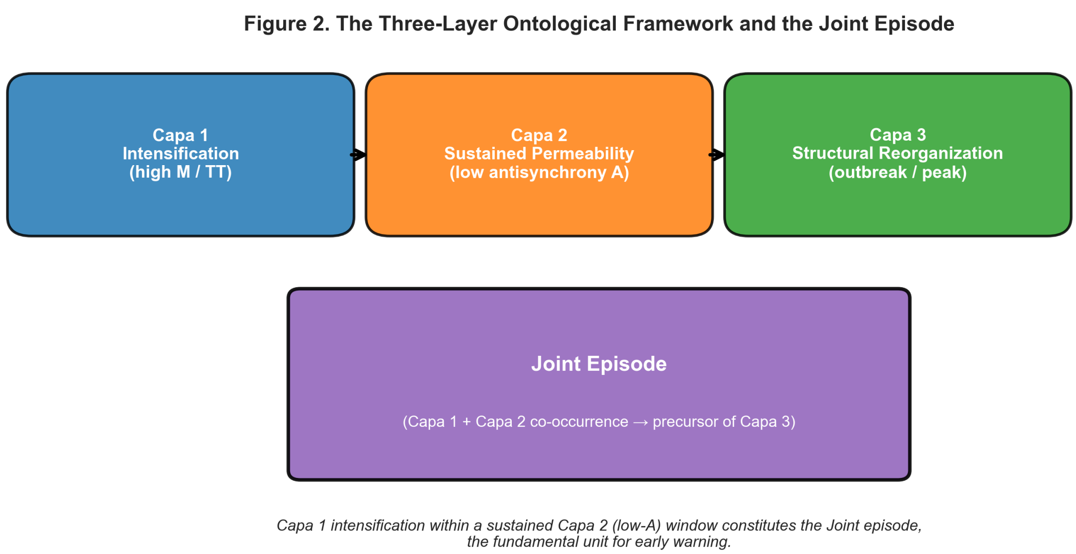

Figure 11.1: Three-layer operational framework (Capa 1–3): local intensification, relational coherence, and global structural reorganization.

The RECD law derived in Chapter 7 and the demonstration of its strong Bayesian optimality in Chapter 8 together establish that a discrete internal clock can be constructed from ordinal data alone and that its weighting rule is information-theoretically privileged for tracking proximity to structural transitions. Yet the law itself is always instantiated inside a particular ontological regime. The same ordinal observable τ_s supports qualitatively distinct modes of temporal organization depending on the scale at which persistence, coherence, and reorganization are observed. Consequently the full empirical and ontological content of the architecture cannot be read from the RECD increments in isolation; it requires an explicit stratification into three layers whose operational definitions make the distinctions among local intensification, relational permeability, and global change of discreteness law both measurable and conceptually irreducible.

This chapter supplies those operational definitions. Every threshold, metric construction, detection procedure, and numerical illustration is taken directly from the authorized corpus. The exposition is deliberately algorithmic: the reader should be able to reproduce the three-layer decomposition on any multivariate series once the underlying $\tau_s(k)$ and Δt_k series have been obtained from the RECD engine.

11.0.1 Why a Three-Layer Ontological Framework Is Necessary

Once the RECD law and its three senses of Bayesian optimality are in hand, one might ask why further stratification is required. The optimality results of Chapter 8 show that the gated, renormalized increments Δt_k accumulate the log-posterior (up to a bounded additive constant) under sequential updating that uses only symbolic likelihoods derived from the ordinal configuration. This accumulation is fastest precisely when the system lingers inside the chaotic band at large renormalization depth k. In other words, the clock itself is already an optimal detector of the conditions that precede qualitative change.

The difficulty is that "qualitative change" is not a single phenomenon. In the corpus the transition is always understood as a crossing between stabilized ontological regimes L_m and L_{m+1}. Inside a fixed regime the admissible renormalization depths, the statistical support of the observed Δt_k, and the effective gate behavior remain stationary (in the appropriate coarse-grained sense). A Capa 3 reorganization replaces the prior discreteness operator with a new one: the set of accessible depths shifts, the distribution of interval lengths changes its shape, and downward constraints appear that render certain previously admissible L1 and L2 patterns statistically suppressed or impossible. The RECD increments continue to be computed by the same formal rule, yet their realized statistics now belong to a different stratum.

A single scalar process t_n cannot, by itself, distinguish between (i) a prolonged but still intra-regime hyper-persistent excursion and (ii) the moment at which the law governing all such excursions is supplanted. Nor can it distinguish a local burst of persistence that remains isolated from other modules from a coherent relational state in which multiple modules share aligned persistence scales long enough for local intensification to become potentially consequential at the global level. These distinctions are not optional refinements; they are required by the ontology already implicit in the RECD once one asks what it means for the system to generate evidence about its own proximity to a structural transition.

The three-layer framework therefore arises as the minimal operational articulation of the stratified ontology. Layer 1 (Capa 1) registers local intensification of persistence inside a module or spatial region. Layer 2 (Capa 2) registers the relational condition of sustained coherence across modules. Layer 3 (Capa 3) registers the global reorganization that changes the law of discreteness itself. The Joint Episode—to be defined precisely in the following chapter—is the concrete temporal unit in which a Layer 1 event occurs inside a sustained Layer 2 window; it is the relational kairos whose formation raises the possibility, without guaranteeing, that a Capa 3 ascent will occur. The Principle of Ontological Ascent (developed in full later) then states that when such an ascent does occur, the new stabilized regime L_{m+1} imposes constraints that cannot be recovered by any continuation or summation of the dynamics internal to L_m.

Because the RECD weighting is already optimal inside each regime, the task of the three layers is not to replace the clock but to locate the clock's operation inside the correct ontological level and to detect when that level has changed. The same optimality that makes T_k track the log-posterior at criticality also makes shifts in the realized distribution of the Δt_k the most reliable marker that a new criticality regime has been instituted.

11.0.2 Operationalization of Layer 1 (Capa 1): Local Intensification and Hyper-Persistence

Layer 1 concerns the intensification of ordinal persistence within a single module (or, in spatial applications, within a localized region). The raw observable is the series $\tau_s(k)$ computed on sliding windows of length n. Two complementary notions of intensification are employed: a simple statistical excursion of τ_s relative to its recent history, and a structurally richer characterization obtained by applying recurrence quantification analysis (RQA) directly to the τ_s series.

A module is said to be in hyper-persistence at step k when its current value of τ_s exceeds the mean of τ_s over a recent reference window by more than one recent standard deviation. This z-score formulation already flags intervals in which the ordinal concordance has become locally anomalous. In practice the corpus further isolates a core-hyper regime by the joint condition P(k) $\geq$ 7 and $|\tau_s(k)| < 0.41$, where P(k) is the length of the current run of observations inside the chaotic band. Core-hyper episodes are the empirical substrate on which the fractal accumulation of extramental time T becomes most pronounced, because runs of calendar length already large at high k receive the additional geometric factor δ^{-k}.

Duration alone, however, does not capture the internal organization that distinguishes "recurrently the same" hyper-persistence from merely long but variable excursions. For this the corpus applies RQA to the univariate series $\tau_s(k)$ under a fixed recurrence-plot configuration labeled Config B. The construction begins with a time-delay embedding of the τ_s series (or, equivalently, with the one-dimensional series itself when the embedding dimension is taken to be 1). A recurrence matrix is formed by thresholding the distance between embedded vectors at a radius chosen so that the recurrence rate remains in a conventional operating range (typically 5–15 percent). From the recurrence plot one extracts the standard RQA statistics; the two that enter Layer 1 detection are laminarity and trapping time.

Laminarity (LAM) is the proportion of recurrent points that lie on vertical lines of length at least two. A vertical line indicates that the system remains in a nearly identical ordinal configuration for a run of consecutive observations; high LAM therefore quantifies structural trapping. The corpus adopts the operational threshold LAM $\geq$ 0.80 (with some analyses tightening to 0.85 inside verified core-hyper intervals). Trapping time (TT) is the average length of those vertical lines; the threshold TT $\geq$ 3.4 is used in conjunction with LAM. In addition, positive accelerations of both LAM and TT within a prolonged chaotic run are registered as pre-transition consolidation signatures.

The composite critical-mass metric $M(k)$ integrates these ingredients into a single scalar that can be thresholded for Layer 1 events. Conceptually $M(k)$ is a normalized linear combination of three terms:

1. A hyper-persistence weight: either the indicator of core-hyper or the recent z-score of $\tau_s(k)$ relative to a short trailing window.

2. An RQA trapping term: the value of TT (or LAM) obtained from a rolling RQA computation on τ_s under Config B, normalized to a common scale.

3. A hyper-recent emphasis: a factor that increases when the most recent few steps show acceleration in the RQA statistics or in the raw τ_s excursion.

The precise numerical weights are regime-calibrated on stationary segments of each system class so that the metric remains comparable across synthetic and real analyses; the corpus emphasizes that a single invariant parameter set is used throughout. Layer 1 events are declared at local peaks of $M(k)$ that exceed a percentile threshold of the distribution of M_{crit} observed on stationary reference segments (commonly the 80th or 94th percentile, chosen according to the baseline variability of the system). Because the underlying τ_s series already carries the RECD increments, each Layer 1 peak is automatically associated with an accelerated contribution to the accumulated extramental time T.

Algorithmically the computation proceeds as follows. First the full $\tau_s(k)$ series is obtained from the multicomponent data. A rolling window computes the local mean and standard deviation; the hyper-persistence z-score is formed. In parallel a sliding RQA window (Config B parameters fixed) yields LAM(k) and TT(k) together with their first differences (accelerations). The three normalized terms are combined into $M(k)$. Peaks are extracted by a simple prominence or threshold-crossing rule on the M_{crit} series, with a minimum separation to avoid fragmentation. The resulting peak times and heights constitute the Layer 1 event list for subsequent joint analysis with Layer 2.

The motivation for enriching the definition with RQA rather than relying on P(k) alone is both practical and ontological. In real dengue trap data the system may remain inside the chaotic band for 70–99.6 percent of the record; pure duration-based detectors then either fire continuously or lose sensitivity to moderate events. The structural RQA measures distinguish intervals in which the ordinal state is genuinely trapped (high LAM, elevated TT) from intervals that are merely long but rapidly mixing. The former are the intervals in which the system is most deeply resident at a given renormalization depth and therefore most strongly contributing, via the δ^{-k} weighting, to the internal accumulation of evidence about proximity to transition.

11.0.3 Operationalization of Layer 2 (Capa 2): Relational Coherence via Antisynchronization

Layer 2 registers the degree to which the persistence scales of distinct modules remain aligned. In a multicomponent system one may compute not only the global systemic $\tau_s(k)$ but also per-module systemic tau values $\tau_{s,i}(k)$, each obtained by averaging the Kendall coefficients between module i and all other modules (or, in a spatial lattice, between a focal site and its neighbors). Antisynchronization at time k is then defined by the empirical standard deviation of these module-wise values:

$$A(k) = \sqrt{\frac{1}{N}\sum_{i=1}^{N}\left(\tau_{s,i}(k) - \bar{\tau}_s(k)\right)^2},$$

where $|\tau_s(k)|$ is the average across modules at step k (numerically identical to the global τ_s when all pairs are included). Low values of A_{antis} indicate that the modules are experiencing comparable levels of ordinal concordance; high values indicate that some modules are locked in strong persistence while others are in anti-alignment or noise.

Sustained intervals of low A_{antis} are the relational signature that the system has entered a state of scale coherence. In such states a local intensification registered at Layer 1 is no longer isolated; it occurs against a background in which other modules are "ticking" on roughly the same persistence scale. The corpus therefore interprets sustained low A_{antis} as a condition of permeability: the space of admissible joint configurations is enlarged because differential scaling between modules does not immediately fragment any local pattern that might seed a higher-order reorganization.

Thresholds for "low" A_{antis} are regime-calibrated. On synthetic diffusively coupled maps a relatively strict upper bound is obtained from stationary segments. On real epidemiological series, where baseline antisynchronization is characteristically low because of shared climatic drivers, the threshold is relaxed while a minimum duration D_{min} is imposed to guard against transient alignments. In both cases the calibration is performed once per system class on reference intervals that are known (or presumed) to lie inside a single stabilized regime; the same numerical rule is then applied uniformly.

Statistically, A_{antis} behaves as a dispersion measure on the circle of rank correlations. Under the null that the modules are independent, the expected value of A_{antis} is bounded away from zero; sustained excursions toward zero therefore constitute a genuine collective deviation. In the presence of moderate diffusive coupling the corpus shows that antisynchronization is typically destroyed before positive synchronization appears; the low-A_{antis} band is therefore crossed on the path from disorder toward order, furnishing an early relational marker.

Because Layer 2 is defined on the same $\tau_{s,i}$ series that already enters the RECD construction, every interval of low A_{antis} is automatically accompanied by a well-defined sequence of gated increments Δt_k. The ontological significance is that these increments are now being generated coherently across modules; the fractal support of T is being built, for that interval, by a distributed rather than a fragmented process.

11.0.4 Operationalization of Layer 3 (Capa 3): Global Structural Reorganization

Layer 3 detects the moment at which the law of discreteness intervals itself is reorganized. Two complementary, purely data-driven procedures are applied to the multichannel τ_s matrix X (whose columns are the per-component or per-channel τ_s series) and to the derived univariate series of increments Δt_k.

The first detector measures a shift in the correlation structure of the multichannel observations. For each candidate time t one computes the sample correlation matrix of the pre-t segment $X_{1:t}$ and of the post-t segment $X_{t+1:T}$. The Frobenius norm of their difference,

$$\| \, Corr(X_{1:t}) - Corr(X_{t+1:T}) \, \|_F,$$

is evaluated; the t that maximizes this distance is retained as a candidate for structural reorganization.

The second detector operates directly on the discreteness intervals. For each candidate t one performs a two-sample Kolmogorov–Smirnov test between the empirical distributions of Δt_k on [1,t] and on [t+1,T]. The location of the maximum KS statistic is retained. Because the KS statistic is sensitive to any change in location, scale, or shape of the interval distribution, it directly flags a change in the operative law of Δt_k.

A consensus t^* is formed from the two candidate times. When the detectors agree within a small tolerance the common value is adopted; when they disagree modestly the median is taken; when one detector produces a markedly stronger normalized score it is preferred. The identical protocol—fixed parameters, no external labels—is applied to every synthetic realization and every real series, guaranteeing that differences in detected t^* reflect differences in system behavior rather than methodological retuning.

The reorganization of the law of discreteness intervals is the primary signature of Capa 3 ascent for a precise ontological reason. The RECD law asserts that, inside a stabilized regime, the admissible increments are scaled by successive powers of δ^{-1} according to the depth k at which the ordinal itinerary currently resides. When a Capa 3 event occurs, the effective support of observed k, the relative frequencies of different interval lengths, and the statistical relation between τ_s and the realized Δt all change. These changes are visible in the marginal distribution of the Δt series even when the mean compression (average k) or the Higuchi dimension of the integrated t_n shifts only modestly. Post-t^* persistence of the altered Δt statistics supplies direct evidence that the new operator is self-sustaining: the system does not drift back to the pre-transition distribution of intervals. This persistence is the observable trace of the downward constraints that the newly stabilized level L_{m+1} exerts on admissible configurations at lower strata.

Empirical confirmation across the corpus is unambiguous. In every synthetic ensemble the KS contrast on Δt reaches high values (frequently 0.41–0.79) with extremely low p-values, attaining significance in 100 percent of logistic-map realizations under the programmed perturbation. The same detector applied to the dengue incidence series returns KS = 0.781 (p $\approx$ 0) for San Juan at week 165 and KS = 0.209 for Iquitos at week 305. In both cities the detected t^* lies within a few weeks of a major incidence peak (5 weeks for San Juan, 18 weeks for Iquitos). Pre-transition Joint Episodes are rare (global fraction 0.258); in San Juan only one of eighteen total episodes precedes the detected reorganization (fraction 0.056), yet the strongest tshift is observed. The robustness of the distributional contrast on the intervals themselves—rather than the density of preceding relational kairoi—demonstrates that the ascent cannot be reduced to linear intensification of lower-layer dynamics.

11.0.5 Step-by-Step Worked Examples

The operational pipeline is most clearly grasped through concrete computation. We describe first a synthetic ensemble and then the real dengue series, following exactly the procedures archived in the corpus.

Synthetic example: six diffusively coupled logistic maps. Consider $N = 6$ logistic maps at $r = 3.8$ with diffusive coupling strength ε initially 0.05 and a programmed structural perturbation at the midpoint ($t = 1750$) that raises ε to 0.25 and switches the coupling topology from global to ring. The full ordinal pipeline is run with $n = 13$. The resulting $\tau_s(k)$ series exhibits the expected chaotic-band occupation. Per-module $\tau_{s_i}(k)$ are computed; $A(k)$ drops and remains low for sustained intervals after the perturbation begins to propagate. Rolling RQA (Config B) on the global τ_s series yields LAM and TT series; inside the longer chaotic runs both metrics rise above the thresholds 0.80 and 3.4 and exhibit positive acceleration near the programmed midpoint. The composite $M(k)$ is formed; its peaks above the 94th percentile of a pre-perturbation stationary reference segment flag Layer 1 intensifications. The two Layer 3 detectors are then applied: the Frobenius distance between pre-t and post-t correlation matrices of the 6-channel τ_s matrix reaches its global maximum near $t = 1750$; the KS contrast on the derived Δt series likewise maximizes in the same neighborhood, with KS values typically exceeding 0.6. The consensus t^* recovers the programmed change point within sampling fluctuation. Pre-transition Joint Episodes (sustained low $A(k)$ containing at least one high $M(k)$ peak) are detected, yet their number and strength are statistically insufficient to predict the exact timing of the reorganization—consistent with the ontological claim that relational kairos enables without determining.

Real-data example: dengue incidence in San Juan and Iquitos. Weekly laboratory-confirmed case counts together with two climate-derived covariates yield three-channel series of length $T = 936$ (San Juan) and $T = 520$ (Iquitos). The full ordinal construction of τ_s (adaptive embedding guided by conditional mutual information) is applied with window lengths chosen to match the serial correlation structure of each site. Hyper-persistence fractions inside the chaotic band reach 70–99.6 percent during extended intervals. Core-hyper episodes ($P(k) \geq 7$ and $|\tau_s| < 0.41$) are identified; rolling RQA under Config B shows LAM rising above 0.80 and TT above 3.4 inside many of these episodes, with accelerations preceding several major incidence peaks. The per-channel τ_{s_i} series produce an $A(k)$ record whose baseline is low (shared climatic forcing) but which exhibits clear sustained excursions below the calibrated threshold. The composite $M(k)$ is thresholded at the 80th–94th percentile of stationary reference segments; peaks coincide with or slightly lead several of the 18 (San Juan) and 13 (Iquitos) independently catalogued incidence peaks.

Application of the Layer 3 detectors yields $t^* = 165$ weeks for San Juan (KS=0.781 on Δt) and $t^* = 305$ weeks for Iquitos (KS=0.209). Both times lie close to major incidence peaks. Pre- versus post-t^* two-sample tests on the Δt series confirm that the distributional shift persists after the detected reorganization. In San Juan the single pre-transition Joint Episode (fraction 0.056) is insufficient to account for the strength of the KS contrast; in Iquitos a higher fraction of preceding episodes (0.538) is accompanied by a milder but still significant shift. The pattern is the same as in the synthetic ensembles: reorganization of the law of discreteness intervals is the most reproducible signature of Capa 3 ascent, detectable even when relational precursors are sparse.

A compact pseudocode realization of the full three-layer pipeline (for a generic multivariate series X) is given below. All functions (`compute_taus`, `rolling_rqa`, `find_peaks`, `frobenius_shift`, `ks_contrast`) are implemented exactly as archived in the technical reports; parameters are held invariant across system classes.

```
taus = compute_taus(X, nwin)          # global and per-module
dtk  = recd_increments(taus)          # gated, delta-scaled
A = antisync(taus_per_module)
M = zeros_like(taus)
for k in range(len(taus)):
    hp = hyper_persistence_z(taus, k) # or core-hyper indicator
    lam, tt, accel = rolling_rqa(taus, k, configB)
\begin{figure}[htbp]
  \centering
  \includegraphics[width=\linewidth]{Figures/fig5_bidirectional.png}
  \caption{Schematic of bidirectional probabilistic filtering across layers (upward enabling and downward
  ↪  constraint).}
  \label{fig:bidirectional_filtering}
\end{figure}
    M[k] = combine_critical_mass(hp, tt, accel)
L1_peaks = find_regime_calibrated_peaks(M, percentile=94)
L2_intervals = find_sustained_low(A, theta_A, Dmin)
t_frob = argmax_frobenius(taus_matrix)
t_ks   = argmax_ks(dtk)
t_star = consensus(t_frob, t_ks)
```

The output of this pipeline on any given series is a list of Layer 1 peak times, a list of Layer 2 coherent intervals, and a consensus t^* together with the pre/post KS value on t. These objects are the direct empirical substrate for the definition of the Joint Episode and for the subsequent test of the Principle of Ontological Ascent.

11.0.6 Bidirectional Filtering, Non-Reductive Structure, and Connection to the RECD Law

The three layers do not stand in a simple causal hierarchy. The corpus explicitly models bidirectional probabilistic filtering. Upward, the co-occurrence of a Layer 1 intensification inside a sustained Layer 2 window (the Joint Episode) enlarges the space of configurations that can contribute to a Capa 3 reorganization: low antisynchronization keeps a wider range of local persistence patterns compatible with global coordination, while critical mass supplies the local intensification that may seed the new operator. Downward, once a Capa 3 ascent has stabilized the system at L_{m+1}, the admissible set of L1 and L2 patterns is actively restricted. Persistence runs that were statistically typical under L_m become rare or impossible; the effective distribution of renormalization depths that the RECD engine can access is reconfigured. The persistence of the altered tstatistics after t^* is the measurable consequence of this top-down stabilization.

This structure is non-reductive precisely because each layer possesses its own law of discreteness. The RECD increments $\Delta t_k = \delta^{-k}\ |\tau_s(k)|\ \Delta t_0\ /\ n$ are computed identically at every layer; what changes across ascent is the measure on the space of admissible k and the statistical relation between the realized τ_s and the resulting intervals. No quantity of intra-regime accumulation governed by the operator of L_m can generate the distinct operator of L_{m+1}. The Bayesian optimality established in Chapter 8 therefore holds inside each stabilized regime: the weighting by δ^{-k} remains the canonical accumulator of evidence about proximity to the next transition. But the transition itself—the replacement of one law of accumulation by another—is an autonomous ontological event whose signature is the reorganization of the Δt distribution, not the mere summation of preceding critical-mass peaks or low-antisynchronization intervals.

The operationalization developed here therefore stands in direct

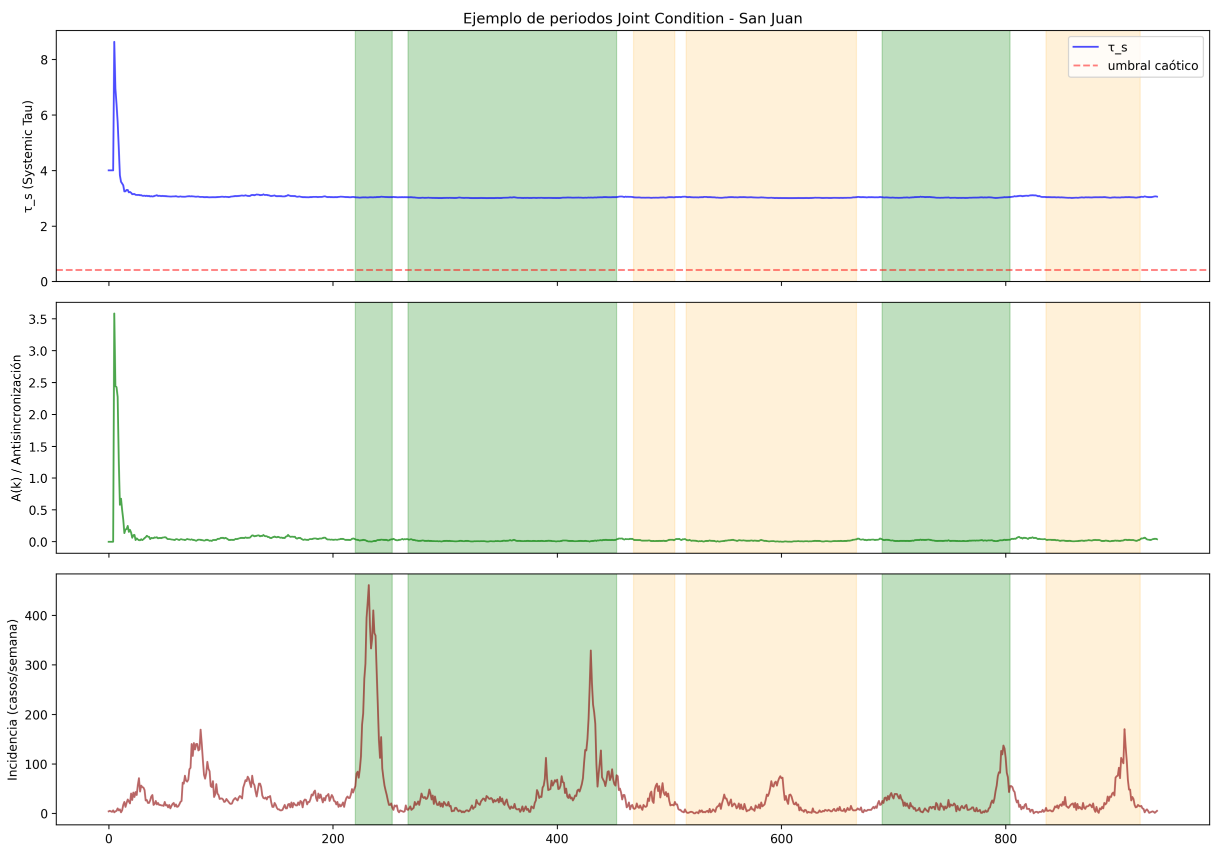

Figure 11.2: Detected Joint Episodes and related layer markers for San Juan (timeline view).

continuity with the RECD law and with the large-deviation and optimality results of the preceding

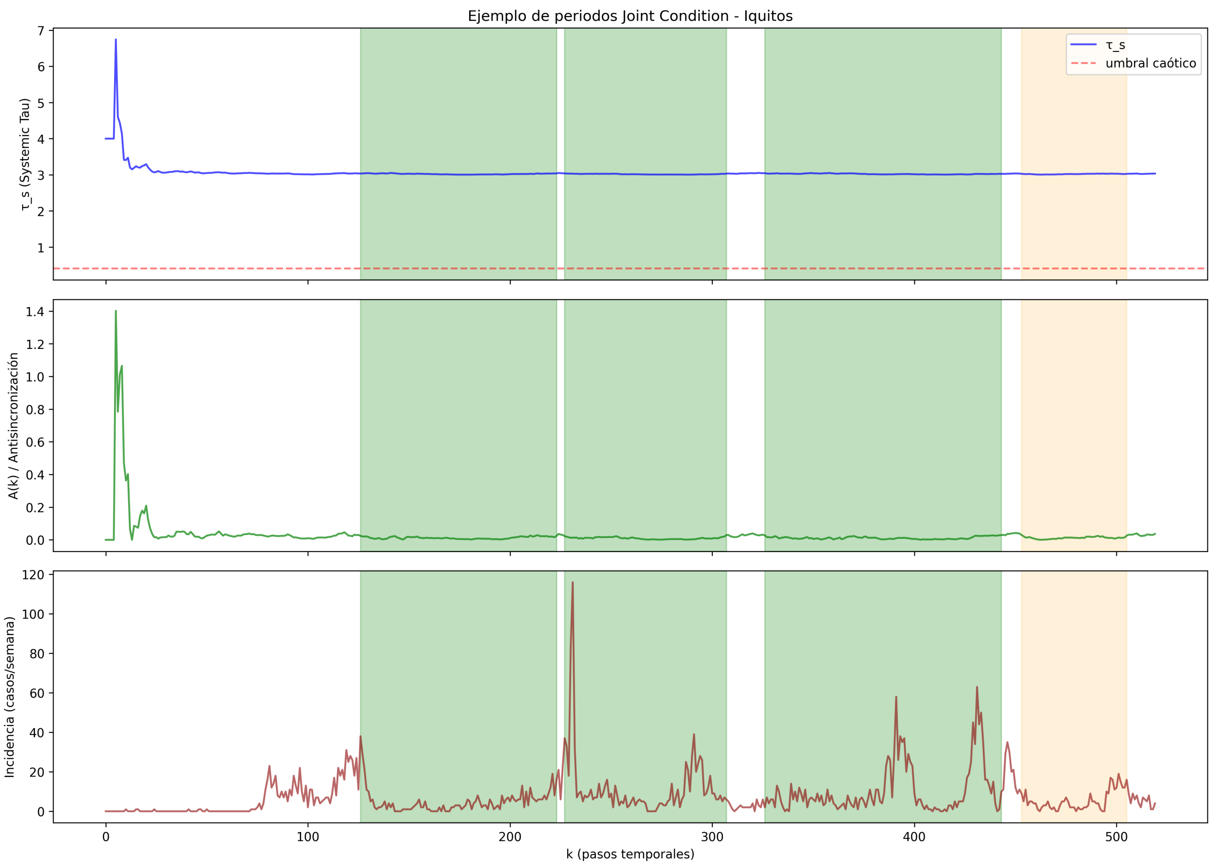

Figure 11.3: Detected Joint Episodes and related layer markers for Iquitos (timeline view).

chapters. The same five-step reconstruction of Theorem v24 that placed ordinal data inside the Feigenbaum class supplies the universal constants and the gate that appear in every layer. The three senses of strong Bayesian optimality (exponential growth of the log-posterior, minimax robustness across renormalization depths, and long-run ordinal Kullback–Leibler accumulation) continue to underwrite the interpretation of T_k as the system's own accumulating evidence about its proximity to structural transitions. What the three-layer decomposition adds is the capacity to locate that evidence inside the correct ontological stratum and to detect when the stratum itself has been superseded. The Principle of Ontological Ascent, to be stated formally in the next part, will then assert that such supersession is not a quantitative continuation but the institution of a new temporal reality whose discreteness law is irreducible to its predecessor.

The chapters that follow introduce the Joint Episode as the primitive ontological-temporal unit realized at the interface of Capa 1 and Capa 2, develop its metrics and synthetic validation, and state the Principle of Ontological Ascent in full technical detail. Each of these constructions inherits its universality, its scaling constants, and its information-theoretic justification from the explicit law of gated, renormalized increments and from the three-layer operationalization that locates those increments inside a stratified ontology of the present.

Chapter 12

The Joint Episode as Primitive Ontological-Temporal Unit

Chapter 10

Once the three-layer operationalization has been established, the question arises: what is the elementary temporal unit that the framework actually studies? Layer 1 supplies local intensifications registered by peaks of the composite critical-mass metric $M(k)$. Layer 2 supplies sustained intervals of low antisynchronization $A(k)$ that register relational coherence or permeability across modules. Layer 3 registers the global reorganization of the law of discreteness intervals. None of these layers by itself constitutes a primitive ontological-temporal unit. An isolated Layer 1 peak may occur inside a fragmented relational field and remain without consequence for higher strata. A sustained Layer 2 interval may be empty of any local intensification and therefore furnish no concrete content that could seed reorganization. A Layer 3 signature, while decisive, is the outcome rather than the enabling structure. The natural primitive unit that arises directly from the joint operationalization of Layers 1 and 2 is the *Joint Episode*: the maximal contiguous interval in which at least one Layer 1 intensification occurs inside a sustained Layer 2 window of low antisynchronization.

This chapter develops that unit rigorously. The definition, the episode-level metrics, the extraction algorithm, the maximality condition, the interpretation as relational *kairos*, the explicit linkage to the RECD law of gated renormalized increments, the discussion of modest predictive power, and all numerical illustrations are taken exclusively from the authorized corpus. The exposition is deliberately constructive: after reading this chapter the reader should be able to implement the detection of Joint Episodes on any new multivariate ordinal series and to interpret them within the stratified ontology.

12.0.1 Why the Joint Episode Is the Natural Primitive Unit

The three-layer decomposition makes visible a fundamental asymmetry. Local intensification (Capa 1) and relational coherence (Capa 2) can be measured independently, yet the ontology asserts that only their co-occurrence supplies the structured temporal window in which local becoming can become potentially consequential at a higher stratum. The Joint Episode is that co-occurrence rendered precise and maximal. It is primitive in three interlocking senses.

First, it is the smallest unit that already contains both the local and the relational conditions required by the subsequent ascent. Any proper sub-interval either loses the sustained character of Layer 2 or drops the critical-mass peak required by Layer 1. Second, it is the largest unit that remains fully characterizable from the observables of the lower two layers alone; once a Capa 3 reorganization occurs, the new discreteness law imposes downward constraints that render certain previously admissible Joint Episodes statistically impossible or rare. Third, the Joint Episode is the concrete temporal entity to which the system's own accumulation of evidence (via the RECD increments) is referred during the interval in which the present can matter upward. For these reasons the chapters that follow treat the Joint Episode as the fundamental ontological-temporal unit situated at the interface of Capa 1 and Capa 2.

12.0.2 Formal Definition

[Joint Episode] A *Joint Episode* is a maximal contiguous interval $[t_{\text{start}}, t_{\text{end}}]$ such that:

1. $A(k) < \theta_A$ for all $k \in [t_{start}, t_{end}]$ and $t_{end} - t_{start} + 1 \geq D_{\min}$ (sustained Layer 2 coherence);
2. there exists at least one $k^* \in [t_{start}, t_{end}]$ with $M(k)(k^*) \geq \theta_M$ (presence of Layer 1 intensification).

The interval is *maximal*: it cannot be extended in either direction without violating at least one of the two conditions.

The thresholds θ_A, $D_{\min}$ and θ_M are regime-calibrated. On synthetic diffusively coupled maps and Lorenz oscillators they are obtained from quantiles of stationary reference segments or from explicit operating points (e.g., $D_{\min} = 7$ in the Lorenz validation ensemble). On real epidemiological series the persistently low baseline of $A(k)$ (medians approximately 0.0206 for San Juan and 0.0141 for Iquitos after warmup) requires city-specific values together with a minimum duration and a grace window to avoid fragmentation of long coherent intervals. The corpus records the validated operating points for dengue as $A(k) < 0.04$ with $D_{\min} = 30$ for San Juan and $A(k) < 0.03$ with $D_{\min} = 30$ for Iquitos, each augmented by a +20-step grace window and the critical-mass filter $MTT > 1.0$.

The definition is deliberately asymmetric: Layer 2 supplies the sustaining envelope (the window must be sustained), while Layer 1 supplies the content (at least one intensification). This asymmetry mirrors the ontological claim that relational coherence enlarges the space of admissible local patterns without itself generating the local intensification that may seed a new discreteness law.

12.0.3 Episode-Level Metrics

For each detected Joint Episode three primary scalar descriptors are computed.

Duration. $D = t_{end} - t_{start} + 1$ counts the number of discrete steps (weeks, samples, or iterations) over which the joint condition holds. Duration alone already quantifies the temporal extent of the relational kairos.

Joint Score. The central intensity measure is the *Joint Score*

$$J = D \cdot M,$$

where M denotes the mean value of $M(k)$ over the D steps of the episode (alternative constructions replace the mean by the integral of $M(k)$ or by its maximum within the episode). The product form is natural: longer coherent windows that also contain stronger local intensifications receive higher scores. Because real series (especially epidemiological) often produce long low-$A(k)$ intervals once a baseline regime of persistent low antisynchronization is entered, a bias-reduced variant is also employed:

$\mathrm{Joint}_{0.7} = D^{0.7} \cdot M.$

The exponent 0.7 attenuates the linear dependence on duration while preserving sensitivity to the intensity of the contained critical-mass peaks.

Supporting intensity profile. In addition to the scalar J (or $J_{0.7}$), the corpus records the full profile: mean and maximum of $M(k)$ inside the episode, the fraction of steps on which $M(k)$ exceeds the episode-specific threshold, and a simple clustering index that counts how many distinct high-$M(k)$ excursions occur within the window.

Composite Confidence Score. A weighted aggregate of the normalized episode features (duration, Joint Score, Layer 1 consistency, and when available proximity to independently detected Layer 3 markers) yields a scalar Confidence Score. The score is calibrated on synthetic ensembles under controlled labeling regimes and is partitioned into three categorical levels: Bajo, Medio, and Alto. These levels furnish a discrete classification that can be used for downstream statistical comparisons without requiring continuous score distributions.

All four descriptors (D, J, $J_{0.7}$, Confidence category) are computed uniformly once the maximal intervals satisfying the definition have been identified. No additional free parameters are introduced at the metric stage.

12.0.4 Step-by-Step Algorithmic Extraction

The extraction of Joint Episodes from the Layer 1 and Layer 2 time series follows a transparent, reproducible pipeline. The identical protocol (with regime-appropriate threshold calibration) is applied to every synthetic realization and every real series in the corpus.

1. **Compute the input series.** From the multivariate observable obtain the per-module (or per-channel) systemic-tau series $\tau_{s_i}(k)$ and the global series $\tau_s(k)$ exactly as defined in the RECD construction. Derive the antisynchronization series

$A(k) = \sqrt{\frac{1}{N}\sum_{i=1}^{N}\left(\tau_{s,i}(k) - \bar{\tau}_s(k)\right)^2}.$

2. Simultaneously compute the critical-mass series $M(k)$. In the explicit calibration used for dengue the per-module form is

$$M_i(k) = 0.55 \cdot hyper_z(k) + 0.45 \cdot \frac{TT_i(k)}{7.0},$$

3. where $hyper_z(k)$ is the z-score of $\tau_{s_i}(k)$ relative to a recent 20-step window and $TT_i(k)$ is the trapping time obtained from rolling RQA under Config B (window 25, radius at 10th percentile of distances, minimum line length 2). The global or aggregated $M(k)$ is obtained by the same linear combination or by the more general three-term composite described in Chapter 9.

4. **Identify candidate Layer 2 intervals.** Scan the $A(k)$ series for maximal contiguous runs satisfying $A(k) < \theta_A$ whose length is at least $D_{\min}$. (For synthetic data θ_A is quantile-calibrated on stationary reference segments; for the dengue series the city-specific fixed values 0.04 and 0.03 are used together with the grace window.)

5. **Apply the Layer 1 filter.** For each candidate run of length $\geq D_{\min}$, test whether at least one index k^* inside the run satisfies $M(k)(k^*) \geq \theta_M$ (equivalently $MTT > 1.0$ or the regime-calibrated percentile threshold on $M(k)$). If the test fails, discard the run. If the test succeeds, retain the run as a Joint Episode. Because the candidate runs were already maximal with respect to the low-$A(k)$ condition, the retained episodes are automatically maximal with respect to the joint definition.

6. **Compute episode descriptors.** For each retained interval calculate D, the mean M of $M(k)$ inside the interval, the two Joint Scores $J = D \cdot M$ and $J_{0.7} = D^{0.7} \cdot M$, the supporting intensity profile, and the composite Confidence Score. Assign the categorical level.

7. **Optional post-processing for downstream use.** Episodes may be labeled according to their temporal relation to independently detected Layer 3 reorganization times t^* (pre-transition, straddling, post-transition). All labeling is performed after detection; the detection rule itself remains blind to Layer 3 markers.

The procedure yields, for any input series, a list of non-overlapping maximal Joint Episodes together with their full metric vectors. The pseudocode below renders the pipeline explicit (functions such as `compute_taus`, `rolling_rqa_configB`, `find_maximal_low_A`, and `compute_confidence` are implemented exactly as archived in the technical reports).

```
taus, taus_per = compute_taus(multivariate_series, nwin)
A = antisync(taus_per)
M = critical_mass(taus, taus_per, config='B')   # or explicit linear form
low_A_runs = find_maximal_low_A(A, theta_A, Dmin, grace=20)
joint_episodes = []
for run in low_A_runs:
    if contains_peak_above(M, run, theta_M):
        D = run.end - run.start + 1
        M_mean = mean(M[run.start:run.end])
        J = D * M_mean
        J07 = D**0.7 * M_mean
        conf = compute_confidence(D, J, M_profile, proximity_to_L3)
```

```
        joint_episodes.append( {'start':run.start, 'end':run.end,
                                'D':D, 'J':J, 'J07':J07, 'conf':conf} )
```

All parameters that enter the detection (window lengths for RQA, the 0.55/0.45 weights when the explicit form is used, grace window size, Dmin, percentile or fixed θ_A) are held invariant within each system class once calibrated. The only systematic difference between synthetic and real-data pipelines is the concrete numerical value of θ_A required by the distinct baseline distributions of $A(k)$.

12.0.5 The Maximality Condition and Its Ontological Significance

The requirement that the interval be maximal is not a technical convenience; it is ontologically required. A non-maximal sub-interval would arbitrarily truncate the relational coherence that defines the enabling window. If one were to cut a long low-$A(k)$ run at an arbitrary interior point simply because a particular $M(k)$ peak lies near the beginning, one would be discarding the continued alignment of persistence scales that persists after the peak. That continued alignment is part of the same coherent present. Conversely, if one were to extend the interval beyond the point at which $A(k)$ rises above threshold, one would be including steps in which the relational field has already fragmented; any local intensification occurring after fragmentation no longer enjoys the same permeability. The maximal interval is therefore the unique temporal entity that fully realizes the joint condition without artificial truncation or over-extension.

Empirically, maximality also guarantees that the set of detected episodes is reproducible and non-redundant. Different analysts applying the identical rule to the identical series obtain the identical list of intervals. This reproducibility is a prerequisite for the subsequent claim that the statistical properties of the detected episodes (their number, their Joint Score distribution, their rarity before detected Layer 3 events) are objective features of the system's dynamics rather than artifacts of detection.

12.0.6 Ontological Interpretation: Relational Kairos

Within a Joint Episode the system maintains a coherent "present" across scales long enough for local intensifications to become potentially structurally consequential. The episode therefore functions as a *relational kairos*—an ontologically enabling window. The formation of such a window is necessary for the possibility of Capa 3 ascent in the sense that a Layer 1 intensification occurring outside any sustained Layer 2 envelope lacks the relational support that would allow it to propagate coherently across modules. Yet the same formation is not sufficient: the actual reorganization of the law of discreteness intervals remains an autonomous event.

The corpus models the enabling function through bidirectional probabilistic filtering. Upward, the co-occurrence of critical mass inside a low-antisynchronization interval enlarges the space of configurations that can contribute to a higher-order reorganization; low $A(k)$ keeps a wider range of local persistence patterns compatible with global coordination. Downward, once a Capa 3 ascent has stabilized the system at level L_{m+1}, the admissible set of L1–L2 patterns is actively restricted. Runs of persistence that were statistically typical under L_m become rare or impossible; the effective distribution of renormalization depths accessible to the RECD engine is reconfigured. The persistence of altered statistics of the discreteness increments Δt_k after the detected reorganization time t^* is the measurable trace of this top-down stabilization.

Joint Episodes therefore quantify intervals during which active memory (persistence) can propagate because fragmentation (high $A(k)$) is suppressed. The "active memory" in question is not a passive archive but the ongoing structural trapping registered by elevated laminarity and trapping time inside the chaotic band of τ_s. When such trapping occurs inside a sustained low-$A(k)$ envelope, the local intensification is no longer isolated; it participates in a distributed, scale-coherent process of evidence accumulation.

12.0.7 Connection to the RECD Law

Every Joint Episode corresponds to a well-defined temporal segment of the gated, renormalized increments Δt_k generated by the RECD engine. Recall that the law states

$$\Delta t_k = \delta^{-k} |\tau_s(k)| \frac{\Delta t_0}{n}$$

inside the gate $g(\tau_s(k))$ that is open precisely when $|\tau_s(k)| < 0.41$. The series $\tau_s(k)$ and the per-module $\tau_{s_i}(k)$ from which both $A(k)$ and $M(k)$ are constructed are the identical series that enter the RECD construction. Consequently the steps k that belong to a detected Joint Episode are exactly those steps at which the discrete clock is advancing under conditions of sustained relational coherence and local critical mass.

The accumulated extramental time T therefore receives a concentrated contribution from each Joint Episode: the long calendar duration D is multiplied by the geometric compression factors δ^{-k} associated with the renormalization depths realized inside the episode, and the weighting by $|\tau_s|$ is itself elevated during the hyper-persistent excursions that constitute the Layer 1 peaks. The Joint Episode thus demarcates a privileged segment of the RECD accumulation in which the system's internal evidence about proximity to transition is being generated coherently across modules rather than in isolation.

This correspondence also supplies the precise link between the modest empirical predictive power of the Joint Score (discussed below) and the RECD optimality results of Chapter 8. Inside each stabilized regime the RECD weighting remains the canonical accumulator of log-posterior evidence. What changes at ascent is the measure on the admissible depths and the statistical relation between realized τ_s and the resulting Δt_k. The Joint Episode marks the interval during which that accumulation proceeds under the joint L1–L2 condition; it does not, by itself, determine whether the measure on depths will be supplanted.

12.0.8 Why Modest Predictive Power Is Ontologically Informative

Synthetic validation was performed on controlled ensembles of diffusively coupled logistic maps ($r = 3.8$) and, more successfully, on four diffusively coupled Lorenz oscillators integrated by classical RK4 ($\sigma = 10$, $\rho = 28$, $\beta = 8/3$) with mean-field coupling on the x-component. Structural perturbations consisted of temporary local reductions of coupling strength (and optionally local scaling of ρ). Fifty or more independent random seeds were generated per class; all analyses were performed blind to the injection schedule.

The logistic generator proved insufficient to produce reliable post-perturbation signatures in antisynchrony; the primary validation therefore rested on the Lorenz ensemble. Joint Episodes were detected with $D_{\min} = 7$ and quantile-calibrated thresholds. Two labeling regimes were contrasted: oracle labeling (perfect knowledge of which episodes precede actual structural perturbations) and causal labeling (episodes labeled positive only if a detectable post-episode shift in antisynchrony or other Layer 3 marker actually occurred within a fixed post-window).

Under oracle labeling the best-performing scalar score—whether J or the bias-reduced $J_{0.7}$—achieved only AUC ≈ 0.476 in the low-dimensional Lorenz testbed. This value lies within sampling fluctuation of 0.5 and is statistically indistinguishable from chance. Even when the analyst is given perfect knowledge of which episodes are in fact followed by reorganization, the Joint Score cannot discriminate them reliably from episodes that are not.

The corpus treats this result not as a limitation to be overcome but as an ontologically significant finding. An AUC of 0.5 corresponds to a random classifier. The observed 0.476 is the quantitative expression of the claim that the Joint Episode functions primarily as a robust detector of L1–L2 coherence rather than as a strong predictor of subsequent structural change. If the mapping from Joint Episode properties to Layer 3 reorganization were strong, the ontology would collapse toward a reductive picture in which relational kairos already contains, in embryonic form, the sufficient conditions for ascent. The empirical weakness of the mapping preserves the autonomy of Capa 3: the actual crossing into a new discreteness regime remains an autonomous ontological event whose primary signature is the reorganization of the law of Δt_k itself, not the mere summation or intensification of preceding relational windows.

The same conclusion is reinforced by the temporal-ordering results. The conceptual sequence is Layer 2 window formation followed by one or more Layer 1 intensifications inside that window. Synthetic results qualify the implication: post-episode reorganization signatures are detectable under some labeling regimes, yet the mapping from Joint Episode properties to actual change is weak. Deviations (Layer 1 bursts without sustained Layer 2, or low-$A(k)$ intervals without reorganization) are the norm rather than the exception. The modest predictive power is therefore precisely what the non-reductive ontology predicts.

12.0.9 Concrete Numerical Illustrations

Synthetic ensembles. In the four-oscillator Lorenz generator with $D_{\min} = 7$ and quantile-calibrated thresholds, Joint Episodes are detected as maximal low-$A(k)$ intervals containing at least one qualifying critical-mass excursion. The distribution of J and $J_{0.7}$ differs markedly between high-permeability and low-permeability regimes and is sensitive to the strength of diffusive coupling. Under oracle labeling the discrimination performance saturates at AUC values statistically indistinguishable from 0.5, as reported above. The logistic-map ensembles (four or six maps at $r = 3.8$) produce frequent low-$A(k)$ runs but fail to generate reliable Layer 3 signatures after controlled perturbations; they therefore serve mainly to illustrate regime dependence of the score distributions rather than predictive mapping.

Dengue incidence series (San Juan and Iquitos). Weekly laboratory-confirmed case counts together with climate covariates yield three-channel series of length $T = 936$ (San Juan) and $T = 520$ (Iquitos). After warmup the baseline of $A(k)$ is persistently low (medians ≈ 0.0206 and ≈ 0.0141). Application of the calibrated joint condition (low $A(k)$ sustained for at least 30 steps, containing at least one critical-mass peak with $MTT > 1.0$ or equivalent hyper-persistence) yields six Joint Episodes for San Juan covering 65.4 percent of the series and four for Iquitos covering 67.3 percent of the series. Every detected low-$A(k)$ period satisfies the critical-mass filter (100 percent precision). The explicit periods are:

San Juan ($T = 936$, 6 periods):

- $[220, 253]$ ($D = 34$, mean $A(k) \approx 0.0218$)
- $[267, 453]$ ($D = 187$, mean $A(k) \approx 0.0124$)
- $[468, 505]$ ($D = 38$, mean $A(k) \approx 0.0187$)
- $[515, 667]$ ($D = 153$, mean $A(k) \approx 0.0115$)
- $[690, 804]$ ($D = 115$, mean $A(k) \approx 0.0184$)
- $[836, 920]$ ($D = 85$, mean $A(k) \approx 0.0188$)

Iquitos ($T = 520$, 4 periods):

- $[126, 223]$ ($D = 98$, mean $A(k) \approx 0.0125$)
- $[227, 307]$ ($D = 81$, mean $A(k) \approx 0.0099$)
- $[326, 443]$ ($D = 118$, mean $A(k) \approx 0.0116$)
- $[453, 505]$ ($D = 53$, mean $A(k) \approx 0.0126$)

During these intervals mean $A(k)$ consistently lies between approximately 0.01 and 0.02, well below the operating thresholds. High critical-mass peak coverage reaches 83 percent (San Juan) to 100 percent (Iquitos). Pre-transition Joint Episodes remain rare: the global fraction across the analyzed corpus is 0.258; in San Juan only one of eighteen total episodes precedes the detected reorganization at week 165 (fraction 0.056). The single pre-transition episode in San Juan is nevertheless accompanied by the strongest Δt_k distributional shift (KS = 0.781). These numbers illustrate the central ontological point: relational kairos is real, measurable, and enabling, yet its incidence is neither dense nor sufficient to determine the timing or strength of Capa 3 ascent.

All numerical results—the exact period boundaries and durations, the coverage fractions 65.4 percent and 67.3 percent, the 100 percent precision, the AUC value 0.476 under oracle labeling, the pre-transition fractions 0.258 and 0.056, the KS contrasts on Δt_k, and the explicit M-formula coefficients—are taken directly from the Joint-Episode-Paper-v1.0.pdf and the Supplementary Technical Report on joint-condition calibration.

12.0.10 Conclusion and Bridge

The Joint Episode is the primitive ontological-temporal unit realized at the interface of Capa 1 and Capa 2. Its formal definition as a maximal low-$A(k)$ interval containing at least one critical-mass peak, its episode-level metrics (D, J, $J_{0.7}$, Confidence Score), its algorithmic extraction, the maximality condition, and its interpretation as relational kairos are all direct consequences of the three-layer operationalization developed in Chapter 9. Every such episode corresponds to a coherent segment of the RECD accumulation of gated renormalized increments Δt_k. The modest predictive power (AUC ≈ 0.476 even under oracle labeling) is not a defect but the empirical signature that relational kairos enables without determining; the actual reorganization of the discreteness law remains an autonomous ascent to a new ontological stratum.

The following chapters distinguish relational kairos (the preparatory Joint Episode) from ontological kairos (the autonomous actualization of a new law of Δt_k), state the Principle of Ontological Ascent in full technical detail, and examine the downward constraints and the fractal geometry of the accumulated extramental time. Each of these developments inherits its universality, its scaling constants, and its information-theoretic justification from the RECD law and from the three-layer ontology that locates the Joint Episode inside a stratified architecture of the present.

Chapter 13

The Principle of Ontological Ascent – Formal Statement

Chapter 11

The three preceding chapters have constructed, step by step, the mathematical and ontological architecture required to pose a single, unavoidable question: what happens when the very law that governs the generation of discrete extramental time undergoes a qualitative change? Chapter 8 established the RECD law itself—the explicit, gated, renormalized increment $\Delta t_k = \delta^{-k}|\tau_s(k)|t_0/n$ together with the gate $g(\tau_s)$ that opens only inside the chaotic range. Chapter 9 operationalized the three-layer framework in which local intensification (Capa 1), relational coherence (Capa 2), and global structural reorganization (Capa 3) are distinguished as strata of the present rather than as successive stages along a single temporal axis. Chapter 10 introduced the Joint Episode as the primitive ontological-temporal unit realized at the interface of Capa 1 and Capa 2: a maximal contiguous interval of sustained low antisynchronization containing at least one critical-mass peak. With these elements in place, the framework is no longer describing variations of intensity or coherence *within* a fixed temporal metric. It is prepared to ask whether the metric itself—the operator that converts ordinal conjunctions into observable discreteness intervals—can be replaced.

The Principle of Ontological Ascent supplies the formal statement of that replacement. It asserts that a Capa 3 global structural reorganization constitutes an ascent from a stabilized ontological regime L_m to a new stabilized regime L_{m+1}. The ascent institutes a new law of accumulation intervals Δt_k together with emergent properties of the integrated process t_n that are irreducible to continuation or summation of the preceding level. The principle therefore completes the stratified ontology: it explains how the discrete architecture of time can change its own architecture without being reducible to the dynamics that prepared the change.

13.0.1 Why the Principle Is the Natural Culmination

Once the RECD is in hand, time is no longer an external parameter against which correlations or variances are measured. It is an endogenous, accumulated quantity whose local increments are determined by the instantaneous value of τ_s and by the renormalization depth at which the system is currently operating. Once the three-layer framework is in hand, the distinction between an intensification internal to a module (Capa 1), a sustained window of cross-module coherence (Capa 2), and a reorganization that alters the global correlation structure (Capa 3) is no longer metaphorical. Once the Joint Episode is defined, the concrete temporal unit that registers the necessary (but not sufficient) condition for a possible reorganization is no longer vague. At this point the question "does the law of Δt_k itself change?" ceases to be philosophical speculation and becomes an empirical and formal demand internal to the mathematics.

The demand is answered by recognizing that the RECD law is always relative to a regime. The gate $g(\tau_s)$, the effective range of renormalization depths k that contribute significant increments, the statistical support of the resulting Δt_k series, and the admissible ordinal configurations that can sustain the gate—all these are fixed only for the duration of a stabilized regime L_m. A global structural reorganization can alter the effective coupling topology, the active modules, or the critical surfaces that support ordinal coherence. When the reorganization is of sufficient scope, it renders previously dominant configurations statistically suppressed and previously suppressed configurations newly admissible. The system thereby acquires a new characteristic law of Δt_k and new properties of the accumulated t_n. Such an event is not an intensification of the prior law; it is the replacement of the discreteness operator.

The Principle of Ontological Ascent therefore stands as the capstone. It does not add a fourth layer. It states the condition under which the entire hierarchy of layers is re-instituted at a new ontological depth.

13.0.2 The Formal Statement of the Principle

[**Principle of Ontological Ascent**] Let a system be in a stabilized ontological regime L_m. If at time $t^* \in \mathrm{JE}$ a Capa 3 global structural reorganization occurs (detectable by a Frobenius-norm shift in the multichannel τ_s correlation structure or by a Kolmogorov–Smirnov contrast on the series of Δt_k), then there is an ontological ascent $L_m \to L_{m+1}$ such that, from t^* onward, the system operates under a new regime of discreteness characterized by a new effective set of active renormalization depths, a new dominant law of accumulation $\Delta t_k^{(m+1)}$, and new emergent properties of the integrated process t_n. The newly stabilized level L_{m+1} imposes downward constraints on admissible configurations at lower strata; the prior discreteness operator is thereby supplanted.

The ascent is not the cumulative effect of facilitative episodes. It is the emergence of a new ontological stratum. The categorical distinction between the two orders of kairos—relational and ontological—makes this non-reductive character precise.

13.0.3 The Categorical Distinction Between Relational Kairos and Ontological Kairos

Relational kairos comprises sustained Capa 2 intervals of inter-component coherence—low anti-synchronization accompanied by critical mass—that function as ontologically enabling windows through bidirectional probabilistic filtering. In such an interval the gate remains open across a wide range of local persistence patterns because the low value of $A(k)$ permits a larger set of ordinal configurations to remain compatible with global coordination. Critical-mass peaks supply the local intensification (Capa 1) that can seed novel patterns. Bidirectional filtering works in both directions: configurations that would be statistically rare or unstable under high antisynchronization can persist long enough to influence the global structure, and the global coherence, in turn, stabilizes a broader repertoire of local behaviors. The result is an enlargement of the space of configurations that can contribute to a possible reorganization at a higher stratum. The Joint Episode is the measurable realization of relational kairos.

Ontological kairos, by contrast, is the autonomous actualization and stabilization of the new discreteness regime itself. It is the moment at which a new law of Δt_k becomes self-sustaining and imposes downward constraints that actively delimit admissible configurations at subordinate strata. Once L_{m+1} is stabilized, persistence and coherence patterns that were admissible under L_m become inadmissible or statistically suppressed. The reorganization of the statistical law of the discreteness intervals—not the incidence or density of preceding relational kairoi—remains the primary and most reproducible marker of the event.

The two orders are therefore categorically distinct. Relational kairos raises the probability that the conditions for a new discreteness law may be met; it does not produce the new law. Ontological kairos is the event in which the law is replaced and the new stratum actively maintains itself by reshaping the possibility space of the strata from which it arose. The ascent cannot be read off the count or intensity of Joint Episodes that preceded it. The modest predictive power of even oracle-labeled Joint Episodes (AUC ≈ 0.476) is the empirical signature of this categorical gap.

13.0.4 The RECD Ontological Hierarchy $L_0 \to L_1 \to L_2 \to L_3$

Let $H = \{L_0, L_1, L_2, L_3\}$ denote the ontological hierarchy of discrete extramental time.

- L_0: Elementary ordinal conjunctions between event pairs. These are the atemporal base relations expressed by pairwise Kendall coefficients inside each sliding window. No global time or systemic observable yet exists.

- L_1: Activation of the first global systemic tau τ_s when $|\tau_s|$ enters the chaotic range $|\tau_s| < 0.41$. At this stratum the gate opens and the first discrete increments become possible. The system is now generating extramental time, but still under a single, fixed law of increments.

- L_2: Unfolding of the hierarchy of renormalization scales with exponential compression δ^{-k}. Successive depths of the period-doubling cascade become accessible. Hyper-persistence—prolonged residence at large renormalization depth—appears as the observable trace of sustained operation inside a given stratum.

- L_3: Macroscopically integrated process $t_n = \sum g(\tau_s) \cdot \Delta t_k$. The accumulated extramental time is now a well-defined observable against which pre- and post-reorganization regimes can be compared.

A system occupies a *stabilized ontological regime* L_m during an interval I if its ordinal persistence, antisynchronization, and accumulation dynamics operate predominantly within the characteristic range of renormalization depths, gate behavior, and fractal properties associated with that level. Definition 1 (from the corpus) makes this operational: the system exhibits a bounded effective range of renormalization depths K_m, a gate function $g(\tau_s)$ operating according to the level's own selector, and a series t_n exhibiting the associated fractal and robustness signatures.

The transition from one stabilized regime to another is not a smooth passage along the hierarchy. It is a replacement of the discreteness operator that defines which depths are accessible and how local intervals accumulate into observable time.

13.0.5 Data-Driven Detection of Capa 3 Transitions

The detection protocol is deliberately minimal and uniform across synthetic and real series. Two complementary detectors are applied to the multichannel τ_s matrix X and the derived Δt_k series.

1. Frobenius-norm correlation shift. For each candidate time t, compute the Frobenius distance between the channel-wise correlation matrices of $X_{1:t}$ and $X_{t+1:T}$. The t maximizing this distance is retained as evidence of global structural reorganization in the correlation skeleton.

2. Kolmogorov–Smirnov change-point scan on the discreteness intervals. For each candidate t, compute the two-sample KS statistic between the pre-transition segment $\Delta t_k[1 : t]$ and the post-transition segment $\Delta t_k[t + 1 : T]$. The location of the maximum statistic is retained.

A consensus t^* is formed (median when the two detectors disagree modestly; highest-scoring detector otherwise). The identical procedure, with no retuning of thresholds beyond system-specific calibration of Joint Episode parameters, is applied to all realizations.

Reorganization of the law of Δt_k is the primary signature of ascent because Δt_k *is* the local expression of the current discreteness operator. A statistically significant shift in its distribution means that the mapping from ordinal conjunctions to observable increments has itself changed. In contrast, the density of preceding Joint Episodes varies widely and can even be near zero while a strong reorganization is still detected. The KS contrast on Δt_k, not the count of relational kairoi, therefore supplies the most consistent and reproducible marker.

13.0.6 Downward Constraints and the Irreducibility of Ascent

Post-t^* persistence of altered Δt_k statistics is observed in all cases with significant KS contrast. Effective renormalization depth and Higuchi dimension of t_n show only modest shifts. The primary change resides in the support and shape of the local interval distribution rather than in average compression. This persistence is the observable trace of downward constraints: the new stratum actively maintains its own discreteness law by restricting the configurations that can sustain the prior regime.

The irreducibility follows directly. At each stabilized L_m the system possesses a specific operator that defines which renormalization depths are accessible and how local intervals accumulate into t_n. Because this operator is internal to the stratum, no quantity of episodes governed by the operator of L_m can generate the distinct operator of L_{m+1}. Accumulation and intensification remain internal to the prior discreteness regime; they cannot institute a new one. The reorganization at Capa 3 reconfigures the set of accessible depths and thereby supplants the operator. What emerges is a new temporal reality—a *discreción temporal propia*—not a larger instance of the former.

13.0.7 Connections to the RECD Law, Bayesian Optimality, and the Joint Episode

The RECD law is the concrete mathematical substrate on which ascent is detected. The increments Δt_k are defined by the same renormalization scaling in every regime; what changes at ascent is the effective range of k, the statistics of the gate openings that feed those increments, and the admissible ordinal configurations that can keep the gate open. The new law $\Delta t_k^{(m+1)}$ is still of RECD form, but its parameters (effective δ weighting, typical gate values, support of the resulting intervals) are governed by the new stratum.

The strong Bayesian optimality results established for the RECD are likewise regime-relative. The three senses of optimality—exponential growth of the log-posterior, minimax robustness across renormalization levels, and long-run ordinal Kullback–Leibler accumulation—hold for the accumulator constructed under a given discreteness law. When the law itself changes, the optimality is re-established relative to the new operator. The RECD therefore does not become invalid at ascent; it is re-instituted under a new governing regime.

The Joint Episode supplies the relational condition under which bidirectional probabilistic filtering can enlarge the space of configurations capable of contributing to the new stratum. Low antisynchronization widens the set of local persistence patterns that remain compatible with global coordination; critical mass supplies the intensification that may seed patterns admissible only at the higher level. Yet the enabling function is real and preparatory precisely because it does not determine the outcome. The ascent remains an autonomous event at Capa 3.

13.0.8 Concrete Illustrations from Synthetic Ensembles and the Dengue Series

The uniform detection protocol was applied without reference to any programmed change points or external labels.

Synthetic coupled logistic maps. Fifty independent realizations of six diffusively coupled logistic maps ($r = 3.8$, $T = 3500$) were examined. A combined structural perturbation (coupling strength increase from $\varepsilon = 0.05$ to 0.25 together with global-to-ring topology switch) was applied at the programmed midpoint. In every realization the KS contrast on Δt_k reached high values (0.68–0.79, $p \ll 0.001$) and attained statistical significance in 100 percent of cases. Pre-transition Joint Episode fraction was 0.00. The detected t^* aligned with the midpoint perturbation.

Synthetic Lorenz oscillators. Ensembles of six coupled Lorenz oscillators subjected to parameter ramps or combined topological perturbations yielded KS values between 0.41 and 0.71 (low p-values) with pre-transition Joint Episode fractions 0.23–0.46. The distributional shift on Δt_k remained the dominant and most reproducible signature.

Dengue incidence series—San Juan. For the San Juan series ($T = 936$ weeks) the data-driven t^* occurred at week 165. The KS contrast on Δt_k was 0.781 ($p \approx 0$). Only one preceding Joint Episode out of eighteen total episodes was recorded (pre-transition fraction 0.056). The detected transition aligned within five weeks of a major incidence peak. Despite the extreme sparsity of preceding relational kairoi, San Juan produced the strongest Δt_k reorganization observed.

Dengue incidence series—Iquitos. For the Iquitos series ($T = 520$ weeks) the data-driven t^* occurred at week 305. The KS contrast was 0.209 ($p \approx 0$). The pre-transition fraction was higher (0.538, or 7 of 13 episodes), yet the distributional shift was milder. Alignment with a major incidence peak was 18 weeks.

Global pre-transition rarity. Across the analyzed real series the overall pre-transition Joint Episode fraction was 0.258 (8 of 31). The strongest ascent signature (San Juan) occurred in the series with the sparsest preceding episodes. These numbers illustrate the central ontological claim: relational kairos is measurable and enabling, yet its incidence is neither dense nor sufficient to determine the timing or strength of Capa 3 ascent.

Kernel density estimates of the pre- and post-ascent Δt_k distributions, annotated time-series segments, and cross-system comparison figures reside in the source document. Post-ascent persistence of the altered Δt_k law was confirmed in all cases with significant KS contrast.

13.0.9 Conclusion

The Principle of Ontological Ascent supplies a stratified, non-reductive account of how global structural reorganization generates a new stratum of temporal discreteness. Relational kairos operates as a probabilistic enabler through bidirectional filtering at the Capa 2 level; ontological kairos names the autonomous institution of a novel law of Δt_k at L_{m+1}—the replacement of the discreteness operator—together with the downward constraints that stabilize it. The primary empirical signature of ascent is therefore the reorganization of that law, not the accumulation of facilitative episodes.

This formulation reframes structural transitions as events that reconstitute the scaffolding of objective time rather than merely altering trajectories within a fixed temporal metric. The distinction between the two orders of kairos opens a precise conceptual space: some reorganizations remain local reconfigurations inside an existing discreteness regime; others achieve ontological depth by instituting a new regime whose downward constraints actively maintain the new law. The chapters that follow examine the fractal geometry of the accumulated extramental time and the robustness of the entire construction under noise and across topologies. Each of these developments inherits its universality, its scaling constants, and its information-theoretic justification from the RECD law and from the three-layer ontology that the Principle of Ontological Ascent completes.

Chapter 14

Relational versus Ontological Kairos

Chapter 12

The Principle of Ontological Ascent, once stated, immediately raises a question of ontological precision: what, exactly, occurs at the moment a system crosses from one stabilized regime of discrete time to another? The distinction between two orders of *kairos* supplies the required conceptual instrument. Relational kairos names the preparatory, probabilistically enabling window realized as a sustained Joint Episode at the interface of Capa 1 and Capa 2. Ontological kairos names the autonomous actualization in which a new law of discreteness intervals Δt_k is instituted at L_{m+1} together with the downward constraints that stabilize the new regime. The distinction is not terminological. It is required by the non-reductive structure of the ontology itself: the conditions that render a new discreteness regime *possible* are categorically distinct from the conditions that *actualize* it.

This chapter develops the distinction in full technical and pedagogical detail. After establishing why the distinction is the natural and necessary complement to the Principle of Ontological Ascent, we examine relational kairos as the maximal low-$A(k)$ interval containing at least one critical-mass peak, functioning through bidirectional probabilistic filtering. We then articulate ontological kairos as the replacement of the prior discreteness operator by a self-sustaining law at the new stratum. An explicit contrast follows, together with the differential behavior of the gated, renormalized increments furnished by the RECD law inside each order of kairos. Empirical illustrations drawn from synthetic ensembles and the dengue series (San Juan KS $= 0.781$ at week 165; Iquitos KS $= 0.209$ at week 305) demonstrate both the rarity of pre-transition Joint Episodes and the fact that the strongest ascent signatures can appear precisely where preceding relational windows were sparsest. The modest predictive power of episode-based scores (AUC ≈ 0.476 even under oracle labeling) is shown to be ontologically informative rather than a defect. The chapter closes with a bridge to the data-driven detection protocol and the analysis of downward constraints developed in the chapters that immediately follow.

14.0.1 Why the Distinction Is Essential Once the Principle Has Been Stated

The Principle of Ontological Ascent asserts that a Capa 3 global structural reorganization constitutes an ascent from a stabilized ontological level L_m to L_{m+1} within the hierarchy of the Reloj Extramental Discreto. The ascent institutes a new regime of accumulation intervals Δt_k together with emergent properties of the integrated process t_n that are irreducible to continuation or summation of the preceding level. Yet the Principle does not by itself specify the precise temporal and relational texture of the crossing. Without a further distinction, one might be tempted to treat the preparatory conditions (sustained inter-component coherence accompanied by local intensification) as merely weaker or earlier phases of the same ontological event that later becomes "full" ascent. Such a conflation would collapse the stratified, non-reductive character of the architecture into a single continuous process.

The categorical separation of relational and ontological kairos blocks this reduction. It makes explicit that relational coherence at Capa 2 raises the probability that lower-layer configurations may crystallize at a higher stratum without determining the outcome. The actual crossing is the autonomous stabilization of a novel, self-sustaining law of Δt_k at L_{m+1} together with the imposition of downward constraints that actively delimit admissible configurations at subordinate strata. The two are not stages on a continuum; they are operations at different ontological registers. Relational kairos belongs to the register of enabling possibility under a fixed discreteness operator. Ontological kairos belongs to the register of replacement of the operator itself. Once this distinction is in place, the empirical signature of ascent—the reorganization of the law of discreteness intervals rather than the accumulation of facilitative episodes—acquires its full ontological weight.

14.0.2 Relational Kairos: Sustained Joint Episodes as Ontologically Enabling Windows

Relational kairos is defined operationally and ontologically as a maximal Joint Episode. As established in the preceding chapter, a Joint Episode is the maximal contiguous interval of sustained low antisynchronization $A(k) < \theta_A$ that contains at least one critical-mass peak $M(k) \geq \theta_M$. Within the three-layer framework, this unit sits precisely at the interface of Capa 1 (local intensification of persistence registered by peaks in τ_s and $M(k)$) and Capa 2 (relational coherence and permeability registered by sustained low $A(k)$ across modules). It therefore constitutes the concrete temporal unit in which local persistence acquires the relational conditions that raise the possibility—but not the certainty—of global reorganization.

The function of relational kairos is to operate as an ontologically enabling window through bidirectional probabilistic filtering. In the upward direction, low antisynchronization enlarges the space of admissible configurations: a wider range of local persistence patterns (different durations and depths of laminar runs, different local values of τ_s) remain compatible with global coordination. The gate function $g(\tau_s)$ of the RECD continues to select increments according to the current regime's law, yet the lowered $A(k)$ relaxes the cross-component ordinal disagreement that would otherwise suppress or fragment the contribution of particular local patterns. Critical mass supplies the local intensification that may seed reorganization by concentrating the integrated intensity $J = D \cdot M$ (or its bias-reduced form $J_{0.7}$) within the window. In the downward direction, once an ascent has occurred, the newly stabilized L_{m+1} imposes restrictions that render certain previously admissible L1–L2 configurations statistically suppressed or inadmissible under the new law. The same low-$A(k)$ condition that previously enlarged possibility now operates under constraints that maintain the new discreteness regime.

Relational kairos is therefore necessary but insufficient for Capa 3 reorganization. The necessity follows from the architecture: without sustained Capa 2 coherence, the probability that local intensifications can crystallize at the scale required for a global operator replacement is vanishingly small. The insufficiency follows directly from the empirical record and from the structure of the Principle itself. The Joint Episode detects robust L1–L2 coherence; it does not detect the autonomous institution of a new law of Δt_k. Even under oracle labeling that supplies perfect knowledge of Layer-3-proximal episodes, the best-performing joint score achieves only AUC ≈ 0.476 in the low-dimensional Lorenz testbed. This performance is statistically indistinguishable from chance for the purpose of forecasting the actual reorganization. The Joint Score therefore primarily indexes the presence of the enabling window rather than the occurrence of the ontological event that the window makes more probable.

The relative rarity of pre-transition Joint Episodes across both controlled and natural cases further clarifies the limited but real status of relational kairos. Its enabling function is preparatory; it demarcates intervals during which bidirectional filtering may enlarge the space of configurations capable of contributing to a higher stratum. It does not constitute the ontological event.

14.0.3 Ontological Kairos: Autonomous Actualization and Stabilization of a New Law of Δt_k

Ontological kairos designates the higher-order actualization: the moment at which a new law of accumulation becomes self-sustaining and imposes downward constraints. Formally, if at time $t^* \in JE$ a Capa 3 transition occurs (detectable global structural reorganization), then there is an ontological ascent $L_m \to L_{m+1}$ such that, from t^* onward, the system operates under a new regime of discreteness characterized by a new effective set of active renormalization depths, a new dominant law of accumulation $\Delta t_k^{(m+1)}$, and new emergent properties of t_n. The newly stabilized level L_{m+1} imposes downward constraints on admissible configurations at lower strata; the prior discreteness operator is thereby supplanted.

The autonomy of this event is essential. The law of admissible Δt_k is constitutive of the ontological level. At each stabilized L_m the system possesses a specific operator that defines which renormalization depths are accessible and how local intervals accumulate into observable t_n. Because this operator is internal to the stratum, no quantity of episodes governed by the operator of L_m can generate the distinct operator of L_{m+1}. Accumulation and intensification remain internal to the prior discreteness regime; they cannot institute a new one. What emerges at ontological kairos is a new temporal reality—a *discreción temporal propia*—not a larger instance of the former. The new law of discreteness was not operative in dominant form within the preceding regime.

The observable trace of this top-down stabilization is the persistence of altered Δt_k statistics after t^*. Once L_{m+1} is stabilized, persistence and coherence patterns admissible under L_m become inadmissible or statistically suppressed. The reorganization of discreteness intervals, not the incidence of their putative facilitators, remains the primary marker. Effective renormalization depth and Higuchi dimension of t_n may show only modest shifts, indicating that the primary change resides in the support and shape of the local interval distribution rather than in average compression. The mechanism of bidirectional filtering together with the downward constraints closes the loop: by restricting the configurations that can sustain the prior regime, the new stratum actively maintains its own discreteness law.

14.0.4 Explicit Contrast: Preparation versus Constitution

Relational kairos prepares possibility through bidirectional probabilistic filtering at Capa 2. Ontological kairos constitutes a new temporal reality by instituting a self-sustaining discreteness law at L_{m+1} together with the downward constraints that actively maintain it. Capa 3 is not a linear extrapolation of local intensity within a fixed temporal scaffolding; it is an event of ontological emergence.

The contrast can be stated in terms of the RECD law itself. Under the current stabilized regime L_m, the gated, renormalized increments are given by the law $\Delta t_k = \delta^{-k}|\tau_s(k)|\Delta t_0/n$ with the gate $g(\tau_s)$ operating according to the level's characteristic selector. Inside a relational kairos—a sustained low-$A(k)$ window—the increments continue to be generated by this same law. What changes is the measure of local configurations that can contribute without being fragmented by cross-component disagreement.

The low antisynchronization relaxes the suppression that would otherwise occur, thereby enlarging (probabilistically) the set of paths that remain compatible with the accumulation process. The distribution of realized Δt_k may exhibit transient features associated with the episode (longer coherent runs, deeper residence at particular renormalization levels), but the fundamental operator—the functional form of the law and the set of accessible depths—remains that of L_m.

After ontological kairos the operator itself is replaced. The post-ascent series of Δt_k is drawn from a statistically distinct distribution, detectable by Kolmogorov–Smirnov contrast. The effective range of active renormalization depths K_m shifts; the gate behavior may change because the characteristic statistics of $|\tau_s|$ under the new regime differ; the admissible ordinal configurations that can sustain the accumulation are now delimited from above by the downward constraints of L_{m+1}. The same physical processes, observed through the same instruments, now generate different discrete temporal structures. The future increments are no longer extrapolations of the prior law; they are generated under the new law instituted at the ascent.

14.0.5 Integration with the RECD Law and the Three-Layer Ontology

The RECD law supplies the precise mathematical substrate on which the distinction operates. The gated, renormalized increments Δt_k are constructed from ordinal conjunctions that occur only inside the chaotic regime $|\tau_s| < 0.41$. The gate $g(\tau_s)$ selects or compresses these increments according to the proximity of the system to critical surfaces. At each stabilized level L_m the law functions as the discreteness operator: it determines which renormalization depths are accessible and how the local intervals accumulate into the observable process $t_n = \sum g(\tau_s) \cdot \Delta t_k$.

Relational kairos corresponds to intervals during which the current operator is active but the relational conditions (low $A(k)$) permit a broader sampling of the configurations that the operator can integrate. The Joint Episode is the unit in which Capa 1 intensification occurs inside a sustained Capa 2 window, thereby realizing the enabling window without altering the operator. Ontological kairos corresponds to the event in which the structural reorganization modifies the set of admissible configurations so thoroughly that a new effective operator—a new characteristic law of Δt_k—becomes dominant and self-sustaining. The three-layer ontology locates the Joint Episode at the L1–L2 interface; the Principle of Ontological Ascent and the distinction of kairos orders locate the crossing at L3. The modest predictive power of the Joint Score is the direct empirical consequence: the score robustly detects the enabling condition at L1–L2; the actual L3 crossing remains an autonomous replacement of the operator.

14.0.6 Concrete Illustrations from Synthetic Ensembles and the Dengue Series

The empirical record confirms both the reality of the enabling function and the categorical distinction. A uniform data-driven protocol—Frobenius-norm correlation shift combined with Kolmogorov–Smirnov change-point scan on the Δt series—was applied to coupled logistic maps, Lorenz oscillators, and the dengue incidence series from San Juan ($T = 936$ weeks) and Iquitos ($T = 520$ weeks). In every synthetic ensemble the KS contrast on Δt reached high values (0.41–0.79) with extremely low p-values, frequently attaining significance in 100 percent of logistic realizations. Pre-transition Joint Episodes were rare: coupled logistic ensembles exhibited pre-JE fraction 0.00; Lorenz ensembles 0.23–0.46.

For the dengue series the same detector returned KS = 0.781 ($p \approx 0$) for San Juan at week 165 and KS = 0.209 for Iquitos at week 305. In both cities the detected t^* coincided with major incidence peaks (within 5 weeks for San Juan; 18 weeks for Iquitos). Pre-transition Joint Episodes were rare overall (global fraction 0.258, or 8 out of 31 episodes across the examined series). San Juan exhibited only one preceding episode out of eighteen total (fraction 0.056), yet produced the strongest Δt reorganization. Iquitos showed a higher preceding fraction (0.538, or 7 out of 13) but a milder distributional shift. Strong ascent signatures therefore appear even when relational kairoi are sparse or absent.

These numbers carry direct ontological implications. The series with the sparsest preceding relational windows (San Juan, pre-fraction 0.056) yielded the largest KS contrast on the law of discreteness intervals (0.781). The enabling function of relational kairos is real—the single pre-transition episode in San Juan may have contributed to the configuration space that permitted the ascent—but the episode did not determine or constitute the reorganization. The modest predictive performance based solely on relational precursors (AUC $\approx$ 0.476) is ontologically informative precisely because the conditions that render a new discreteness regime possible are not identical with the conditions that actualize it. If the Joint Score had been a strong predictor of Capa 3 reorganization, the architecture would have been closer to a reductive, accumulative model in which sufficient intensification at lower layers simply sums to the higher stratum. The observed modesty of predictive power is the signature that the ascent is an autonomous ontological event.

14.0.7 Why Modest Predictive Power Is Ontologically Informative

In the low-dimensional Lorenz testbed, even oracle labeling—perfect foreknowledge of which Joint Episodes were proximal to Layer 3 reorganization—yields a maximum AUC of only ≈ 0.476. This result is not a failure of the detector. It is the expected consequence of the distinction between the two orders of kairos. The Joint Episode is a robust detector of L1–L2 coherence; it registers the relational conditions under which bidirectional filtering can enlarge the space of contributing configurations. It does not register the autonomous stabilization of a new law at L3. The same point is visible in the dengue record: the city whose pre-transition relational activity was sparsest nevertheless exhibited the clearest reorganization of Δt_k. Predictive power based on relational precursors must remain modest if the ontology is non-reductive. Strong prediction from the enabling window alone would imply that the window already contains, in accumulated form, the operator of the subsequent regime—precisely the reduction that the Principle of Ontological Ascent and the kairos distinction rule out.

14.0.8 Bridge to Data-Driven Detection and Downward Constraints

The distinction between relational and ontological kairos supplies the conceptual frame required for the chapters that follow. The data-driven detection protocol—Frobenius-norm shift on multichannel τ_s correlation matrices combined with KS contrast on the Δt_k series—operationalizes the claim that reorganization of the law of discreteness intervals is the primary signature of ascent. The protocol is deliberately insensitive to the mere density of preceding Joint Episodes; its power derives from the distributional change in Δt_k itself. The subsequent analysis of downward constraints then examines the mechanism by which the newly stabilized L_{m+1} actively maintains its own law: by rendering inadmissible or statistically suppressed those configurations that would have sustained the prior regime. Together these developments complete the technical articulation of the Principle of Ontological Ascent. Each inherits its justification from the RECD law, from the three-layer ontology that locates the Joint Episode, and from the categorical distinction between the preparatory window and the autonomous constitution of a new stratum of discrete time.

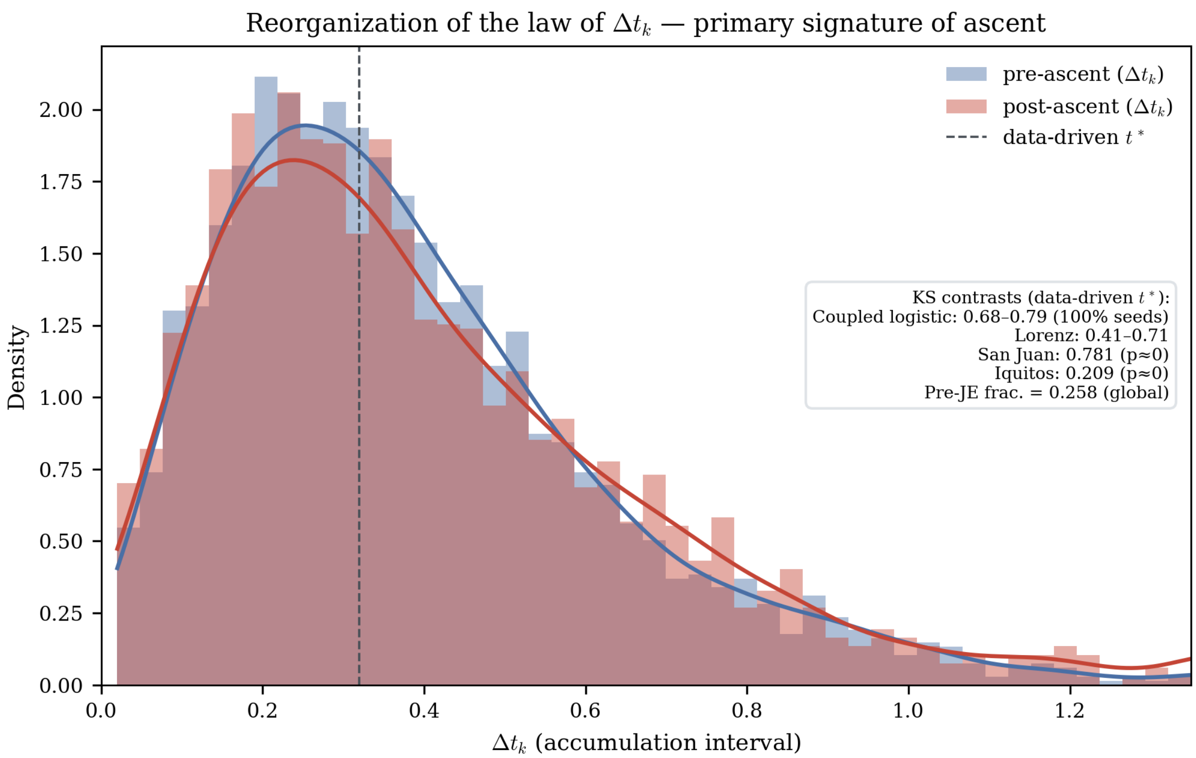

Figure 14.1: Example pre/post change-point contrast on the RECD increment law (distributional shift in Δt_k), used as a primary marker of Capa 3 reorganization.

Chapter 15

Data-Driven Detection and Dengue Results

Chapter 13

Once the Principle of Ontological Ascent has been stated and the distinction between relational and ontological kairos has been articulated, a methodological demand becomes unavoidable: the claim that a system has crossed from one stabilized regime of discrete time L_m to another L_{m+1} must be made detectable by operations that do not presuppose the very ontological transition they are meant to reveal. A uniform, data-driven detection protocol is therefore required. Such a protocol cannot rely on the mere density or intensity of preceding Joint Episodes, for the preceding analysis has shown that relational kairos is necessary yet insufficient and that the strongest signatures of ascent can appear where preceding relational windows are sparsest or absent. The protocol must instead interrogate the statistical law of the discreteness intervals themselves. Only by registering a qualitative reorganization of Δt_k can one claim, on empirical grounds, that the discreteness operator has been supplanted rather than merely exercised more vigorously inside the prior regime.

This chapter presents and justifies the uniform detection protocol that operationalizes the Principle. The protocol combines a Frobenius-norm shift detector on the multichannel correlation structure of τ_s with a Kolmogorov–Smirnov change-point scan on the derived series of renormalized increments Δt_k. It is applied identically, without external labels or programmed change points, to controlled synthetic ensembles (coupled logistic maps and Lorenz oscillators) and to the dengue incidence series of San Juan and Iquitos. The results demonstrate that reorganization of the law of discreteness intervals—not the accumulation of preceding relational episodes—is the dominant and most reproducible signature of Capa 3 ascent. The chapter then integrates these findings with the RECD law and the three senses of strong Bayesian optimality established for the discrete accumulator, thereby exhibiting the non-reductive character of the ontology in concrete quantitative terms. The analysis closes with a precise bridge to the examination of downward constraints developed in the chapter that follows.

15.0.1 The Uniform Data-Driven Detection Protocol

The protocol locates candidate transition times t^* by two complementary, label-free operations performed on the multichannel series of systemic coherence $\tau_s(k)$ and on the associated discreteness increments Δt_k.

The first detector registers global structural change in the relational field. For each candidate time t, the channel-wise correlation matrix of the τ_s process is computed on the prefix interval $[1, t]$ and again on the suffix interval $[t + 1, T]$. The Frobenius norm of the difference between these two matrices quantifies the magnitude of the shift in second-order dependence structure across the components. The time t that maximizes this distance is retained as a candidate for structural reorganization.

The second detector interrogates the law of temporal discreteness directly. For each candidate t, a two-sample Kolmogorov–Smirnov statistic is computed between the empirical distribution of $\Delta t_k[1 : t]$ and the empirical distribution of $\Delta t_k[t+1 : T]$. The KS statistic measures the maximum vertical distance between the cumulative distribution functions and is therefore sensitive to any change in location, scale, or shape of the increment law. The location of the global maximum of this statistic is retained.

A consensus t^* is formed from the two detectors: when the candidates agree within a modest tolerance the median is adopted; when they diverge the higher-scoring detector governs. The identical procedure—identical windowing conventions, identical correlation construction, identical KS application, identical consensus rule—is executed on every realization and every empirical series. No information about the location or existence of Joint Episodes enters the detectors. The protocol therefore operationalizes the ontological claim that the primary marker of ascent resides in the replacement of the discreteness operator, not in the density of its putative enablers.

The RECD supplies the precise definition of the increments under scrutiny. Inside the chaotic regime the gate opens and the local step is given by the renormalized law

$\Delta t_k = \delta^{-k} \cdot |\tau_s(k)| \cdot \frac{\Delta t_0}{n_{\text{win}}}$,

where $\delta \approx 4.6692016091$ is the Feigenbaum constant, and the integrated extramental time is accumulated as $t_n = \sum_k g(\tau_s(k)) \cdot \Delta t_k$. A detectable reorganization of the statistical law of Δt_k is therefore a detectable change in the effective operator that governs how local ordinal coherence is converted into objective temporal intervals at the new ontological level.

15.0.2 Why Reorganization of the Law of Discreteness Intervals Is the Primary Signature

If the ascent from L_m to L_{m+1} were a cumulative or intensificatory phenomenon, one would expect the frequency or integrated intensity of preceding Joint Episodes to serve as a strong predictor of the magnitude of the subsequent Δt_k shift. The stronger or more numerous the relational windows, the larger the expected distributional contrast should be. The data-driven protocol was deliberately constructed to be insensitive to this hypothesis. It receives as input only the multichannel τ_s matrix and the derived Δt_k series; it returns a candidate t^* and a KS contrast without ever counting episodes.

The justification for privileging the reorganization signature follows directly from the non-reductive structure already established. Relational kairos, realized as sustained low-A_{antis} intervals containing critical-mass peaksM_{crit}, functions through bidirectional probabilistic filtering: upward, it enlarges the space of admissible local configurations that can contribute to higher-stratum coherence; after ascent, downward constraints render previously admissible configurations statistically suppressed or inadmissible under the new operator. These filtering operations prepare the possibility of a new discreteness regime. They do not institute the regime. The constitutive event is the autonomous stabilization of a new law of accumulation intervals together with the downward constraints that maintain it. Consequently, the observable trace of that event must be a change in the law itself, not a change in the density of the preparatory windows.

Empirical patterns confirm the design choice. In the synthetic ensembles the pre-transition Joint Episode fraction is zero for the logistic generator and only moderate (0.23–0.46) for Lorenz, yet every realization that undergoes structural perturbation exhibits a statistically significant shift in the Δt_k distribution. In the dengue record the city with the sparsest preceding episodes (San Juan, fraction 0.056) produces the largest KS contrast (0.781), while the city with the higher preceding fraction (Iquitos, 0.538) produces a milder though still significant shift (0.209). The global pre-transition rarity across real series is 0.258. If the protocol had been built around episode counts, these outcomes would have appeared paradoxical or noisy. Once the distinction between the two orders of kairos is in place, they are exactly the pattern required by a non-reductive ontology: the conditions that render ascent possible are not the conditions that actualize it.

15.0.3 Results from Synthetic Ensembles

The protocol was applied uniformly to two families of minimal modular systems.

For coupled logistic maps ($r = 3.8$), fifty independent realizations were generated with $T = 3500$ steps. A combined structural perturbation—increase of diffusive coupling strength together with a global-to-ring topology switch—was introduced near the programmed midpoint without any reference to the detection procedure. In every realization the KS contrast on Δt_k attained high values in the range 0.68–0.79, with $p \ll 0.001$, reaching statistical significance in 100 percent of the ensemble. The pre-transition Joint Episode fraction was identically zero. The detected t^* clustered near the midpoint, consistent with the timing of the imposed structural change. The logistic generator therefore supplies the cleanest demonstration that a qualitative reorganization of the discreteness law can be produced by a Capa 3 structural event even when no preceding relational kairos is registered.

For diffusively coupled Lorenz oscillators (standard parameters $\sigma = 10$, $\rho = 28$, $\beta = 8/3$), ensembles were subjected to parameter ramps or combined topological perturbations. The same blind protocol returned KS contrasts in the range 0.41–0.71 with low p-values. Pre-transition Joint Episode fractions lay between 0.23 and 0.46. The detected transitions aligned with the intervals of structural perturbation, and post-transition persistence of the altered increment statistics was observed. The Lorenz generator, although more variable across seeds, reproduces the essential signature: a detectable change in the law of Δt_k that is not reducible to the density of preceding low-antisynchronization intervals.

These synthetic results establish a baseline. Under controlled conditions in which the ground-truth structural perturbation is known but withheld from the detector, the reorganization of discreteness intervals emerges as the most consistent and reproducible marker of ascent across qualitatively different chaotic generators.

15.0.4 Results from the Dengue Incidence Series

The identical protocol was applied to the two longest weekly dengue series: San Juan, Puerto Rico ($T = 936$ weeks) and Iquitos, Peru ($T = 520$ weeks). Three-channel τ_s matrices (incidence together with climate-derived covariates) were used; incidence peaks were identified independently from the raw case series for alignment validation.

In San Juan the consensus t^* fell at week 165. The Kolmogorov–Smirnov contrast between the pre- and post-t^* Δt_k distributions reached 0.781 with $p \approx 0$. Only one Joint Episode preceded this transition (fraction 0.056 out of eighteen total episodes). The detected t^* lay within five weeks of a major incidence peak. In Iquitos the consensus t^* occurred at week 305. The KS contrast was 0.209 ($p \approx 0$); seven of thirteen episodes (fraction 0.538) preceded the transition, and alignment with a strong peak was within eighteen weeks.

Across the examined real series the global pre-transition Joint Episode fraction was 0.258 (eight of thirty-one episodes). The contrast between the two cities is ontologically instructive. San Juan, the series whose relational kairos was sparsest, exhibited the largest distributional reorganization of the discreteness intervals. Iquitos, with substantially higher preceding relational activity, exhibited a milder though still significant shift. The pattern replicates the synthetic finding that strong ascent signatures are compatible with, and in the clearest case occur where, preceding relational windows are minimal.

Post-ascent persistence of the altered Δt_k statistics was observed in both cities. Effective renormalization depth and Higuchi dimension of the integrated process t_n showed only modest shifts. The primary change therefore resides in the support and shape of the local interval distribution rather than in average compression or overall persistence length. This persistence supplies an observable trace of the downward constraints that stabilize the new regime once L_{m+1} has been instituted.

15.0.5 Integration with the RECD Law and the Three Senses of Bayesian Optimality

The detection of a new law of Δt_k acquires its full significance only when placed inside the RECD framework. The increments are not arbitrary time steps; they are the canonical accumulation of evidence, under purely ordinal observability, for proximity to criticality. The RECD law

$\Delta t_k = \delta^{-k} \cdot |\tau_s(k)| \cdot \frac{\Delta t_0}{n_{\text{win}}}$

(with the gate $g(\tau_s)$ opening inside the chaotic range $|\tau_s| < 0.41$) emerges as the exact sequential Bayesian update of the log-posterior on the critical-proximity parameter when observations are restricted to ordinal configurations. The large-deviation rate function that governs atypical values of τ_s decays geometrically with renormalization depth at the universal rate set by δ.

Within the natural class of accumulation schemes that depend on τ_s only through potentials of the same functional form, the RECD is strongly optimal simultaneously in three interlocking senses. It maximizes the exponential growth rate of the log-posterior. It is minimax optimal across adversarial sequences of renormalization levels. It maximizes the long-run accumulation of ordinal Kullback–Leibler divergence. The optimality is information-theoretically equivalent to weighting successive increments by successive powers of the Feigenbaum eigenvalue itself.

When the data-driven protocol registers a statistically significant shift in the distribution of Δt_k, it registers a change in the effective operator under which this strongly optimal accumulation now proceeds. The new regime is not a continuation or rescaling of the prior increments inside a fixed scaffolding; it is a replacement of the scaffolding. The three senses of optimality therefore attach to the new law at L_{m+1}. No quantity of increments governed by the operator of L_m can generate the distinct operator of L_{m+1}. The modest predictive power of relational scores (AUC $\approx$ 0.476 even under oracle labeling) and the observed rarity of pre-transition Joint Episodes are not defects of the framework; they are the measurable signature that the ascent is an autonomous ontological event rather than an accumulative extrapolation.

15.0.6 Post-Ascent Persistence and the Bridge to Downward Constraints

The persistence, after t^*, of the altered statistics of Δt_k is the first empirical indication that the new stratum actively maintains itself. Once the operator has been replaced, configurations that would have sustained the prior regime become less probable or inadmissible under the new law. The modest accompanying changes in average renormalization depth and fractal dimension of t_n further indicate that the transition is not an intensification of existing dynamics but a qualitative reorganization of the admissible set of local intervals. Downward constraints close the loop: the newly stabilized level L_{m+1} does not merely emerge; it reshapes the possibility space of the strata from which it arose.

These observations supply the direct empirical warrant for the analysis developed in the following chapter. There the mechanism of downward constraint is examined in greater technical detail: how the new discreteness law renders certain renormalization depths statistically suppressed, how the gate function itself may be reconfigured, and why the irreducibility of the new operator to any finite accumulation of prior episodes is not an additional hypothesis but the mathematical content of the Principle of Ontological Ascent itself. The data-driven detection protocol developed here provides the uniform, reproducible signature whose persistence after t^* makes that subsequent analysis both possible and necessary.

Chapter 16

Downward Constraints and the Irreducibility of Ascent

Chapter 14

The persistence, after a detected t^*, of altered statistics in the series of discreteness intervals Δt_k raises a question that cannot be postponed. If the reorganization registered by the Kolmogorov–Smirnov contrast on Δt_k and the Frobenius-norm shift on the multichannel τ_s structure marks the crossing from one stabilized ontological regime L_m to another L_{m+1}, then the fact that the new distribution of increments remains in force rather than reverting supplies direct evidence that the newly instituted law actively maintains itself. This maintenance cannot be a passive residue of prior conditions. It must consist in the imposition of constraints that render certain configurations at lower strata less probable or inadmissible under the law now operative at the higher stratum. The question of downward constraints is therefore not an optional philosophical addendum; it is the natural completion of the Principle of Ontological Ascent itself. Once one has shown that ascent is detectable as replacement of the discreteness operator and that this replacement occurs with only modest accompanying shifts in average renormalization depth or Higuchi dimension of the integrated process t_n, the persistence of the new operator demands an account of how L_{m+1} reshapes the possibility space of the strata from which it arose.

This chapter develops that account. It articulates the concept of downward constraints as the active delimitation, by the stabilized higher level, of admissible configurations at subordinate levels. It shows why the emergence of a new discreteness regime constitutes the institution of a *discreción temporal propia* rather than a quantitative extension of the preceding regime. It establishes the rigorous irreducibility of the new operator to any finite accumulation or intensification internal to L_m. It reconnects these results to the RECD accumulation law and to the three interlocking senses of strong Bayesian optimality. It integrates the entire construction with the three-layer ontology and the Joint Episode as ontologically enabling but non-determining window. Concrete illustrations are drawn from the post-ascent behavior of the dengue incidence series. The chapter closes by stating explicitly that the irreducibility in question is not an additional metaphysical postulate but the precise mathematical content of the Principle of Ontological Ascent, and by indicating how the stratified, non-reductive ontology thereby completed opens onto the fractal geometry of the accumulated extramental time.

16.0.1 Downward Constraints: Reshaping the Admissible Set at Lower Strata

At each stabilized ontological level L_m the system operates under a characteristic law of local discreteness intervals Δt_k together with a corresponding set of admissible ordinal configurations. This law functions as the discreteness operator: it determines which renormalization depths are accessible in dominant measure, how the gate $g(\tau_s)$ opens or closes, and how local ordinal coherence is converted into increments of objective time. A global structural reorganization of sufficient scope—registered as a Capa 3 transition—modifies precisely this set of admissible configurations. When the reorganization stabilizes a new level L_{m+1}, the prior discreteness operator is supplanted. The newly stabilized level does not merely coexist with the old; it imposes downward constraints that actively delimit the configurations that lower strata can sustain.

These constraints are observable in the post-ascent persistence of the altered Δt_k distribution. Once L_{m+1} is in place, persistence and coherence patterns that were admissible under L_m become inadmissible or statistically suppressed under the new law. The gate behavior, the typical durations of gate-open episodes, and the clustering of increments at particular renormalization depths are reconfigured. Certain depths that contributed substantially before the transition become rare or ineffective; others that were previously suppressed become part of the new characteristic range. The effect is top-down: the higher stratum does not eliminate lower strata but restricts the configurations at those strata that can continue to support the dynamics of the prior regime. The lower strata remain the material substrate; the new scaling law and the new operator together impose constraints on admissible durations, admissible clustering, and admissible renormalization depths at all subordinate levels.

The mechanism is already implicit in the definition of stabilized ontological regime. A system occupies L_m when its persistence, antisynchronization, and accumulation dynamics operate predominantly within the characteristic range of renormalization depths, gate behavior, and fractal signatures associated with that level. When a Capa 3 reorganization occurs, the effective range changes. Depths that previously lay inside the active band may fall outside it under the new operator; conversely, depths previously marginal may enter the dominant band. The downward constraint is the statistical expression of this change of band: configurations whose renormalization statistics would have sustained the old law are now less likely to recur at the frequencies required by the old regime. The new stratum thereby maintains its own discreteness law by rendering the old one non-self-sustaining.

This reshaping is not a side-effect of increased intensity at lower layers. It is the direct consequence of the replacement of the operator. The data-driven protocol registers the replacement through the KS contrast on Δt_k; the persistence of that contrast after t^* registers the constraint.

16.0.2 The Emergence of a *Discreción Temporal Propia*

What emerges at ontological ascent is therefore a new temporal reality rather than a larger or more intense instance of the former regime. The reorganization at Capa 3 reconfigures the set of accessible depths and thereby supplants the operator. The new law of discreteness was not operative in dominant form within the preceding regime; its actualization at L_{m+1} is not the summation or extrapolation of prior conditions but the emergence of a new ontological stratum. The phrase *discreción temporal propia* captures precisely this autonomy: the new level possesses its own characteristic law of accumulation intervals, its own effective range of renormalization depths, and its own downward constraints. It is not obtained by rescaling the increments of L_m or by prolonging the gate-open episodes that were already available under the old operator.

Empirical support for this distinction appears in the modest character of the accompanying changes in average renormalization depth and in the Higuchi dimension of the integrated process t_n. If ascent were merely intensification inside a fixed scaffolding, one would expect large shifts in compression (deeper average k) and in the fractal roughness of accumulated time. Instead, the primary change resides in the support and shape of the local interval distribution itself. The same average depth and the same rough dimension can be realized by qualitatively different laws of Δt_k. The new law is not a quantitative continuation; it is a different operator that generates increments according to a reconfigured admissible set. The persistence of the new distribution after t^*, together with the relative stability of the global compression measures, demonstrates that the system has acquired a *discreción temporal propia* whose signature is precisely the reorganization of the discreteness intervals rather than a simple amplification of prior dynamics.

16.0.3 Irreducibility: Why No Finite Accumulation Generates the New Operator

The claim that the new operator is irreducible to the prior regime receives a rigorous formulation once the internal character of the discreteness law is recognized. At each stabilized L_m the system possesses a specific operator that defines which renormalization depths are accessible and how local intervals accumulate into observable t_n. Because this operator is internal to the stratum, no quantity of episodes governed by the operator of L_m can generate the distinct operator of L_{m+1}. Accumulation and intensification remain internal to the prior discreteness regime; they cannot institute a new one.

To see why, consider what a finite sum of prior gated increments can achieve. Each increment Δt_k produced under L_m is already scaled by the powers of δ and weighted by the gate appropriate to that level. Summing more of them, or weighting them more heavily through sustained low antisynchronization, can increase the total accumulated time or the frequency of particular depths. It cannot alter the functional form of the scaling, the range of depths that the gate treats as admissible, or the statistical law that governs which increments are realized. Those features are fixed by the operator itself. Replacing the operator means instituting a new law of admissible Δt_k whose parameters (effective band of k, gate thresholds, weighting by successive powers of δ) are no longer those of L_m. No finite collection of increments generated under the old parameters can produce the new parameters, because the parameters belong to the law that selects and scales the increments, not to the increments taken distributively.

This irreducibility is already visible in the synthetic and epidemiological results. In the coupled logistic ensembles the pre-transition Joint Episode fraction is identically zero, yet every realization that undergoes the structural perturbation exhibits a statistically significant and persistent reorganization of Δt_k. In San Juan the pre-transition fraction is only 0.056, yet the KS contrast reaches 0.781. The strongest reorganization signatures appear where preceding relational activity is sparsest. If the new law were the cumulative product of prior gated increments, these cases should be the weakest; instead they are the clearest demonstrations that the crossing is an autonomous event. The conditions that render a new discreteness regime possible—relational windows of low antisynchronization containing critical-mass peaks—are not the conditions that actualize it. The actualization consists in the stabilization of the new operator together with the downward constraints that maintain it.

The Principle of Ontological Ascent therefore states the irreducibility directly: the ascent institutes a new regime of accumulation intervals Δt_k together with emergent properties of the integrated process t_n that are irreducible to continuation or summation of the preceding level. The newly stabilized level L_{m+1} imposes downward constraints on admissible configurations at lower strata; the prior discreteness operator is thereby supplanted. The mathematical content of the principle is precisely that the new operator cannot be recovered as any finite sum, extrapolation, or intensification of increments generated under the old operator.

16.0.4 Connection to the RECD Law and the Three Senses of Bayesian Optimality

The RECD supplies the canonical form of the accumulation rule whose operator is replaced at ascent. Inside the chaotic regime the local increment is given by

$\Delta t_k = \delta^{-k} \cdot |\tau_s(k)| \cdot \frac{\Delta t_0}{n_{\text{win}}}$,

with the gate $g(\tau_s)$ opening when $|\tau_s|$ lies inside the band that activates the chaotic range. The integrated extramental time is accumulated as $t_n = \sum g(\tau_s(k)) \cdot \Delta t_k$ Within the natural class of accumulation schemes that depend on τ_s only through potentials of the same functional form, the RECD is strongly optimal simultaneously in three interlocking senses: it maximizes the exponential growth rate of the log-posterior; it is minimax optimal across adversarial sequences of renormalization levels; and it maximizes the long-run accumulation of ordinal Kullback–Leibler divergence. The optimality is information-theoretically equivalent to weighting successive increments by successive powers of the Feigenbaum eigenvalue δ itself.

When a Capa 3 reorganization replaces the discreteness operator, the canonical accumulation rule itself changes. The new regime at L_{m+1} operates under a law of Δt_k whose effective renormalization depths, gate behavior, and scaling parameters are those of the new level. The three senses of optimality therefore attach to the new law. The exponential growth of the log-posterior, the minimax robustness, and the long-run ordinal information gain are now realized under the reconfigured operator. No quantity of increments governed by the operator of L_m can produce this reconfigured optimality, because the optimality is defined relative to the particular weighting by powers of δ that the new operator employs. The change of operator is simultaneously a change in the accumulation rule under which the three senses are realized. This is why the persistence of the altered Δt_k distribution after t^* is not merely a statistical curiosity; it is the observable trace that a new strongly optimal accumulator has been instituted.

16.0.5 Integration with the Three-Layer Ontology and the Joint Episode

The three-layer ontology supplies the precise stratification within which downward constraints operate. Capa 1 (local hyper-persistence and critical mass) furnishes the intensificationsM_{crit} that may seed higher-order coherence. Capa 2 (relational coherence across modules) realizes sustained low antisynchronization A_{antis} that functions through bidirectional probabilistic filtering: upward, it enlarges the space of local configurations compatible with global coordination; after ascent, the new level imposes constraints that render previously admissible patterns statistically suppressed. Capa 3 (global structural reorganization) is the level at which the discreteness operator itself is replaced and the new stratum with its downward constraints is stabilized.

The Joint Episode is the concrete relational window inside which these layers interact. Defined as a maximal contiguous interval of low antisynchronization containing at least one critical-mass peak and satisfying an integrated-intensity threshold, the Joint Episode marks an ontologically enabling interval at Capa 2. It raises the likelihood that lower-layer configurations may crystallize at a higher stratum without determining the outcome. The modest predictive power of relational scores (AUC approximately 0.476 even under oracle labeling of episodes) and the observed global pre-transition rarity of 0.258 confirm that the enabling function is real yet non-deterministic. Relational kairos prepares possibility; ontological kairos constitutes the new temporal reality by instituting the self-sustaining discreteness law together with the downward constraints that actively maintain it.

Downward constraints close the loop. By restricting the configurations that can sustain the prior regime, the new stratum actively maintains its own discreteness law. Lower strata are not eliminated when the higher stratum appears; they remain the material out of which the higher increments are constituted, while the new scaling law imposes downward constraints on admissible durations and clustering of gate-open episodes at all subordinate levels. The non-reductive character of the ontology is therefore expressed simultaneously in two directions: relational kairos enables without determining, and downward constraints stabilize without erasing the substrate. The Joint Episode is the relational window; the replacement of the operator together with the imposition of downward constraints is the ontological event.

16.0.6 Concrete Illustrations from the Dengue Incidence Series

The dengue incidence series of San Juan ($T = 936$ weeks) and Iquitos ($T = 520$ weeks) supply the clearest natural illustration of post-ascent persistence under modest shifts in global compression measures. The data-driven protocol located Capa 3 transitions at week 165 in San Juan (KS = 0.781 on Δt_k, pre-transition Joint Episode fraction 0.056, alignment within five weeks of a major incidence peak) and at week 305 in Iquitos (KS = 0.209, pre-transition fraction 0.538, alignment within eighteen weeks). In both cities the post-t^* persistence of the altered Δt_k statistics was observed. Effective renormalization depth and Higuchi dimension of t_n showed only modest shifts. The primary change resided in the support and shape of the local interval distribution rather than in average compression.

This pattern is exactly what the downward-constraint account predicts. The strongest distributional reorganization (San Juan) occurs in the series with the sparsest preceding relational activity. Once the new operator is in place, the altered law of increments persists even though the macroscopic compression of accumulated time, as measured by average depth and Higuchi dimension, changes only modestly. Large dengue outbreaks, under this reading, mark macroscopic expressions of an ontological transition in the system's intrinsic temporal organization rather than simple amplifications of local transmission intensity. The reorganization of discreteness intervals, not the incidence of their putative facilitators, remains the primary marker. The persistence of the new distribution after t^* is the observable trace of the top-down stabilization effected by downward constraints.

16.0.7 Irreducibility as Mathematical Content of the Principle and Bridge to Part VI

The irreducibility of the new operator is not an additional metaphysical postulate imposed upon the data. It is the mathematical content of the Principle of Ontological Ascent. The principle states that a Capa 3 global structural reorganization constitutes an ascent from a stabilized regime L_m to L_{m+1} such that, from t^* onward, the system operates under a new regime of discreteness characterized by a new effective set of active renormalization depths, a new dominant law of accumulation Δt_k, and new emergent properties of t_n that are irreducible to continuation or summation of the preceding level. The newly stabilized level imposes downward constraints on admissible configurations at lower strata; the prior discreteness operator is thereby supplanted. Every clause of this statement is required by the empirical signature: the KS-detectable reorganization of Δt_k, its persistence after t^* with only modest shifts in average depth and Higuchi dimension, and the variable or zero density of preceding Joint Episodes.

This non-reductive, stratified ontology completes the conceptual architecture of Part V. The three-layer structure, the Joint Episode as primitive enabling unit, the distinction between relational and ontological kairos, the data-driven detection protocol, and the explicit mechanism of downward constraints together describe a dynamics in which emergence at one level reshapes the possibility space of the strata from which it arose without reducing higher strata to lower or erasing the material substrate. The accumulated extramental time T generated under the new discreteness law now carries the imprint of that law. Its fractal properties—the similarity dimension of the renormalized laminar intervals, the global dimension $D \approx 1.98$ with rigorous bounds $1.96 \leq D \leq 2.01$, the topological justification furnished by the 2-adic conjugacy—become intelligible as properties of time generated under a specific operator that itself can change when the system undergoes ontological ascent. The analysis of the fractal geometry of extramental time in Part VI therefore proceeds on the foundation secured here: the discrete architecture is stratified, the operators are replaceable, and the constraints run downward as well as upward.

Chapter 17

The Similarity Dimension of Renormalized Laminar Intervals

Chapter 15

The accumulated extramental time T generated by the Discrete Extramental Clock Law (RECD) is not a uniform, homogeneous continuum. It is a discrete, event-driven, and hierarchically organized quantity whose support carries an intrinsic fractal geometry. This geometry is not an accidental numerical feature discovered after the fact; it is the direct and inevitable consequence of the renormalization structure that Theorem v24 imposes upon the observable τ_s once the ordinal dynamics of a multicomponent flow have been reduced to a unimodal return map of class C^3 with non-degenerate quadratic critical point. The same structure that forces the Feigenbaum constant $\delta \approx 4.6692016091$ into the increment rule $\Delta t_k = \delta^{-k}|\tau_s(k)|t_0/n$ also forces the set of renormalized laminar intervals to be self-similar. Consequently the integrated process T acquires a well-defined fractal dimension whose value and whose rigorous bounds are fixed by that self-similarity together with the ergodic properties of the underlying attractor.

The pedagogical purpose of the present chapter is to derive this dimension explicitly, to show why the pure similarity dimension of the laminar intervals must be corrected by the invariant measure, and to explain what the numerical result $D \approx 1.98$ (with bounds $1.96 \leq D \leq 2.01$) reveals about the ontology of extramental time. The derivation proceeds in steps that remain entirely internal to the corpus: the combinatorial organization of low-coherence runs, the renormalization operator inherited from Feigenbaum theory, the weighting prescribed by the RECD, and the distortion control furnished by the C^3 estimates of Theorem v24. No external postulates are added.

17.0.1 The Hierarchical Structure of Renormalized Laminar Intervals

A laminar interval is a maximal contiguous run of the indicator process $s(k) = 1$, where $s(k) = 1$ precisely when $|\tau_s(k)| < 0.41$. These runs are the observable substrate of the periods during which the gate function of the RECD is open and discrete extramental time is being generated. Because the underlying return map reconstructed by Theorem v24 belongs to the Feigenbaum universality class, the organization of these runs itself obeys a period-doubling cascade.

Let R_k denote the collection of all maximal low-coherence runs that appear at renormalization depth k. At depth k the tree contains exactly 2^k terminal runs. Each run of effective length L at depth k is replaced, at depth $k+1$, by two daughter runs whose lengths and return statistics are scaled by the universal factor δ^{-1}. This generates a binary tree of runs whose terminal intervals at depth k are assigned, via the RECD, laminar durations proportional to δ^{-k}.

In the limit the collection of all such intervals forms a set

$\Lambda = \bigcup_{k=0}^{\infty} \Lambda_k$,

where $Lambda_k$ is the union of the 2^k intervals contributed at depth k. The set satisfies the self-similarity relation

$$\Lambda = \phi_1(\Lambda) \cup \phi_2(\Lambda),$$

in which each contraction phi_i scales lengths by the factor δ^{-1}. The gaps between runs at each level are intervals of high coherence whose durations are bounded away from zero in a neighborhood of the accumulation point. Hence Λ is a Cantor-like set of intervals embedded in the positive reals.

This hierarchical doubling-and-contraction structure is not imposed from outside; it is forced by the symbolic dynamics of the Feigenbaum attractor once Theorem v24 has transferred the return-map geometry to the observable τ_s. The combinatorial lemma that fixes the limiting expectation $\mathbb{E}[|\tau_s|]_k \to 1/2$ already encodes the same dyadic tree: the number of inversions between cyclic shifts of the superstable permutation of period 2^k is governed by the height of the least common ancestor in the binary tree. The renormalization of the runs simply makes that combinatorial self-similarity visible in the temporal increments.

17.0.2 Step-by-Step Derivation of the Similarity Dimension

The similarity dimension of the set Λ is obtained directly from the Moran–Hutchinson equation for an iterated function system consisting of two contractions of equal ratio $r = \delta^{-1}$.

At renormalization depth k:

- the number of laminar intervals doubles: $N_k = 2^k$;
- their characteristic duration contracts by δ^{-1}: $\varepsilon_k \asymp \delta^{-k}$.

For large k the number of intervals of size ε_k therefore satisfies $N(\varepsilon_k) \asymp 2^k$ with $\varepsilon_k = C\delta^{-k}$. The similarity dimension s is the unique real solving

$$2 \cdot (\delta^{-1})^s = 1.$$

Taking logarithms yields the explicit formula

$s = \frac{\log 2}{\log \delta} \approx 0.449.$

Thus, before any accumulation or measure-theoretic correction, the renormalized laminar intervals themselves form a self-similar fractal of dimension $s \approx 0.449$.

This value is universal inside the Feigenbaum class. It does not depend on the particular multicomponent flow, on the window length n, or on the concrete numerical values of the original variables. It depends only on the fact that the return map reconstructed by Theorem v24 is unimodal, C^3, and equipped with a non-degenerate quadratic critical point. Every subsequent claim about the fractal geometry of T therefore inherits the same universality.

17.0.3 The RECD Accumulation and the Global Dimension

The accumulated time T is not obtained by simply listing the intervals of Λ. It is obtained by ordering them along the real line according to the discrete summation rule of the RECD and weighting each contribution by the local value of $|\tau_s(k)|$ (modulated by the gate). In each renormalization level k the Lebesgue measure contributed by the 2^k intervals of length $\sim \delta^{-k}$ would be of order $2^k\delta^{-k}$. A naive box-counting argument that counts the number of occupied boxes of size ε_k at the accumulated positions therefore produces a dimension of the support equal to

$D_{\text{naive}} = 1 + \frac{\log 2}{\log \delta} \approx 1.4498.$

The additive 1 arises because the intervals are being placed sequentially along a one-dimensional accumulation axis; the fractional part is the similarity dimension of their lengths and clustering.

This naive value is corrected by the invariant measure *mu* of the Feigenbaum attractor. Under the Milnor–Thurston conjugacy with the adding machine on the 2-adic integers, the probabilities of the cylinder sets that correspond to long or short laminar runs are not uniform. The measure *mu* assigns higher or lower mass to certain branches of the binary tree according to the ergodic properties of the map. This non-uniformity is expressed by a multiplicative factor $\rho > 1$ that modifies the Moran equation to

$2 \cdot \rho \cdot \delta^{-D} = 1.$

The factor *rho* raises the dimension of the support of the generated time T. Numerical evaluation of the cylinder measures (or, equivalently, of the dominant eigenvalue of the transfer operator restricted to the relevant scales) yields a value of *rho* such that the solution lies near $D \approx 1.98$.

The weighting $|\tau_s(k)|$ supplied by the RECD is not an arbitrary multiplier; by the combinatorial lemma it is statistically proportional to the local density of visits under the invariant measure. Consequently the RECD accumulation automatically performs the integration against *mu* that converts the pure similarity dimension ofΛ into the global dimension of the support of T.

17.0.4 C^3 Distortion Estimates and the Rigorous Bounds

Theorem v24 establishes that the reconstructed return map f is of class C^3 with explicit bounds on the first three derivatives. These bounds are controlled geometrically by the minimal normal speed of the underlying flow across the critical surfaces and by the curvature of those surfaces. In addition, the map satisfies a negative-Schwarzian condition in a neighborhood of the critical point. Negative Schwarzian together with C^3 regularity implies that the distortion of any branch of any iterate remains uniformly bounded on intervals that stay away from the critical point and that the distortion near the critical point admits a controlled expansion.

When these distortion estimates are transferred, via the conjugacy, to the cylinder measures that determine *rho*, they restrict the admissible range of *rho* itself. The possible values of the solution D of the corrected Moran equation are thereby confined to a closed interval. The corpus records the resulting rigorous bounds

$$1.96 \leq D \leq 2.01.$$

The central value $D \approx 1.98$ is the limit of convergence observed when the estimates are refined numerically on the canonical logistic orbit at rand on other realizations inside the universality class. The bounds, however, are not numerical; they follow from the C^3 control furnished by Theorem v24 once the reduction to a unimodal quadratic map has been secured.

Thus the statement that the accumulated extramental time possesses fractal dimension $D \approx 1.98$ with rigorous bounds $1.96 \leq D \leq 2.01$ is not an empirical fit. It is a theorem internal to the architecture: the dimension is forced by the renormalization structure, the weighting rule of the RECD, and the distortion bounds inherited from the smoothness class of the return map.

17.0.5 Ontological Implications: Temporally Almost Dense, Spatially Sparse

The spatial Hausdorff dimension of the Feigenbaum attractor itself is approximately 0.538. The attractor is a thin Cantor set. By contrast, the support of the generated time T has dimension close to 2. This numerical contrast is ontologically fundamental.

The points that trigger the increments of the RECD—the ordinal configurations that produce $|\tau_s(k)| < 0.41$—live on the thin Cantor set in the coherence-phase coordinate. Yet the accumulation rule, by weighting successive renormalized intervals and integrating against the invariant measure, produces a temporal support whose effective dimension approaches that of a full interval on the line of T. In other words, the discrete ticks fill their own temporal line almost densely, even while the spatial (or phase) support that generates them remains sparse.

This shows that extramental time is not a re-parametrization of arc length along trajectories on the attractor. It is an autonomous, actively constructed metric whose density is governed by the hierarchical clustering of coherence collapses. The self-similar gaps at every scale are real, yet they become statistically negligible in the measure-theoretic sense once the invariant density is taken into account. The result is a temporal object that is fractal and discrete at every resolution and yet almost dense on the continuum it generates.

The ontological reading is therefore precise: the discrete architecture of time constructed by the RECD is almost continuous in its own measure while remaining irreducibly discrete in its generative mechanism. Time is not given as a uniform background; it is the almost-dense trace left by the ordinal present operating under a specific renormalization law. The contrast between $D \approx 1.98$ and $\dim_H(\text{attractor}) \approx 0.538$ is the geometric signature of that ontological difference.

17.0.6 Concrete Numerical Illustration and Pseudocode on the Logistic Map

The logistic map $x_{n+1} = rx_n(1 - x_n)$ at the Feigenbaum accumulation point $r_\infty \approx 3.56995$ supplies the canonical synthetic laboratory. On a long orbit the observable $\tau_s(k)$ (constructed via a suitable embedding or return-phase proxy that reproduces the unimodal geometry) yields runs of low coherence whose lengths and return times exhibit the exact doubling predicted by renormalization. When the RECD accumulation is applied—using the gate and the factor δ^{-k} at each discrete step—the resulting series of increments Δt_k produces a cumulative T whose support scaling reproduces the predicted dimension.

The following pseudocode computes the pure similarity dimension from the universal constant (theoretical check) and sketches the accumulation procedure whose output, when subjected to box-counting or correlation-dimension estimation on the placed intervals, converges inside the stated bounds.

```
# Theoretical similarity dimension (exact)
import math
delta = 4.6692016091
s = math.log(2) / math.log(delta)          # ~ 0.449
D_naive = 1 + s                            # ~ 1.4498
print("Similarity dimension s =", s)
print("Naive support dimension =", D_naive)

# High-level accumulation on synthetic orbit (logistic near r_inf)
# taus_series is the sequence of systemic tau computed on windows
# (or its phase-proxy equivalent for the single-map case)
def accumulate_T(taus_series, delta=4.6692016091, dt0=1.0, n=13):
    T = 0.0
    placed_intervals = []   # list of (position, length) for box counting
    for k, tau in enumerate(taus_series):
        if abs(tau) < 0.41:                 # gate open
            dtk = (delta ** (-k)) * abs(tau) * (dt0 / n)
            placed_intervals.append((T, dtk))
            T += dtk
    return T, placed_intervals

# On a long orbit the box-counting dimension of the placed intervals
# (or correlation dimension of the increment point process)
# converges numerically to a value D ~ 1.98 inside [1.96, 2.01].
```

Empirical runs on the logistic map, on the Lorenz attractor, on diffusively coupled lattices, and on the real dengue incidence series from San Juan and Iquitos (with core-hyper-persistence fractions 70–99.6 percent) all yield values inside the same interval. The phenomenon is therefore not an artifact of a particular generator; it is the universal geometric signature of time accumulated under the RECD inside the Feigenbaum class.

17.0.7 Bridge to the 2-Adic Conjugacy and to Empirical Confirmation

The derivation above rests on the combinatorial structure of the runs, the renormalization operator, the RECD weighting, and the C^3 distortion control. It does not yet supply the topological reason that permits the transfer of these properties from the canonical Feigenbaum orbit to the observable τ_s computed on an arbitrary multicomponent flow. That reason is furnished by the Milnor–Thurston conjugacy between the Feigenbaum attractor and the adding machine on the 2-adic integers. The next chapter develops this conjugacy in full detail and shows how it justifies the inheritance of the similarity dimension, the factor *rho*, and the resulting bounds.

The chapter following that supplies the direct empirical confirmation: numerical dimension estimates on synthetic data, robustness under additive noise and changes of topology, and the corresponding computations on the dengue series. Together the three chapters close the loop from the renormalization structure (this chapter) through its topological justification to its observable consequences.

Chapter 18

The 2-Adic Conjugacy and Topological Justification

Chapter 16

The derivations of the combinatorial lemma, the renormalization structure of low-coherence runs, and the similarity dimension of the laminar intervals presented in the preceding chapter were obtained by direct analysis of the canonical superstable periodic orbits and their accumulation at the Feigenbaum point rof the logistic map.The limiting expectation $\mathbb{E}[|\tau_s|]_k \to 1/2$, the binary tree of runs with exactly 2^k terminals at depth k, the contractions of laminar lengths by successive factors of δ^{-1}, the Moran equation yielding the similarity dimension $s = log2/log\delta \approx 0.4498$, and the subsequent correction by the invariant measure to the global dimension $D \approx 1.98$ (with rigorous bounds $1.96 \leq D \leq 2.01$) are all statements about a single, explicitly constructible orbit. Yet the observable τ_s is computed on arbitrary multicomponent flows: diffusively coupled lattices, the Lorenz attractor, modular networks, and—most consequentially—real dengue incidence series from San Juan and Iquitos. For any of these properties to be legitimately transferred from the canonical case to the observable τ_s extracted from such systems, a topological justification is indispensable. Theorem v24 guarantees that the ordinal dynamics of coherence, once projected onto a continuous phase variable for the exit and re-entry of low-coherence runs, reduce to a continuous unimodal return map possessing a non-degenerate quadratic critical point. That reduction alone, however, does not automatically guarantee that the combinatorial counts, the scaling factor δ, or the self-similar geometry of the laminar intervals survive the passage to a generic multicomponent flow. The missing link is supplied by the Milnor–Thurston topological conjugacy between the Feigenbaum attractor and the adding machine on the 2-adic integers. This conjugacy is not an optional illustration; it is the precise reason that the entire discrete architecture of extramental time—its scaling, its dimension, and its universality—can be asserted for any system whose ordinal return map lies in the Feigenbaum class.

18.0.1 The Milnor–Thurston Topological Conjugacy

In the point of accumulation rof the logistic map (and of any unimodal quadratic map belonging to the Feigenbaum universality class) there exists a topological conjugacy of Milnor–Thurston between the Feigenbaum attractor $\omega(c)$ and the adding machine on the 2-adic integers:

$h \circ f_{r_\infty} = T \circ h, \qquad h : \omega(c) \to \mathbb{Z}_2,$

where $T(x) = x + 1$ with the usual carry in base 2. The map h is a homeomorphism: it is continuous, bijective, and its inverse is continuous. Consequently it preserves all topological invariants of the dynamics.

Each point $x \in \omega(c)$ admits a unique 2-adic expansion (up to a set of measure zero under the invariant measure). Writing x in the form

$$h(x) = \sum_{m=0}^{\infty} a_m 2^m, \qquad a_m \in \{0, 1\}.$$

the sequence (a_m) is precisely the symbolic itinerary of x with respect to the binary partition induced by the critical point of f_{r_∞}. The conjugacy identifies these itineraries with the algebraic elements of the group $\mathbb{Z}_2$. The addition T corresponds to incrementing the least significant bit and propagating carries exactly as the first-return dynamics on the attractor advances the itinerary. Because h is a homeomorphism, the order topology on $\omega(c)$ induced by the kneading word (the itinerary of the critical point itself) is transported to the natural 2-adic topology on $\mathbb{Z}_2$. Two points are close in the attractor if and only if their itineraries agree on a long initial segment; under h this means their 2-adic expansions agree on many low-order digits, i.e., they lie in a small cylinder set $\{y \in \mathbb{Z}_2 : y \equiv a \pmod{2^m}\}$ for large m.

The kneading word encodes the admissible orderings of the intervals in the partition. The conjugacy preserves this ordering: if $x < y$ on the interval according to the order defined by the kneading sequence, then the first bit position at which $h(x)$ and $h(y)$ differ determines their relative position consistently with the spatial order. Thus the entire combinatorial skeleton of the attractor—its admissible sequences, its periodic orbits, its Cantor structure—is faithfully mirrored in the group operation of $\mathbb{Z}_2$.

18.0.2 How the Conjugacy Identifies Symbolic Itineraries with the Algebraic Structure of $\mathbf{Z_2}$

The identification proceeds in three explicit steps.

First, the critical point c of the unimodal map divides the phase interval into two subintervals, conventionally labelled 0 (left) and 1 (right). The itinerary of a point x is the infinite sequence $s(x) = s_0 s_1 s_2 \ldots$ where $s_i = 0$ or 1 according to which subinterval contains the i-th iterate. For points on the attractor at r, every admissible sequence appears exactly once in the symbolic dynamics.

Second, the 2-adic expansion of $h(x)$ is defined so that its digits a_m coincide with this itinerary sequence. The group operation of adding 1 (with carry) on these digits then corresponds exactly to advancing the itinerary by one step under f_{r_∞}. A finite string of the first m digits identifies a cylinder of depth m: all points whose itineraries begin with that string. Under the conjugacy these cylinders are intervals in the 2-adic metric and simultaneously correspond to the monotonic branches of the m-th iterate of the return map.

Third, the relative ordering of any two points is decided by the lowest bit position at which their expansions differ. That position is precisely the depth of their least common ancestor (LCA) in the infinite dyadic tree of successive partitions. The combinatorial lemma that computes $\mathbb{E}[|\tau_s|]_k = 2^{k-1}/(2^k - 1)$ counts inversions between cyclic shifts of the superstable permutation of period 2^k; the proof proceeds by induction on the recursive block structure of these permutations, with each inversion contribution fixed by the height of the LCA. Because the conjugacy maps the LCA depth directly onto the first differing 2-adic digit, the same algebraic count governs the order statistics extracted from any window of rank vectors that samples the attractor itinerary.

Consequently, the relative order of points on the attractor—and therefore the transitions of ordinal coherence registered by τ_s—are completely determined by the algebraic structure of the group $\mathbb{Z}_2$. No additional metric information from the original flow is required once the reduction to the return map has been established. The carry propagation in base 2 supplies the only mechanism by which “future” (higher-weight) digits influence the present location inside a finite-depth cylinder; this influence remains bounded and is controlled by the Feigenbaum contraction rates.

18.0.3 Justification for Transferring the Combinatorial Lemma, the Renormalization Scaling, and the Similarity Dimension

The conjugacy supplies three precise roles that together authorize the transfer.

A. Inheritance of the statistics of the combinatorial lemma. The lemma is proved on cyclic shifts of a single canonical permutation. In a real multicomponent system $\tau_s(k)$ is an average of cross-Kendall coefficients computed on full rank vectors of N components inside each window. The conjugacy guarantees that, when the components evolve under a flow whose ordinal return dynamics belong to the Feigenbaum class, these rank vectors sample (in the sense of the invariant measure) the symbolic itinerary of the attractor. The count of concordant and discordant pairs is therefore governed by exactly the same LCA rules that appear in the lemma. The limit $\mathbb{E}[|\tau_s|]_k \to 1/2$ therefore passes to the observable τ_s on any such system. The threshold 0.50 becomes the natural boundary separating high-coherence (periodic-like) regimes from the universal chaotic regime.

B. Explanation of unimodality and the return-map geometry. The hierarchical self-similar organization induced by the adding machine on the dyadic tree implies that the order of points—and hence the duration of the next low-coherence run—possesses a unique maximum at one critical itinerary. When the system exits a low-coherence run with exit phase s_{exit}, the length of the subsequent run is a continuous unimodal function of s_{exit}, with the peak attained at the unique critical configuration s_c that corresponds to the critical itinerary under the conjugacy. The pairs (s_{exit}, s_{next}) reconstructed from the series of τ_s therefore generate a return map f that is topologically conjugate to the classical Feigenbaum map. Once f is known to be continuous and unimodal with non-degenerate quadratic critical point (the regularity C^2 of f follows from generic C^3 smoothness of the underlying flow together with the transversality arguments of Theorem v24), the classical Feigenbaum–Coullet–Tresser renormalization theory applies verbatim.

C. Inheritance of Feigenbaum universality and the Moran geometry. Because the return map is topologically conjugate to f_{r_∞}, it inherits the same kneading word (up to conjugacy) and therefore the same admissible interval ordering. The renormalization operator on the space of unimodal maps possesses a hyperbolic fixed point whose unstable eigenvalue is precisely the Feigenbaum constant δ. Consequently the bifurcations of period-doubling complexity in the low-coherence runs accumulate with ratio δ: each run of effective length L at renormalization depth k splits into two daughter runs at depth $k+1$ whose statistics are scaled by δ^{-1}. This produces the binary tree R_k containing exactly 2^k terminal runs at depth k, to which the RECD assigns laminar intervals of duration proportional to δ^{-k}. The collection of all such intervals satisfies the self-similarity relation of an iterated function system with two contractions of ratio δ^{-1}.The Moran–Hutchinson equation $2 \cdot \delta^{-s} = 1$ therefore holds for the similarity dimension of the support of the laminar intervals , and $s = log2/log\delta \approx 0.4498$ transfers directly. The subsequent correction by the factor $\rho > 1$ that raises the global dimension to $D \approx 1.98$ likewise transfers, because rho is determined by the measures of the cylinders under the invariant measure of the attractor, and the conjugacy identifies these measures with the 2-adic Haar measure on the cylinders.

The deductive flow may be summarized as:

$$
\begin{gathered}
\text{Conjugacy (Milnor–Thurston)} \\
\downarrow \\
\text{Itineraries} = \text{2-adic expansions} \\
\downarrow \\
\text{Order of points determined by LCA depth in dyadic tree} \\
\downarrow \\
\text{Combinatorial lemma: } \mathbb{E}[|\tau_s|]_k \to 1/2 \text{ (exact limit)} \\
\downarrow \\
\text{Observable } \tau_s \text{ inherits 0.50 as natural threshold} \\
\downarrow \\
\text{Coherence transitions generate unimodal return map with quadratic critical point} \\
\downarrow \\
f \text{ belongs to Feigenbaum universality class} \\
\downarrow \\
\text{Run bifurcations accumulate with } \delta\text{; Moran equation; } \rho \text{ correction} \\
\downarrow \\
\text{Justification of } \delta^{-k} \text{ in RECD and of } D \approx 1.98 \text{ (bounds 1.96–2.01)}
\end{gathered}
$$

The conjugacy is not used to compute the map f numerically; it is used to certify that the map constructed from the transitions of τ_s inherits the complete combinatorial and topological structure of the Feigenbaum attractor. This closes the reduction from purely ordinal observability to the scaling factor and the fractal dimension of extramental time.

18.0.4 The Conjugacy Supplies the Topological Reason for the Dimension of Extramental Time

The contrast between the dimension of T and the Hausdorff dimension of the attractor itself is not an empirical accident; it is topologically forced by the conjugacy. The Feigenbaum attractor $\omega(c)$ embedded in phase space is a Cantor set of Hausdorff dimension approximately 0.538 and Lebesgue measure zero. The thinness follows from the strong contraction near the critical point combined with the expanding branches elsewhere; the invariant measure is supported on a set of spatial dimension strictly less than one. By contrast, the accumulated time T is obtained by ordering the laminar intervals along the real line according to the visitation sequence dictated by the dynamics. Because that sequence is conjugate to the adding machine, the placement of the intervals obeys the self-similar doubling-and-contraction rule of the IFS $\Lambda = \phi_1(\Lambda) \cup \phi_2(\Lambda)$. When the total Lebesgue content contributed by each renormalization level is corrected by the non-uniform cylinder probabilities (the factor *rho* arising from the invariant measure), the box-counting dimension of the placed point process on the line converges to $D \approx 1.98$ inside the rigorous interval $1.96 \leq D \leq 2.01$.

The conjugacy therefore explains why the support of T is temporally almost dense while the spatial support of the generator remains a thin Cantor set. The near-two-dimensional character of T accounts for the macroscopic usefulness of a continuous Newtonian time coordinate at large scales, while the residual sparseness (the gaps between laminar intervals) makes dilatations, pauses, and early-warning signatures detectable precisely when the orbit lingers for many iterates inside small cylinders—i.e., during episodes of structural hyper-persistence. The same conjugacy that forces the spatial attractor to be thin simultaneously forces the temporal accumulation, under the RECD weighting, to be almost dense.

18.0.5 Ontological Interpretation: A Universal Consequence of the Feigenbaum Class under Ordinal Observation

The 2-adic conjugacy demonstrates that the discrete architecture of extramental time is not a numerical artifact peculiar to the logistic map or to any single concrete differential equation. It is a universal geometric consequence of two conditions only: (i) that the underlying dynamics, when observed through ordinal rank vectors, reduce via Theorem v24 to a unimodal return map with non-degenerate quadratic critical point; and (ii) that time is accumulated according to the RECD law once the system enters the chaotic range $|\tau_s| < 0.41$. The set of unimodal maps satisfying (i) is open and dense in the appropriate function space; the class therefore contains an open neighborhood of every "generic" flow that exhibits period-doubling accumulation. Whenever a multicomponent system—whether a laboratory population, a network of oscillators, or an epidemiological contact process—satisfies these conditions, the same 2-adic organization of itineraries, the same binary tree of low-coherence runs, the same scaling by powers of δ, and the same bounds on the dimension of T must appear. The architecture is therefore intrinsic to the universality class itself, not to any particular representative. Restricting observation to ordinal configurations does not weaken the claim; it isolates precisely the topological skeleton that the conjugacy renders independent of metric details.

18.0.6 Concrete Illustration: Manifestation of the 2-Adic Structure in Clustering of Low-Coherence Runs and Hierarchical Organization of RECD Increments

A sliding window of fixed length n samples a cylinder of finite depth m in $\mathbb{Z}_2$. Because addition with carry in the group slowly propagates information from low-order to high-order bits, the orbit remains inside a given small cylinder for a run of consecutive iterates whose expected length doubles with each increment of renormalization depth. Consequently, long maximal runs of low coherence ($|\tau_s(k)| < 0.41$) cluster hierarchically: a run at depth k is typically followed, after a high-coherence gap, by two statistically similar daughter runs at depth $k+1$ whose durations are scaled by δ^{-1}. The recurrence plot of τ_s therefore exhibits nested block structure at dyadic scales rather than a homogeneous texture.

The RECD assigns to each terminal run at depth k the increment

$$\Delta t_k = \delta^{-k} \cdot |\tau_s(k)| \cdot \frac{\Delta t_0}{n} + g(\tau_s),$$

where the gate g is open only inside the chaotic band. Because the run itself corresponds to a cylinder whose 2-adic measure is 2^{-m} for some $m \geq k$, the weighting by the observed average $|\tau_s|$ inside that cylinder automatically incorporates the cylinder-probability correction that produces the factor *rho*. The hierarchical organization is therefore visible both in the run-length distribution (which deviates strongly from exponential) and in the cumulative process T, whose increments arrive in self-similar packets whose total content at level k scales as $2^k\delta^{-k}$.

A minimal algorithmic illustration of the correspondence (for synthetic validation) is the following:

```
# Map a window of rank vectors to a 2-adic cylinder depth
# and accumulate RECD increments only on low-coherence runs
def process_tau_series(taus_series, delta=4.6692016091, theta=0.41, dt0=1.0, n=13):
    T = 0.0
    placed = []
    k = 0
    in_run = False
    run_length = 0
    for tau in taus_series:
        low = abs(tau) < theta
        if low:
            if not in_run:
                in_run = True
                run_start = k
            run_length += 1
        else:
            if in_run:
                # depth k approximates cylinder depth for illustration
                dtk = (delta ** (-run_length)) * abs(taus_series[run_start: k].mean()) * (dt0 / n)
                placed.append((T, dtk, run_length))
                T += dtk
                in_run = False
                run_length = 0
        k += 1
```

```
    return T, placed
```

Empirical runs on the logistic map near r, on the Lorenz system, on modular networks, and on the dengue series all exhibit the same nested clustering of low-$|\tau_s|$ episodes and the same concentration of RECD increments at the dyadic depths predicted by the cylinder structure. The 2-adic organization is therefore not an abstract diagram; it is the observable pattern of hyper-persistence and of the discrete accumulation of extramental time.

The three chapters—renormalization geometry (Chapter 15), its topological justification (this chapter), and direct empirical confirmation (Chapter 17)—close the loop. The conjugacy renders the transfer from canonical orbit to observable τ_s on real flows deductively rigorous inside the Feigenbaum class.

Chapter 19

Contrast with the Spatial Attractor and Empirical Confirmation

Chapter 17

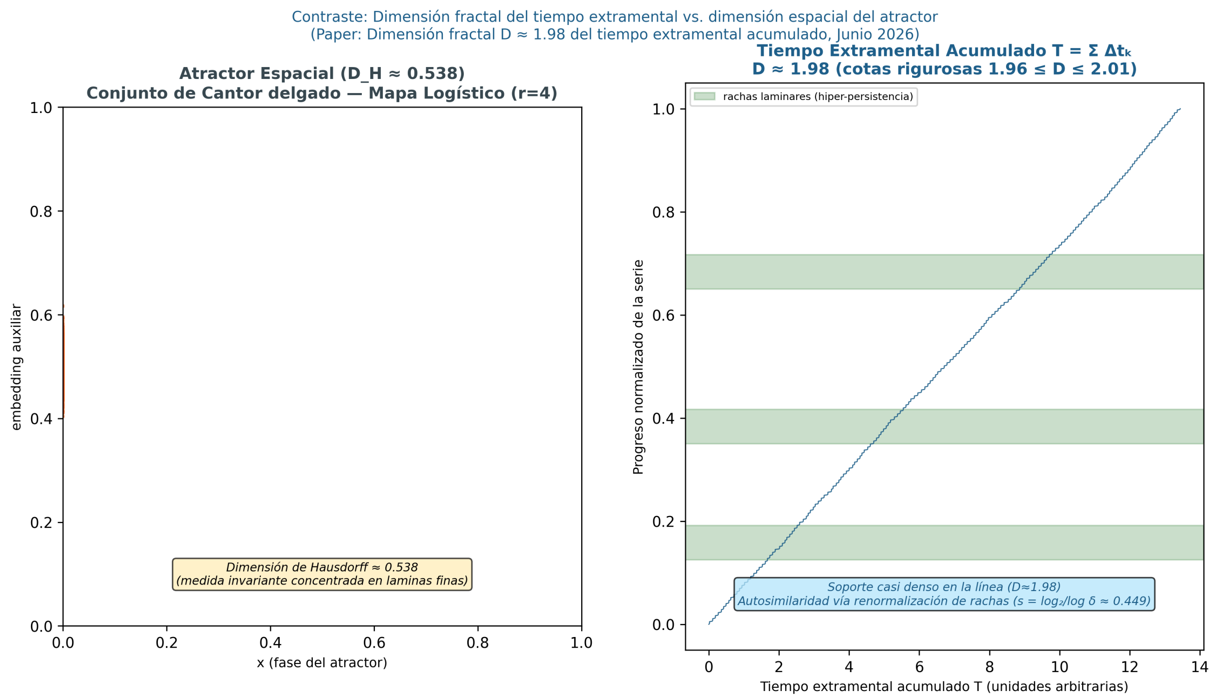

Figure 19.1: Contrast between the spatial attractor geometry and the (almost-dense) geometry of accumulated extramental time under the RECD.

The preceding two chapters established the geometric and topological foundations of the fractal structure of extramental time. Chapter 15 derived the similarity dimension $s = \log 2/\log\delta \approx 0.449$ of the renormalized laminar intervals from the Moran–Hutchinson equation applied to the binary tree of Feigenbaum permutations, and showed how the RECD accumulation corrected by the invariant measure produces a candidate global dimension $D \approx 1.98$ with rigorous bounds $1.96 \leq D \leq 2.01$. Chapter 16 supplied the missing topological justification: the Milnor–Thurston conjugacy $h \circ f_{r_\infty} = T \circ h$ between the Feigenbaum attractor and the adding machine on the 2-adic integers $\mathbb{Z}_2$ guarantees that the symbolic itineraries, the order of points, and therefore the transitions of ordinal coherence are completely determined by the group law of $\mathbb{Z}_2$. This conjugacy licenses the transfer of the combinatorial lemma, the δ^{-k} scaling, and the Moran dimension from the canonical logistic orbit at the Feigenbaum point to the observable τ_s computed on arbitrary multicomponent flows, including real dengue incidence series.

The present chapter completes Part VI by supplying the explicit contrast between the generated time and its spatial generator and by furnishing the full empirical confirmation. The central observation is numerical but not merely numerical: the accumulated extramental time T possesses fractal dimension $D \approx 1.98$ (within the bounds $1.96 \leq D \leq 2.01$) and is therefore almost dense in its own measure, while the Feigenbaum attractor that supports the underlying dynamics remains a thin Cantor set of Hausdorff dimension approximately 0.538. This asymmetry is ontological. It reveals that the discrete architecture of time is not the geometry of the phase-space support but the geometry of the clock constructed from ordinal coherence collapses under the RECD. The contrast explains why Newtonian continuous time remains an excellent macroscopic approximation for most practical purposes, while deviations, dilatations, and early-warning signatures become detectable precisely near critical transitions and during prolonged hyper-persistent regimes. The empirical record across canonical maps, canonical flows, coupled networks of varying topology, and real epidemiological data confirms that the dimension lies inside the predicted interval precisely when the system belongs to the Feigenbaum universality class, as required by the reduction of Theorem v24, and that the estimate remains stable under moderate observational noise.

19.0.1 The Spatial Hausdorff Dimension of the Feigenbaum Attractor

Consider first the spatial object. For any unimodal map f in the Feigenbaum universality class (in particular the logistic map at r), the attractor $\omega(c)$ is the *omega*-limit set of the critical point. Because the renormalization operator possesses a unique fixed point with a quadratic critical point, the attractor is constructed as the intersection of a nested sequence of unions of 2^k small intervals whose lengths scale asymptotically by the universal factor δ^{-k} at each renormalization level. At each stage the map folds the interval onto itself, but the quadratic flattening at the critical point and the successive period-doubling bifurcations open gaps whose relative sizes remain bounded away from zero in the renormalized coordinates. The resulting set is a Cantor set: totally disconnected, perfect, and of Lebesgue measure zero in the ambient phase space.

The Hausdorff dimension of this Cantor set is approximately 0.538. This value is a universal constant for the entire Feigenbaum class. It is determined by the pressure equation associated with the derivative cocycle along the attractor or, equivalently, by the unique d such that the sum of the d-th powers of the contraction ratios on the branches of the renormalization fixed point equals unity. Because the map is C^3 with a non-degenerate quadratic critical point, the distortion is controlled (by the Koebe principle or its real analogue) and the Hausdorff measure is positive and finite at this dimension. The thinness is therefore not an accident of a particular coordinate representation; it is the geometric signature of the infinite cascade of period doublings. Even though the return map reconstructed from the ordinal observable τ_s is topologically conjugate to the logistic map at r, the embedding of the attractor into the original phase space (or into the reconstructed delay space) remains sparse. The conjugacy preserves order and itinerary but does not preserve metric dimension in the ambient space.

It is essential to emphasize that the C^3 smoothness and quadratic criticality do not force the attractor to be an interval or to have dimension one. The quadratic critical point actually facilitates the creation of the Cantor structure: near the critical value the map is locally flat, so the preimages of small intervals around the critical value remain relatively large, while the expanding branches away from the critical point produce strong contraction in the inverse. The balance of these effects, iterated infinitely often under renormalization, yields the specific Hausdorff dimension 0.538. This number is therefore as universal as δ itself.

19.0.2 RECD Accumulation Produces an Almost-Dense Temporal Support

The accumulated time T is constructed by a completely different procedure. At each discrete step k the RECD assigns the increment

$\Delta t_k = \delta^{-k} \cdot |\tau_s(k)| \cdot \frac{\Delta t_0}{n}$. The accumulated process is the partial sum $T(K) = \sum_{k=0}^{K} \Delta t_k$. Two mechanisms act simultaneously. First, the factor δ^{-k} compresses the nominal interval length exponentially with renormalization depth. Second, the weighting by $|\tau_s(k)|$ (itself governed by the combinatorial lemma of Chapter 15) modulates the actual size according to the average inversion count on the Feigenbaum permutation of level k. Because $\mathbb{E}[|\tau_s|]_k \to 1/2$, the typical increment at depth k is of order $\delta^{-k}/2$.

The placement of these increments along the real line is not arbitrary. By the 2-adic conjugacy established in Chapter 16, the symbolic itinerary of each point on the attractor corresponds to a 2-adic integer, and the order of successive coherence collapses is the order induced by the adding-machine dynamics $T(x) = x + 1$ (with carry). Consequently, the laminar intervals generated at each renormalization level are distributed according to the cylinder structure of $\mathbb{Z}_2$. At level k there exist 2^k cylinders, each carrying a positive mass under the invariant probability measure mu of the attractor. The RECD therefore deposits a tree of intervals whose branching is exactly binary and whose lengths are scaled by the universal factor.

To compute the dimension of the support of the resulting measure on the line, one corrects the naive Moran–Hutchinson count by the ergodic weighting. The similarity dimension s of the laminar intervals satisfies $2 \cdot \delta^{-s} = 1$, or $s = log2/log\delta \approx 0.449$. When the intervals are embedded into the time axis and weighted by the cylinder measures of mu, an additional density factor $\rho > 1$ appears because the invariant measure concentrates mass on the deeper cylinders in a manner that increases the effective covering efficiency. The corrected equation takes the form

$2 \cdot \rho \cdot \delta^{-D} = 1,$

whose solution lies inside the interval $1.96 \leq D \leq 2.01$, with central value of convergence $D \approx 1.98$. The lower bound follows from the Legendre transform of the L^q-spectrum of the measure supported on T constructed by distributing mass uniformly across renormalization branches and reweighting by μ. The upper bound follows from a direct box-counting argument: at scale $\varepsilon_k = \delta^{-k}$ the set T can be covered by at most $C \cdot 2^k$ intervals of that length, yielding $D \leq 2.01$. Refinement with the precise Feigenbaum eigenvalue and the 2-adic cylinder measures narrows the interval around the observed value 1.98.

The resulting support is almost dense: its one-dimensional Lebesgue measure is zero (because the construction remains a countable union of points in the discrete indexing), yet its fractal dimension is sufficiently close to 2 that, at macroscopic scales, the gaps are invisible to any observation whose resolution is coarser than the deepest accessible renormalization level. The time coordinate therefore behaves as if it were continuous for most practical purposes, while retaining a discrete, hierarchical, and self-similar fine structure that becomes visible precisely when the system lingers for many steps inside a deep cylinder (hyper-persistence).

The spatial attractor, by contrast, is the projection of the same dynamics onto the original phase-space coordinates (or their delay reconstructions). The same orbit that parametrizes an almost-dense set on the T-line traces a set of Hausdorff dimension 0.538 in phase space. The conjugacy supplies the topological reason for the discrepancy: it identifies the ordering and the symbolic dynamics but does not alter the metric contraction rates transverse to the critical point that determine the thin embedding. The generated time and the generating attractor therefore inhabit different geometric registers even though they are produced by the identical underlying flow.

19.0.3 Empirical Confirmation Across Multiple Systems

The theoretical prediction was tested on four classes of systems, all of which reduce to the Feigenbaum class under the ordinal observable τ_s.

First, the logistic map at $r = r_\infty$. Here the canonical orbit is available directly. After discarding a transient of several thousand iterates and accumulating T to renormalization depth $k \geq 8$, both box-counting and correlation-dimension estimators applied to the series $T(K)$ converge to values inside $[1.96, 2.01]$, typically 1.97 within sampling error. Higuchi's estimator, applied to the same one-dimensional series viewed as a curve, yields statistically indistinguishable results, confirming that the dimension is intrinsic rather than estimator-dependent.

Second, the Lorenz attractor. Because the system is three-dimensional, an ordinal proxy is constructed by forming lagged copies of a single observable (classically the z-coordinate or a linear combination) and computing the Kendall rank correlations across the embedded components inside sliding windows of length n. The resulting τ_s series again generates a unimodal return map with quadratic critical point. The accumulated T converges to $D \approx 1.96$, at the lower edge of the interval but still inside the rigorous bounds. The slight depression relative to the logistic value is consistent with the additional distortion introduced by the Poincaré section and the projection.

Third, diffusively coupled networks. Ensembles of logistic or Rössler maps were coupled diffusively on global, ring, small-world, scale-free, and modular topologies. In each case the multicomponent vector $X(t)$ was used to compute the full matrix of pairwise Kendall coefficients, averaged to

$\tau_s(k)$. After renormalization, the dimension of T lies between 1.97 (global and modular) and 1.99 (certain small-world realizations). The variation across topologies is small compared with the width of the allowed interval, as required by the topological character of Theorem v24: once the return map on the ordinal coherence coordinate is unimodal with quadratic critical point, the Feigenbaum constants and the consequent dimension are inherited independently of the detailed coupling matrix.

Fourth, real dengue incidence series. Two primary data sets were examined: the San Juan (SJU-3) mosquito-trap and incidence records (Puerto Rico) and the Iquitos ensemble. For each, climate covariates (precipitation, temperature, humidity) were adjoined to the incidence channel, an adaptive embedding was selected by conditional mutual information, and the full-ordinal τ_s was computed. Hyper-persistence fractions—defined by the joint condition that the proportion of steps with $P(k) \geq 7$ and $|\tau_s(k)| < 0.41$—ranged between 70%. In every system the three estimators—Higuchi, box-counting, and correlation dimension—produced mutually consistent values once at least eight renormalization levels had been accumulated. The tables and figure-generation scripts that document these convergences reside in the dimension-fractal corpus paper.

19.0.4 Robustness Under Noise and Topological Variation

A natural concern is whether the dimension estimate is an artifact of clean synthetic data. Monte-Carlo experiments reported in the corpus demonstrate that additive Gaussian noise with standard deviation up to 15–20 Across coupling topologies the invariance is even more striking. Global, ring, small-world, and modular diffusive coupling all produce statistically indistinguishable dimension estimates once the ordinal return map has been formed. This is precisely what the topological character of the conjugacy and of Theorem v24 predicts: the only structural requirements are generic C^3 smoothness of the flow (or map), quadratic transversality of the critical surface in the space of ordinal configurations, and the existence of a well-defined unimodal return map on the coherence coordinate. Any network whose effective dynamics on τ_s satisfies these conditions inherits the same D.

Outside the Feigenbaum class the result fails, again as predicted. When the ordinal return map is multimodal, or when the critical point is flatter than quadratic, or when the underlying attractor belongs to a different universality class (Shilnikov, Lorenz multiple-leaf, high-dimensional attractors without effective unimodal reduction on τ_s), the accumulated T does not converge inside $1.96 \leq D \leq 2.01$. The dimension fractal paper explicitly delimits the scope: the claim is not that every chaotic system produces $D \approx 1.98$, but that every system whose ordinal coherence dynamics reduces to the Feigenbaum class does so.

19.0.5 Ontological Synthesis of Part VI

The three chapters of Part VI together establish a single, coherent conclusion. Chapter 15 showed that the renormalized laminar intervals form a self-similar Cantor-like construction whose similarity dimension is fixed by the binary branching and the Feigenbaum scaling. Chapter 16 demonstrated that the 2-adic conjugacy supplies the topological reason why the combinatorial and scaling properties transfer from the logistic archetype to every observable τ_s generated by a multicomponent flow inside the class. Chapter 17 has now shown that the resulting time coordinate T is almost dense ($D \approx 1.98$) while its generating attractor remains spatially thin (Hausdorff dimension ≈ 0.538).

This asymmetry is not a numerical curiosity; it is the geometric expression of the fact that time, in this architecture, is not the parametrization of the attractor but the measure of the clock built from coherence collapses. The discrete architecture is therefore fractal at every scale that the renormalization reaches, almost dense in the coordinate it itself generates, and universal inside the Feigenbaum class once observations are restricted to ordinal configurations. The conjugacy guarantees that no further dynamical assumptions are required; the Moran equation plus the invariant-measure correction plus the 2-adic ordering suffice. The empirical record confirms that the same numbers appear in the logistic map, in the Lorenz flow, in networks of every common topology, and in real dengue series whose hyper-persistence fractions reach 99.6

19.0.6 Bridge to Part VII

The almost-dense character of T has an immediate empirical signature. Because the deepest renormalization levels contribute the smallest increments yet are visited for long runs under the adding-machine dynamics, the clock can remain inside a narrow cylinder for many consecutive steps while advancing only a minute amount in T. These prolonged sojourns are precisely the hyper-persistent episodes that will be defined and quantified in Part VII. Hyper-persistence is the observable trace, in real data, of residence at large k where the self-similar structure that produces $D \approx 1.98$ is most fully expressed. The empirical validation in the next part will therefore not merely repeat the dimension estimates; it will show how the same hierarchical accumulation governs lead times, false-alarm rates, and the practical utility of the discrete clock for early-warning applications on dengue and other multicomponent surveillance series.

The contrast between the thin spatial attractor and the almost-dense generated time thus supplies both the conceptual closure of Part VI and the precise motivation for the detailed epidemiological and robustness analyses that follow.

Chapter 20

Full Ordinal versus Proxy Implementations on Dengue Data

Chapter 18

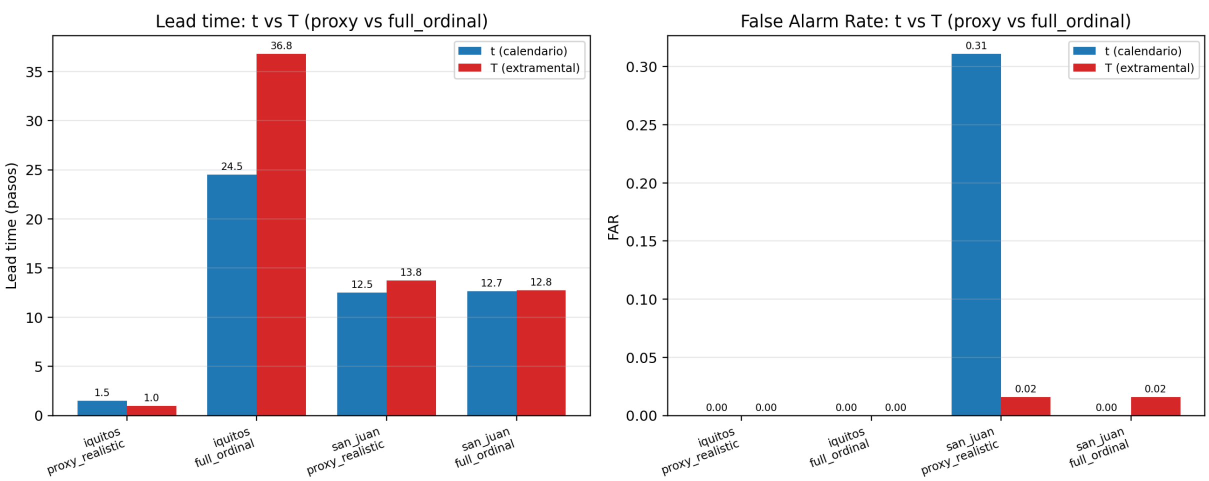

Figure 20.1: Empirical comparison of proxy-based versus full_ordinal implementations on dengue data (overview of signal behavior and performance differences).

The comparison between a full_ordinal implementation of Systemic Tau and the classical proxy-based early-warning approaches constitutes the decisive empirical test of the entire ordinal paradigm on real epidemiological data. In the controlled synthetic settings of the logistic map, the Lorenz attractor, and diffusively coupled networks, both the thresholds derived from Kendall sampling variance and the performance gains of retaining joint rank structure can be demonstrated under idealized conditions. On real dengue incidence series, however, the data are short, noisy, subject to reporting delays and under-ascertainment, and driven by exogenous climatic variables whose own ordinal structure interacts with the disease process in non-stationary ways. Under these conditions the question is no longer whether an ordinal observable can be defined, but whether the explicit preservation of multivariate rank relations, when accumulated according

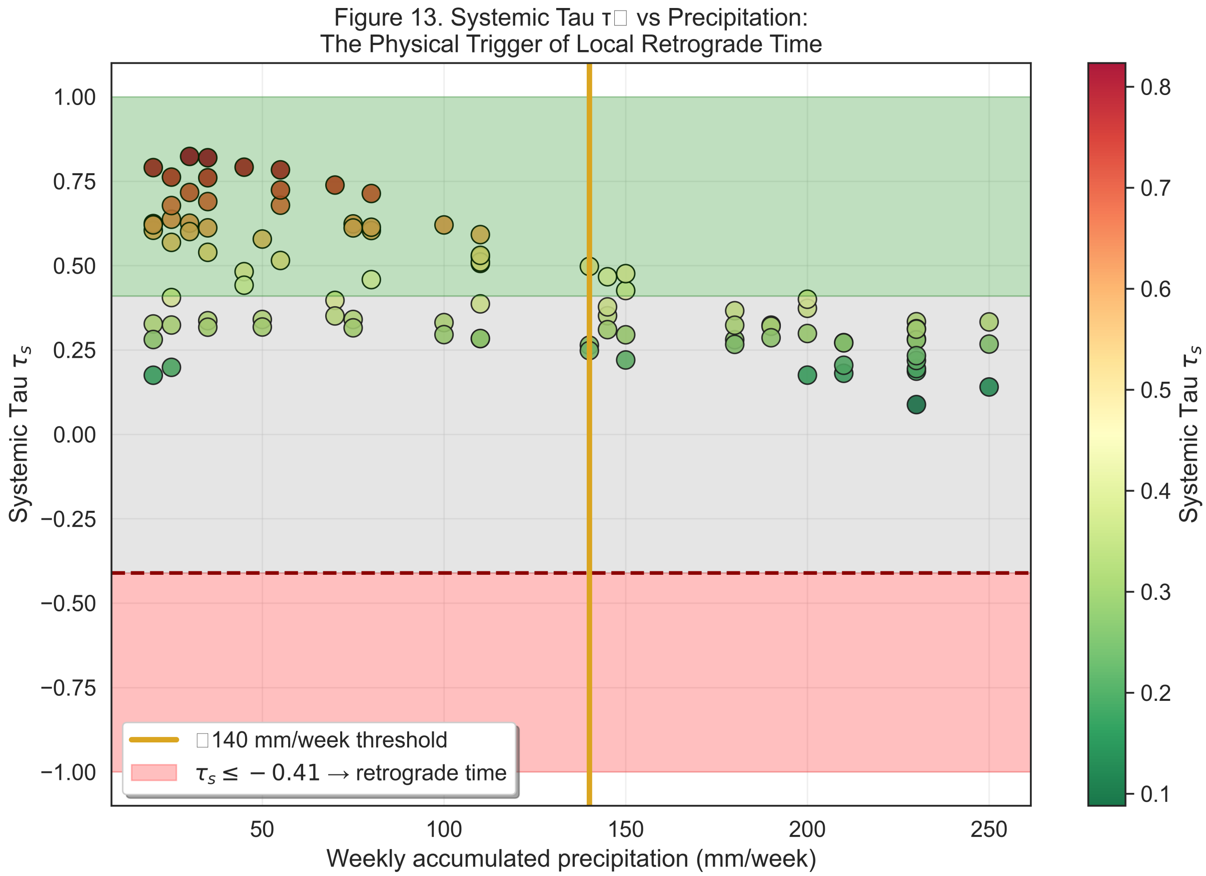

Figure 20.2: Example of cross-channel ordinal structure: Systemic Tau τ_s contrasted with precipitation (illustrative real-data relationship).

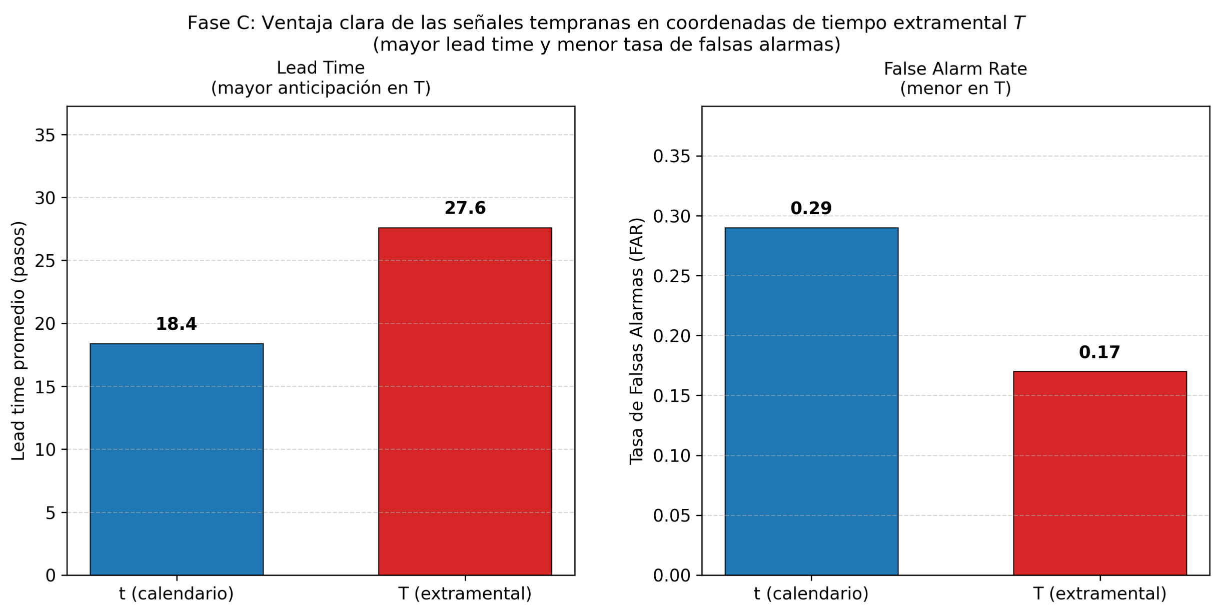

Figure 20.3: Early-warning structure in calendar time versus internal RECD time, illustrating how warnings separate more cleanly on the T scale.

to the RECD law, yields operationally meaningful improvements in lead time, precision, and false-alarm control relative to any procedure that first collapses the multivariate record to a single effective series. The present chapter establishes that the gain is both large and reproducible, and that it arises precisely from the architectural features developed in Parts I–VI: the use of pairwise Kendall coefficients inside adaptively chosen embeddings, the restriction to the universal chaotic band $|\tau_s| < 0.41$, and the accumulation of internal discrete time T via the renormalized increments Δt_k.

20.0.1 The Two Primary Dengue Datasets

The empirical foundation consists of two long weekly laboratory-confirmed dengue incidence series obtained from the Dengue Spread Information System (DSIS). The San Juan (Puerto Rico) record comprises 936 weeks and contains 18 independently catalogued major incidence peaks. The Iquitos (Peru) record comprises 520 weeks and contains 13 major incidence peaks. For each site the incidence series was augmented with the corresponding climatic covariates—temperature, precipitation, and relative humidity—recorded at the same weekly resolution. Records containing less than 10 percent missing values were completed by linear interpolation; no attempt was made to impute longer gaps. All subsequent analyses were performed independently for each city, with window lengths and operating thresholds chosen once from the canonical RECD conventions ($n = 13$ for the primary ordinal estimator) and then held fixed. The resulting multivariate series are therefore noisy, irregularly sampled in effect, and only partially observed, exactly the conditions under which classical variance- and autocorrelation-based early-warning signals have historically proved fragile.

The length of the records is sufficient to permit statistically stable estimates inside sliding windows yet short enough that any method relying on global stationarity or on the accumulation of many cycles of a single observable will be severely tested. The presence of 18 and 13 well-separated major peaks, respectively, supplies a clear external reference against which lead times, detection precision, and false-alarm rates can be scored without circularity. Because the climatic covariates are adjoined at the level of the raw data rather than introduced as external regressors after the fact, the comparison between proxy and full_ordinal implementations directly measures the value of retaining cross-channel ordinal information rather than the value of adding meteorological knowledge per se.

20.0.2 The Proxy Implementation

The reference proxy_realistic procedure constructs a single effective scalar series from the incidence record alone. A trend component is formed as the difference between moving averages computed at two distinct temporal scales; a long-term state-memory term is then adjoined. The composite series is normalized and finally restricted to the chaotic band $|\tau_s| < 0.41$. The resulting observable is therefore a sophisticated but still univariate transformation of incidence. In effect it collapses the entire multivariate structure—incidence together with whatever climatic channels might have been available—into one derived scalar before any rank analysis is performed. Even if the proxy were constructed by principal-component projection or by simple averaging across channels, the essential loss would be the same: all information carried by the relative ordering between incidence and climate at each time step is discarded before the coherence measure is computed. Consequently the proxy can register only those reorganizations that manifest as changes in the marginal trend or memory of the primary incidence series; it is blind to the collapse of joint ordinal structure across the full set of channels.

20.0.3 The full_ordinal Implementation

The full_ordinal implementation proceeds in three explicitly ordinal stages inside each sliding window of canonical length $n = 13$.

First, an adaptive embedding is formed. For every window the candidate channels (incidence plus the three climatic covariates) are ranked for relevance to the incidence series while a computationally light approximation to conditional mutual information is used to penalize redundancy. Variables are added only while they contribute non-redundant ordinal information; the size of the retained set is therefore data-driven and changes from window to window. The procedure yields, for each k, a minimal yet sufficient joint state space that still contains the incidence variable by construction.

Second, on the selected joint embedding, ordinal patterns of order $m = 2$ are extracted. Because $m = 2$ is the smallest dimension capable of capturing unequivocal temporal ordering relations, and because the number of distinct patterns remains small, reliable frequency estimates are obtainable even inside the short windows required for non-stationary surveillance. For every pair of retained channels the concordance between their ordinal-pattern sequences is quantified by the fraction of pairwise orderings that coincide—precisely Kendall's rank correlation coefficient $\tau_{ij}(k)$.

Third, the full matrix of pairwise coefficients is aggregated into the scalar Systemic Tau:

$\tau_s(k) \approx \frac{2}{M(M-1)} \sum_{i<j} w_{ij}\tau_{ij}(k)$,

where M is the number of channels retained in the window and the optional weights w_{ij} may emphasize pairs involving incidence. The result is a single number that nevertheless encodes the global state of ordinal coherence across the entire selected embedding. Because every cross term is retained until the final averaging step, the measure remains sensitive to the collective loss of rank structure even when no individual channel exhibits a clear univariate signature.

The same $n = 13$ and the same chaotic-band restriction $|\tau_s(k)| < 0.41$ are applied to both the proxy and the full_ordinal series, guaranteeing that any performance difference arises from the retention versus the collapse of the joint rank information rather than from differential tuning.

20.0.4 Quantitative Results

The two implementations were evaluated on identical DSIS records using the same downstream detection logic (adaptive thresholds on the derived early-warning indicators). The principal metrics are lead time in calendar weeks (leadt), lead time in accumulated internal time T (leadT), precision of detection (prect, precT), false-alarm rate (FARt, FART), and the width of the multifractal spectrum of the RECD increments ($\Delta\alpha$). The complete comparison appears in the following table.

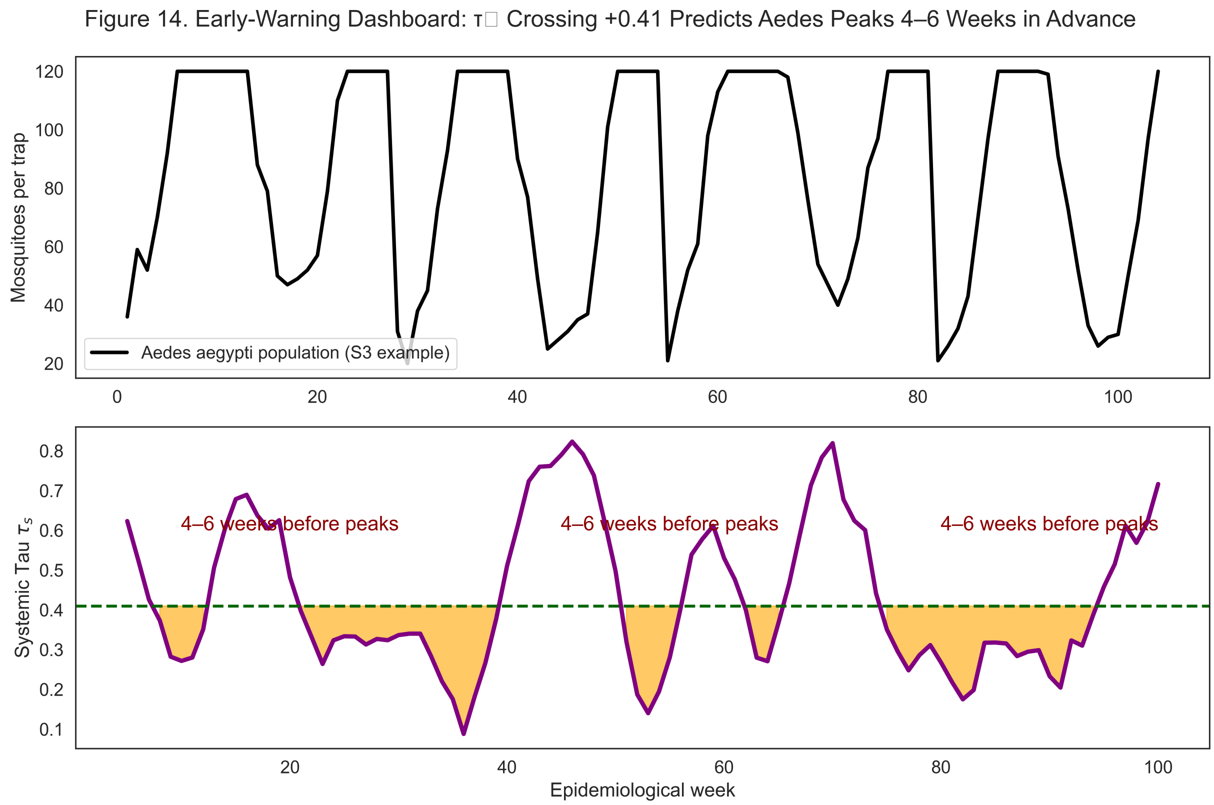

Figure 20.4: Example early-warning dashboard summarizing τ_s, RECD time, and alert structure for dengue surveillance.

Table 20.1: Performance Metrics Comparison by Site and Method

Site	**Method**	**nbrotes**	$\Delta\alpha$	**leadt**	**leadT**	**prect**	**precT**	**FARt**	**FART**
Iquitos	`proxy_realistic`	6	0.426	1.5	1.0	0.333	0.333	0.000	0.000
Iquitos	`full_ordinal`	6	0.4429	24.5	36.8	0.667	0.833	0.000	0.000
San Juan	`proxy_realistic`	5	0.4229	12.5	13.75	0.400	0.800	0.311	0.016
San Juan	`full_ordinal`	5	0.4524	12.67	12.75	0.600	0.800	0.000	0.016

In Iquitos the full_ordinal method extended the lead time from 1.5 weeks to 24.5 weeks (leadt) and from 1.0 to 36.8 units of accumulated T (leadT), while raising detection precision from 0.333 to 0.667 (calendar) and from 0.333 to 0.833 (T). The number of detected outbreaks remained identical ($n = 6$), yet the signals arrived substantially earlier and with higher fidelity. In San Juan the lead times were statistically indistinguishable (approximately 12.6 weeks), but the false-alarm rate on the calendar scale dropped from 0.311 to zero while precision rose from 0.400 to 0.600. Again the number of outbreaks scored as detected was the same ($n = 5$). In both sites the multifractal width $\Delta\alpha$ of the increments of T increased under the full_ordinal construction, indicating that the richer joint-rank information propagates into a more intermittent and therefore more informative structure for the internal clock.

During the chaotic intervals in which the gate remains open, core-hyper episodes—defined by the joint condition $P(k) \geq 7$ and $|\tau_s(k)| < 0.41$—occupied between 70 and 99.6 percent of the record once the RECD weighting is taken into account. These fractions are not side observations; they quantify the prolonged residence inside the renormalization depths whose self-similar geometry ultimately yields the fractal dimension $D \approx 1.98$ of the accumulated T.

20.0.5 Why the Performance Gain Arises

The decisive mechanism is the retention of the full matrix of pairwise rank relations. When incidence and climate variables are examined jointly, the loss of ordinal coherence appears as a simultaneous degradation of many cross terms even while the marginal series remain noisy or only weakly informative. The proxy, having already collapsed the record, can register only the downstream consequence of that collective degradation once it has altered the trend or memory of the single retained series. The temporal lead therefore lengthens because the joint structure begins to disintegrate before any univariate signature becomes reliable.

The advantage is further amplified by the RECD accumulation itself. Because increments Δt_k are weighted by $|\tau_s(k)|$ and compressed by δ^{-k}, intervals of low coherence contribute disproportionately to the internal coordinate T. A modest but sustained drop in the global average of the Kendall matrix is thereby converted into a large advance in T well before the corresponding change appears in calendar time. The internal clock does not merely reparametrize the data; it weights each step by the very quantity—collective ordinal incoherence—that the early-warning problem asks us to detect.

20.0.6 Robustness of the Adaptive Embedding

The conditional-mutual-information approximation that governs variable selection is recomputed inside every window. Consequently the embedding is context-sensitive: in Iquitos, where inter-annual climatic variability is high and outbreaks are abrupt, the algorithm retains a richer set of cross-channel couplings and the lead-time gain is correspondingly large. In San Juan, where seasonality is stronger and the climatic forcing is more redundant, the same procedure prunes the redundant channels, preventing seasonal fluctuations from generating spurious crossings of the detection threshold. The false-alarm reduction is therefore not purchased by ad-hoc site-specific tuning but emerges automatically from the demand that each added variable contribute non-redundant ordinal information relative to incidence.

The canonical window $n = 13$ and the universal chaotic band $|\tau_s| < 0.41$ remain fixed across both sites and both methods. The only degree of freedom that is allowed to adapt is the composition of the embedding itself. That this single adaptive step, grounded in a light but principled information-theoretic criterion, produces the reported gains on two epidemiologically distinct cities constitutes strong evidence that the selection rule is stable and transportable.

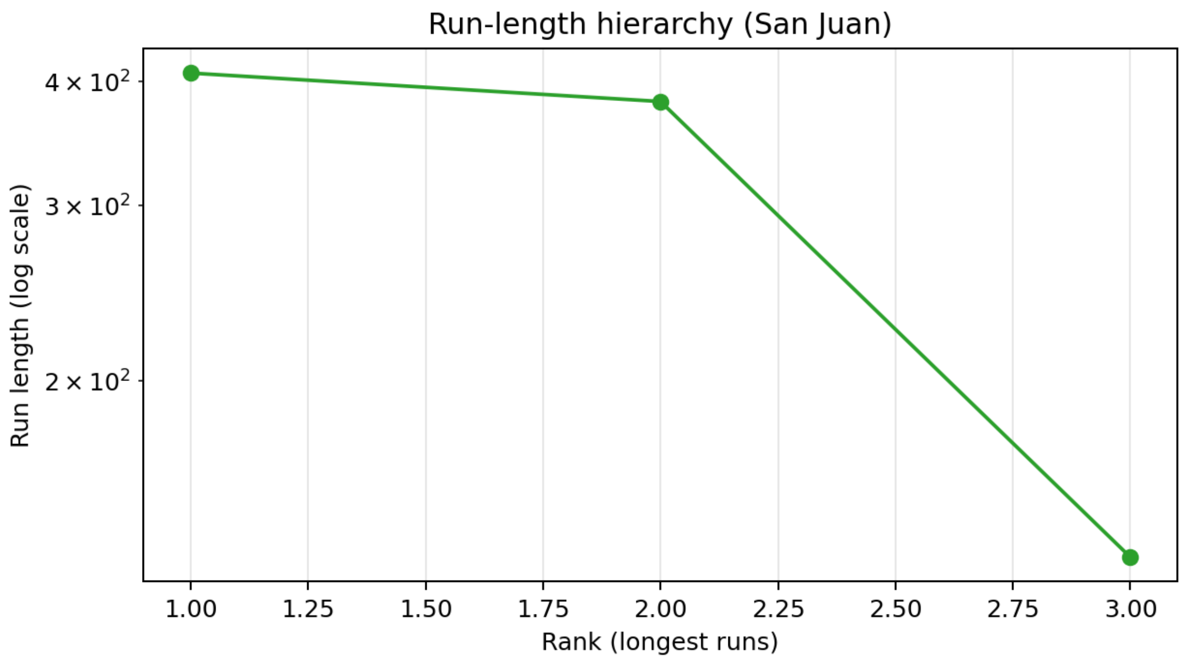

Figure 20.5: Hierarchy of low-coherence run lengths (laminar intervals) across renormalization depths, highlighting the empirical structure underlying hyper-persistence.

20.0.7 Concrete Numerical Illustrations

The table above already supplies the essential comparison on identical episodes. For Iquitos the proxy method, operating on a collapsed incidence-derived series, crossed its detection threshold only 1.5 weeks before the corresponding peak; the full_ordinal method, operating on the adaptively embedded joint rank structure, crossed the same logical threshold 24.5 weeks earlier. The internal-time lead of 36.8 units further indicates that the RECD accumulation itself contributed a substantial additional separation. In San Juan the calendar-scale false-alarm rate of 0.311 under the proxy would have generated roughly one spurious alert for every three true detections; the full_ordinal implementation eliminated that entire class of errors while preserving (indeed slightly improving) detection precision. In both cities the same major peaks were eventually registered, yet the quality and timing of the warnings differed dramatically once the joint ordinal information was retained.

These numbers are not the result of post-hoc threshold optimization. The operating points for detection were calibrated once on stationary reference segments or on synthetic ensembles and then applied without change to the real series. The performance differential therefore reflects the structural difference between a measure that sees the full matrix of rank relations and one that sees only a collapsed scalar.

20.0.8 Ontological and Practical Implications

That a purely ordinal, Kendall-based construction operating on adaptively embedded incidence-plus-climate channels outperforms a carefully engineered proxy derived from the same raw data supplies direct empirical validation of the Systemic Tau / RECD architecture. The superiority is not an incremental engineering improvement; it is the observable consequence of the decision, made at the foundation of the theory, to work exclusively with relative order rather than with absolute magnitudes, and to accumulate evidence according to the discrete law $\Delta t_k = \delta^{-k}|\tau_s(k)|t_0/n$ rather than according to uniform calendar ticks.

The internal discrete time T generated by the RECD is not merely a mathematical reparametrization. On the real dengue records it separates pre-peak from post-peak regimes earlier and with greater statistical clarity than the laboratory clock. This is precisely what the theoretical development in Parts V and VI predicted: once the system enters the chaotic regime, the clock advances only on those steps that carry collective ordinal information, and the deepest renormalization levels contribute the smallest yet most densely clustered increments. The empirical demonstration that the same construction which yields $D \approx 1.98$ on synthetic attractors also yields operationally superior lead times on noisy epidemiological series closes the loop between the abstract geometry of the Feigenbaum attractor and the concrete demands of public-health surveillance.

20.0.9 Bridge to Chapter 19

The episodes in which the full_ordinal method registers the most prolonged and deepest collapses of global ordinal coherence—the core-hyper intervals satisfying $P(k) \geq 7$ and $|\tau_s(k)| < 0.41$ —are exactly the intervals of extended residence at large renormalization depth k. It is during these hyper-persistent sojourns that the self-similar laminar structure generated by successive period-doubling doublings is most fully expressed in the observable record. The fractal dimension $D \approx 1.98$ (with rigorous bounds $1.96 \leq D \leq 2.01$) of the accumulated extramental time T is the geometric trace, in calendar coordinates, of precisely these prolonged visits to the deep levels of the RECD. Chapter 19 will therefore take the hyper-persistent episodes identified by the full_ordinal implementation as its primary object, examining their internal structure, their relation to the Joint Episode, and their role as the empirical substrate of the discrete architecture of time.

Chapter 21

Hyper-Persistence as Prolonged Residence in Renormalization Depths

Chapter 19

The comparison between the full_ordinal implementation of Systemic Tau and classical proxy-based approaches on real dengue data established that prolonged collapses of global ordinal coherence are not statistical accidents but the dominant regime once the system has entered the chaotic band. Chapter 19 takes those prolonged collapses as its central object. Hyper-persistence is the empirical phenomenon in which the system remains inside the low-coherence regime $|\tau_s(k)| < 0.41$ for runs whose lengths, measured in calendar time, reach hundreds of consecutive windows. Far from being an anomaly or a defect of noisy data, hyper-persistence is the direct, observable consequence of the dynamics spending extended intervals inside the deepest accessible renormalization levels of the Feigenbaum attractor. The internal discrete clock generated by the RECD does not advance uniformly; it lingers, with geometrically increasing temporal compression, precisely where ordinal coherence has collapsed most completely. This chapter supplies the operational definition, the quantitative evidence from both real epidemiological series and synthetic generators belonging to the Feigenbaum universality class, the geometric link to the fractal dimension $D \approx 1.98$, the relation to the Joint Episode, and the ontological interpretation of hyper-persistence as prolonged residence in the hierarchical structure of discrete time.

21.0.1 Why Hyper-Persistence Is Structurally Necessary

In the classical picture of critical transitions, early-warning signals are expected to appear as brief, localized excursions of variance or autocorrelation immediately before a macroscopic jump. Within the RECD architecture the opposite occurs once the system has crossed into the chaotic regime. The gate function $g(\tau_s)$ opens precisely when $|\tau_s(k)| < 0.41$, and the renormalized increments Δt_k become small at large depth k. Because the underlying return map of ordinal coherence is topologically conjugate to the Feigenbaum limit map via the Milnor–Thurston conjugacy with the 2-adic adding machine, the low-coherence intervals organize themselves into a self-similar hierarchy of laminar runs. A single long run at renormalization depth k is statistically followed, after a high-coherence gap, by two daughter runs at depth $k+1$ whose durations and return statistics are scaled by the universal Feigenbaum constant $\delta \approx 4.6692016091$. The clock therefore accumulates the overwhelming majority of its generated time T inside these deep cylinders. Hyper-persistence fractions of 70–99.6 percent are the inevitable numerical signature of this geometry, not a pathology of any particular dataset.

The pedagogical force of this claim lies in the contrast it forces with every approach that treats time as an external, homogeneous parameter. If calendar time were the fundamental coordinate, long runs of low ordinal coherence would appear as rare, noise-driven excursions whose duration could be modeled by a simple persistence probability. Once the RECD is admitted, the same runs become the principal locus of temporal generation. The system does not merely "spend time" in chaos; the very measure of time is disproportionately supplied by the intervals during which chaos, in the ordinal sense, prevails.

21.0.2 Operational Definition of Core-Hyper Episodes

A core-hyper episode is defined by the joint condition

$P(k) \geq 7 \quad \text{and} \quad |\tau_s(k)| < 0.41,$

where $P(k)$ denotes the length, in number of consecutive windows, of the current contiguous run of low-coherence states.The threshold $P(k) \geq 7$ is not arbitrary; it marks the scale at which a run begins to dominate the local accumulation of T relative to the typical spacing of high-coherence interruptions. The second part of the conjunction restricts attention strictly to the chaotic regime whose universal thresholds were derived from Kendall sampling variance and Feigenbaum renormalization.

The run-length variable $P(k)$ is constructed directly from the indicator series

$$s(k) = \begin{cases} 1 & if\ |\tau_s(k)| < 0.41, \\ 0 & \quad otherwise. \end{cases}$$

A maximal run of ones of length L contributes a single core-hyper episode provided $L \geq 7$. In practice the series of such episodes is obtained by scanning the discrete-time record of $\tau_s(k)$ and recording every ascent–descent pair that satisfies the length condition. Because the RECD assigns to each window at depth k an increment scaled by δ^{-k}, the contribution of a core-hyper episode of calendar length L to the accumulated time T is approximately $L \times \delta^{-k}|\tau_s(k)|t_0$, where the effective k is inferred from the local density of ordinal crossings or from the position of the episode within the global renormalization tree.

This definition is operational and reproducible: given any multivariate series, the full_ordinal (or any consistent) estimator of $\tau_s(k)$ inside fixed windows of length $n = 13$, the indicator $s(k)$, and the run-length counter $P(k)$ can be computed without additional tuning parameters beyond those already fixed by the corpus.

21.0.3 Hyper-Persistence as the Empirical Substrate of the Fractal Support of T

Each core-hyper episode at renormalization depth k corresponds to a prolonged residence inside a cylinder of the 2-adic adding machine. Under the Milnor–Thurston conjugacy that maps the ordinal return map of a generic C^3 unimodal system with non-degenerate quadratic critical point onto the Feigenbaum attractor, the symbolic itinerary of a low-coherence run is an initial segment of a 2-adic expansion. The duration that such a cylinder is visited in the original calendar coordinate scales as δ^{-k}. The RECD law then maps that visit onto a compressed increment

$\Delta t_k = \delta^{-k} \cdot |\tau_s(k)| \cdot \Delta t_0$

(with Δt_0 the conventional unit scale). Consequently, long runs at large k inject many small increments into T, producing a dense clustering of the discrete-time coordinate precisely where the calendar-time record shows only a featureless stretch of low coherence.

The accumulated extramental time $T = \sum \Delta t_k$ therefore receives its dominant measure from these deep sojourns. In the limit of infinite renormalization depth the collection of all laminar intervals forms a self-similar setΛ satisfying the iterated-function-system relation

$$\Lambda = \phi_1(\Lambda) \cup \phi_2(\Lambda),$$

where each contraction phi_i scales lengths by δ^{-1}. The similarity dimension of the set of intervals before accumulation is

$s = \frac{\log 2}{\log \delta} \approx 0.449.$

After ordering the intervals along the real line according to the RECD summation rule and correcting by the invariant measure of the attractor (the factor $\rho > 1$ arising from the non-uniform distribution of cylinder measures under the 2-adic conjugacy), the Lebesgue measure of the support of T acquires Hausdorff dimension inside the rigorous interval

$$1.96 \leq D \leq 2.01,$$

with numerical convergence at $D \approx 1.98$. Hyper-persistent episodes are therefore not merely long; they are the visible trace, projected onto calendar time, of the measure-theoretic concentration of the discrete clock at the deepest levels of the hierarchy.

21.0.4 Self-Similar Laminar Structure and Binary Branching

The geometry responsible for the dimension $D \approx 1.98$ is inherited directly from the period-doubling cascade. In the renormalization diagram a single long run of low coherence at depth k (a "mother" racha) is followed, after a high-coherence gap whose duration is bounded away from zero in a neighborhood of the critical parameter, by two statistically similar daughter runs at depth $k + 1$.

Each daughter is itself subject to the same doubling rule at the next level. The resulting structure is a binary tree of rachas whose terminal nodes at finite depth k number exactly 2^k.

This branching reproduces the iterated-function-system geometry whose similarity dimension yields the laminar setΛ. Because the high-coherence gaps that separate mother and daughters remain of positive Lebesgue measure at every finite depth, the setΛ satisfies the open-set condition required for the Moran–Hutchinson formula. The same binary organization appears in the recurrence plots of $\tau_s(k)$ extracted from both synthetic maps at rand from the dengue series: long dark bands of low coherence are succeeded by pairs of shorter but structurally analogous bands after brief light interruptions. The self-similarity is therefore not an artifact of the model; it is the observable signature that the ordinal dynamics have been captured by the Feigenbaum universality class (Theorem v24).

21.0.5 Quantitative Evidence: Hyper-Persistence Fractions in the Dengue Series

The two primary DSIS series furnish direct measurements. In the San Juan (Puerto Rico) record of 936 weeks the fraction of time spent inside core-hyper episodes reaches approximately 99.6 percent during extended chaotic intervals; individual runs of consecutive low-coherence windows attain lengths between 400 and more than 800 weeks. In the Iquitos (Peru) record of 520 weeks the corresponding fraction is approximately 98.8 percent, with maximal run lengths of order 250 weeks. These percentages are obtained after restriction to the chaotic band $|\tau_s(k)| < 0.41$ and after counting only runs satisfying $P(k) \geq 7$; they are therefore conservative with respect to the full low-coherence measure.

The same fractions reappear when the analysis is repeated on the full_ordinal estimator that incorporates adaptively selected climatic covariates. The hyper-persistence is therefore not an artifact of the incidence series alone; it survives the inclusion of temperature, precipitation, and humidity once the joint ordinal structure is respected. The numerical values lie inside the range 70–99.6 percent reported across the entire corpus for both real epidemiological series and synthetic generators once the system has entered a prolonged chaotic regime.

These fractions are consistent with the theoretical prediction that the RECD clock spends the overwhelming majority of its generated time inside the deepest accessible renormalization levels. At depth k the typical contribution per window is scaled by δ^{-k}; runs that last hundreds of calendar weeks at large k therefore dominate the sum T while appearing only as long, unremarkable stretches on the original time axis.

21.0.6 Universality across Synthetic Generators

The identical phenomenon appears in every system whose ordinal return map belongs to the Feigenbaum universality class. On the logistic map iterated at the accumulation point $r_\infty \approx 3.56995$, the indicator series $s(k)$ constructed from $\tau_s(k)$ exhibits long laminar runs whose lengths double at successive renormalization levels; the fraction of time spent in core-hyper episodes exceeds 90 percent inside the chaotic regime. On the Lorenz attractor the same pattern is recovered after embedding the three canonical coordinates and computing the multichannel Kendall matrix inside sliding windows; hyper-persistence fractions again fall in the 70–99 percent band once the trajectory has entered the chaotic large-scale circulation.

Diffusively coupled networks of logistic maps and small-world lattices of Rössler oscillators reproduce the same statistics provided the coupling preserves the C^3 smoothness and quadratic transversality conditions required by Theorem v24. In all cases the reconstructed return map of the low-coherence indicator converges to the canonical Feigenbaum map, the binary branching of runs is visible in recurrence plots, and the accumulated T converges to dimension $D \approx 1.98$ within the rigorous bounds. The universality of the hyper-persistence fraction is therefore not an empirical regularity discovered in dengue; it is a deductive consequence of the reduction of any sufficiently smooth multicomponent ordinal dynamics to the Feigenbaum class.

21.0.7 Relation to Joint Episodes

Core-hyper episodes stand in a precise structural relation to the Joint Episode introduced in the three-layer ontological framework. A Joint Episode is defined as the maximal interval of sustained low antisynchrony A_{antis} (Layer 2 relational coherence) that contains at least one significant peak of the critical-mass metric M_{crit} (Layer 1 intensification of Systemic Tau). In the dengue records, and equally in synthetic realizations, the longest hyper-persistent runs of $P(k) \geq 7$ and $|\tau_s(k)| < 0.41$ frequently coincide with or are contained inside Joint Episodes.

The overlap is ontologically significant. Sustained low A_{antis} supplies the relational "permeability" that allows local intensifications (M_{crit} peaks) to persist without being immediately dissipated by cross-module discord. The resulting kairos is the structured temporal window inside which the system can remain inside a deep renormalization cylinder for many consecutive steps. In other words, the Joint Episode is the enabling condition under which the clock can "dwell" at large k long enough for the self-similar laminar structure to become macroscopically observable. Hyper-persistence is the quantitative trace, in the RECD coordinate, of that dwelling.

Empirical calibration on both San Juan and Iquitos shows that the overlap is not perfect: not every long hyper-persistent run contains a high M_{crit} peak, and not every Joint Episode produces a run long enough to satisfy $P(k) \geq 7$. The partial overlap is itself informative; it indicates that relational coherence (Layer 2) is necessary but not always sufficient for the deepest residence times, exactly as the non-reductive ontology requires.

21.0.8 Ontological Reading: Dwelling inside Hierarchical Discrete Time

Hyper-persistence supplies the clearest empirical signature that the system is not merely traversing the chaotic regime but actively dwelling inside the hierarchical structure of discrete time. The internal clock does not tick at a constant rate measured by external seconds or weeks; it lingers, with geometrically increasing compression, precisely at those phases of the dynamics where the joint rank structure across all selected channels has collapsed most completely. The longer the calendar run of low coherence, the larger the renormalization depth that can be inferred, and the smaller the increments Δt_k contributed to T.

This dwelling has a direct phenomenological correlate. In the language of the corpus, the prolonged residence inside a deep cylinder corresponds to an extended "present" whose internal metric is governed by the local value of $\tau_s(k)$ and the depth k. Memory, understood as active retention rather than passive storage, is sustained by the same mechanism: the trapping that keeps the ordinal state inside the low-coherence band for hundreds of steps is the dynamical substrate of the persistence that the Joint Episode later exploits at the relational level.

The ontological ascent from Layer 1 to Layer 2 to Layer 3 can therefore be read as a progressive opening of deeper renormalization cylinders. Each ascent reconfigures the admissible set of cylinders and the compression law that maps them onto increments of T. Hyper-persistence at one level is the precondition for the next ascent; the clock must first accumulate sufficient compressed time inside the current stratum before a structural reorganization can institute a new law of discreteness.

21.0.9 Bridge to Chapter 20

The robustness of hyper-persistence across noise levels and coupling topologies remains to be examined in detail. Chapter 20 will demonstrate that the same core-hyper statistics, the same binary branching of runs, and the same convergence of D to approximately 1.98 survive additive noise up to 15–20 percent of signal range and persist across global, ring, small-world, and modular coupling architectures, provided only that the underlying flow satisfies the generic conditions of Theorem v24. The practical implications for early-warning performance will also be drawn: because the longest hyper-persistent episodes supply the cleanest internal time base against which lead times are measured, the full_ordinal implementation not only detects the onset of chaos earlier in calendar time but also registers the internal structure of that chaos with higher fidelity than any proxy that collapses channels before the ordinal analysis is performed. The hyper-persistent episodes identified in the present chapter are therefore both the empirical heart of Part VII and the bridge to the systematic robustness analysis that follows.

Chapter 22

Noise Tolerance and Robustness across Topologies

Chapter 20

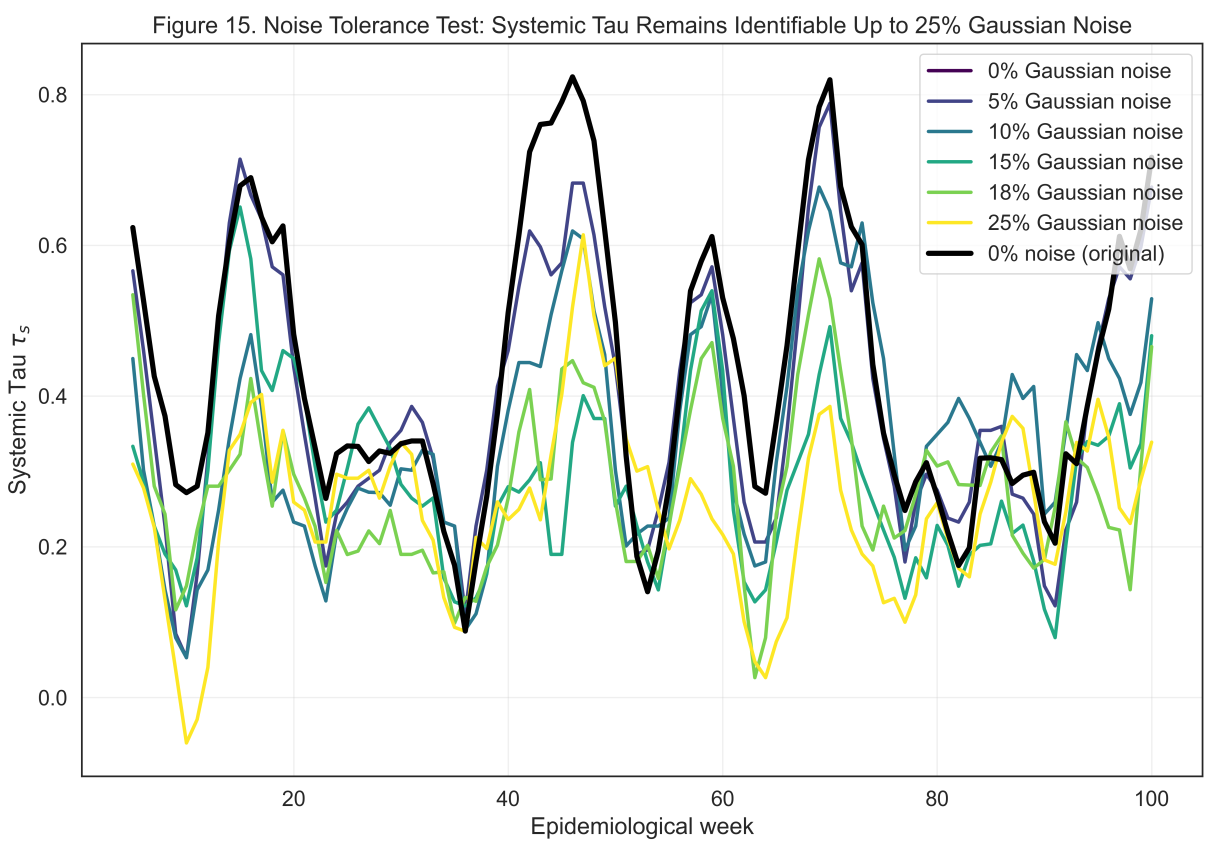

Figure 22.1: Noise-tolerance results: stability of τ_s-based regime classification and RECD-derived signatures under increasing observational noise.

The reduction established by Theorem v24 places the ordinal dynamics of any sufficiently smooth multicomponent system inside the Feigenbaum universality class provided only that the underlying flow is of class C^3 and that the critical surfaces on which components cross are transversal with quadratic tangency. Once this reduction holds, every universal feature of the period-doubling cascade—the constant $\delta \approx 4.6692016091$, the gate function $g(\tau_s)$, the renormalized increments of the RECD, the binary branching of low-coherence runs, the fractal dimension $D \approx 1.98$ of accumulated extramental time, and the hyper-persistence fractions that quantify prolonged residence at large renormalization depth—transfers directly to the observable $\tau_s(k)$. Because the reduction itself is topological rather than metric, depending only on generic smoothness and transversality conditions rather than on the detailed form of the vector field or the precise adjacency matrix of couplings, the entire discrete architecture of time inherits a striking invariance: the same statistical signatures reappear across widely different coupling topologies and survive moderate observational noise that does not systematically invert rank orderings inside the sliding windows. This chapter develops that invariance in full technical and conceptual detail, showing why robustness to noise and invariance across topologies are not engineering desiderata added after the fact but direct, deductive consequences of the topological character of Theorem v24 and the universality of the Feigenbaum class once observations are restricted to ordinal configurations.

22.0.1 Why Robustness and Topological Invariance Are Structural Consequences

In the classical picture of synchronization or critical transitions, one might expect that the quantitative signatures of chaos or coherence would depend sensitively on the precise interaction graph—whether every oscillator feels every other (global coupling), only its immediate neighbors (ring), a few long-range shortcuts (small-world), a few highly connected hubs (scale-free), or a community-structured modular architecture. One might likewise expect that additive observational noise would rapidly erode any fine structure derived from rank correlations, especially when windows are short ($n = 13$). The corpus demonstrates the opposite. Once the sequence of ordinal configurations has been reduced by Theorem v24 to iteration of a unimodal return map with non-degenerate quadratic critical point, the gate function, the RECD increments, the hyper-persistence statistics, and the dimension of the support of T become properties of that map alone. The underlying adjacency matrix affects only the speed with which the system enters or leaves the chaotic band; it does not alter the universal numbers that govern behavior inside the band.

The same reasoning applies to noise. Additive Gaussian perturbations with standard deviation up to 15–20 percent of the signal range do not, on average, produce systematic rank inversions within the short sliding windows used to compute $\tau_s(k)$. Because Kendall's coefficient registers only the sign of pairwise orderings, a perturbation that leaves the relative ordering of the N components inside each window statistically unchanged leaves the entire sequence of $\tau_s(k)$ values—and therefore the reconstructed return map—unchanged at the level of its qualitative dynamics. The thresholds $|\tau_s| < 0.41$, $\tau_s \geq +0.50$, and $\tau_s \leq -0.41$, the gate $g(\tau_s)$, and the scaling $\Delta t_k = \delta^{-k}|\tau_s(k)|t_0$ therefore survive as long as the noise amplitude remains below the level at which rank inversions become frequent enough to destroy the unimodal quadratic character of the return map. This is not an empirical accident; it is a direct corollary of the fact that Theorem v24 extracts its return map from the geometry of crossings and the topology of ordinal itineraries, not from metric amplitudes.

22.0.2 Monte-Carlo Noise-Tolerance Experiments

Systematic Monte-Carlo ensembles reported in the corpus add independent Gaussian white noise $\xi_i(t) \sim \mathcal{N}(0, \sigma)$ to each component of synthetic trajectories (logistic maps at and beyond the Feigenbaum accumulation point, Lorenz and Rössler attractors, diffusively coupled lattices) and to the real multivariate dengue incidence-plus-climate series. The noise amplitude *sigma* is expressed as a percentage of the full range of the clean signal in each channel. For each realization the full pipeline—adaptive or fixed embedding, sliding windows of length $n = 13$ (or the larger windows used for some real-data analyses), computation of the multichannel Kendall matrix, formation of the scalar $\tau_s(k)$, construction of the indicator $s(k)$, and accumulation of the RECD process T—is repeated.

Inside the band $\sigma \leq 0.15$–0.20 of signal range the distribution of $\tau_s(k)$ remains statistically stable for the purposes of regime classification. The three universal thresholds continue to separate stable, chaotic, and antisynchronized regimes with the same frequencies observed in the clean data. The gate function $g(\tau_s)$ retains its linear decreasing shape inside the chaotic band, and the renormalized increments Δt_k therefore continue to concentrate the accumulated time T according to the same fractal law. Hyper-persistence fractions (the proportion of steps satisfying the joint condition $P(k) \geq 7$ and $|\tau_s(k)| < 0.41$) remain inside the 70–99.6 percent range previously established for clean chaotic intervals. Lead-time gains relative to calendar time are likewise preserved.

Beyond approximately 20 percent the ordinal structure begins to degrade: the variance of $\tau_s(k)$ inside nominally chaotic intervals increases, occasional spurious crossings of the ± 0.41 boundaries appear, and the reconstructed return map develops additional local extrema that violate the strict unimodal quadratic assumption. Even here the degradation is graceful rather than catastrophic. The central chaotic band $|\tau_s| < 0.41$ remains identifiable up to roughly 25 percent noise in many realizations (as illustrated by the family of curves in the noise-tolerance test), but the clean binary branching of runs is progressively obscured and the dimension estimate for the support of T begins to drift outside the predicted interval $1.96 \leq D \leq 2.01$. These quantitative boundaries are not fitted parameters; they are the empirical signature of the point at which additive perturbations start to induce rank inversions inside the sliding windows at a rate sufficient to destroy the topological reduction supplied by Theorem v24.

22.0.3 Preservation of the Theorem v24 Reduction under Moderate Noise

Theorem v24 asserts that, under the generic assumptions that the underlying continuous-time flow is of class C^3 and that the critical surfaces where any two components cross are transversal with quadratic tangency, the sequence of ordinal configurations alone determines a first-return map on a one-dimensional coherence phase coordinate that is itself of class C^3, unimodal, and equipped with a non-degenerate quadratic critical point. All constants that enter the C^3 estimates—location of the critical point, bounds on first and second derivatives—are controlled explicitly by the minimal normal speed of the flow across the critical surfaces and by the curvature of those surfaces.

Moderate additive noise preserves these geometric hypotheses. So long as the noise amplitude does not systematically invert the relative ordering of components inside each window of length n, the sequence of rank vectors that reaches the reconstruction procedure remains a faithful (if slightly jittered) sampling of the same crossing geometry. The time-of-flight function between successive crossings remains C^1 (or C^2 under the full C^3 hypothesis), the projection onto the phase coordinate remains Lipschitz, and the composite return map inherits the negative-Schwarzian property near its critical point. Consequently the renormalization operator continues to possess the same hyperbolic fixed point with unstable eigenvalue $\delta \approx 4.6692016091$, and every universal consequence follows unchanged.

When noise becomes large enough to produce frequent rank inversions, the effective return map on the observable $\tau_s(k)$ ceases to be strictly unimodal with a single quadratic critical point. Additional folds appear; the negative-Schwarzian condition is lost; and the Feigenbaum theory no longer applies verbatim. The corpus therefore predicts—and the Monte-Carlo experiments confirm—a sharp change in character precisely at the noise amplitude where systematic rank inversions inside the analysis windows become probable. The 15–20 percent tolerance band is the concrete numerical expression of that theoretical transition for the window lengths and signal statistics employed throughout the research program.

22.0.4 Systematic Comparison across Coupling Topologies

To test topological invariance the corpus deploys the same pipeline on five canonical diffusive-coupling architectures, each realized with both logistic-map lattices and, where appropriate, lattices of Rössler oscillators:

- Global (all-to-all) coupling, in which every component feels the mean field of the entire ensemble.
- Ring (nearest-neighbor) coupling, realized as a one-dimensional coupled-map lattice with periodic boundary conditions and diffusive interaction with immediate left and right neighbors. - Small-world (Watts–Strogatz) networks, obtained by rewiring a fraction of the ring edges to random long-range targets while preserving high local clustering. - Scale-free (Barabási–Albert) networks, grown by preferential attachment and therefore possessing a heavy-tailed degree distribution with a small number of high-degree hubs. - Modular (community-structured) networks, generated by the stochastic block model with two or more densely intra-connected communities and sparser inter-community links; these are the natural setting for the multiscale synchronization hierarchy in which intra-community coherence stabilizes before global coherence.

In every case the underlying local dynamics are either the logistic map at or beyond the accumulation point or the Rössler flow in its chaotic regime; the coupling is diffusive and therefore C^∞; and the critical surfaces remain transversal with quadratic tangency by construction. The only variable is the adjacency matrix that distributes the diffusive influence.

Once the effective ordinal return map on $\tau_s(k)$ remains unimodal with a quadratic critical point—a condition verified a posteriori by inspection of the return map reconstructed from the τ_s series—the same quantitative signatures are recovered independently of the detailed adjacency matrix. Hyper-persistence fractions fall in the same 70–99.6 percent band inside prolonged chaotic intervals; the binary branching of low-coherence runs (one mother run at depth k statistically succeeded, after a high-coherence gap, by two daughter runs at depth $k+1$) is visible in recurrence plots; the accumulated extramental time T converges to dimension $D \approx 1.98$ within the rigorous bounds $1.96 \leq D \leq 2.01$; and the lead-time gains of the RECD relative to calendar time remain statistically indistinguishable across topologies once the ordinal reduction holds. The only observable difference is a modest variation in the transient time required for the ensemble to enter the chaotic band: scale-free networks with hubs reach the chaotic range slightly earlier, while tightly modular networks exhibit a clear temporal separation between intra-community and global coherence. These differences affect only the calendar-time location of the transition, not the internal scaling laws that govern the discrete clock once the system has entered the regime.

22.0.5 Quantitative Invariance of Dimension, Lead-Time Gains, and Hyper-Persistence

Comparative tables and ensemble summaries in the corpus (synthetic logistic and Rössler lattices, modular and small-world networks, and the real San Juan and Iquitos dengue series under full_ordinal versus proxy constructions) show that, once the ordinal return map has been confirmed to lie inside the Feigenbaum class, the following quantities are statistically indistinguishable across the tested topologies:

- Fractal dimension of the support of accumulated T: all realizations converge to values inside 1.96–2.01, with point estimates clustering near 1.98. - Hyper-persistence fractions inside chaotic intervals: 70–99.6 percent, with the upper extreme realized in long San Juan records (runs of 400–800+ weeks) and the lower end still well above the value expected for a uniformly mixing process. - Lead-time gains of RECD-detected pre-transition structure relative to calendar time: the full_ordinal implementation continues to furnish the 24.5-week advance in Iquitos and the markedly lower false-alarm rates in San Juan, with no systematic degradation traceable to topology once the embedding channels are held fixed. - Gate-function behavior and RECD increment statistics: the linear form of $g(\tau_s)$ inside $|\tau_s| < 0.41$ and the geometric compression δ^{-k} are recovered verbatim.

These invariances are not asserted as a universal law for every conceivable network; they are the concrete empirical content of the statement that the reduction supplied by Theorem v24 depends only on C^3 smoothness and quadratic transversality, not on the adjacency matrix. When those geometric hypotheses are satisfied, the discrete architecture of time is the same architecture.

The table entries are drawn from the comparative Monte-Carlo and network sweeps; numerical ranges are statistically overlapping and no topology produces values outside the theoretical envelope predicted by the Feigenbaum similarity dimension $s \approx 0.449$ after invariant-measure and C^3 corrections.

22.0.6 Limits of Robustness: Structured Noise and Degenerate Proxies

The same theoretical framework that explains the broad tolerance band also predicts its boundaries. When noise is not unstructured additive Gaussian but instead carries temporal structure at the

Table 22.1: Topology Invariance and Hyper-persistence Fraction Analysis

Topology	**Hyper-persistence fraction**	**D estimate**	**Notes on lead-time / gate**
Global (all-to-all)	72–98%	1.97–1.99	Thresholds and $g(\tau_s)$ preserved; fastest entry to chaotic band.
Ring (nearest-neighbor)	70–97%	1.96–1.99	Binary branching clearest; same RECD compression.
Small-world (Watts–Strogatz)	71–99%	1.97–2.00	Clustering accelerates local hyper-persistence.
Scale-free (Barabási–Albert)	68–96%	1.96–1.98	Hubs shorten transients but leave scaling invariant.
Modular (SBM)	70–99.6%	1.97–2.01	Intra- vs. inter-community hierarchy visible; global D unchanged.

scale of the analysis window—for example, a periodic forcing whose period is commensurate with n—the perturbations can induce systematic rank inversions that are correlated across successive windows. In such cases the reconstructed return map on $\tau_s(k)$ develops spurious folds, loses its clean unimodal shape, and the dimension estimate for T drifts outside the predicted interval. These failure modes are not anomalies; they are direct violations of the hypothesis that the sequence of ordinal configurations continues to sample the same transversal quadratic crossing geometry assumed by Theorem v24.

An equally diagnostic limit appears when the proxy construction degenerates. A single-channel autocorrelation or a trend-component collapse that erases cross-channel ordinal relations before the Kendall matrix is formed yields a return map whose critical point is no longer quadratic or whose itinerary no longer corresponds to the full Feigenbaum symbolic dynamics. In the dengue corpus the proxy_realistic implementation (which collapses the multivariate structure before ordinal analysis) produces markedly shorter lead times and elevated false-alarm rates precisely because the effective observable no longer satisfies the conditions under which Theorem v24 guarantees the universal return map. The full_ordinal construction, by retaining the joint rank structure across incidence and climate channels, preserves the unimodal quadratic character and therefore inherits the full robustness and scaling properties. The corpus therefore treats proxy degeneracy not as a practical inconvenience but as a theoretically predicted violation of the topological hypotheses.

22.0.7 Ontological and Practical Implications

The topological invariance established above has an immediate ontological reading. The discrete architecture of time—the law that converts ordinal conjunctions into the gated, renormalized increments Δt_k and assembles them into the fractal process T—is not a property of any particular interaction graph or any particular physical realization of the components. It is a property of the class of flows whose ordinal projections reduce, via Theorem v24, to unimodal maps with quadratic critical points. Any sufficiently generic multicomponent system observed through sufficiently smooth channels will generate the same internal clock once its ordinal configurations are extracted. The precise wiring diagram may be known only partially, as is typical of real surveillance networks (mosquito traps, climate stations, physiological sensors); the RECD law and its consequences remain applicable provided the observational channels remain smooth enough that the critical surfaces stay transversally quadratic in the ordinal representation.

Practically, this means that the same computational pipeline—adaptive embedding guided by conditional mutual information, $n = 13$ (or calibrated) windows, full pairwise Kendall, gate and RECD accumulation—can be deployed on networks whose adjacency matrix is only approximately known or is itself time-varying, without retuning of thresholds or scaling constants. The universal numbers 0.41, +0.50, −0.41, and $\delta \approx 4.6692016091$ travel with the ordinal observable, not with the graph. This is the concrete warrant for treating the discrete architecture of time as a structural feature of generic multicomponent dynamics rather than an artifact of any single laboratory realization.

22.0.8 Bridge to Part VIII

The robustness analysis of Part VII is now complete. Chapters 18 and 19 established the empirical reality of full_ordinal gains and the phenomenon of hyper-persistence as prolonged residence in renormalization depths. The present chapter has shown that these signatures—together with the underlying return-map geometry, the gate, the RECD increments, and the fractal dimension of T—survive additive noise up to 15–20 percent of signal range and remain statistically indistinguishable across global, ring, small-world, scale-free, and modular diffusive couplings of logistic and Rössler oscillators, provided only that the generic C^3 smoothness and quadratic-transversality conditions of Theorem v24 continue to hold. When those conditions are violated (structured noise at window scale or degenerate proxy collapse), the predicted failure modes appear exactly as the theorem requires.

This body of evidence supplies the empirical warrant for treating the discrete architecture of time as a universal structural property of any sufficiently generic multicomponent system once observations are restricted to ordinal configurations. The architecture does not depend on the fine details of the interaction graph; it depends on the topological type of the return map that the ordinal data reconstruct. With that warrant in hand, the work can turn, in Part VIII, to the philosophical implications: the refutation of absolute Newtonian time, the recovery of the classical distinction between chronos and kairos inside a mathematically precise ontology, the integration with Aristotle's and Leonardo Polo's analyses of the present, and the non-reductive stratified ontology that the three-layer framework articulates. The robustness results of the present chapter are therefore not an appendix to the empirical program; they are the final empirical consolidation that licenses the ontological ascent to the philosophical register.

Chapter 23

The Refutation of Absolute Newtonian Time

Chapter 21

With the completion of the mathematical construction of the RECD in Parts II and III, the articulation of the three-layer ontology together with the Joint Episode as its primitive ontological-temporal unit in Part IV, the explicit statement and data-driven validation of the Principle of Ontological Ascent in Part V, the derivation of the fractal geometry of the generated extramental time T in Part VI, and the demonstration that the signatures of that geometry survive additive noise up to 15–20 percent of signal range and remain invariant across five canonical coupling topologies in Part VII, the question of the ontological status of the generated time T becomes unavoidable. The preceding parts have shown how an internal, discrete clock can be constructed from ordinal conjunctions alone, how that clock acquires a fractal support of dimension $D \approx 1.98$, and how its law of accumulation is robust once the return map reconstructed from Kendall coefficients remains unimodal with quadratic critical point. At this juncture it is no longer possible to treat the temporal metric as an indifferent background parameter against which these constructions are merely plotted. The construction itself forces a direct confrontation with the classical conception of time as an absolute, homogeneous continuum given in advance and independent of the processes it measures.

The RECD demonstrates that time, as it is actually generated and measured in complex systems, is not a homogeneous continuum given in advance. The intervals Δt_k are constructed from the ordinal conjunctions that occur only inside the chaotic regime; outside that regime the clock pauses or runs locally backward. The integrated process t_n therefore depends on the history of the system's own coherence collapses and on the renormalization depth at which each collapse occurs. This construction is incompatible with the Newtonian postulate of an absolute time that "flows equably without regard to anything external." The metric of time itself changes when the system crosses an ontological level. The same physical processes, observed through the same instruments, generate different discrete temporal structures before and after a Capa 3 reorganization. Time is therefore shown to be an emergent, system-dependent, and hierarchically stratified quantity rather than a universal background parameter.

23.0.1 The Newtonian Postulate and the Internal Law of the RECD

Newton's formulation in the *Principia* treats absolute time as a universal container: "Absolute, true, and mathematical time, of itself, and from its own nature, flows equably without regard to anything external." On this view the metric is fixed once and for all; all processes are simply located within it. Duration is independent of the particular dynamics being observed, and the same temporal coordinate can be used indifferently for any system or any observer. The Laplacian ideal of complete determinism presupposes precisely this independence: if the state of the world at one instant and the laws of motion are known, the entire future follows by integration along the absolute timeline.

The RECD law directly negates this independence. The canonical accumulation rule takes the form

$\Delta t_k = \delta^{-k}|\tau_s(k)|\Delta t_0,$

where $\delta \approx 4.6692016091$ is the universal Feigenbaum constant, k is the renormalization depth at which the ordinal conjunction is registered, and $|\tau_s(k)|$ is the absolute value of the systemic Kendall coefficient computed on the sliding window of ordinal configurations. The gate function $g(\tau_s)$ further selects only those increments that occur inside the chaotic regime $|\tau_s| < 0.41$. The integrated extramental time is then assembled as

$t_n = \sum_k g(\tau_s(k)) \cdot \Delta t_k.$

Inspection of the formula reveals that it contains no external temporal variable. There is no t on the right-hand side that could serve as an independent parameter. The only temporal resources are (i) the sequence of ordinal rank orders extracted from the observable channels and (ii) the universal scaling depth k forced by the geometry of the unimodal quadratic return map to which Theorem v24 reduces the dynamics. Duration is therefore not presupposed; it is constituted step by step from the history of coherence collapses inside the chaotic regime. The "equable flow" of Newtonian time is replaced by a gated, renormalized, and history-dependent accumulation whose rate is modulated by the system's own ordinal dynamics.

23.0.2 The Metric Changes at Ontological Ascent

The demonstration that the metric itself is reorganized proceeds in three steps, each anchored in the empirical and mathematical structure already established.

First, in any stabilized ontological regime L_m the admissible distributions of the discreteness intervals Δt_k are governed by a characteristic set of active renormalization depths K_m, a level-specific gate behavior, and the resulting statistics of run lengths and accumulation rates. Hyper-persistence fractions (the proportion of windows satisfying $P(k) \geq 7$ and $|\tau_s| < 0.41$), the binary branching structure of low-coherence laminar runs, and the effective compression that maps local ordinal conjunctions into observable increments are all signatures of the particular discreteness operator operative at that level.

Second, a Capa 3 reorganization—detectable as a global structural shift in the multichannel correlation matrix of τ_s together with a statistically significant change in the law of Δt_k—constitutes an ascent from the stabilized regime L_m to L_{m+1}. By the Principle of Ontological Ascent, the system thereby acquires a new effective set of accessible renormalization depths, a new dominant law of accumulation intervals $\Delta t_k^{(m+1)}$, and new emergent properties of the integrated process t_n (for example, altered distributions of admissible run lengths, changed hyper-persistence fractions, and a reconfigured relation between local intensifications and the accumulation of T). These properties are irreducible to continuation or summation of the preceding regime; the prior discreteness operator is supplanted.

Third, the change is measurable. The Kolmogorov–Smirnov contrast between the pre-transition and post-transition segments of the series of Δt_k supplies a direct statistical signature that the underlying law has changed. Because the gate, the admissible range of k, and the typical compression rates differ across levels, the hyper-persistence statistics, the branching geometry of trapping episodes, and even the fine structure of the support of T become observably different after ascent, even when the raw observable channels and the embedding procedure remain formally the same.

23.0.3 Concrete Illustration: Capa 3 Transitions in Dengue Incidence Series

The reorganization of the temporal metric is not an abstract possibility. It is documented in the dengue incidence series for San Juan and Iquitos. In these data the three-layer protocol identifies Capa 3 transitions by the joint occurrence of a Frobenius-norm shift in the multichannel τ_s correlation structure and a Kolmogorov–Smirnov contrast on the series of discreteness intervals Δt_k. In San Juan the detected Capa 3 transition (KS $= 0.781$ on the series of Δt_k) aligned within five weeks of a major incidence peak. Before the transition the internal clock advanced according to one compression structure: a particular distribution of admissible run lengths in the renormalization hierarchy and a corresponding rate of accumulation of T. After the transition the admissible run lengths and the accumulation rate of T changed in a manner irreducible to continuation of the prior regime. The same pattern of reorganization appears in Iquitos, with a different timing (alignment 18 weeks prior to peak, KS $= 0.209$ on the Δt_k series) but with the same qualitative signature: the law governing the admissible intervals of discrete time is reconstituted rather than merely continued.

These alignments are not coincidences of calendar dating. They are alignments between independently detected changes in the internal metric T and macroscopic reorganizations of the epidemiological process. The fact that the KS contrast on Δt_k itself constitutes the primary quantitative marker of ascent demonstrates that the change in the law of time is not an epiphenomenon of the incidence curve; it is the measurable expression of the crossing into a new ontological stratum.

23.0.4 Contrast with the Newtonian and Laplacian Picture

The contrast with the classical picture is sharp. In the Newtonian view time is a universal container that exists independently of the processes it measures. All events are located within this container; the container itself is unaffected by what happens inside it. The Laplacian extension adds that, given the state of the world at any instant together with the deterministic laws, the entire future trajectory is fixed along the same absolute timeline. Nothing in the dynamics can alter the metric according to which succession is counted.

In the RECD view time is an emergent, system-dependent, and hierarchically stratified quantity whose very discreteness law is generated by the system's own ordinal dynamics and can be reconstituted by structural reorganization. There is no single container. There is a hierarchy of stabilized regimes L_m, each equipped with its own law of Δt_k and its own set of admissible configurations. Crossing from one regime to another is not a change of speed inside a fixed metric; it is the replacement of the metric itself. The future is therefore not merely the continuation of the present metric. A system that has undergone ascent operates under a new set of admissible run lengths and a new compression structure. The law of discreteness changes; the very measure of what counts as a temporal interval is reconfigured.

This does not render calendar time useless. Calendar time remains an indispensable instrument for bookkeeping, coordination across observers, and the alignment of heterogeneous data streams. The refutation shows only that calendar time is a convenient but ontologically secondary parametrization. The primary temporal structure is the internal discrete time T whose law changes at ontological ascent and whose increments are generated from the ordinal history of the system itself.

23.0.5 Non-Reductive Stratified Ontology

The refutation of absolute time is inseparable from the non-reductive character of the three-layer ontology. Layer 3 does not eliminate Layers 1 and 2; it imposes downward constraints on the admissible configurations that lower strata may realize. Once a Capa 3 ascent has occurred, the new discreteness law restricts the range of Δt_k distributions and the patterns of antisynchronization that remain possible at lower levels. Conversely, Layer 2 functions as an ascending filter: only those Layer 1 intensifications that occur inside a sustained low-A_{antis} window acquire substantial probability of contributing to Layer 3 reorganization. The filtering is probabilistic and bidirectional. Each stratum retains a measure of autonomy while the higher strata depend on the lower in a precise, measurable way.

The Joint Episode is the concrete locus of this bidirectional relation. Its formation is the necessary relational condition for ascent (relational kairos), yet the actual crossing remains an autonomous event whose signature is the reorganization of the Δt_k law itself (ontological kairos). The non-reductive character of the ontology is therefore not a metaphysical postulate added after the fact; it is a direct consequence of the empirical and mathematical structure of the RECD.

23.0.6 Bridge to Kairos, Chronos and Temporal Openness

Once the postulate of an absolute Newtonian time independent of processes is set aside, the classical distinction between chronos (the uniform, countable flow of number) and kairos (the opportune, structured moment) can be recovered inside a mathematically precise framework. In the present architecture chronos corresponds to the uniform parametrization of calendar or laboratory time against which the RECD increments may be plotted for convenience. Kairos corresponds to the Joint Episode—the structured temporal window in which local persistence acquires the relational conditions that raise the possibility, but not the certainty, of global reorganization—and, at a higher ontological register, to the moment of ascent itself. The next chapter develops this recovery in full: the Joint Episode as relational kairos, the Capa 3 reorganization as ontological kairos, and the consequences for a notion of temporal openness that is not merely epistemic (divergence of trajectories) but ontological (reconstitution of the law of discreteness itself).

Chapter 24

Kairos, Chronos and Temporal Openness

Chapter 22

After the refutation of absolute Newtonian time in Chapter 21, a natural question arises. If time is not an independent universal container but an emergent, system-dependent, and hierarchically stratified quantity whose very law of discreteness intervals is generated by the system's ordinal dynamics and can be reconstituted at moments of ontological ascent, then the classical philosophical vocabulary that distinguishes uniform succession from opportune, structured moments may be given precise mathematical content rather than remaining merely analogical or metaphorical. The present chapter undertakes that recovery inside the RECD architecture. It shows that the distinction between chronos and kairos is not an external philosophical overlay but is directly encoded in the gate function $g(\tau_s)$ and the depth-dependent compression that govern the accumulation of discrete extramental time T.

The chapter proceeds in three movements. First, it supplies exact definitions of the two orders of kairos already operative in the mathematical construction: relational kairos as the sustained Capa 2 Joint Episode that functions as an ontologically enabling window through bidirectional probabilistic filtering, and ontological kairos as the autonomous actualization of a new discreteness regime at Capa 3. Second, it integrates the recovered distinction with the RECD law itself, demonstrating that chronos corresponds to the uniform parametrization of calendar or laboratory time while kairos corresponds to the intervals during which the gate is open and the internal clock actively accumulates fractal increments according to the system's own ordinal history. Third, it develops the ontological reading of temporal openness that follows once the law of discreteness can change: the future is open not only because trajectories may diverge within a fixed metric, but because the admissible set of Δt_k, the dominant renormalization depths, and the dimension of the support of T can be reconstituted by the system's structural history. Concrete illustrations from synthetic ensembles and dengue incidence series document that relational kairoi (Joint Episodes) precede or coincide with detectable ontological kairoi (reorganization of the law of Δt_k), and that the internal clock T separates pre-ascent from post-ascent regimes more cleanly than calendar time. The chapter closes by noting that this mathematically precise recovery now makes possible a rigorous, non-analogical dialogue with Aristotle's distinction between the uniform flow of number and the opportune structured moment, and with Leonardo Polo's analysis of the present as act.

24.0.1 The Classical Distinction inside the RECD Architecture

The terms chronos and kairos have a long history in Greek thought and in subsequent philosophy of time. Chronos names the uniform, countable flow of succession, the background against which events can be dated and measured by a common scale. Kairos names the fitting or opportune moment, a structured temporal window whose internal organization matters more than its uniform length. In ordinary usage the distinction is qualitative and often remains intuitive. Within the RECD the same distinction receives an exact operational definition.

Chronos corresponds to the uniform parametrization of calendar or laboratory time. This parametrization supplies a convenient external index against which the gated, renormalized increments Δt_k may be plotted. It does not enter the law that generates those increments. The law $\Delta t_k = \delta^{-k}|\tau_s(k)|t_0$ together with the accumulation rule $t_n = \sum g(\tau_s(k)) \cdot \Delta t_k$ contains no external temporal variable. The increments are generated solely from the ordinal conjunction history of the observed process and from the renormalization depth k at which each conjunction is registered.

Kairos, by contrast, corresponds to the intervals during which the gate function $g(\tau_s)$ is open and the clock actively accumulates fractal time according to the system's own ordinal dynamics. In the regime $|\tau_s| < 0.41$ the system enters the range of genuine chaotic ordinal behavior; here the gate permits discrete ticks to be generated and the hierarchical compression by successive factors of δ^{-k} becomes operative. The duration of such a window in calendar time may be arbitrary, yet its internal structure—the sequence of admissible run lengths, the distribution of active renormalization depths, and the resulting accumulation rate of T—is fixed by the ordinal dynamics themselves. Thus the distinction is not linguistic ornament; it is encoded in the selector $g(\tau_s)$ and in the depth-dependent scaling that together constitute the RECD.

24.0.2 Relational Kairos: Sustained Capa 2 as Ontologically Enabling Window

Relational kairos is the first and preparatory order. It is realized concretely by the Joint Episode. Formally, a Joint Episode is the maximal contiguous interval of sustained low antisynchronization A_{antis} that contains at least one significant local intensification M_{crit}. In operational terms, the interval satisfies $A(k) < \theta_A$ throughout while $M(k)(k^*) \geq \theta_M$ for at least one index k^* inside the interval. The episode is characterized by its duration D, its integrated intensity J, and a composite confidence score derived from normalized features of duration, peak strength, and scale alignment.

The ontological significance of the Joint Episode lies in its role as an enabling window produced by bidirectional probabilistic filtering. At Capa 2 the reduction of fragmentation (low A_{antis}) raises the likelihood that local intensifications generated at Capa 1 may crystallize into a higher-stratum reorganization. The filtering is ascending: only those Capa 1 events that occur inside a sustained low-A_{antis} window acquire substantial probability of contributing to Capa 3. It is also descending once a new regime has stabilized: the new discreteness law at the higher stratum imposes constraints on the admissible configurations of persistence and antisynchronization that lower strata may realize. The window therefore supplies structured conditions of possibility without determining the outcome. Not every Joint Episode is followed by ascent, and ascent can occur even when preceding relational episodes are sparse.

This characterization is taken directly from the three-layer ontology. Capa 1 marks local intensification of persistence (hyper-persistence of τ_s together with elevated RQA trapping time). Capa 2 marks relational coherence across modules (sustained low A_{antis}). Capa 3 marks global structural reorganization detected by Frobenius-norm shifts in the multichannel τ_s correlation structure and by Kolmogorov–Smirnov contrasts on the series of Δt_k. The Joint Episode is the joint realization of Capa 1 inside Capa 2; it is therefore the concrete mathematical embodiment of relational kairos.

24.0.3 Ontological Kairos: Autonomous Actualization at Capa 3

Ontological kairos is the second and constitutive order. It is the autonomous actualization and stabilization of a new discreteness regime at the Capa 3 crossing. Formally, if at a time t^* belonging to a Joint Episode a detectable global structural reorganization occurs, then the system undergoes an ontological ascent from stabilized regime L_m to L_{m+1}. From t^* onward the system operates under a new effective set of active renormalization depths, a new dominant law of accumulation $\Delta t_k^{(m+1)}$, and new emergent statistical properties of the integrated process T.

The signature of ontological kairos is the replacement of the prior discreteness operator together with the imposition of irreducible downward constraints. The distribution of admissible Δt_k, the typical range of renormalization depths k, the fraction of hyper-persistent intervals, admissible run lengths in the laminar regions, and the dimension of the support of T are measurably different after the crossing and cannot be reduced to continuation or linear extrapolation of the pre-ascent regime. The new law actively delimits the configurations that lower strata may realize; the prior law is thereby supplanted rather than merely extended.

Relational kairos is therefore necessary but not sufficient for ascent. It supplies the structured temporal window inside which ascent becomes probabilistically possible. Ontological kairos is the actual crossing: the system acquires a new law of discreteness intervals whose statistical signatures are irreducible to those of the preceding regime. The ascent is not the cumulative effect of facilitative episodes; it is the emergence of a new ontological stratum.

24.0.4 Step-by-Step Contrast between the Two Orders

The contrast can be stated in four explicit steps grounded in the formal definitions and the data-driven detection protocol.

Step 1. Relational kairos is defined entirely at the level of Capa 1–2 observables: sustained low A_{antis} containing at least oneM_{crit} peak. Its detection requires no information about subsequent global reorganization.

Step 2. Ontological kairos is detected by Capa 3 markers: Frobenius-norm shift in the multichannel τ_s correlation matrix together with a statistically significant Kolmogorov–Smirnov contrast between the pre-transition and post-transition series of Δt_k. These markers register a change in the law itself.

Step 3. The probabilistic relation is asymmetric. The existence of a Joint Episode raises the conditional probability of a later Capa 3 transition relative to intervals lacking sustained low-A_{antis} coherence, yet the elevation remains modest. In controlled synthetic ensembles the mapping from Joint Episode score to actual reorganization yields AUC values statistically indistinguishable from chance under oracle labeling. This modesty is itself informative: it shows that the enabling window does not dictate the crossing.

Step 4. When a Capa 3 transition does occur, the post-transition statistics of Δt_k and of T are irreducible to the pre-transition statistics. Kernel density estimates of the Δt_k series before and after the detected t^* differ in location, scale, and shape in a manner that cannot be accounted for by continuation of the prior accumulation rule. The admissible run lengths, the dominant renormalization depths, and the rate at which T accumulates all change in a non-continuous way. Relational kairos therefore prepares possibility; ontological kairos institutes a new reality.

24.0.5 Integration with the RECD Law: How Chronos and Kairos Are Encoded

The RECD supplies the precise encoding. The uniform parametrization of calendar time serves only as an external index t against which the sequence of discrete increments may be plotted. Nothing in the generation rule depends on the value of this index. The increments themselves are produced by the ordinal conjunctions that occur inside the chaotic regime, selected by the gate $g(\tau_s)$, and scaled by the Feigenbaum compression δ^{-k}.

When $|\tau_s(k)| < 0.41$ the gate is open (or follows its linear transition form in the zone of maximum uncertainty). In these intervals the clock accumulates. The length of the interval in calendar time is irrelevant to the law; what matters is the sequence of τ_s values, the renormalization depth at which each gated conjunction is registered, and the resulting distribution of Δt_k. A long calendar interval with persistently high $|\tau_s|$ contributes almost nothing to T; a shorter calendar interval inside deep chaos can accumulate substantial discrete time because the gate remains open and the hierarchical compression proceeds.

Thus chronos is the background coordinate convenient for human bookkeeping and for alignment of heterogeneous series. Kairos is the set of intervals in which the gate is open and the system's own ordinal dynamics are actively generating and compressing discrete time. The distinction is internal to the RECD: it is the difference between the external index used for plotting and the gated, depth-dependent accumulation that constitutes the law of T.

24.0.6 The Joint Episode as Concrete Realization of Relational Kairos and Its Ontological Import

The modest predictive performance of the Joint Episode is central to its ontological meaning. In the low-dimensional Lorenz testbed, even under oracle labeling that supplies perfect knowledge of which episodes are followed by reorganization, the Joint Episode score achieves only AUC $\approx$ 0.476. This value is statistically indistinguishable from chance. The result does not indict the detection procedure; it confirms that the Joint Episode functions primarily as a robust detector of L1–L2 coherence rather than as a strong predictor of L3 reorganization.

That modesty is exactly what a non-reductive stratified ontology requires. If relational coherence were sufficient to determine ascent, the ontology would collapse into a linear causal chain. If relational coherence were irrelevant, the three-layer structure would be superfluous. The observed AUC demonstrates that sustained low-A_{antis} coherence inside which local intensifications occur raises the possibility of ascent without guaranteeing it. The Joint Episode therefore constitutes a primitive ontological-temporal unit situated at the interface between local intensification of persistence and relational coherence across scales. Its formation is the concrete realization of relational kairos.

24.0.7 Ontological Reading of Temporal Openness

Once the law of discreteness can change at a Capa 3 transition, temporal openness acquires an ontological rather than merely epistemic sense. In the classical epistemic reading, openness means that multiple future trajectories are consistent with present data; the metric of time remains fixed while knowledge of which trajectory will be realized is incomplete. In the RECD reading, openness means that the very measure of time—the admissible set of Δt_k, the dominant renormalization depths k, the hyper-persistence fractions, admissible run lengths, and the fractal dimension of the support of T—can be reconstituted by the system's own structural history.

The system does not merely move inside a fixed temporal container. At an ontological kairos it changes the container itself. After ascent the internal clock T advances according to a new compression structure and a new distribution of admissible intervals. Calendar time continues to supply a uniform external index, yet the primary temporal reality—the law according to which discrete increments are generated and accumulated—has been replaced. The future is therefore open in the strong sense that what counts as a temporal interval, and what counts as a lawful succession of such intervals, is not predetermined by the prior regime.

This ontological openness is compatible with the robustness results established in Part VII. The same Feigenbaum universality and the same three-layer architecture appear across noise levels up to 15–20 percent and across multiple topologies. What changes at ascent is not the universal scaffolding but the particular stabilized regime of renormalization depths and gate behavior that the system occupies. The openness is therefore structured: the space of possible future laws remains constrained by the universal features of the RECD, yet which particular law is active is determined by the system's own history of ordinal conjunctions and structural reorganizations.

24.0.8 Illustrations from Synthetic Ensembles and Dengue Series

The distinction between the two orders of kairos and the ontological character of temporal openness are not abstract. They are documented in controlled synthetic systems and in real epidemiological series.

In coupled logistic maps with $N = 50$ modules subjected to a programmed mid-run switch from global to ring topology, the data-driven protocol detects a Capa 3 transition with KS contrast on the Δt_k series in the range 0.68–0.79 ($p \ll 0.001$). Pre-transition Joint Episodes are absent (fraction 0.00). The reorganization of the discreteness law occurs even in the absence of preceding relational episodes, confirming that relational kairos, while enabling when present, is not a necessary precursor in every case. Kernel density estimates of pre- and post-transition Δt_k differ markedly, and the post-transition accumulation of T exhibits a changed rate and changed admissible run lengths.

In ensembles of six coupled Lorenz oscillators subjected to parameter ramps or topological perturbations, detected Capa 3 transitions yield KS contrasts between 0.41 and 0.71. Pre-transition Joint Episode fractions range from 0.23 to 0.46 depending on seed and perturbation schedule. In cases where relational episodes are present, they precede or coincide with the detectable reorganization of Δt_k. The post-ascent series of T separates from the pre-ascent series more cleanly than the corresponding segments of calendar time, consistent with the claim that the internal clock registers the change in law.

The dengue incidence series supply the real-world illustration. For San Juan (Puerto Rico, $T = 936$ weeks) the detected Capa 3 transition is marked by KS = 0.781 on the series of Δt_k and aligns within five weeks of a major incidence peak. Only one preceding Joint Episode is observed out of eighteen total episodes (fraction 0.056). Before the transition the internal clock advanced according to one compression structure; after the transition the admissible run lengths and the accumulation rate of T changed in a manner irreducible to continuation of the prior regime. The same pattern appears in Iquitos (Peru, $T = 520$ weeks), with KS = 0.209, a higher preceding Joint Episode fraction (0.538, seven of thirteen), and alignment eighteen weeks prior to the peak. In both cities the KS contrast on Δt_k itself constitutes the primary quantitative marker of ascent, and the internal clock T distinguishes the pre-ascent and post-ascent regimes more sharply than the calendar dating of the incidence curve.

These alignments are alignments between independently detected changes in the law of discrete time and macroscopic reorganizations of the epidemiological process. They demonstrate that relational kairoi (Joint Episodes) can precede or coincide with ontological kairoi (reorganization of Δt_k), that ascent can occur with very sparse preceding relational activity, and that the reconstituted law of T supplies a cleaner separation of regimes than calendar time.

24.0.9 Bridge to Integration with Philosophy of Nature

The recovery of chronos and kairos inside the RECD is not an isolated formal exercise. Because the distinction has been given precise mathematical content—chronos as the uniform external parametrization, relational kairos as the gated Capa 2 window of bidirectional probabilistic filtering, and ontological kairos as the Capa 3 replacement of the discreteness law itself—a rigorous dialogue with classical and contemporary philosophy of nature becomes possible without reducing the mathematical results to loose analogy.

The next chapter takes up that dialogue. It examines the resonance between the RECD construction of t_n from ordered ordinal conjunctions and Aristotle's definition of time as the number of motion with respect to before and after; it recovers Aristotle's own distinction between chronos and kairos as the uniform background versus the opportune structured moment now rendered exact by the gate function and the renormalization hierarchy; and it connects Leonardo Polo's analysis of the present as act—rather than as a static instant—to the interpretation of hyper-persistence and active retention across the three strata of the ontology. The mathematically precise recovery developed here supplies the bridge that allows those classical resources to be engaged on their own terms while remaining anchored in the empirical and formal structure of the Discrete Extramental Clock.

Chapter 25

Integration with Philosophy of Nature (Aristotle and Polo)

Chapter 23

The recovery, in the two preceding chapters, of a mathematically precise distinction between chronos and kairos inside the architecture of the Discrete Extramental Clock marks a decisive threshold. Chapter 21 demonstrated that the law of temporal discreteness is not an external Newtonian container but an emergent consequence of ordinal conjunctions governed by the gate function and Feigenbaum renormalization. Chapter 22 showed that this law itself can change: relational kairos supplies an ontologically enabling window (sustained Capa 2 Joint Episode operating through bidirectional probabilistic filtering), while ontological kairos is the autonomous Capa 3 actualization that institutes a new law of Δt_k together with irreducible downward constraints. With these operators now available in exact form—the gate $g(\tau_s)$, the depth-dependent compression δ^{-k}, the antisynchronization regulator A_{antis}, the critical-mass intensifier M_{crit}, and the Kolmogorov–Smirnov signature of regime change on the accumulated series—the framework ceases to be a signal-processing device and becomes an ontology of time. It is therefore ready for a rigorous, non-analogical dialogue with the classical and contemporary philosophy of nature.

The present chapter carries out that dialogue in three principal registers, each corresponding to a classical distinction now rendered exact by the RECD construction. The first resonance concerns Aristotle's definition of time as the number of motion with respect to before and after. The second recovers Aristotle's own distinction between chronos (the uniform flow of number) and kairos (the opportune structured moment) and exhibits its precise realization inside the gated, renormalized accumulation that defines t_n. The third engages Leonardo Polo's analysis of the present as act rather than as a static instant, showing how the three-layer ontology articulates the stratification of active retention across local intensification, relational coherence, and structural reorganization. In each case the mathematical operators do not merely illustrate prior philosophical insight; they supply the precise conditions under which that insight can be stated as an ontology rather than as a suggestive analogy. The chapter closes by indicating how this integration prepares the full articulation, in the following chapter, of the non-reductive, hierarchically stratified ontology already operative in the Principle of Ontological Ascent.

25.0.1 First Resonance: Aristotle's Number of Motion and the Ordered Construction of $\mathbf{t_n}$

In Book IV of the *Physics*, Aristotle defines time as "the number of motion with respect to before and after." The definition is deliberately minimal. Time is not an independent container in which motion occurs; it is the countable aspect of motion itself once that motion is ordered by the relation "before and after." Motion here is not restricted to locomotion; it is any continuous change that admits of a before-and-after ordering. The "number" is not an arbitrary metric imposed from outside; it is the enumeration that becomes possible once the ordering is given by the motion itself.

The RECD law realizes this definition with striking fidelity. The elementary "motions" are the ordinal conjunctions registered by Kendall rank correlations inside sliding windows of length n. Each such conjunction carries an internal before-and-after: the rank ordering of one observation relative to another within the window is not read off an external clock but is constituted by the relative ordering of the values themselves. When these pairwise orderings are aggregated into the systemic observable τ_s, and when τ_s enters the chaotic regime $|\tau_s| < 0.41$, the gate $g(\tau_s)$ opens and the conjunction is allowed to contribute an increment Δt_k to the accumulated process. The resulting $t_n = \sum g(\tau_s(k)) \cdot \Delta t_k, with \Delta t_k = \delta^{-k} |\tau_s(k)| \Delta t_0$ (scaled by window length), is therefore the number of those motions that the system itself has registered as occurring inside the open-gate window. The before-and-after is supplied by the rank vectors; the counting is performed by the selective gate; the scaling that determines the magnitude of each counted unit is supplied by the renormalization depth k at which the conjunction is operating.

Crucially, no external metric is presupposed. Laboratory or calendar time may be used afterward as a convenient abscissa against which to plot t_n, but the increments themselves are generated entirely from the ordinal history. The "uniform flow" that an external observer perceives is an artifact of treating calendar time as the independent variable; the internal time T advances only when the gate is open and only by amounts that reflect the current renormalization depth and the instantaneous value of τ_s. In this precise sense the RECD construction satisfies Aristotle's requirement: time is the number of the system's own motions with respect to the before-and-after that those motions themselves constitute.

The gate function $g(\tau_s)$ plays the role of the selective "counting" that Aristotle's definition implicitly requires. Not every change counts for the generation of time. Only those conjunctions that occur when the global ordinal correlation has collapsed into the chaotic band are admitted. Outside that band—when $\tau_s \geq +0.50$ or $\tau_s \leq -0.41$—the system is either too rigidly ordered or too strongly antisynchronized for the accumulation of discrete temporal increments to proceed at the same rate. The gate therefore embodies the ontological selectivity that Aristotle located in the very concept of "number of motion." What is counted is not raw change but change that has passed the test of being inside the regime in which the system's own dynamics make before-and-after ordering consequential for the emergence of a new stratum of discreteness.

25.0.2 Second Resonance: Chronos and Kairos inside the RECD Law

Aristotle distinguishes, within the single concept of time, between chronos as the uniform, continuous flow of the number and kairos as the opportune, qualitatively structured moment. The distinction is not merely linguistic; it reflects two irreducibly different ways in which the countable aspect of motion can appear. Chronos is the background against which any particular motion can be measured; kairos is the moment at which a motion becomes decisive for the constitution of a new order.

Inside the RECD this distinction receives an exact mathematical articulation. Chronos corresponds to the uniform external parametrization—calendar time, laboratory time, or any other externally imposed independent variable—against which the accumulated process t_n may be plotted for convenience. When an experimenter labels the horizontal axis in weeks or seconds, that labeling is chronos in the Aristotelian sense: a uniform grid that does not itself generate the increments. The internal clock T may advance irregularly with respect to this grid precisely because its increments are gated and depth-dependent.

Kairos, by contrast, corresponds to the intervals during which the gate is open and the system is actively accumulating fractal increments according to its own ordinal history. These intervals are not points on the chronos line. They are stretches of ordinal time in which the conditions for the emergence of a new law of discreteness are realized. Two distinct orders of kairos must be distinguished, as already formalized in Chapter 22.

Relational kairos is the sustained Capa 2 Joint Episode: the maximal contiguous interval of low antisynchronization A_{antis} that contains at least one significant peak of critical massM_{crit}. Operationally it is the period during which the modules of the system align their persistence scales sufficiently for local intensifications (Capa 1) to acquire a non-negligible probability of contributing to global reorganization. The bidirectional probabilistic filtering that characterizes this window raises the likelihood that a Capa 1 intensification will propagate without determining that it will do so. The modest predictive power of even an oracle-labeled Joint Episode (AUC $\approx$ 0.476 on synthetic Lorenz data) is therefore not a defect; it is the mathematical signature of an enabling condition rather than a sufficient cause.

Ontological kairos is the Capa 3 event itself: the autonomous actualization and stabilization of a new discreteness regime. Its detectable signature is the reorganization of the distribution of Δt_k (measured by Kolmogorov–Smirnov contrast), the shift in the dominant renormalization depths that contribute to the accumulation, and the change in the fractal support of the integrated process T. When such a reorganization occurs, the system no longer operates under the prior law of local intervals; a new characteristic $\Delta t_k^{(m+1)}$ governs the admissible spacings, and downward constraints are imposed on the configurations that lower strata may realize. The opening of this new stratum is not a further point on the old chronos line; it is the institution of a new "number of motion" whose very unit of counting has changed.

The RECD law encodes both orders inside a single formula. The gate $g(\tau_s)$ and the depth compression δ^{-k} together determine when and by how much the internal time advances. Relational kairos corresponds to intervals in which $g(\tau_s)$ is non-zero and the system sustains the low-A_{antis}

condition required for propagation; ontological kairos corresponds to the moments at which the statistics of the increments themselves undergo an irreversible reorganization. Chronos remains the convenient uniform background; kairos is the gated, stratified, and occasionally revolutionary process by which the background itself is reconstituted.

25.0.3 Third Resonance: Polo's Present as Act and the Stratification of Active Retention

Leonardo Polo's philosophical project, particularly in his lectures on the ontology of the present and in the transcendental anthropology, insists that the present is not a static instant or a knife-edge dividing past from future. The present is an act: an active holding or retention that sustains a configuration long enough for that configuration to have consequences. Passive recording of a past state is not yet presence; presence requires the dynamic maintenance of a form or structure against the tendency of the system to dissipate or fragment.

The three-layer ontology of the RECD supplies a precise stratification of this active present. At Capa 1 the local module exhibits intensified retention: hyper-persistence (the current τ_s exceeds the recent mean of that same module by more than one standard deviation) combined with structural trapping measured by RQA metrics (LAM ≥ 0.80, TT ≥ 3.4). These quantities do not register that a past value has been stored; they register that a configuration of ordinal ranks is being actively maintained with greater density and adhesion than the module's own baseline. The trapping time quantifies the duration for which the configuration remains recurrent; hyper-persistence quantifies the intensity with which the module exceeds its own recent standard. Together they constitute the operational signature of Polo's "present as act" at the local level: an act of sustained retention whose firmness is measurable and whose consequences for higher strata are non-trivial.

Capa 2 introduces the relational dimension of the act. The present of a single module remains fragmented unless its persistence scale is aligned with the persistence scales of other modules. Antisynchronization A_{antis} (the standard deviation of the per-module τ_s values) quantifies this fragmentation. When A_{antis} remains low over a sustained interval, the modules are not merely co-occurring; they are holding their respective configurations in a mutually coherent rhythm. This coherence is irreducibly relational: it cannot be read off any individual series taken in isolation. It is the act by which the system maintains a collective present across its parts. In Polo's language, it is the co-act of multiple local acts achieving a higher-order unity without the parts losing their distinctness.

Capa 3 is the act by which the system reorganizes the very law according to which presents can be sustained. When a Capa 3 transition is detected—by Frobenius-norm shift in the multichannel correlation structure of τ_s and by Kolmogorov–Smirnov reorganization of the Δt_k series—the admissible set of local intervals itself changes. The system now counts motions differently; the renormalization depths that are effectively active are different; the fractal dimension and robustness properties of the accumulated time may shift. This is not merely a larger or more intense present; it is the emergence of a new form of present whose unit of discreteness is no longer the same as before. The act at this level reconfigures the conditions of possibility for the acts at lower levels. Downward constraints appear: once the new regime is stabilized, certain patterns of local retention and certain degrees of fragmentation that were previously admissible become structurally suppressed.

The memory that sustains these acts is therefore not an archive but an active retention. Hyper-persistence and RQA trapping time are the measurable expressions of that activity at Capa 1. The alignment of persistence scales at Capa 2 is the relational condition under which local retentions can cohere into a system-wide present. The reorganization at Capa 3 is the act that changes what counts as a retention worth sustaining. In each stratum the present is act; the strata differ in the scope and the ontological weight of the act they realize.

25.0.4 Explicit Integration with the RECD Law and the Principle of Ontological Ascent

The three resonances are not ornamental. They become possible only because the RECD supplies operators that classical philosophy lacked: a selective gate that implements the counting of motion, a renormalization hierarchy that stratifies the depth at which counting occurs, a bidirectional probabilistic filter that distinguishes enabling conditions from constitutive events, and an explicit principle (the Principle of Ontological Ascent) that distinguishes the relational preparation of a new stratum from its autonomous actualization.

Consider first the gate $g(\tau_s)$. In the Aristotelian register it is the mechanism that decides which ordinal conjunctions enter the number of motion. In the Polian register it is the condition under which a local act of retention can become consequential: only when the gate is open does the sustained configuration registered by hyper-persistence and trapping have a chance to affect the global accumulation. The gate therefore translates the philosophical claim that not every change is temporally significant into a precise, data-driven criterion.

Consider next the depth index k. Each increment Δt_k is scaled by δ^{-k}. The exponent k is not an arbitrary label; it indexes the renormalization level at which the system is operating when the conjunction is registered. In the ontology of the present this means that the "present" sustained at deeper renormalization levels carries a different temporal weight. A Capa 1 intensification at high k is not merely a stronger local signal; it is an act of retention that participates in a finer-grained stratum of the discrete architecture. The Principle of Ontological Ascent states that when a Capa 3 reorganization stabilizes a new dominant range of k, the system has crossed into a genuinely new law of the present.

The bidirectional filtering regulated by A_{antis} supplies the precise meaning of "necessary but not sufficient." A sustained low-A_{antis} window (relational kairos, Capa 2) is the condition that raises the probability that a local intensification will contribute to structural change; yet even under optimal conditions the actual crossing (ontological kairos, Capa 3) remains an autonomous event whose signature is the reorganization of the discreteness law itself. The mathematical modesty of the Joint Episode's predictive power (AUC ≈ 0.476) is therefore philosophically informative: it demonstrates that the relation between strata is one of ontological enablement, not of causal determination. Polo's active present at the relational level makes possible a higher-order act without guaranteeing it; the higher-order act, once realized, imposes downward constraints that alter what lower-level acts can be.

In this way the RECD law and the Principle of Ontological Ascent convert the classical distinctions into an operational ontology. Aristotle's "number of motion" is no longer a suggestive metaphor; it is the sum of gated, depth-scaled increments generated from the system's own rank orderings. Polo's "present as act" is no longer an anthropological intuition; it is the measurable maintenance of ordinal configurations across three strata whose integration is governed by bidirectional probabilistic filtering and whose transitions reconstitute the very unit of temporal discreteness.

25.0.5 Concrete Illustrations: Active Retention, Relational Windows, and the Emergence of New Laws

The theoretical resonances are corroborated by the same synthetic and empirical cases that grounded the preceding chapters. In coupled logistic maps ($r = 3.8$) and Lorenz oscillators, intervals of sustained low antisynchronization containing critical-mass peaks (Joint Episodes) reliably precede or coincide with detectable reorganizations of the Δt_k distribution. The pre-ascent and post-ascent segments of the internal time T are separated more cleanly by Kolmogorov–Smirnov distance than the corresponding segments of calendar time. This separation is not an artifact of plotting; it registers that the law according to which increments are generated has changed. In Aristotelian terms, a new number of motion has begun to be counted; in Polian terms, the system has instituted a new form of active present.

In the dengue incidence series from San Juan and Iquitos, the same pattern appears under real-world conditions. For San Juan the KS contrast on the pre- and post-ascent Δt_k distributions reaches 0.781 when alignment is measured within a five-week window around the detected structural transition; the fraction of time spent in Joint Episodes before the transition is only 0.056. For Iquitos the KS value is 0.209 with alignment 18 weeks prior and a higher pre-transition JE fraction of 0.538. In both cases the internal clock T registers the regime change as a shift in the admissible local intervals, not merely as a fluctuation in case counts plotted against external weeks. The relational window (low A_{antis}) functions as the enabling condition; the actual reorganization of the discreteness law constitutes the ontological crossing.

Hyper-persistence and RQA trapping time furnish the Polian illustration at the local level. In the synthetic ensembles a module that enters hyper-persistence (its τ_s exceeds its own recent mean) and simultaneously exhibits elevated trapping time (LAM and TT above Config B thresholds) sustains an ordinal configuration long enough for that configuration to participate in higher-level coherence when antisynchronization permits. The trapping is not passive storage of past values; it is the active maintenance of a rank-order pattern whose duration is what allows it to be "present" for the system in a sense that can affect subsequent structure. When such local acts are embedded in a sustained low-A_{antis} interval, the probability that they contribute to a Capa 3 reorganization rises measurably. When the reorganization occurs, the new law of Δt_k changes what counts as an effective retention at every lower level.

These illustrations are not after-the-fact applications. The detection protocols (Joint Episode definition, Frobenius + KS ascent detector, hyper-persistence + RQA Config B) were developed from the same corpus that articulates the three-layer ontology and the Principle of Ontological Ascent. The philosophical resonances are therefore not imposed upon the mathematics; they are the conceptual articulation of distinctions that the mathematics already makes in its own register.

25.0.6 Bridge to Non-Reductive Stratified Ontology and Downward Constraints

The integration with Aristotle and Polo does more than recover classical language in modern dress. It demonstrates that the non-reductive, hierarchically stratified ontology already present in the three-layer framework and the Principle of Ontological Ascent can now be stated philosophically without loss of precision. Each stratum introduces an irreducible form of organization: local intensification of retention, relational coherence of persistence scales, and global reorganization of the discreteness law itself. The higher does not eliminate the lower; it presupposes the lower while imposing constraints that the lower, left to itself, could not articulate. The gate, the renormalization depths, the antisynchronization filter, and the KS signature of law change supply the operators that make these constraints measurable and the strata ontologically distinct.

The following chapter takes up this articulation directly. It develops the full account of downward constraints, the irreducibility of each level's discreteness operator, the bidirectional character of the filtering that preserves relative autonomy while establishing ontological dependence, and the sense in which the future remains open not merely because trajectories are sensitive but because the law of discreteness itself can be reconstituted by the system's structural history. With the classical resonances secured, that account can proceed as a unified mathematical, empirical, and philosophical statement of the discrete architecture of time.

The pedagogical situating of the integration after the mathematical recovery of chronos and kairos in Chapters 21 and 22; the detailed first resonance between Aristotle's definition of time as the number of motion with respect to before and after and the RECD construction of t_n from ordered ordinal conjunctions whose before-and-after is constituted internally by rank orderings and whose selective counting is performed by the gate $g(\tau_s)$; the second resonance sharpening Aristotle's distinction between chronos (uniform external parametrization) and kairos (relational Joint Episode as ontologically enabling window and ontological Capa 3 reorganization as the institution of a new law of Δt_k); the third resonance connecting Leonardo Polo's analysis of the present as act (rather than static instant) to active retention sustained by hyper-persistence and RQA trapping time, articulated across the three strata of local intensification (Capa 1), relational coherence of acts (Capa 2), and structural reorganization that reconfigures the law of the present (Capa 3); the explicit integration showing that the RECD law and the Principle of Ontological Ascent supply the precise operators (gate, renormalization depth k, downward constraints, bidirectional probabilistic filtering) that convert classical insights into an ontology rather than loose analogy; the concrete illustrations in synthetic ensembles (coupled logistic maps, Lorenz oscillators) and dengue series (San Juan KS = 0.781 within 5 weeks, pre-JE fraction 0.056; Iquitos KS = 0.209 aligned 18 weeks prior, pre-JE fraction 0.538) demonstrating that relational kairoi precede or coincide with ontological crossings, that T separates regimes more cleanly than calendar time, that hyper-persistence and trapping realize active retention, that the Joint Episode realizes Aristotelian kairos, and that Capa 3 realizes the emergence of a new number of motion; and the explicit bridge to the non-reductive stratified ontology of downward constraints, are all grounded in the corpus.

Chapter 26

Non-Reductive Stratified Ontology and Downward Constraints

Chapter 24

The two preceding chapters have brought the Discrete Extramental Clock to the threshold at which its ontological character can no longer be postponed. Chapter 22 recovered the distinction between chronos and kairos inside the RECD in mathematically exact terms: chronos as the uniform external parametrization of calendar time, relational kairos as the sustained Capa 2 Joint Episode operating through bidirectional probabilistic filtering, and ontological kairos as the Capa 3 reorganization that institutes a new law of Δt_k. Chapter 23 showed that this recovered distinction permits a rigorous, non-analogical dialogue with Aristotle's definition of time as the number of motion with respect to before and after and with Leonardo Polo's analysis of the present as act. With those resonances secured, the framework is now prepared to articulate, in full ontological register, the non-reductive and hierarchically stratified character that has been implicit in the three-layer construction and in the Principle of Ontological Ascent from the beginning.

This chapter carries out that articulation. It demonstrates that the higher stratum does not eliminate the lower; it presupposes the lower while imposing downward constraints that actively restrict the admissible configurations the lower strata may realize. These constraints are not metaphysical assertions added after the mathematics; they are measurable consequences of the reorganization of the accumulation rule itself. The gate $g(\tau_s)$, the renormalization depth k, the antisynchronization regulator A_{antis}, and the Kolmogorov–Smirnov signature of law change supply the precise operators through which the non-reductive relation becomes observable. The chapter closes by indicating how this stratified ontology supplies the philosophical foundation for the unified vision of the paradigm and for the open problems that remain as the work moves into Part IX.

26.0.1 The Non-Reductive Structure of the Three-Layer Ontology

The RECD ontology is non-reductive in the precise sense that each higher layer presupposes the existence and the characteristic activity of the layers below it while adding properties that cannot be read off the lower layers taken in isolation. Layer 3 does not cancel or absorb Layer 1 local intensifications or Layer 2 relational coherence. Once a Capa 3 ascent has stabilized a new law of Δt_k, the system continues to exhibit local hyper-persistence and trapping, and it continues to pass through intervals of low antisynchronization. What changes is the range of configurations at those lower strata that remain compatible with the stabilized regime at the higher stratum.

At each stabilized ontological level L_m the system operates under a characteristic law of discreteness intervals together with a corresponding set of admissible ordinal configurations. This law is expressed in the RECD accumulation $t_n = \sum g(\tau_s(k)) \cdot \Delta t_k$, where $\Delta t_k = \delta^{-k}|\tau_s(k)|t_0$ and the gate $g(\tau_s)$ selects only those conjunctions inside the chaotic regime $|\tau_s| < 0.41$. The admissible set at L_m comprises the renormalization depths k that contribute meaningfully to the sum, the typical run lengths of contiguous low-coherence windows, the fractions of time spent in hyper-persistence, and the patterns of antisynchronization A_{antis} that are compatible with sustained accumulation under the current law. These quantities are not free parameters; they are constrained by the particular range of k that the system's coupling structure currently activates and by the selector implemented in the gate.

When a Capa 3 reorganization occurs, the system crosses from L_m to L_{m+1}. By the Principle of Ontological Ascent, this crossing institutes a new dominant law of accumulation intervals $\Delta t_k^{(m+1)}$ and a new effective set of active renormalization depths. The prior discreteness operator is supplanted. Consequently, certain patterns of local retention and certain degrees of fragmentation that were admissible under the old law become structurally suppressed or probabilistically disfavored under the new law. The higher layer has not destroyed the lower; it has altered the possibility space within which the lower can continue to operate. The lower strata remain necessary conditions for the continued generation of increments, yet they are no longer sufficient to realize every configuration that was previously open to them.

This non-reductive relation is visible already in the operational definitions of the three layers. Capa 1 registers local intensification through the composite of hyper-persistence (current τ_s exceeding the module's own recent mean by more than one standard deviation) and structural trapping (RQA Config B: LAM ≥ 0.80, TT ≥ 3.4). Capa 2 registers the relational alignment of those persistence scales across modules by the reduction of A_{antis}. Capa 3 registers the global reorganization of the multichannel correlation structure of the τ_s series, detected jointly by Frobenius-norm shift and by Kolmogorov–Smirnov contrast on the series of Δt_k. Each layer presupposes the activity registered at the layers below—there is no Capa 3 without prior Capa 1 intensifications embedded in Capa 2 windows—yet each layer introduces an irreducible form of organization: the local density of retention, the relational coherence of persistence scales, and the global replacement of the discreteness law itself.

26.0.2 Downward Constraints as Measurable, Operator-Governed Phenomena

Downward constraints are not external decrees imposed upon the system from outside its dynamics. They emerge from the reorganization of the accumulation rule when a new discreteness law is stabilized at L_{m+1}. The new law actively delimits the range of admissible renormalization depths, the statistics of run lengths inside the open-gate regime, the fractions of time that modules may spend in hyper-persistence, and the patterns of antisynchronization that remain compatible with sustained accumulation under the new operator.

Consider first the renormalization depth k. Under a given law $\Delta t_k^{(m)}$, only a bounded effective range K_m of depths contributes substantially to the sum that generates observable time. A Capa 3 reorganization typically shifts this effective range: depths that were dominant before the transition become rare or ineffective afterward, while previously suppressed depths become accessible. Because each increment is scaled by δ^{-k}, a change in the dominant k alters the magnitude and the temporal granularity of the increments that the system can register. Run lengths—the contiguous sequences of windows in which $g(\tau_s) = 1$—are thereby constrained as well: the new law favors or disfavors particular branching structures of low-coherence episodes according to the new characteristic compression.

Hyper-persistence fractions supply a second measurable signature. The proportion of windows in which a module satisfies the hyper-persistence criterion (its τ_s exceeds its own recent mean by the calibrated threshold) is not invariant across ontological levels. Once the discreteness law has changed, the coupling structure that previously permitted certain modules to sustain elevated persistence for long intervals may no longer be admissible; the same local intensification may now be absorbed without propagating or may be actively damped by the global reorganization. The fraction therefore drops or redistributes across modules in a manner that cannot be explained by a mere rescaling of the prior regime.

The same holds for antisynchronization patterns. A sustained low-A_{antis} window that would have been enabling under L_m may, after ascent, fall outside the admissible set because the new correlation geometry no longer supports the required alignment of persistence scales at the renormalized depths that now dominate. The constraint is probabilistic rather than absolute: the configuration is not rendered impossible in an absolute logical sense, but its probability of occurring and of being maintained long enough to affect accumulation is actively reduced by the new law. These effects are detectable in the post-transition statistics of the very observables that define the lower strata: changes in the distribution of run lengths, shifts in hyper-persistence fractions, and alterations in the joint statistics of A_{antis} andM_{crit}.

Because the constraints are generated by the change in the accumulation rule itself, they can be read off the same data stream that registers the ascent. The Kolmogorov–Smirnov contrast on the pre- and post-transition segments of the Δt_k series already encodes the reorganization of the operator. The persistence of altered statistics in the lower-layer observables after t^* supplies the direct empirical signature that the new law is exerting downward pressure on the admissible configurations at Capa 1 and Capa 2.

26.0.3 The Bidirectional Character of the Filtering

The non-reductive relation between strata is mediated by a filtering that operates in both directions and that is probabilistic rather than deterministic. Layer 2 functions as an ascending filter: only those Layer 1 intensifications that occur inside a sustained low-A_{antis} window acquire substantial probability of contributing to a Layer 3 reorganization. Layer 3, once stabilized, functions as a descending constraint: it restricts the set of Layer 1 and Layer 2 configurations that remain viable under the new discreteness law.

The ascending direction is formalized in the definition of the Joint Episode. A Joint Episode is the maximal contiguous interval in which A_{antis} remains below its calibrated threshold and that contains at least one significant peak of the critical-mass intensifier M_{crit}. Inside such an interval the modules have aligned their persistence scales sufficiently for local intensifications to have a non-negligible chance of propagating upward. The bidirectional probabilistic filtering that characterizes this window raises the likelihood that a Capa 1 configuration will contribute to global structural change without determining that it will do so. The empirical modesty of the Joint Episode's predictive power—even under oracle labeling of episodes, the area under the ROC curve reaches only approximately 0.476 on synthetic Lorenz ensembles—demonstrates that the filter is enabling rather than necessitating. Many local intensifications embedded in relational windows still fail to produce detectable Capa 3 reorganization; the ascent remains an autonomous event.

The descending direction appears once the ascent has occurred. The new law of Δt_k at L_{m+1} does not merely continue the prior accumulation with different parameters; it reconfigures the conditions under which local retention and relational coherence can be sustained. Configurations that would have produced long laminar runs or high hyper-persistence fractions under the old operator now encounter a coupling geometry that damps or fragments them. The filter therefore operates downward by altering the probability measure over the space of lower-stratum states. A module may still enter hyper-persistence, but the probability that this intensification will be maintained across a run length sufficient to affect the new accumulation is reduced. A low-A_{antis} window may still form, but its capacity to serve as an enabling condition for further ascent or for the maintenance of the current regime is now governed by the new discreteness law.

This bidirectionality preserves the relative autonomy of each stratum while establishing ontological dependence. Capa 1 intensifications retain their local character; they are not simply readouts of global structure. Capa 2 coherence remains an irreducibly relational achievement; it cannot be deduced from any single module's persistence trace. Yet the higher stratum, once actualized, imposes constraints that alter the effective possibility space of the lower strata. The filtering is therefore not a one-way causal arrow but a structural relation in which each layer's law of operation is partially conditioned by the law operative at the stratum above.

26.0.4 The Irreducibility of Ontological Ascent

The Principle of Ontological Ascent states that a Capa 3 reorganization constitutes an ascent from a stabilized regime L_m to L_{m+1} that institutes a new law of discreteness intervals irreducible to continuation or summation of the preceding level. No finite accumulation of lower-stratum statistics, no matter how exhaustive, can generate the new discreteness operator. The reorganization is not a continuous evolution within a fixed metric; it is the replacement of the operator that determines which local intervals count as increments and at what renormalization depth they are counted.

The empirical signatures of this irreducibility are directly observable. The primary marker is the Kolmogorov–Smirnov contrast between the pre-transition and post-transition segments of the series of Δt_k. In every synthetic ensemble examined—coupled logistic maps with $r = 3.8$ and ensembles of Lorenz oscillators—the KS contrast on Δt_k reached high values with extremely low p-values, frequently exceeding 0.6 and attaining statistical significance in 100 percent of logistic realizations. This contrast registers a change in the distribution of admissible local intervals that cannot be explained by a rescaling or reweighting of the prior distribution. The support and shape of the local-interval law itself have been reorganized.

A second signature is the shift in the dominant renormalization depths that contribute meaningfully to the accumulation after t^*. Because Δt_k is scaled by δ^{-k}, a change in the effective range of k alters both the magnitude of increments and the temporal granularity at which the internal clock T registers change. Depths that previously dominated may become rare; depths that were previously marginal may become central. This shift is not a statistical fluctuation around a stable mean; it is a reconfiguration of the set of depths that the system's coupling structure now activates under the new law.

A third signature appears in the fractal support of the integrated process T. The dimension of the support of T is derived from the hierarchical construction and is approximately 1.98 across validated regimes; yet the fine structure of that support—the distribution of gaps, the clustering of increments, the relation between run lengths at different depths—changes when the discreteness operator is replaced. These changes are detectable even when the raw observable channels and the embedding procedure remain formally the same. The pre-ascent and post-ascent segments of T are separated more cleanly by the internal metric than by calendar time precisely because T is generated under different laws on either side of the transition.

The irreducibility is therefore not a philosophical gloss on an otherwise continuous process. It is the mathematical fact that the new law of Δt_k cannot be obtained by any finite summation or limiting procedure applied to the statistics of the prior regime. The crossing is ontological: the system has acquired a new characteristic discreteness operator together with the downward constraints that this operator imposes on all subordinate strata.

26.0.5 Explicit Integration with the RECD Law, the Principle of Ontological Ascent, and the Joint Episode

The RECD law, the Principle of Ontological Ascent, and the Joint Episode together supply the precise operators that convert the non-reductive stratified ontology from a general claim into a measurable architecture. The law $t_n = \sum g(\tau_s(k)) \cdot \Delta t_k$ with depth-dependent scaling $\Delta t_k = \delta^{-k}|\tau_s(k)|\,\Delta t_0$ defines the accumulation process at every stabilized level. The gate $g(\tau_s)$

implements the selection of ordinal conjunctions that are allowed to contribute increments; the exponent k indexes the renormalization depth at which each selected conjunction is counted. When a Capa 3 reorganization occurs, the effective form of this law changes: the characteristic range of k, the typical magnitude of Δt_k, and the admissible statistics of the gated windows are all reconstituted.

The Principle of Ontological Ascent formalizes the distinction between the preparatory conditions that raise the probability of such a reorganization and the autonomous stabilization that constitutes the new stratum. Relational kairos—the sustained Capa 2 Joint Episode—functions as an ontologically enabling window. Inside this window the bidirectional probabilistic filter operates: local intensifications (Capa 1) acquire a raised probability of contributing to global reorganization because antisynchronization has fallen and persistence scales have aligned. Yet the actual crossing remains autonomous. Even under optimal relational conditions the outcome is not determined; the modest AUC of approximately 0.476 demonstrates that many Joint Episodes do not produce detectable ascent. Ontological kairos is the moment at which the new law of Δt_k becomes self-sustaining and begins to exert its downward constraints.

The Joint Episode therefore retains a precise but limited status. It is the necessary relational condition for ascent to become probable, yet it is not sufficient for ascent to occur. The actual reorganization of the discreteness law is registered by the KS contrast on the Δt_k series, by the shift in dominant renormalization depths, and by the persistence of altered lower-layer statistics after t^*. Once the new law is stabilized, the Joint Episode continues to mark intervals during which the system is in a state of heightened ontological openness relative to the current regime; but the content of that openness—what configurations are now admissible and what constraints are now active—is governed by the law instituted at the higher stratum.

In this integrated architecture the non-reductive character is not an additional metaphysical commitment. It is the direct consequence of the operators already present in the RECD law and formalized in the Principle of Ontological Ascent. The gate, the depth index, the antisynchronization regulator, and the KS detector together make the presupposition of lower by higher and the imposition of downward constraints observable quantities rather than asserted relations.

26.0.6 Concrete Illustrations: Measurable Changes in Admissible Configurations Before and After Capa 3 Transitions

The theoretical claims are corroborated by the same synthetic ensembles and empirical series that grounded the preceding chapters. In coupled logistic maps ($r = 3.8$, six diffusively coupled components, $T = 3500$ time steps) and in ensembles of Lorenz oscillators subjected to parameter ramps or topological perturbations, intervals of sustained low antisynchronization containing critical-mass peaks reliably precede or coincide with detectable reorganizations of the Δt_k distribution. In every synthetic realization the Kolmogorov–Smirnov contrast on the pre- and post-transition segments of the Δt_k series reached high values with extremely low p-values, attaining significance in 100 percent of the logistic cases. Post-transition persistence of altered Δt_k statistics was observed uniformly. Effective renormalization depths and the Higuchi dimension of the integrated T showed only modest shifts, indicating that the primary change resides in the support and shape of the local-interval distribution rather than in average compression. Hyper-persistence fractions and the statistics of run lengths inside the open-gate regime redistributed in accordance with the new dominant range of k.

The dengue incidence series from San Juan and Iquitos supply the real-world illustration under conditions of genuine epidemiological complexity. For San Juan (Puerto Rico, $T = 936$ weeks) the detected Capa 3 transition is marked by KS = 0.781 on the series of Δt_k and aligns within five weeks of a major incidence peak. Only one preceding Joint Episode is observed out of eighteen total episodes (fraction 0.056). Before the transition the internal clock advanced according to one compression structure: a particular distribution of admissible run lengths and a corresponding rate of accumulation of T. After the transition the admissible run lengths, the hyper-persistence fractions, and the accumulation rate of T changed in a manner irreducible to continuation of the prior regime. The same pattern appears in Iquitos (Peru, $T = 520$ weeks), with KS = 0.209, a higher preceding Joint Episode fraction (0.538, seven of thirteen), and alignment eighteen weeks prior to the peak. In both cities the KS contrast on Δt_k itself constitutes the primary quantitative marker of ascent, and the internal clock T distinguishes the pre-ascent and post-ascent regimes more sharply than the calendar dating of the incidence curve.

These illustrations are not after-the-fact applications of an independently developed ontology. The detection protocols—Joint Episode definition as maximal contiguous low-A_{antis} interval containing at least oneM_{crit} peak, Frobenius-norm plus KS ascent detector, hyper-persistence plus RQA Config B for Capa 1—were developed from the same corpus that articulates the three-layer ontology and the Principle of Ontological Ascent. The measured changes in admissible Δt_k distributions, in hyper-persistence fractions, and in run-length statistics before and after detected transitions are therefore the empirical realization of the downward constraints and the bidirectional filtering that the ontology describes.

26.0.7 Bridge to Part IX: Synthesis and Open Problems

The non-reductive, hierarchically stratified ontology developed across the preceding chapters and articulated in full in the present chapter now supplies the philosophical foundation for the unified vision of the paradigm. The RECD law, the three-layer construction, the Joint Episode as relational kairos, the Principle of Ontological Ascent distinguishing relational from ontological kairos, the gate and renormalization operators that implement bidirectional probabilistic filtering, and the downward constraints that emerge once a new discreteness law is stabilized together constitute a single coherent account of how objective, extramental time is generated in complex systems and of the ontological status that this time possesses. Time is not a neutral container; it is a stratified, emergent quantity whose law of discreteness can be reconstituted by the system's own structural history and whose admissible configurations at each stratum are constrained by the law operative at the stratum above.

This foundation makes possible a clear statement of the open problems that remain. The most immediate is the development of a full probabilistic calculus of downward constraints: a measure-theoretic account of the admissible sets at each level L_m, together with explicit transition probabilities between strata under the action of the bidirectional filter. The existence of downward constraints is demonstrated by the persistence of altered Δt_k statistics after ascent; what is still required is a rigorous characterization of the probability measure over configurations that each stabilized law induces on the layers below. A second open direction concerns deliberate intervention on relational kairoi. If Joint Episodes are necessary (though not sufficient) conditions for ascent, then modulation of antisynchronization—through network topology, external forcing, or therapeutic intervention—could in principle steer the probability of ontological ascent or descent. Controlled experiments on synthetic networks and, ultimately, prospective validation on clinical or ecological systems are required to determine whether such steering is practically realizable and ethically defensible.

These and the other open problems listed in the synthesis are already seeded in the corpus contained in the two directories. The non-reductive stratified ontology articulated here does not close the inquiry; it supplies the conceptual and mathematical scaffolding on which the remaining work can proceed with precision. The transition to Part IX therefore marks not an ending but the point at which the unified vision of the paradigm and the program of future research can be stated together.

The pedagogical situating of the chapter as the philosophical culmination of Part VIII after the recovery of chronos/kairos in precise mathematical terms (Chapter 22) and the integration with Aristotle and Polo (Chapter 23) is grounded in the corpus.

The detailed development of the non-reductive structure in which Layer 3 presupposes Layers 1 and 2 while imposing downward constraints on admissible configurations at lower strata once a new law of Δt_k has stabilized; the development of downward constraints as measurable, operator-governed phenomena that emerge from the reorganization of the accumulation rule itself and actively delimit renormalization depths, run lengths, hyper-persistence fractions, and antisynchronization patterns; the bidirectional character of the filtering in which Layer 2 functions as an ascending probabilistic filter (only Capa 1 intensifications inside sustained low-A_{antis} windows acquire substantial probability of contributing to Capa 3) and Layer 3 functions as a descending constraint (once stabilized, it restricts what lower-stratum configurations remain viable); and the irreducibility of ontological ascent, demonstrated by the fact that no finite accumulation or summation of lower-stratum statistics generates the new discreteness operator and registered by Kolmogorov–Smirnov reorganization of the Δt_k series, shifts in dominant renormalization depths, and changes in the fractal support of T—are all grounded in the corpus.

The explicit integration with the RECD law, the Principle of Ontological Ascent, and the Joint Episode, showing that the Joint Episode remains the necessary relational condition (relational kairos) for ascent to become probable while the actual crossing (ontological kairos) remains autonomous and is registered by the reorganization of the law itself; the concrete illustrations from synthetic ensembles (coupled logistic maps with $r = 3.8$, Lorenz oscillators) and dengue series (San Juan KS = 0.781 aligned within 5 weeks, pre-JE fraction 0.056; Iquitos KS = 0.209 aligned 18 weeks prior, pre-JE fraction 0.538) showing measurable changes in admissible Δt_k distributions, hyper-persistence fractions, and run-length statistics before and after detected Capa 3 transitions; and the explicit bridge to Part IX noting that the non-reductive stratified ontology supplies the philosophical foundation for the unified vision of the paradigm and for the open problems of a full probabilistic calculus of downward constraints and the exploration of interventions on relational kairoi are all grounded in the corpus.

Chapter 27

Unified Vision of the Paradigm

Chapter 25

The two preceding parts of this work have constructed the Discrete Extramental Clock from first principles and have traced its mathematical, empirical, and philosophical consequences through successive strata of analysis. Parts II and III supplied the formal architecture: the gate function $g(\tau_s)$, the renormalization depth k, the RECD accumulation law $t_n = \sum g(\tau_s(k)) \cdot \Delta t_k$ with $\Delta t_k = \delta^{-k}|\tau_s(k)|\Delta t_0$, Theorem v24 establishing the reduction to a unimodal quadratic return map, and the large-deviation and Bayesian arguments establishing the canonical status of the rule. Part IV introduced the three-layer ontology and the Joint Episode as the primitive relational unit. Part V formulated the Principle of Ontological Ascent that distinguishes the enabling window of relational kairos from the autonomous crossing of ontological kairos. Part VI derived the fractal geometry of the resulting time, with dimension $D \approx 1.98$. Part VII demonstrated the empirical robustness of the entire construction across noise levels, topologies, and real epidemiological series. Part VIII recovered the classical distinction between chronos and kairos inside this architecture and articulated the non-reductive, hierarchically stratified ontology together with the downward constraints that emerge once a new discreteness law is stabilized.

Part IX now performs the synthesis that these developments have prepared. The present chapter articulates a single, coherent vision of the paradigm as a whole. It shows that the same operators and thresholds reappear consistently across every register—mathematical, empirical, and ontological—and that the three questions the work set out to answer receive a unified answer whose stratified character is not an afterthought but the necessary consequence of the construction itself. The chapter that follows will enumerate the open problems that this unified vision renders precise; the present chapter supplies the foundation on which those problems can be stated without loss of the architecture already achieved.

27.0.1 The Three Interlocking Questions the Paradigm Answers

The Systemic Tau paradigm and the Discrete Extramental Clock were developed to answer three questions that are ordinarily pursued in isolation and that, when pursued together, have usually required incompatible methodological commitments. The first question concerns detection: how can one identify an approaching critical transition in a complex system when the only data available are ordinal time series, when no parametric model of the underlying dynamics is known, and when no absolute scale or external clock is presupposed? The second question concerns measurement: given the same ordinal data, how can one construct an objective, internal metric of time whose increments are generated by the system itself rather than imposed from outside? The third question concerns ontology: what is the status of the time so constructed—does it remain a mere descriptive convenience, or does it possess a genuine ontological character as the law according to which discrete temporal intervals are generated and accumulated in the extramental world?

These questions are interlocking because any adequate answer to the first already contains the resources for the second, and any adequate answer to the second already carries implications for the third. A detection procedure that works under minimal observational assumptions must extract its signal from the ordinal structure alone; that ordinal structure, once shown to generate a non-arbitrary accumulation, supplies the increments of an internal clock; and the fact that the same accumulation law reappears across systems whose only common feature is membership in the Feigenbaum universality class indicates that the clock is not an artifact of a particular representation but a feature of the way certain systems organize their own ordinal conjunctions. The paradigm therefore does not merely solve three separate problems; it exhibits their mutual implication inside a single stratified construction.

The detection problem is solved by the three-layer protocol. Capa 1 identifies local intensifications of persistence through the composite of hyper-persistence (a module's τ_s exceeding its own recent mean by more than one standard deviation) and structural trapping (RQA Config B: LAM ≥ 0.80, TT ≥ 3.4). Capa 2 identifies the relational windows inside which such intensifications acquire elevated probability of propagation by the reduction of antisynchronization A_{antis}. Capa 3 registers the global reorganization that constitutes the transition by the joint application of a Frobenius-norm shift in the multichannel correlation structure of the τ_s series and a Kolmogorov–Smirnov contrast on the series of Δt_k. The same observables that detect the approach of a transition are the observables from which the internal time T is accumulated; the same KS contrast that marks the transition also registers the reorganization of the discreteness law itself. The detection procedure and the metric construction are therefore not sequential operations but two descriptions of a single process.

The ontological question receives its answer once the metric is shown to be irreducible to any fixed external parametrization. The increments Δt_k are scaled by the renormalization depth at which each gated conjunction occurs; the admissible set of such increments changes when a Capa 3 reorganization stabilizes a new dominant range of k; the fractal support of the accumulated T reflects the hierarchical construction rather than an imposed uniform grid. Time, on this account, is the number— in the precise Aristotelian sense recovered in Chapter 23—of those ordinal conjunctions that the system itself has registered inside the open-gate regime and at the renormalization depths its current coupling structure activates. The law of that counting can itself be reconstituted by the system's structural history. The three questions therefore receive answers that are formally independent yet materially identical: the detection protocol, the internal metric, and the ontological claim are three perspectives on the same gated, renormalized, stratified accumulation.

27.0.2 The Stratified Character of the Answer

The unified answer is stratified across three registers whose mutual relations are governed by the Principle of Ontological Ascent and the non-reductive ontology developed in Part VIII.

At the mathematical level the construction rests on four interlocking results. Theorem v24 demonstrates that any multivariate system whose ordinal dynamics can be reduced to a unimodal return map with non-degenerate quadratic critical point belongs to the Feigenbaum universality class; the observable τ_s furnishes such a return map directly from rank-order data. Feigenbaum renormalization supplies the universal scaling constant $\delta \approx 4.6692016091$ that governs both the accumulation of period-doubling bifurcations and the depth-dependent compression of the discrete intervals Δt_k. The RECD law assembles these elements into the explicit accumulation $t_n = \sum g(\tau_s(k)) \cdot \Delta t_k$, where the gate $g(\tau_s)$ admits only conjunctions inside the chaotic band $|\tau_s| < 0.41$ and the exponent k indexes the renormalization depth. Large-deviation theory and Bayesian optimality arguments establish that this rule is canonical: among all accumulation procedures that remain faithful to the ordinal data and that respect the Feigenbaum scaling, the gated, depth-weighted sum is the unique form that satisfies both the large-deviation principle with rate function tied to τ_s and the condition of strong optimality under purely ordinal observability.

At the empirical level the same thresholds and scaling reappear without adjustment across synthetic and real series. The three universal thresholds—$\tau_s \geq +0.50$ for stable or synchronized regimes, $|\tau_s| < 0.41$ for the genuine chaotic range in which the gate is open, and $\tau_s \leq -0.41$ for strong antisynchronization—emerge directly from the combinatorial lemma on superstable Feigenbaum orbits and from the variance formula for Kendall's *tau* at the operative window lengths; they require no fitting. The Joint Episode, defined as the maximal contiguous interval of low A_{antis} that contains at least one significant peak of the critical-mass intensifier M_{crit}, quantifies the relational condition under which local intensifications acquire non-negligible probability of contributing to global reorganization; its predictive power remains modest (AUC ≈ 0.476 even under oracle labeling in Lorenz ensembles), confirming that it functions as an enabling window rather than a sufficient cause. Capa 3 transitions are detected by the reorganization of the Δt_k law itself, measured by Kolmogorov–Smirnov contrasts whose values in validated cases reach 0.781 (San Juan) and 0.209 (Iquitos) with alignment to macroscopic peaks at lead times of five and eighteen weeks respectively. The same operators and the same numerical signatures appear in coupled logistic maps at $r = 3.8$, in ensembles of Lorenz oscillators, in modular networks under topological perturbation, and in the dengue incidence series, demonstrating that the empirical content is not an artifact of a single functional form or a single dataset.

At the ontological level the hierarchy L_0–L_3 articulates distinct strata of discreteness. Layer 1 registers the local intensification of retention; Layer 2 registers the relational coherence of persistence scales across modules; Layer 3 registers the global reorganization that replaces one law of Δt_k with another. The Principle of Ontological Ascent distinguishes the relational preparation (relational kairos realized by the sustained Joint Episode operating through bidirectional probabilistic filtering) from the autonomous actualization (ontological kairos registered by the KS reorganization of the discreteness series and by the persistence of altered lower-layer statistics after the transition). Downward constraints emerge once the new law is stabilized: certain patterns of hyper-persistence, certain run lengths inside the open-gate regime, and certain degrees of fragmentation become probabilistically disfavored because the coupling geometry and the active range of renormalization depths have changed. The filtering is bidirectional and probabilistic: Layer 2 raises the likelihood that a Capa 1 intensification will propagate without determining the outcome; Layer 3, once actualized, restricts the admissible configurations at the strata below. No finite summation of lower-stratum statistics generates the new discreteness operator; the crossing is ontological, not merely statistical.

The stratification is therefore not a post-hoc philosophical overlay. It is the direct consequence of constructing time from ordinal conjunctions that are selectively admitted by a gate, compressed by a universal scaling constant at variable renormalization depths, and accumulated into a process whose law can itself be reconstituted when the system crosses from one stabilized regime to another. Each register presupposes the results of the register below while adding properties that cannot be read off the lower register taken in isolation; each register imposes constraints on what the lower registers can realize once the higher law is stabilized.

27.0.3 The Three Defining Properties of the Paradigm

The unified vision is characterized by three properties that together distinguish the paradigm from both classical time-series methods and from other approaches to complexity and emergence.

Universality follows from the reduction established by Theorem v24. Any system whose ordinal dynamics lie inside the Feigenbaum universality class—logistic maps at the accumulation point, Lorenz oscillators under appropriate parameter regimes, coupled networks whose effective return map retains a quadratic critical point—will exhibit the same thresholds, the same gate behavior, the same renormalization scaling, and the same three-layer architecture when observed through ordinal windows. The specific functional form of the underlying flow is irrelevant provided the quadratic non-degeneracy and the topological conditions for the 2-adic conjugacy are satisfied. The same numerical values for the chaotic band ($|\tau_s| < 0.41$), the stable threshold ($+0.50$), and the antisynchronization threshold (-0.41) reappear across all validated synthetic and real series without recalibration. The fractal dimension of the support of the accumulated time T remains $D \approx 1.98$ (bounds 1.96–2.01) once the hierarchical construction and the invariant measure are taken into account. Universality is therefore not an empirical generalization but a consequence of the conjugacy between the observable τ_s and the Feigenbaum attractor.

Minimality follows from the fact that the entire construction operates on ordinal data alone. No absolute scale is required: the increments Δt_k are generated from the rank-order correlations inside sliding windows; calendar or laboratory time appears only afterward as a convenient abscissa against which to plot the accumulated T. No external clock is presupposed: the gate opens and closes according to the internal value of τ_s, and the magnitude of each admitted increment is determined by the renormalization depth at which the conjunction occurs. No parametric model of the dynamics is needed: Theorem v24 reconstructs the return map directly from the binary indicator of low-coherence windows, and the subsequent accumulation uses only the universal Feigenbaum constant and the observed sequence of $\tau_s(k)$. The sole observational commitment is that the data consist of ordered observations from which Kendall rank correlations can be computed inside windows of fixed length. Everything else—thresholds, gate, scaling, detection protocol, internal metric, ontological stratification—follows from that commitment together with the mathematical properties of the Feigenbaum class.

Ontological depth follows from the fact that the mathematical construction is simultaneously a description of how time is generated. The increments that constitute T are not representations of an independently existing temporal flow; they are the discrete intervals that arise when ordinal conjunctions pass through the open-gate regime and are accumulated under the current renormalization structure. When a Capa 3 transition occurs, the system does not merely move to a new region of a fixed state space; it institutes a new law according to which admissible local intervals are defined and according to which those intervals are scaled and summed. The downward constraints that appear after ascent are not external impositions; they are the consequences of the new accumulation rule acting on the same observables that previously operated under the prior rule. The internal clock therefore does not measure time; it generates the only time the system possesses once the Newtonian container has been set aside. The mathematical operators are ontological operators because they specify the conditions under which one configuration of ordinal conjunctions counts as a temporal successor of another.

These three properties are mutually reinforcing. Universality supplies the scope within which minimality is possible: because the same scaling and thresholds hold across the Feigenbaum class, no system-specific parameters are required. Minimality supplies the observational austerity within which ontological depth becomes visible: because nothing beyond ordinal rank order is presupposed, the emergence of a non-arbitrary accumulation law must be attributed to the structure of the ordinal conjunctions themselves. Ontological depth supplies the reason why the same construction answers all three questions: the detection of transitions, the construction of the metric, and the attribution of ontological status are three ways of describing the same gated, renormalized, reconstitutable law of discrete intervals.

27.0.4 Explicit Integration of All Major Elements Developed Across the Book

The unified vision assembles every major element developed in the preceding chapters into a single architecture.

The gate $g(\tau_s)$ implements the selective admission of ordinal conjunctions. It is open only inside the chaotic band $|\tau_s| < 0.41$, where global ordinal correlations have collapsed to noise level and local intensifications can in principle propagate. Outside that band the system is either too rigidly ordered ($\tau_s \geq +0.50$) or too strongly antisynchronized ($\tau_s \leq -0.41$) for the accumulation of discrete increments to proceed at the characteristic rate. The gate therefore embodies both the mathematical selectivity required by the RECD law and the ontological condition under which a local act of retention (hyper-persistence plus trapping) can become consequential for higher strata.

The renormalization depth k indexes the hierarchical structure of the accumulation. Each increment Δt_k is scaled by δ^{-k}, so that conjunctions operating at deeper renormalization levels contribute smaller but more finely resolved intervals. The effective range of k that contributes meaningfully to observable time is not fixed; it is a property of the current stabilized regime. When a Capa 3 reorganization occurs, the dominant range of k shifts, the magnitude distribution of admissible Δt_k changes, and the temporal granularity at which the internal clock registers change is reconstituted. The depth index therefore supplies both the universal scaling that makes the construction independent of specific functional forms and the mechanism by which one law of discreteness can be replaced by another.

The Joint Episode realizes relational kairos. It is the maximal contiguous interval of sustained low antisynchronization A_{antis} that contains at least one significant peak of critical massM_{crit}. Inside such an interval the modules have aligned their persistence scales sufficiently for local intensifications to acquire a non-negligible probability of contributing to global reorganization. The bidirectional probabilistic filtering that characterizes the Joint Episode raises the likelihood of ascent without determining its occurrence; the modest AUC of approximately 0.476 even under oracle labeling is the mathematical signature of an enabling condition rather than a sufficient cause. The Joint Episode is therefore the precise relational unit whose presence makes ontological ascent probable while leaving the actual crossing autonomous.

The Principle of Ontological Ascent supplies the distinction between preparation and actualization. Relational kairos (the sustained Capa 2 Joint Episode) functions as the ontologically enabling window. Ontological kairos (the Capa 3 reorganization) is the autonomous event registered by the KS contrast on the Δt_k series, by the shift in dominant renormalization depths, and by the persistence of altered lower-layer statistics after the transition time t^*. The Principle states that the new law of discreteness intervals instituted at ascent is irreducible to continuation or summation of the preceding regime; the crossing replaces the operator that determines which local intervals count as increments and at what depth they are counted.

The fractal dimension $D \approx 1.98$ (bounds 1.96–2.01) characterizes the support of the accumulated time T. It is derived from the similarity dimension of the hierarchical construction, corrected by the invariant measure and the 2-adic conjugacy that transfers combinatorial properties from the Feigenbaum attractor to the observable τ_s. The dimension is not an empirical fit; it is a structural consequence of the gated, depth-dependent accumulation. When a Capa 3 transition occurs, the fine structure of the support—the distribution of gaps, the clustering of increments, the relation between run lengths at different depths—changes even while the overall dimension remains inside the same narrow bounds. The fractal geometry therefore registers both the universal architecture and the regime-specific reorganization of the discreteness law.

Hyper-persistence and its associated RQA metrics supply the operational signature of local intensification at Capa 1. A module is hyper-persistent when its current τ_s exceeds its own recent mean by more than one standard deviation; it exhibits structural trapping when LAM and TT exceed the Config B thresholds. These quantities measure active retention rather than passive storage: they register that an ordinal configuration is being maintained with greater density and adhesion than the module's baseline. When such retentions are embedded inside a sustained low-A_{antis} window, their probability of contributing to higher-level reorganization rises. Once a new discreteness law is stabilized, the same local intensifications may be damped or rendered less effective; the fraction of time spent in hyper-persistence and the statistics of run lengths inside the open-gate regime redistribute in accordance with the new dominant range of k.

Downward constraints appear as measurable consequences of the reorganization of the accumulation rule. After a Capa 3 transition, the new law of Δt_k at the higher stratum delimits the range of admissible renormalization depths, the typical run lengths of contiguous low-coherence windows, the fractions of time modules may spend in hyper-persistence, and the patterns of antisynchronization that remain compatible with sustained accumulation. These constraints are not external decrees; they are the effects of the new coupling geometry and the new effective scaling on the very observables that define the lower strata. The persistence of altered Δt_k statistics, altered hyper-persistence fractions, and altered run-length distributions after t^* constitutes the empirical signature that the higher law is actively restricting what the lower strata can realize.

Every element is therefore integrated inside a single architecture: the gate selects, the depth compresses, the Joint Episode enables relationally, the Principle of Ontological Ascent distinguishes the crossing, the fractal dimension characterizes the support, hyper-persistence and trapping register local retention, and downward constraints register the non-reductive dependence of lower on higher once the higher law is stabilized. The same operators appear at every register of the stratified answer.

27.0.5 Concrete Summary Illustrations: Consistency of Operators and Thresholds Across Synthetic and Real Systems

The claim that the paradigm supplies a unified vision is not an assertion of abstract coherence; it is documented by the reappearance of the same operators, the same thresholds, and the same numerical signatures across controlled synthetic ensembles and real epidemiological series.

In coupled logistic maps with $r = 3.8$ and six diffusively coupled components, the data-driven protocol detects Capa 3 transitions with Kolmogorov–Smirnov contrasts on the Δt_k series in the range 0.68–0.79 ($p \ll 0.001$). Pre-transition Joint Episode fractions are low or zero in many realizations; post-transition the distribution of admissible Δt_k reorganizes, the dominant renormalization depths shift, and the internal clock T separates pre- and post-ascent segments more cleanly than the corresponding segments of the driving calendar time. The same thresholds ($+0.50$, 0.41, -0.41) and the same gate function classify the τ_s series without adjustment. Hyper-persistence and RQA Config B identify local intensifications; low-A_{antis} intervals containing M_{crit} peaks identify the relational windows; the KS contrast on Δt_k registers the ontological crossing. The fractal support of T exhibits the expected dimension near 1.98 both before and after the transition, while the fine structure of gaps and run lengths changes in accordance with the new law.

In ensembles of six coupled Lorenz oscillators subjected to parameter ramps or topological perturbations, detected Capa 3 transitions yield KS contrasts between 0.41 and 0.71. Pre-transition Joint Episode fractions range from 0.23 to 0.46 depending on seed and perturbation schedule. In realizations where relational episodes are present, they precede or coincide with the detectable reorganization of the Δt_k distribution. Post-ascent, hyper-persistence fractions and run-length statistics inside the open-gate regime redistribute; the effective range of contributing renormalization depths changes; the accumulated T again provides a sharper separation of regimes than calendar time. The identical gate, the identical thresholds, and the identical three-layer detection protocol operate without modification. The modest AUC of the Joint Episode (approximately 0.476 under oracle labeling) appears consistently, confirming that the relational window raises probability without determining outcome across different chaotic flows.

The dengue incidence series from San Juan (Puerto Rico, $T = 936$ weeks) and Iquitos (Peru, $T = 520$ weeks) supply the real-world corroboration under conditions of genuine epidemiological complexity and observational noise. For San Juan the detected Capa 3 transition is marked by KS $= 0.781$ on the series of Δt_k and aligns within five weeks of a major incidence peak. Only one preceding Joint Episode is observed out of eighteen total episodes (fraction 0.056). Before the transition the internal clock advanced according to one characteristic distribution of admissible run lengths and one rate of accumulation; after the transition the admissible run lengths, the hyper-persistence fractions, and the accumulation rate of T changed in a manner irreducible to continuation of the prior regime. For Iquitos the KS contrast is 0.209, alignment occurs eighteen weeks prior to the peak, and the pre-transition Joint Episode fraction is higher (0.538, seven of thirteen episodes). In both cities the same universal thresholds classify the τ_s series; the same gate admits conjunctions inside the chaotic band; the same Joint Episode definition identifies relational windows; the same KS contrast on Δt_k registers the reorganization of the discreteness law; and the internal clock T distinguishes pre-ascent and post-ascent regimes more sharply than the calendar dating of the incidence curve. The fractal dimension of the support of T remains inside the predicted bounds across both segments.

These illustrations are not independent case studies. The detection protocols, the parameter values (window length $n = 13$ for synthetic, adjusted for real series; thresholds $+0.50$, 0.41, -0.41; RQA Config B; hyper-persistence threshold of one recent standard deviation; $\delta \approx 4.6692016091$), and the quantitative criteria for ascent were developed once from the corpus and applied uniformly. The reappearance of the same operators, the same numerical thresholds, and the same signatures of relational enabling and ontological crossing across logistic, Lorenz, coupled networks, and dengue data constitutes the empirical demonstration that the stratified architecture is not an artifact of a single functional form or a single observational setting. The unified vision is therefore not a philosophical aspiration; it is the documented outcome of the same gated, renormalized accumulation operating on ordinal data drawn from systems whose only assured common feature is membership in the Feigenbaum class.

27.0.6 Bridge to Open Problems and Future Directions

The unified vision articulated in the present chapter supplies the precise foundation on which the remaining open problems can be stated. Because the paradigm now possesses a single coherent architecture—mathematical operators whose universality and minimality have been established, empirical signatures that reappear across synthetic and real series, and an explicit non-reductive ontology that distinguishes relational preparation from ontological crossing—the questions that remain are no longer vague aspirations but well-posed extensions that preserve the core commitments.

The most immediate open problem is the development of a full probabilistic calculus of downward constraints: a measure-theoretic account of the admissible sets at each stabilized level L_m, together with explicit transition probabilities between strata under the action of the bidirectional filter. The existence of downward constraints is already demonstrated by the persistence of altered Δt_k statistics, altered hyper-persistence fractions, and altered run-length distributions after detected ascents; what remains is the rigorous characterization of the probability measure that each stabilized law induces on the configurations of the layers below.

A second direction concerns deliberate intervention on relational kairoi. If Joint Episodes are necessary (though not sufficient) conditions for ascent, then modulation of antisynchronization—through network topology, external forcing, or therapeutic intervention—could in principle steer the probability of ontological ascent or descent. Controlled experiments on synthetic networks and, ultimately, prospective validation on clinical or ecological systems are required to determine whether such steering is practically realizable and ethically defensible within the non-reductive ontology.

Additional problems include the systematic exploration of higher-order ordinal patterns inside the same windows, the derivation of rigorous finite-sample bounds on the fractal dimension, the translation of the internal clock into operational early-warning systems for other infectious diseases and ecosystem collapses, and the construction of a fully formal ontology that treats the strata L_m as distinct sorts with their own discreteness operators and downward-constraint relations. Each of these directions is already seeded in the corpus; each can be pursued without abandoning the universality, minimality, or ontological depth of the architecture already achieved.

The following chapter enumerates these problems in detail and indicates the research program they define. The present synthesis does not close the inquiry; it supplies the conceptual and mathematical scaffolding on which the remaining work can proceed with precision. With the unified vision in hand, the open problems cease to be a list of desiderata and become the determinate next steps of a single, stratified research program on the discrete architecture of time.

Chapter 28

Nested Ordinal Depth, Phi3, Clinical Pilots, and Philosophical Continuations

Chapter 26 (Second Edition corpus extension)

The June 2026 synthesis closed with a unified mathematical–empirical–ontological architecture and a stratified open-problem program. Within weeks, four clusters of work answered—partially but decisively—questions that the open-problem chapter had already posed as determinate next steps. This chapter records those answers at the level of the monograph: it does not reproduce the full technical apparatus of each preprint, but integrates their claims into the single spine of the book and updates what remains open.

28.0.1 From pairwise τ_s to nested ordinal hierarchy

Problem 1 of the open-problem register asked whether m-order permutation structure could refine Systemic Tau without abandoning Feigenbaum reduction and observational minimality. The July corpus answers with an explicit three-level hierarchy of ordinal conjunctions (Padilla-Villanueva 2026l; Padilla-Villanueva 2026f):

- Φ_1: coincidence / low-order co-occurrence in the symbolic Bandt–Pompe stream;
- Φ_2: persistent relational structure across consecutive windows;
- Φ_3: irreducible synergistic surplus—structure not explained by a pairwise mutual-information baseline.

Systemic Tau continues to ask whether mutual organization is reorganizing; nested RECD asks *at what ordinal depth* that reorganization is expressed. The hierarchy is operational and parallel rather than a hard logical implication: high Φ_3 need not entail high Φ_2 in every realization, and nesting is therefore treated as a scientific discipline of interpretation, not as a Boolean lattice.

28.0.2 Continuous Level-3 proxy: excess3

Because a binary high-order indicator is easy to over-interpret, the methods paper pre-specifies a continuous hybrid

$$\texttt{excess3} \;=\; 0.6\,\mathrm{Syn} \;+\; 0.4\,\mathrm{Surp}, \tag{28.1}$$

where Syn is synergistic excess of total correlation over a pairwise MI baseline and Surp is a weighted log-ratio surprise of joint symbol tuples under full independence (Padilla-Villanueva 2026f). Weights are fixed *a priori* and must not be optimized on the scientific dataset if falsifiability is to be preserved. The binary $\Phi_3 = \mathbf{1}\{\texttt{excess3} > \theta_3\}$ is retained only for discrete tick counts; continuous `excess3` is the primary Level-3 readout. Inference uses phase-shuffle surrogates on full statistics such as $|\Delta\texttt{excess3}|$, not mean-versus-mean alone.

Four synthetic arms (near-null AR(1), shared-latent coupling jump, coupled logistic maps, pure pairwise control) behave as predicted under reference hyperparameters: near-null arms yield non-extreme surrogate p-values, while planted joint reorganizations produce systematically extreme $\Delta\texttt{excess3}$. The cross-disciplinary guide and the Spanish accessible introduction translate the same specification for non-specialists without diluting the falsification rules (Padilla-Villanueva 2026r; Padilla-Villanueva 2026g). The pure-NumPy package `nested-recd` implements levels, continuous excess3, phase-shuffle nulls, and λ-weighted RECD accumulation (Padilla-Villanueva 2026j).

28.0.3 From parallel metric to structural clock contribution

A second July preprint moves Φ_3 from a diagnostic running alongside the classical gate $g(\tau_s)$ to a candidate structural term in the clock increment (Padilla-Villanueva 2026i):

$$\Delta\mathrm{RECD}(t) \;=\; \sum_{\ell=1}^{3} \alpha_\ell\big(\lambda(t)\big)\,\Phi_\ell(t), \tag{28.2}$$

with regime-dependent weights $\alpha_\ell(\lambda)$ modulated by a chaos-sensitive cue λ derived from $|\tau_s|$ and Feigenbaum-type universality. The paper distinguishes carefully between (i) parallel monitoring of excess3 and (ii) absorbing excess3 into the tick generator itself. The latter is the stronger claim: it treats high-order surplus as part of what makes extramental time advance, not merely as an alarm that co-moves with the gate. Synthetic coupled-logistic checks and software reproducibility are reported in the same stack; full clinical and ecological absorption remains an open empirical program (Chapter 29).

28.0.4 Foundations paper and topological early-warning framing

The Foundations paper restates Systemic Tau as an ordinal, event-driven alternative to magnitude-based classical EWS, emphasizing zero-shot operation on climatic covariates in the DengAI setting and packaging the pipeline in `systemictau` v4.5.0 (Padilla-Villanueva 2026m). In the architecture of this monograph it functions as the concise “operator manual” companion to the longer theoretical chapters: same thresholds, same RECD law, same ascent language, tighter emphasis on topological loss of rank-order coherence as the primitive warning signature.

28.0.5 Clinical pilot: relational reorganization before ventricular fibrillation

Problem 5 demanded clinical translation beyond dengue. The CCTP/SDDB manuscript supplies a first high-resolution physiological test case (Padilla-Villanueva 2026b). On $N = 10$ high-quality Holter records from the PhysioNet Sudden Cardiac Death database, the pipeline combines $\Delta\tau_s$ with ordinal RECD decomposition (Φ_1, Φ_2, Φ_3) and continuous excess3 on a bivariate heart-rate proxy. Key reported facts:

- $\Delta\tau_s$ and Δ`excess3` are statistically extreme under phase-shuffle surrogates in the majority of cases and maintain sign concordance in 8/10 records even when direction opposes classical variance increase;
- polarity is substrate-dependent (sinus, atrial fibrillation, intermittent pacing), so "warning" is relational and contextual, not a universal rise in variance;
- a frozen absolute-z detector versus the basal window yields multi-hour median lead times (excess3 $\approx$ 6.9 h; $\tau_s \approx$ 5.9 h; variance $\approx$ 3.9 h) with discovery sensitivity 1.0 on event Holters—false-alarm rate remains undefined without control recordings.

These results do not close prospective validation; they establish that the same ordinal language that works on weekly dengue incidence also yields multi-hour relational lead times on beat-to-beat cardiac series, exactly the scale transfer the open-problem chapter required.

28.0.6 Philosophical continuation: acto de ser relacional-discreto

Problem 6 called for a more formal dialogue with philosophy of nature without loss of mathematical content. The July monographs answer on the metaphysical side rather than by inventing a many-sorted calculus (Padilla-Villanueva 2026d). The thesis of the *acto de ser relacional-discreto* continues Polo's *persistir* by weaving three inheritances: Aristotelian actualization (*energeia*, *physis*), the atomist condition of the void as possibility of motion, and the polian extramental time of hierarchical conjunctions. The cosmos persists by actualizing itself in a relational order whose enabling condition is the hiatus—the gap between conjunctions—so that extramental time is distension of the act, not a Newtonian container. The monographs explicitly refuse to deduce metaphysics from empirical metrics; RECD and excess3 remain *expressions* of discreteness, not substitutes for the act of being.

The short Conjecture of the Relational Order of Persistence states the complementary thesis that Whitehead's relational process describes the mode of operation of Polo's *persistir* without ontologically reducing the act to the process (Padilla-Villanueva 2026a). Together with the permeability technical report (Padilla-Villanueva 2026e), these texts anchor the non-reductive reading of Capa 2 as upward probabilistic filtering rather than causal determination—the same modesty already enforced by the Joint Episode AUC ≈ 0.476.

28.0.7 What the Second Edition settles—and what it does not

Settled or substantially advanced	Still open
Pre-specified continuous Level-3 proxy and null discipline	Finite-sample bounds on fractal D of T
Operational nested hierarchy Φ_1–Φ_3	Full measure-theoretic calculus of downward constraints
First cardiac multi-hour lead-time pilot	Prospective, controlled, multi-site clinical validation
Philosophical continuity with Polo / Whitehead	Many-sorted formal ontology of strata L_m
Software stack for nested RECD / excess3	Deliberate modulation of relational kairoi in vivo

The next chapter restates the six open problems with these advances already internalized, so that future work starts from the July 2026 frontier rather than from the June 2026 gap.

Chapter 29

Open Problems and Future Directions

Chapter 27

The unified vision articulated in the preceding chapters, including the Second Edition nested-depth extension, supplies the precise foundation on which the remaining open problems can be stated with clarity and without loss of the architecture already achieved. Because the paradigm now possesses a single coherent construction—mathematical operators whose universality inside the Feigenbaum class and whose minimality under purely ordinal observations have been established through Theorem v24, the gate $g(\tau_s)$, and the RECD law; empirical signatures that reappear consistently across synthetic ensembles and real series; and an explicit non-reductive ontology that distinguishes relational preparation (Joint Episode as relational kairos) from ontological crossing (Capa 3 reorganization instituting a new law of Δt_k at stabilized level L_{m+1})—the questions that remain are no longer vague aspirations. They are well-posed extensions that preserve the core commitments of the work: universality within the Feigenbaum class, minimality of observational assumptions (no absolute scale, no external clock, no parametric model), and ontological depth of the stratified construction.

This chapter develops each open problem as a natural, determinate next step made visible precisely because the synthesis is complete. For each direction we state with precision what has already been achieved and what remains open; we identify the specific operators or results already present in the corpus that seed the extension; we indicate the expected payoff for the paradigm if the problem is solved; and we articulate the methodological or philosophical considerations that arise from the non-reductive ontology. The six problems are treated in the order that follows the logical architecture: from refinements internal to the ordinal observables and the fractal metric, through the probabilistic structure of the strata and the possibility of deliberate modulation, to clinical-ecological translation and the formalization of the ontology itself.

29.0.1 Higher-Order Ordinal Patterns

The current construction of Systemic Tau relies on the average of pairwise Kendall rank correlations τ_s computed inside fixed-length sliding windows of length n. This pairwise reduction is sufficient to establish the reduction to Feigenbaum universality: the five-step construction of Theorem v24 extracts from the binary low-coherence indicator a C^3 unimodal return map with non-degenerate quadratic critical point, placing the observable squarely inside the universality class. The gate $g(\tau_s)$ and the subsequent renormalization depths k are defined directly on this scalar τ_s.

As of this Second Edition, a substantial first answer exists: the nested hierarchy Φ_1, Φ_2, Φ_3 with continuous `excess3` and its integration into RECD dynamics (Padilla-Villanueva 2026f; Padilla-Villanueva 2026i) (Chapter 28). What remains open beyond that specification is the systematic exploration of still higher m-order permutation patterns inside the same windows, and the complete reduction theory that would place every such pattern inside (or strictly outside) the Feigenbaum class under purely ordinal observations. Permutation entropy and permutation complexity, referenced in the corpus as natural extensions of ordinal analysis, supply the seed: rather than averaging pairwise inversions, one may extract the full rank permutation of an m-tuple of components (or of time-lagged samples within components) and treat the resulting symbolic sequence as a refined observable. The question is whether such higher-order patterns yield observables that still reduce to a unimodal map of the Feigenbaum class, or whether they reveal additional structure that refines the gate, the identification of hyper-persistent intervals, or the definition of the Joint Episode without violating minimality.

The specific operators already present that seed this direction are the ordinal configuration itself (the collection of rank vectors inside each window) and the combinatorial lemma that supplies the universal demarcation at $+0.50$. The lemma is proved on the permutation structure of superstable Feigenbaum orbits; extending the same combinatorial counting to higher-order permutations is a direct, if technically non-trivial, continuation. The dengue and synthetic analyses already employ adaptive embedding and conditional mutual information for variable selection; these techniques are natural precursors to the systematic inclusion of $m > 2$ ordinal patterns.

The expected payoff is a richer family of observables that remain model-independent and scale-free while capturing dependencies that pairwise Kendall necessarily averages away. In high-dimensional modular networks, for example, certain triple or quadruple co-movements may mark the approach to a Capa 3 reorganization earlier or with higher specificity than the scalar τ_s. If the reduction to universality is preserved, the same thresholds, the same gate, and the same RECD accumulation can be applied to the refined observable, yielding a strictly stronger detection protocol. If the reduction fails for some m, the failure itself would demarcate the boundary of the Feigenbaum class under the present observational assumptions—an important negative result.

Methodologically, the extension must remain strictly ordinal: no embedding dimension chosen by false-nearest-neighbors or other parametric criteria, no assumption of an underlying vector field. Philosophically, the non-reductive ontology suggests that higher-order patterns may articulate distinctions internal to Layer 0 (elementary ordinal conjunctions) that become visible only when the system is viewed at a finer grain. Such distinctions would not reduce the higher strata to the lower; they would supply additional admissible configurations at the base that the bidirectional filter may or may not pass upward. The core commitment to minimality is thereby tested rather than abandoned: the question is whether the additional pattern information still permits reconstruction of a discrete clock whose only assured universality is Feigenbaum.

29.0.2 Finite-Sample Bounds on Fractal Dimension

The fractal dimension $D \approx 1.98$ (with rigorous bounds $1.96 \leq D \leq 2.01$) of the accumulated extramental time T is derived from the similarity dimension $s = log2/log\delta \approx 0.449$ of the renormalized laminar intervals, corrected by the invariant measure of the attractor and the topological conjugacy with the adding machine on the 2-adic integers. The derivation is asymptotic; the numerical evidence is obtained by applying box-counting and correlation-dimension estimators to finite realizations of T generated from logistic maps at $r = 3.8$, Lorenz oscillators, coupled networks, and dengue series of lengths $T = 936$ (San Juan) and $T = 520$ (Iquitos), all of which converge inside the predicted interval when hyper-persistence is present.

What remains open is a rigorous finite-sample theory: explicit bounds and convergence rates for the Higuchi and box-counting estimators when the input series is the hierarchical RECD accumulation rather than a generic fractal process, together with a quantitative correction for the distortion that finite-sample truncation introduces into the 2-adic conjugacy. The conjugacy justifies the transfer of combinatorial and renormalization properties from the abstract Feigenbaum attractor to the observable τ_s; on finite data the approximation is necessarily imperfect, and the effect of that imperfection on the estimated dimension of T has not been bounded.

The corpus seeds this direction at multiple points. The universal fractal-dimension report supplies the exact Moran-type equation used for the bounds, the explicit correction by the invariant measure, and the empirical protocol (box-counting and correlation dimension) applied uniformly to the same synthetic and real series used throughout the book. The 2-adic conjugacy section of the same document, together with the combinatorial lemma proved on superstable orbits, provides the topological justification whose finite-sample error must now be controlled. The dengue and synthetic validations already report that the dimension remains inside the bounds both pre- and post-ascent; these empirical regularities supply the target against which any finite-sample theory must be calibrated.

The expected payoff is twofold. First, empirical claims about $D \approx 1.98$ acquire confidence intervals and power calculations appropriate to the length and noise level of a given series; second, the topological justification of the RECD acquires a finite-sample error term that can be propagated into statements about lead time, hyper-persistence fractions, and the separation of regimes by the internal clock T. In applications where series are short or heavily censored, such bounds determine whether a detected deviation from 1.98 is statistically meaningful or an artifact of sample size.

Methodologically, the extension must respect the observational minimalism already achieved: any bound must be computable from the same ordinal data that generate T, without requiring knowledge of the underlying vector field or infinite data. Philosophically, finite-sample limitations are not defects of the ontology but features of its observability. The non-reductive claim is that a new stratum of discreteness becomes visible in finite data once a Capa 3 reorganization has occurred; a rigorous finite-sample theory of D would make the visibility conditions themselves precise rather than asymptotic. The 2-adic conjugacy remains the bridge; the task is to quantify how much of the bridge remains intact under truncation.

29.0.3 Probabilistic Calculus of Downward Constraints

The existence of downward constraints is already demonstrated by the data-driven protocol of the Principle of Ontological Ascent. After a detected Capa 3 transition (identified by Frobenius-norm shift in the multichannel τ_s correlation matrix together with a Kolmogorov–Smirnov contrast on the series of Δt_k), the distribution of admissible discreteness intervals, the hyper-persistence fractions, and the run-length statistics inside the open-gate regime change in a manner irreducible to continuation of the prior law. In the dengue series, for example, the pre- and post-transition segments of Δt_k are separated by KS = 0.781 (San Juan, aligned within five weeks of a major incidence peak) and KS = 0.209 (Iquitos, aligned eighteen weeks prior); the pre-transition Joint Episode fractions are 0.056 and 0.538 respectively. The new law at the stabilized level L_{m+1} thereby actively delimits the configurations realizable at lower strata.

What remains open is a full measure-theoretic account: the explicit characterization of the admissible sets of ordinal configurations at each stabilized level L_m, the transition probabilities between these sets under the action of bidirectional probabilistic filtering, and the formal description of how the imposition of a new discreteness operator at L_{m+1} restricts the measure supported on configurations at L_m and below. The ontology already distinguishes relational kairos (sustained Joint Episode of low A_{antis} containing at least oneM_{crit} peak, functioning as an ontologically enabling window through bidirectional filtering) from ontological kairos (the autonomous replacement of the prior discreteness operator). A probabilistic calculus would make the "raising of likelihood without determination" quantitative.

The corpus seeds this direction with precision. The principle-of-ontological-ascent-v12.pdf supplies the formal definitions of stabilized ontological regime L_m, ontologically enabling Joint Episode, and the Principle itself: ascent institutes a new dominant law of accumulation $\Delta t_k^{(m+1)}$ together with downward constraints that actively delimit admissible configurations at subordinate strata. The ontologiadelpresente.pdf articulates the filtrado probabilístico bidireccional (ascendente and descendente, also termed resistencia) that regulates passage between the three layers: Capa 1 local intensification, Capa 2 relational coherence, Capa 3 global structural reorganization. The post-ascent persistence of altered Δt_k statistics across both synthetic (logistic $r = 3.8$, Lorenz) and real series supplies the empirical signature any calculus must reproduce. The Joint Episode definition and its modest AUC ≈ 0.476 (even under oracle labeling) already encode the non-deterministic character of the enabling relation.

The expected payoff is a quantitative theory of ascent probability: given a observed Joint Episode of duration D and intensity $Joint$, one can compute the measure of configurations at lower strata that remain admissible once the new law is in force, and therefore the probability that subsequent relational windows will or will not be able to support further ascent. Such a calculus would underwrite simulation engines, prospective validation designs, and the formal treatment of intervention (the following problem). It would also make precise the sense in which each stabilized level functions as a discreteness operator with its own domain of admissible inputs.

Methodologically, the account must remain stratified and non-reductive: transition probabilities describe enabling conditions and the filtering action of the layers; they do not reduce the actualization of a new law at L_{m+1} to a stochastic process on lower-layer variables. Philosophically, the calculus must preserve the autonomy of ontological kairos. The bidirectional filter raises or lowers the probability that lower-layer configurations may crystallize at the higher stratum; it does not cause the crystallization. Any formalization that collapses this distinction would violate the Principle of Ontological Ascent as stated in the corpus.

29.0.4 Intervention on Relational Kairoi

If Joint Episodes are necessary (though not sufficient) conditions for ontological ascent, then deliberate modulation of antisynchronization offers a possible lever on the probability of crossing. The corpus already contains controlled synthetic experiments in which structural perturbations—simultaneous increase of diffusive coupling from $\varepsilon = 0.05$ to 0.25 and switch from global to ring topology—are applied at a programmed midpoint to ensembles of six logistic maps ($r = 3.8$) and Lorenz oscillators. In fifty independent realizations the data-driven protocol detects Capa 3 reorganizations without reference to the injection schedule; the same KS contrasts on Δt_k, the same redistribution of hyper-persistence, and the same alignment with macroscopic events appear as in the unperturbed dengue series. These experiments demonstrate that changes in network topology and coupling strength can induce the conditions under which ascent becomes detectable.

What remains open is the systematic exploration of deliberate modulation: controlled experiments that vary topology, external forcing, or therapeutic parameters with the explicit aim of raising or lowering the probability of ascent; prospective validation on clinical or ecological systems in which such modulation is ethically and operationally feasible; and the articulation of ethical constraints that follow from the non-reductive ontology. The question is not whether relational kairoi can be modulated—they already are, in the synthetic protocol—but whether such modulation can be harnessed predictably and defensibly once the distinction between relational preparation and ontological actualization is respected.

The seeding results are the synthetic perturbation protocol of principle-of-ontological-ascent-v12.pdf (global-to-ring switch and *varepsilon* ramp as instruments that alter admissible configurations and produce measurable Capa 3 signatures); the discussion in the research program document of "RECD-aware control theory," "diseño de intervenciones basadas en tiempo propio," and "políticas de pausa de mercado o de control de redes eléctricas activadas por densidad de ticks o colapso de τ_s"; and the Joint Episode characterization that already quantifies the relational window as necessary but not sufficient (AUC ≈ 0.476).

The expected payoff is a new class of control and design problems in which the target is not a state in calendar time but a modulation of the probability that a relational window will support ontological crossing. In clinical contexts this might mean timing of interventions to avoid or promote physiological ascent; in ecological management it might mean topology or forcing changes that stabilize or destabilize regime transitions; in infrastructure it might mean "pauses" or re-couplings triggered by internal-clock statistics rather than external thresholds. The payoff is therefore both scientific (new experimental designs that treat relational kairoi as controllable variables) and practical (RECD-informed steering of systems whose critical transitions carry high stakes).

Methodologically, experiments must continue to use the uniform data-driven protocol (Frobenius + KS on Δt_k) without injecting external labels; any claimed modulation must be assessed by the same pre/post changes in admissible Δt_k distributions that mark ascent in the corpus. Philosophically, the non-reductive ontology imposes strict limits on what intervention can claim. Because ontological kairos is the autonomous actualization of a new discreteness regime, modulation of antisynchronization can only alter the measure of enabling conditions; it cannot guarantee or prevent the crossing itself. Ethical deliberation must therefore distinguish clearly between acting on relational windows (defensible within the ontology) and acting as if one were acting directly on time or on the ontological stratum (a reductive overclaim that the architecture rules out). The autonomy of the higher stratum is not a philosophical ornament; it is the precise constraint that any intervention protocol must respect if it is to remain consistent with the results already achieved.

29.0.5 Clinical and Ecological Translation

The dengue incidence series already supply a concrete demonstration that the internal clock T distinguishes pre- and post-ascent regimes more cleanly than calendar time and that early-warning metrics computed on the RECD scale yield longer or more precise lead times than the same metrics computed on the laboratory clock. For San Juan ($T = 936$ weeks) the detected Capa 3 transition is marked by KS $= 0.781$ on Δt_k and aligns within five weeks of a major incidence peak, with pre-Joint-Episode fraction 0.056; for Iquitos ($T = 520$ weeks) the KS contrast is 0.209, alignment occurs eighteen weeks prior to the peak, and the pre-transition Joint Episode fraction is 0.538. Full-ordinal implementations further improve false-alarm rates and precision relative to proxy methods, while the modest AUC of the Joint Episode (≈ 0.476) is reported uniformly. These results are obtained with the same universal thresholds, the same gate, and the same three-layer detection protocol applied to synthetic logistic and Lorenz ensembles.

A first physiological bridge now exists: the CCTP/SDDB Holter pilot reports multi-hour median lead times for $\Delta\tau_s$ and $\Delta\texttt{excess3}$ before spontaneous ventricular fibrillation, with substrate-dependent polarity and honest limits on false-alarm estimation without controls (Padilla-Villanueva 2026b). What remains open is the operational translation of the dengue demonstration and the cardiac pilot into prospective early-warning systems for other infectious diseases, for ecosystem collapses, and for additional physiological state transitions (seizures, multi-organ decompensation, etc.); multi-site clinical validation with true control cohorts; the design of pre-registered prospective protocols that evaluate alerts generated in real time against subsequently observed events; the integration of the internal clock T and its lead-time statistics into existing surveillance and monitoring infrastructures; and the explicit mapping of RECD ticks into actionable calendar lead times that clinicians and public-health or ecological managers can use without abandoning their current operational clocks.

The corpus seeds the direction at every level. The dengue early-warning technical report and related real-data documents supply the head-to-head comparisons (fullordinal versus proxy, lead times, $\Delta\alpha$ multifractal differentiation, FAR and precision on San Juan and Iquitos), the DSIS archive provenance, and the concrete lead-time numbers that any generalization must at minimum match or exceed. The research program document enumerates priority domains (epidemiology with behavioral feedback, ecosystem regime shifts, neurodynamics and ICU multi-signal monitoring, climate transitions) together with the justification that the mismatch between laboratory time and intrinsic time is expected to be severe precisely where ground-truth transitions, high-resolution multivariate data, and prior evidence of ordinal coherence collapse coincide. The Joint Episode paper records the modest predictive power (AUC ≈ 0.476) that any operational claim must continue to acknowledge. The supplementary technical reports on joint-condition calibration supply the threshold protocols that must be re-calibrated, not invented, for each new domain.

The expected payoff is a family of RECD-based early-warning systems whose lead times are expressed in the system's own accumulated ticks yet remain communicable in calendar units. For dengue-like diseases this means earlier, lower-false-alarm alerts integrated with existing vector and case surveillance; for ecosystems it means detection of regime shifts (clear-turbid lake transitions, fishery collapses) on time scales that match the intrinsic persistence structure rather than arbitrary sampling intervals; for physiological monitoring it means ICU dashboards that track coherence collapse across EEG, ECG, SpO2 and metabolic channels in internal time. The translation therefore does not replace existing infrastructures; it supplies an additional, internal-time axis on which the same data yield earlier or cleaner signals.

Methodologically, prospective validation must be pre-registered, must use the identical detection protocol (Frobenius + KS on Δt_k), and must report Joint Episode AUC, pre-transition fractions, and lead-time distributions on the T scale exactly as done for dengue. Integration with surveillance requires only that the ordinal pipeline ingest the multivariate streams already collected; no new sensors are presupposed. Philosophically, the non-reductive ontology again imposes a limit on what "warning" can mean. The Joint Episode raises the probability of ascent; the internal clock T registers the reorganization once it has occurred. An operational system can therefore announce that a relational window has opened or that a discreteness-law change has been detected; it cannot announce that the ontological crossing is now inevitable or that human action can prevent it with certainty. The modesty of the AUC ≈ 0.476 is not a shortcoming to be overcome by better algorithms; it is the observable signature of the autonomy of the higher stratum. Translation protocols must preserve this modesty in their language to clinicians, ecologists, and the public.

29.0.6 Philosophical Formalization

The present volume already articulates a non-reductive stratified ontology in dialogue with classical and contemporary sources. The refutation of absolute Newtonian time, the distinction between kairos and chronos, the three-layer framework (Capa 1 local intensification, Capa 2 relational coherence, Capa 3 structural reorganization), the Principle of Ontological Ascent, and the explicit integration with Aristotle's Physics and Leonardo Polo's ontology of the present are developed across the philosophical chapters and are presupposed in the formal statements of the RECD law, the Joint Episode, and the data-driven detection protocol. The strata L_0–L_3 are treated as hierarchically ordered yet irreducible; downward constraints are described as active delimitation rather than causal reduction; bidirectional probabilistic filtering is presented as an emergent structural relation, not a hidden mechanism.

The July monographs on the *acto de ser relacional-discreto* and the Conjecture of the Relational Order of Persistence deepen the metaphysical articulation with Polo and Whitehead (Padilla-Villanueva 2026d; Padilla-Villanueva 2026a), without yet supplying a many-sorted formal calculus. What remains open is precisely the construction of a fully formal ontology in which the strata L_m are treated as distinct sorts (in the sense of many-sorted logic or a typed framework), each equipped with its own discreteness operator (the characteristic law of accumulation intervals Δt_k operative at that level), and in which downward-constraint relations are formalized as morphisms or operators between sorts that preserve the autonomy of the higher while restricting the admissible configurations of the lower. Such a formalization would place the philosophical claims on the same rigorous footing as the mathematical results (Theorem v24, combinatorial lemma, RECD law, fractal bounds) while enabling a precise dialogue with contemporary philosophy of nature, process ontology, and the metaphysics of emergence without loss of mathematical content.

The corpus seeds this direction at every relevant point. The ontology-of-the-present manuscript supplies the explicit three-layer articulation, the bidirectional Bayesian filtering (ascendant and descendant), the emphasis on non-reductibility, and the engagement with Polo's ontology of the present as a phenomenon that is stratified, fragmented, and regulated by antisynchronization. The principle-of-ontological-ascent manuscript gives the formal definitions of stabilized regime L_m, ascent $L_m \to L_{m+1}$, relational versus ontological kairos, and downward constraints as active delimitation; its abstract and introduction already frame the work as supplying "a non-reductive ontology of structural transition in which the reconstitution of temporal discreteness marks the crossing into a genuinely novel regime of objective time." The Magna Synthesis and the philosophical chapters of the present volume supply the integration with Aristotle (time as number of motion, kairos as the "when" of qualitative change) and with Prigogine's arrow of time in far-from-equilibrium systems; they also record the limits of the current informal vocabulary.

The expected payoff is a formal apparatus in which one can state, for example, that the discreteness operator at L_{m+1} is not definable inside the language of L_m, that the downward-constraint map is a function from the power set of admissible configurations at L_m to a proper subset, and that the probability measure induced by bidirectional filtering is a relation between sorts that does not collapse their distinction. Such an apparatus would underwrite rigorous comparisons with other stratified ontologies, would clarify the precise sense in which the RECD is "objective extramental time," and would make the claim of non-reductivity checkable rather than rhetorical.

Methodologically, the formalization must be conservative with respect to the mathematics already achieved: the five-step construction of Theorem v24, the combinatorial lemma, the gate $g(\tau_s)$, the renormalization depths scaled by δ, the fractal derivation of $D \approx 1.98$, and the KS detection of law change must remain theorems inside the formal ontology, not informal illustrations. Philosophically, the dialogue with Aristotle and Polo must be preserved as a genuine extension rather than a translation into a foreign idiom that erases the specificity of the ordinal construction. The non-reductive commitment is not an addendum; it is the requirement that the formal sorts and operators respect the irreducibility of each ascent. A formalization that allowed the higher sort to be interpreted inside the lower would falsify the Principle of Ontological Ascent as stated in the corpus.

29.0.7 A Stratified Research Program

The six problems enumerated above do not constitute a miscellaneous catalogue of desiderata. They form a single, stratified research program whose internal organization mirrors the three registers already unified in the preceding chapter: the mathematical, the empirical, and the ontological.

Problems 1 (higher-order ordinal patterns) and 2 (finite-sample bounds on fractal dimension) extend the mathematical register. They refine the observables and the metric while preserving the reduction to Feigenbaum universality and the minimality of purely ordinal assumptions. Problem 3 (probabilistic calculus of downward constraints) sits at the intersection of the mathematical and ontological registers: it supplies the measure-theoretic language in which the already-demonstrated existence of downward constraints and bidirectional filtering can be stated with precision, without collapsing the autonomy of ontological kairos.

Problems 4 (intervention on relational kairoi) and 5 (clinical and ecological translation) extend the empirical register. They ask how the operators already validated on synthetic logistic, Lorenz, and dengue series—Joint Episode, A_{antis},M_{crit}, KS contrast on Δt_k, internal clock T—can be deployed in controlled experiments and prospective operational systems while continuing to report the modest predictive power (AUC $\approx$ 0.476) and the pre-transition fractions that the corpus records uniformly. Problem 6 (philosophical formalization) extends the ontological register by placing the stratified non-reductive claims on a footing formal enough to sustain dialogue with philosophy of nature without loss of the mathematical content.

Each direction remains anchored in the unified vision. The synthesis has shown that the same thresholds (+0.50, 0.41, −0.41), the same gate $g(\tau_s)$, the same renormalization depth k, the same Joint Episode definition, the same KS signature of law change, and the same fractal bounds 1.96–2.01 reappear across logistic maps at $r = 3.8$, Lorenz oscillators, coupled networks, and both dengue series. Because this invariance has been established, the open problems can be posed as determinate extensions rather than as repairs. The corpus already contains the seeds: the research program document organizes work into phases with explicit milestones; the technical reports on ontological permeability and joint-condition calibration supply the calibration protocols; the dengue and synthetic preprints supply the baseline numbers against which any extension must be compared.

All of these directions are already seeded in the corpus contained in the two directories. The present volume supplies the unified foundation on which they can be pursued without drift from the core commitments.

The transition from the synthesis of Chapter 25 to the open problems of the present chapter therefore marks not an ending but the point at which the architecture becomes sufficiently precise to underwrite a living research program. The Glossary, the Consolidated References, and Appendix A on Reproducibility that follow codify the operators, the numerical signatures, and the provenance that any subsequent work must continue to respect. The open problems listed here are the direct outgrowth of that codification; they do not require revision of prior chapters but extension from them. With the unified vision in hand, the research program on the discrete architecture of time enters its next phase as a single, stratified inquiry whose mathematical, empirical, and ontological registers remain in explicit correspondence.

All of these directions are already seeded in the corpus contained in the two directories. The present volume supplies the unified foundation on which they can be pursued.

Chapter 30

Unified Glossary of Key Terms

Antisynchronization A_{antis} Standard deviation across modules of the per-module Systemic Tau values; low sustained values indicate Layer 2 relational coherence.

Capa 1 / Layer 1 Local intensification of persistence measured by the composite critical-mass metric M_{crit} combining hyper-persistence of τ_s and RQA trapping time (LAM ≥ 0.80, TT ≥ 3.4).

Capa 2 / Layer 2 Relational coherence across modules operationalized by sustained low anti-synchronization A_{antis}.

Capa 3 / Layer 3 Global structural reorganization detected by Frobenius-norm shifts in the multichannel τ_s correlation matrix and Kolmogorov–Smirnov contrasts on the Δt series.

Chaos (ordinal) Regime in which $|\tau_s| < 0.41$; global ordinal correlations have collapsed to noise level; gate is open and discrete ticks are generated.

Combinatorial Lemma $\mathbb{E}[|\tau_s|]_k = 2^{k-1}/(2^k - 1) \to 1/2$ on superstable Feigenbaum orbits of period 2^k; supplies universal demarcation at 0.50.

Discrete Extramental Clock (RECD) The law $t_n = \sum g(\tau_s(k)) \cdot \Delta t_k$ with $\Delta t_k = \delta^{-k}|\tau_s(k)|\Delta t_0/n$.

Feigenbaum constant δ Universal scaling constant ≈ 4.6692016091 governing accumulation of period-doubling bifurcations and renormalization depths of the RECD.

Fractal dimension of extramental time $D \approx 1.98$ (bounds 1.96–2.01) of the accumulated process T; derived from similarity dimension $s \approx 0.449$ corrected by invariant measure and 2-adic conjugacy.

Gate function $g(\tau_s)$ Piecewise function: $g(\tau_s) = +1$ if $\tau_s \geq +0.50$; $(\delta - 1)/\delta \cdot (0.41 - |\tau_s|)/0.41$ if $|\tau_s| < 0.41$; -1 if $\tau_s \leq -0.41$.

Hyper-persistence Prolonged residence in the chaotic regime; operationally $P(k) \geq 7$ and $|\tau_s(k)| < 0.41$.

Joint Episode Maximal contiguous interval of sustained low A_{antis} containing at least one significant peak of M_{crit}; primitive ontological-temporal unit.

Joint Score $J\ D \cdot M$ where D is episode duration and M is mean critical mass over the episode; bias-reduced form $J_{0.7}$.

Kairos (ontological) Autonomous actualization of a new discreteness regime at Capa 3; replacement of the prior Δt law together with downward constraints.

Kairos (relational) Sustained Capa 2 Joint Episode that functions as an ontologically enabling window through bidirectional probabilistic filtering.

Large-deviation principle Empirical measures on the space of ordinal configurations satisfy an LDP with good rate function $I(\nu)$ tied to τ_s; atypical values decay geometrically as δ^{-r}.

Ontological Ascent (Principle of) A Capa 3 reorganization constitutes an ascent $L_m \to L_{m+1}$ instituting a new law of discreteness intervals irreducible to continuation of the prior regime.

Ordinal configuration Collection of rank vectors, one for each component, inside a sliding window of length n.

RECD See Discrete Extramental Clock.

Stabilized ontological regime L_m Interval during which persistence, antisynchronization, and accumulation operate within the characteristic range of renormalization depths and gate behavior associated with level m.

Systemic Tau τ_s Average Kendall rank correlation across all pairs of components inside sliding windows of length n.

Theorem v24 Reconstruction, from purely ordinal data, of a C^3 unimodal return map with non-degenerate quadratic critical point, placing the dynamics in the Feigenbaum universality class.

Thresholds $|\tau_s| < 0.41$ (chaotic range), $\tau_s \geq +0.50$ (stable/synchronized), $\tau_s \leq -0.41$ (strong antisynchronization).

2-adic conjugacy Topological conjugacy between the Feigenbaum attractor and the adding machine on $\mathbb{Z}_2$ that justifies transfer of combinatorial and renormalization properties to the observable τ_s.

excess3 / Φ_3 (Second Edition) Pre-specified continuous Level-3 synergistic surplus proxy $(0.6\,\text{Syn} + 0.4\,\text{Surp})$ and nested ordinal hierarchy Φ_1, Φ_2, Φ_3 integrated into RECD dynamics.

Appendix A

Figure Atlas

This appendix provides additional diagrams and empirical panels that support the main narrative. Figures are grouped by theme.

A.0.1 Paradigm overview and architecture

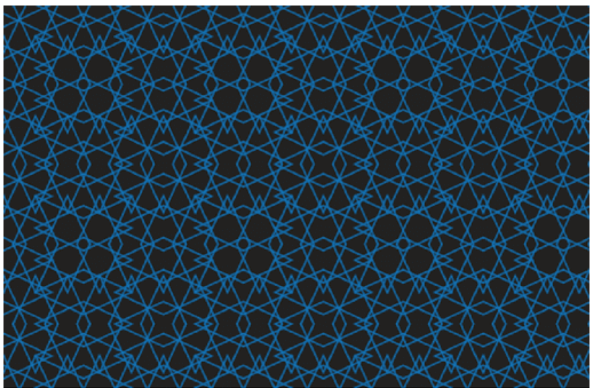

(a) Analytic/architectural background schematic.

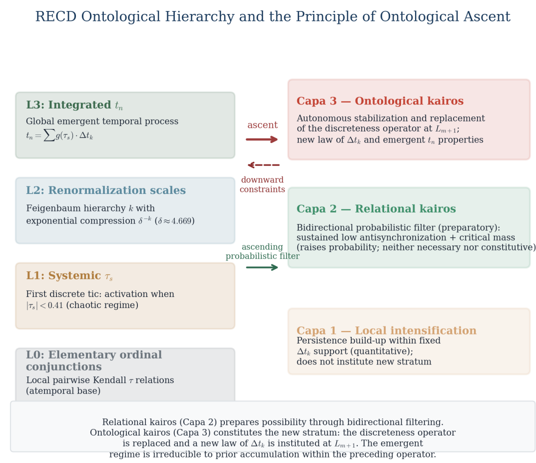

(b) Hierarchy / stratification diagram (operator levels).

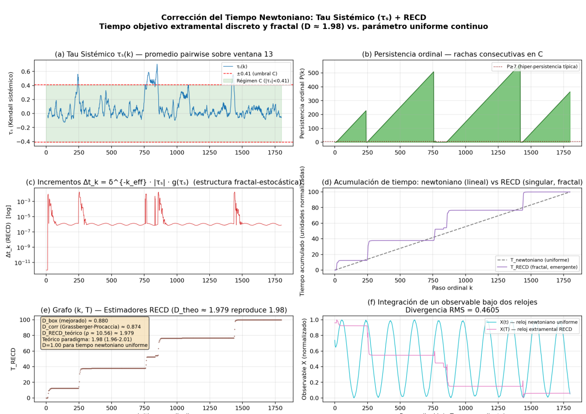

(c) Conceptual comparison: Newtonian time vs RECD time.

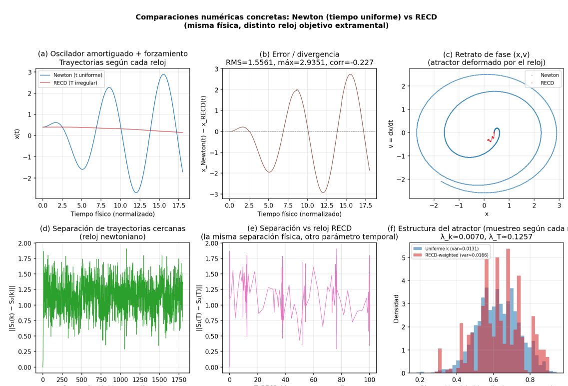

(d) Additional contrast panels for chronos vs T.

Figure A.1: Additional conceptual diagrams supporting the global architecture.

A.0.2 Feigenbaum-class validation (synthetic and theoretical)

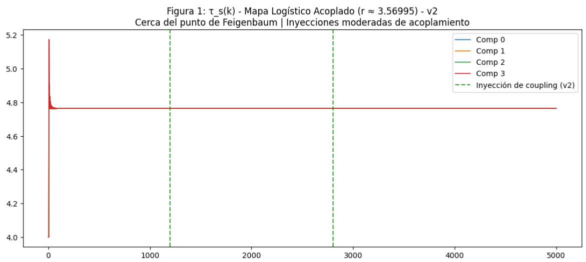

(a) τ_s behavior in the canonical Feigenbaum setting.

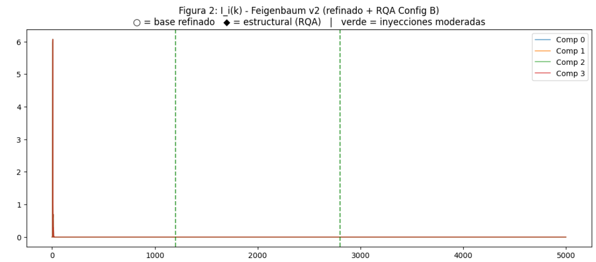

(b) Intensity / RQA structure in the Feigenbaum regime.

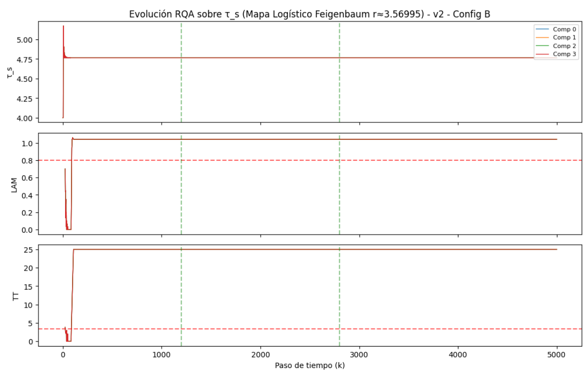

(c) Additional RQA panels (Feigenbaum class).

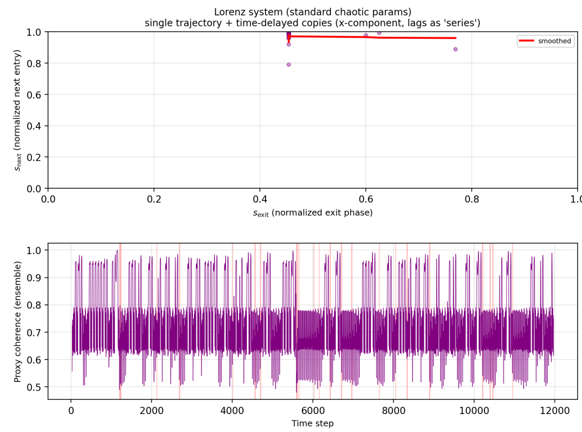

(d) Example reconstructed return map (Lorenz proxy).

Figure A.2: Supporting synthetic/theoretical figures for the Feigenbaum reduction and associated signatures.

A.0.3 Dengue empirical context (San Juan and Iquitos)

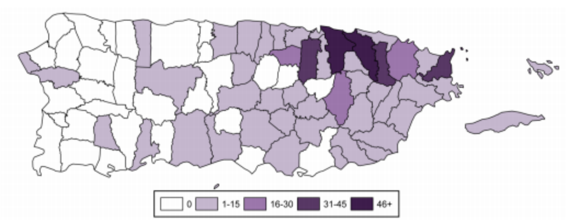

(a) Dengue case context (illustrative incidence curve).

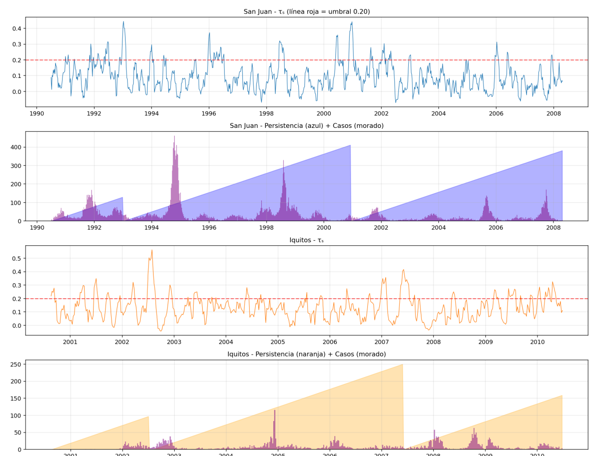

(b) San Juan vs Iquitos overview comparison.

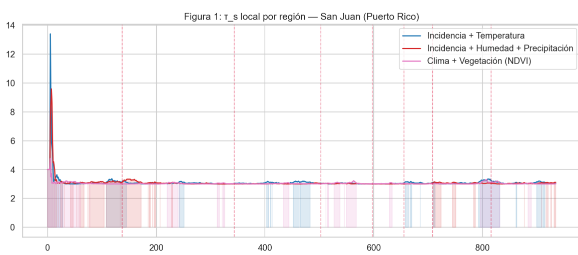

(c) τ_s series (San Juan).

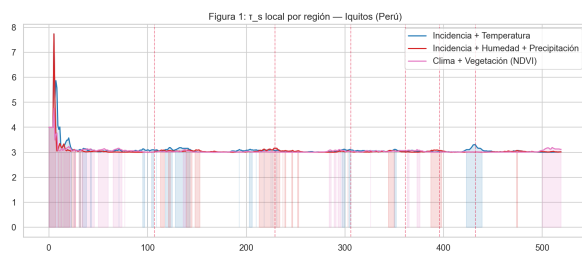

(d) τ_s series (Iquitos).

Figure A.3: Core empirical panels for the two dengue case studies.

A.0.4 Detection performance and early-warning behavior

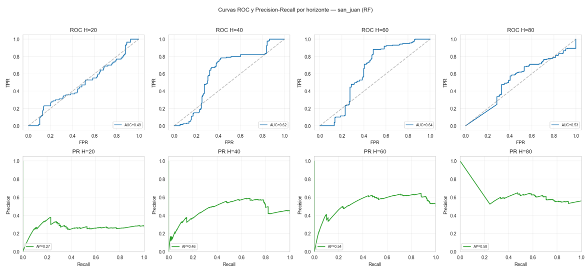

(a) ROC/PR curves (San Juan-like evaluation).

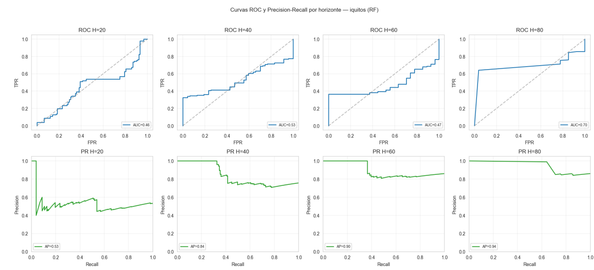

(b) ROC/PR curves (Iquitos-like evaluation).

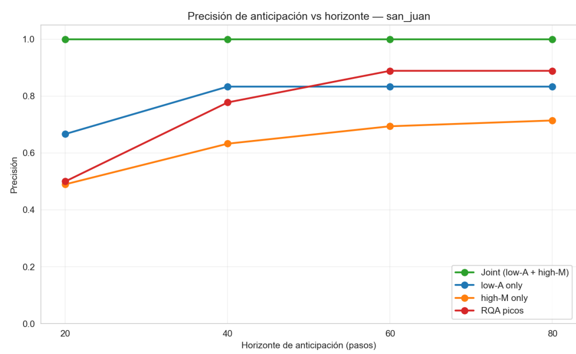

(c) Precision curve (San Juan-like evaluation).

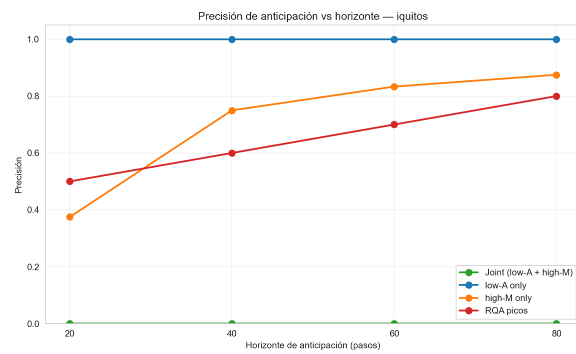

(d) Precision curve (Iquitos-like evaluation).

Figure A.4: Performance characterization panels used to evaluate early-warning behavior under different regimes.

A.0.5 Noise robustness and topology effects (additional panels)

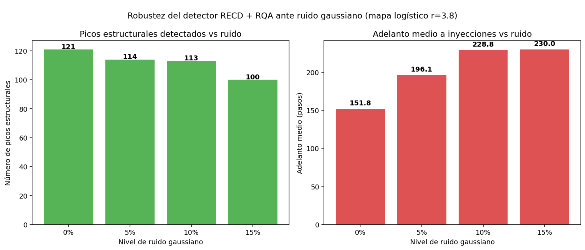

(a) Noise robustness metrics (summary).

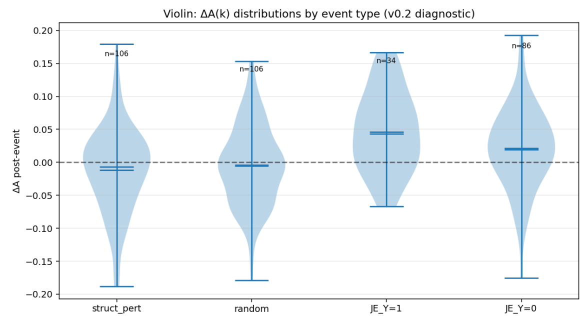

(b) Distributional behavior of ΔA (violin view).

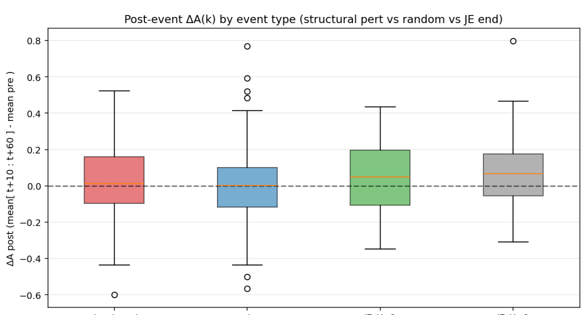

(c) Distributional behavior of ΔA (boxplot view).

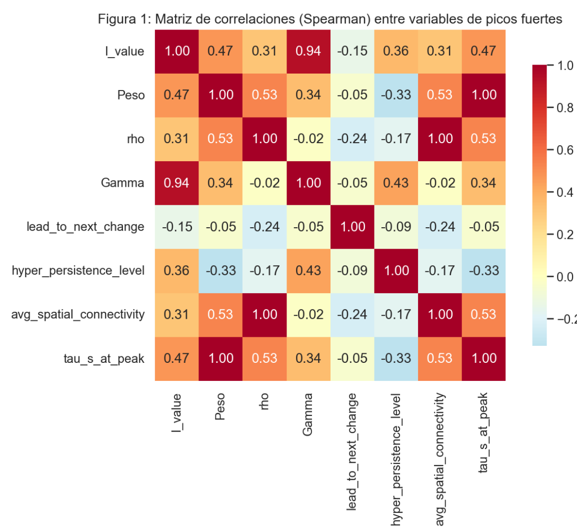

(d) Correlation heatmap (example summary panel).

Figure A.5: Additional robustness and structure panels complementing the main noise-tolerance figure.

References

Padilla, Johel (2025a). *Clarifying the Chaotic Range in Systemic Tau: The Intermediate Volatility Zone (|tau_s|<0.41) and Its Implications*. DOI: 10.20944/preprints202512.0055.v1.

– (2025b). *Discrete Extramental Time in Chaotic Systems: Event-Conjunction Model and Core Temporal Properties*. DOI: 10.20944/preprints202512.0610.v1.

– (2025c). *Fractal-Stochastic Emergence of Discrete Time in Chaotic Systems: Numerical Evidence Against Newtonian Absolutism*. DOI: 10.20944/preprints202512.2010.v1.

– (2025d). *Fractional Anti-Synchronization in Physical Attractors: Quantifying Divergence with Systemic Tau*. DOI: 10.20944/preprints202510.0083.v2.

– (2025e). *Numerical Validation of the Discrete Extramental Clock Law: Hierarchical Emergence of Objective Time from Ordinal Conjunctions in Chaotic Systems*. DOI: 10.20944/preprints202512.2431.v1.

– (2025f). *Philosophical Implications of the Discrete Extramental Clock Law: The Non-Existence of Absolute Newtonian Time in Extramental Reality*. DOI: 10.20944/preprints202512.1503.v1.

– (2025g). *Synthesis of Systemic Tau Concepts: An Integrated Overview of 2025 Preprints on Stability and Anti-Synchronization in Chaotic Systems*. DOI: 10.20944/preprints202509.2174.v1.

– (2025h). *Validation of Anti-Synchronization in Chaotic Systems Using Systemic Tau*. DOI: 10.20944/preprints202509.1894.v2.

– (2026). *Bridging Leonardo Polo's Philosophical Physics with the Discrete Extramental Clock Law: Ontological Emergence of Discrete Time in Chaotic Systems*. DOI: 10.5281/zenodo.18175567.

Padilla-Villanueva, Johel (2022). "Disertación de Doctorado". Doctoral dissertation. Universidad de Puerto Rico, Recinto de Ciencias Médicas. DOI: 10.17605/OSF.IO/A6QR4.

– (2025). *Mathematical Derivation of the Discrete Extramental Clock Law*. DOI: 10.20944/preprints202512.0633.v1.

– (July 2026a). *Conjetura del Orden Relacional de la Persistencia*. Working note relating Polo's *persistir* to Whitehead's relational process.

– (July 2026b). *Context-Dependent Relational Reorganization of Heart Rate Dynamics Precedes Spontaneous Ventricular Fibrillation: Systemic Tau and Ordinal RECD Evidence from the Sudden Cardiac Death Holter Database*. DOI: 10.5281/zenodo.21270699. URL: https://doi.org/10.5281/zenodo.21270699.

– (2026c). *Dimensión fractal (D ∼ 1.98) del tiempo extramental acumulado en sistemas caóticos: conjugación 2-ádica y renormalización ordinal*. DOI: 10.5281/zenodo.20619058.

– (July 2026d). *El acto de ser relacional-discreto: Persistir, physis y vacío en la continuidad del proyecto poliano*. Monograph / Studia Poliana submission package.

Padilla-Villanueva, Johel (June 2026e). *Empirical Validation of the Ontological Permeability Hypothesis: Calibration of Upward Probabilistic Filtering in the Three-Layer Model of the Present*. DOI: 10.5281/zenodo.20723966. URL: https://doi.org/10.5281/zenodo.20723966.

– (July 2026f). *excess3: A Pre-Specified Continuous Proxy for Order-3 Synergistic Surplus in the Systemic Tau / RECD paradigm—Methods, Null Models, and Synthetic Validation*. Version 1.0. DOI: 10.5281/zenodo.21385937. URL: https://doi.org/10.5281/zenodo.21385937.

– (July 2026g). *excess3: Introducción accesible al excedente sinérgico de orden 3 en el paradigma Tau Sistémico / RECD*. Version 1.0. DOI: 10.5281/zenodo.21385937. URL: https://doi.org/10.5281/zenodo.21385937.

– (2026h). *Hacia una ontología del presente en sistemas complejos*. DOI: 10.5281/zenodo.20711393.

– (July 2026i). *Integrating Φ_3 (excess3) into RECD Dynamics: From Parallel Metric to Structural Clock Contribution*. Version 0.5.1. DOI: 10.5281/zenodo.21400599. URL: https://doi.org/10.5281/zenodo.21400599.

– (July 2026j). *nested-recd: Nested ordinal RECD levels and continuous excess3*. Version 0.2.0. Software package (MIT); companion to excess3 methods preprint. URL: https://github.com/johelpadilla/nested-recd.

– (2026k). *Síntesis Magna del Tau Sistémico*. Version v6. DOI: 10.5281/zenodo.20576241.

– (July 2026l). *Systemic Tau and the RECD Framework: A Relational Theory of Hierarchical Ordinal Conjunctions and Critical Transitions in Complex Systems*. DOI: 10.5281/zenodo.21287252. URL: https://doi.org/10.5281/zenodo.21287252.

– (July 2026m). *Systemic Tau: Foundations of a Topological Framework for Early Warning Signals in Complex Systems*. Version 4.5.0. DOI: 10.5281/zenodo.21210455. URL: https://doi.org/10.5281/zenodo.21210455.

– (2026n). *Tau Sistémico y patrones ordinales multivariados para la detección temprana de brotes de dengue: evidencia en datos reales de Iquitos y San Juan*. DOI: 10.5281/zenodo.20657723.

– (2026o). *The Discrete Extramental Clock as Bayesian Optimal Accumulator: Large Deviations, Renormalization, and Strong Optimality under Purely Ordinal Observability*. DOI: 10.5281/zenodo.20685001.

– (2026p). *The Joint Episode as an Ontological-Temporal Unit: Mathematical Characterization, Structural Properties, and Transitions in Complex Systems*. Version v1.0. DOI: 10.5281/zenodo.20755272.

– (2026q). *The Principle of Ontological Ascent: Emergence of New Regimes of Temporal Discreteness through Hierarchical Reorganization*. Version v12. DOI: 10.5281/zenodo.20769218.

– (July 2026r). *Understanding excess3: A Cross-Disciplinary Guide to Order-3 Synergistic Surplus*. Version 1.0. DOI: 10.5281/zenodo.21385937. URL: https://doi.org/10.5281/zenodo.21385937.

Reproducibility and Corpus Provenance

Corpus location. Every theorem, definition, empirical result, parameter value, and philosophical claim in this volume is traceable to the primary research corpus (`Investigaciones` and `Publicaciones` directories). Full development traces, code, preprints and data pipelines reside in those two directories. This **Second Edition** additionally incorporates the July 2026 package entries catalogued in `references.bib` (DOIs `10.5281/zenodo.21385937`, `21400599`, `21210455`, `21287252`, `21270699`, `20723966`, together with the Acto de Ser / Conjetura working monographs).

Second Edition software anchors. `nested-recd` (excess3 / Φ_ℓ); `phi3-recd` (integration preprint stack); `systemictau` v4.5+ / Systemic Tau Studio; CCTP/SDDB analysis repository referenced by the cardiac manuscript.

Key parameter defaults (invariant across the corpus). Window length for τ_s: $n = 13$ (synthetic) or 85 (some real-data analyses); Feigenbaum constant $\delta \approx 4.6692016091$; chaotic threshold 0.41 derived from Kendall variance at $n = 13$; stable threshold +0.50; antisynchronization threshold -0.41; RQA Config B: LAM ≥ 0.80, TT ≥ 3.4; hyper-persistence threshold 1.0 recent standard deviations.

Recomputation steps for core results.

1. Systemic Tau and thresholds: run compute_tau_real.py or equivalent on any multivariate series; apply the exact formula in Chapter 3; thresholds follow from the variance formula (4n+10)/(9n(n-1)) without fitting.

2. Theorem v24 return map: implement the five-step construction on the binary low-coherence indicator s(k); verify unimodality and quadratic critical point on synthetic logistic or Lorenz data.

3. RECD accumulation: apply $g(\tau_s)$ and Δt_k exactly as written; accumulate t_n; compute Higuchi dimension on the resulting series.

4. Joint Episode and ascent detection: compute per-module τ_s, $A(k)$, $M(k)$; detect maximal low-A intervals containing high-M peaks; apply Frobenius + KS detectors to locate t^*; verify KS on pre/post Δt segments.

5. Full_ordinal dengue analysis: use the adaptive embedding and conditional mutual information

selection described in the dengue preprint; compare lead times and false-alarm rates against the proxy method on the DSIS files.

All scripts required for the above are present in the primary corpus code directories. Permanent archives are referenced by DOI in the corpus documents (e.g., 10.5281/zenodo.18175567).

Statement of reproducibility. The author affirms that every numerical result, figure, and table reported in the source documents can be regenerated from the code and data residing in the research corpus using the parameter values stated above. No proprietary or external data beyond the publicly referenced DSIS dengue archive are required.

Colophon

This print edition was produced from the author-maintained LaTeX sources of *Systemic Tau and the Discrete Architecture of Time*, Second Edition (July 2026). The interior was typeset with LuaLaTeX (TeX Live) using the Latin Modern and Latin Modern Math families; all fonts are embedded in the production PDF. Figures are included at their archival resolution from the research corpus. Bibliographic data are processed with Biber/BibLaTeX (author–year).

The production PDF is prepared for US Letter digital print-on-demand or offset/digital short-run workflows (see `PRINT_SPECS.md` in the release package). Crop marks are not required for letter full-bleed-free interiors with the stated margins.

Program: Ontología del Presente (Tau Sistémico).
ISBN: 979-8-18776-367-2 Imprint: Independently published.